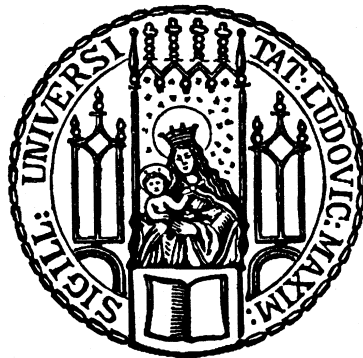


**ONTOGENETIC, MACROEVOLUTIONARY AND
MORPHOFUNCTIONAL PATTERNS IN ARCHOSAUR SKULLS: A
MORPHOMETRIC APPROACH**



Dissertation der Fakultät für Geowissenschaften der Ludwig-Maximilians-
Universität München zur Erlangung des Doktorgrades in den
Naturwissenschaften (Dr. rer. nat.)

von Dipl.-Biol. Christian Foth
geb. am 12.11.1984 in Rostock

22. Juli 2013

Supervisor and 1st reviewer: PD Dr. Oliver W. M. Rauhut

Bayerische Staatssammlung für Paläontologie und Geologie, Department of Earth and Environmental Sciences, Ludwig-Maximilians-Universität München, Richard-Wagner-Str. 10, D-80333 München, Germany

2nd reviewer: Prof. Dr. Johannes Müller

Museum für Naturkunde, Leibniz-Institut für Evolutions- und Biodiversitätsforschung an der Humboldt-Universität zu Berlin, Invalidenstraße 43, D-10115 Berlin, Germany

Date of thesis defense: 13.11.2013

Contents

Abbreviations	VI
Anatomical abbreviations for the skull	VI
Institutional abbreviations	VI
Technical abbreviations	VII
Abstract of the thesis	VIII
Kurzfassung der Dissertation	XII
Acknowledgements	XVI
Chapter 1: Introduction and summery of the thesis	1
Introduction	2
Characteristics and diversity of archosaur skulls	3
Previous work on archosaur skull diversity, ecology and function	4
Objective of the thesis	7
Introduction to results of Chapter 2 to Chapter 6	8
Ontogenetic and heterochronic patterns in archosaur skulls	23
Conclusions	50
Chapter 2: The good, the bad, and the ugly: the influence of skull reconstructions and intraspecific variability in studies of cranial morphometrics in theropods and basal saurischians	52
Abstract	53
Introduction	54
Material and methods	55
Institutional abbreviations	59
Results	59
Discussion	64
Conclusions	72
Acknowledgements	73
Chapter 3: Intraspecific variation in the skull morphology of the black caiman <i>Melanosuchus niger</i> (Alligatoridae, Caimaninae)	74
Abstract	75
Introduction	76

Material and methods	79
Results	86
Discussion	91
Conclusions	98
Acknowledgements	99
Chapter 4: Do different disparity proxies converge on a common signal?	
Insights from the cranial morphometrics and evolutionary history of	
Pterosauria (Diapsida: Archosauria)	
	101
Abstract	102
Introduction	103
Methods	107
Results	115
Discussion	122
Conclusions	127
Acknowledgements	128
Chapter 5: Macroevolutionary and morphofunctional patterns in theropod	
skulls: a morphometric approach	
	129
Abstract	130
Introduction	131
Material and Methods	134
Results	144
Discussion	153
Conclusions	163
Acknowledgements	166
Chapter 6: An exceptionally preserved juvenile megalosauroid theropod	
dinosaur with filamentous integument from the Late Jurassic of Germany	
	167
Abstract	168
Introduction	169
Systematic paleontology	169
Holotype	170
Etymology	170
Type locality and horizon	170
Diagnosis	170

Description and Comparisons	170
Discussion	179
Acknowledgements	184
References	186
Curriculum vitae	247
Eidesstattliche Versicherung	253
Appendix	S1
Supplementary information of Chapter 1	S2
Supplementary information of Chapter 2	S17
Supplementary information of Chapter 3	S27
Supplementary information of Chapter 4	S34
Supplementary information of Chapter 5	S49
Supplementary information of Chapter 6	S68

Abbreviations

ANATOMICAL ABBREVIATIONS FOR THE SKULL

AOF	antorbital fenestra	N	nasal
BOC	basioccipital	NAOF	nasoantorbital fenestra
EN, N	nares	O	orbit
EO	exoccipital	OP	opisthotic
HY	hyoid	PA	parietal
J	jugal	PM	premaxilla
JF	jugal foramen	PO	postorbital
L	lacrimal	Q	quadrate
LF	lacrimal fenestra	QJ	quadratojugal
LTF	lateral temporal fenestra	SNF	subnarial foramen
M	maxilla	SOC	supraoccipital
MF	maxillary fenestra	SQ	squamosal

INSTITUTIONAL ABBREVIATIONS

AMNH	American Museum of Natural History, New York (USA)
BHI	Black Hills Institute, Hill City (USA)
BMMS	Bürgermeister Müller Museum Solnhofen (Germany)
BP	Bernard Price Institute for Palaeontological Research, University of the Witwatersrand, Johannesburg (South Africa)
FMNH	The Field Museum, Chicago (USA)
GPIT	Geologisch-Paläontologisches Institut, Tübingen (IFGT Institut für Geowissenschaften, Eberhard-Karls-Universität, Tübingen) (Germany)
IVPP	Institute of Vertebrate Palaeontology and Palaeoanthropology, Beijing (China)
LACM	Los Angeles County Museum, Los Angeles (USA)
MB	Museum für Naturkunde, Berlin (Germany)
MOR	Museum of the Rockies, Bozeman (USA)
NHMW	Naturhistorisches Museum Wien (Austria)
NM	National Museum, Bloemfontein (South Africa)
NMC	National Museum of Canada, Ottawa (Canada)
NMMNH	New Mexico Museum of Natural History and Science, Albuquerque (USA)

NCSM	North Carolina Museum of Natural Sciences, Raleigh (USA)
PIN	Paleontological Institute, Russian Academy of Sciences, Moscow (Russia)
PVSJ	Museo de Ciencias Naturales, Universidad Nacional de San Juan, San Juan (Argentina)
QMNS	Qatar Museum of Nature and Science (Qatar)
SMA	Sauriermuseum, Aathal (Switzerland)
SMNS	Staatliches Museum für Naturkunde Stuttgart, Stuttgart (Germany)
SMF	Senckenberg Naturmuseum Frankfurt (Germany)
TMP	Royal Tyrrell Museum of Palaeontology, Drumheller (Canada)
TTU	Texas Tech University, Lubbock (USA)
ULBRA	Museu de Ciências Naturais, Universidade Luterana do Brasil, Canoas (Brazil)
USNM	National Museum of Natural History (= formerly United States National Museum), Smithsonian Institution, Washington, D.C. (USA)
UUVP	Utah Museum of Natural History, Salt Lake City (USA)
ZFMK	Zoologisches Forschungsmuseum Alexander Koenig, Bonn (Germany)
ZMH	Zoologisches Museum Hamburg (Germany)
ZPAL	Institute of Palaeobiology, Polish Academy of Sciences, Warsaw (Poland)
ZSM	Zoologische Staatssammlung München (Germany)

TECHNICAL ABBREVIATIONS

AMS	average maximum stress
CVA	Canonical Variate Analyses
FEA	Finite Element Analysis
GPA	Generalized Procrustes Analyses
NPMANOVA	non-parametric multivariate ANOVA
PC	principal component
PCA	Principal Component Analysis
PCO	Principal Coordinates Analysis
PIC	phylogenetic independent contrast
SSI	skull strength indicator
2B-PLS	two-block partial least squares analysis
UPGMA	Unweighted Pair Group Method with Arithmetic mean
UV	ultraviolet

Abstract of the thesis

The Archosauria represent the most successful clade within tetrapods, having a large diversity in terms of species, diet spectra, body plans and locomotion styles. This is also true for the skull morphology, which shows a wide variety in shape and size, as well as in the common formation of beaks, crests, domes or horns. Archosaur skulls have been studied intensively in terms of their morphology, ontogeny, function, ecology and behavior in the past, but most of these studies have largely been restricted to case studies of single species or only a small number of taxa. The aim of the current thesis is to obtain better and comprehensive insight into skull shape diversity of archosaurs by using a two-dimensional geometric morphometric approach, with a special focus on ontogenetic and macroevolutionary patterns and their relation to function and ecology. Skull shape variation was quantified for Crocodylomorpha (including an ontogenetic series of the recent caimanine alligatorid *Melanosuchus niger*), Pterosauria, Sauropodomorpha and Theropoda. The material used for the analyses consists of skull reconstructions published in the scientific literature and photographs of skull material. The most important results of the thesis are summarized as follows:

- The use of different skull reconstructions of the same specimen from the scientific literature has no significant influence on the results of morphometric analyses. However, the results could be potentially falsified by the use of reconstructions based on highly incomplete, strongly deformed or pathologic specimens.
- In some cases the degree of intraspecific variation of one species can be as great as the interspecific variation of closely related species with similar ecological

niches. Thus, species with great intraspecific diversity could have an impact on the results of morphometric analyses.

- The skull shape of Archosauria is strongly correlated with function. A closer examination within theropod skulls reveals that the shape of the postrostrum is probably more affected by functional constraints than the snout, but the greatest correlation to the function was found in the orbital shape. The latter result supports previous studies on the biomechanics of theropod skulls. A comparison of the ontogenetic bite force performance with the cranial growth in the alligatorid *Melanosuchus* and biomechanical studies on crocodile skulls reveals that ontogenetic shape changes, especially in the orbital and postorbital region, are functional constrained.
- Both ontogenetic and interspecific skull shape variation in archosaurs is correlated to diet preferences and feeding behaviour. A comparison between carnivorous and non-carnivorous (i.e. omnivorous and herbivorous) theropods reveals that both ecological groups occupy large areas within the morphospace without showing a significant overlap. Furthermore, small-bodied theropods tend to have a larger diet spectrum, suggesting that diet preferences within theropods are probably size related.
- The distribution of taxa within the morphospace of Crocodylomorpha, Pterosauria, Sauropodomorpha and Theropoda is strongly correlated with the phylogenetic interrelationship of these clades: Closely related taxa appear closer to one another within the morphospace than more distantly related taxa. This result indicates that skull shape in archosaurs is further constrained by phylogeny.

- When inferred from geometric morphometric data, disparity results proved to be similar to those based on limb measurements and discrete characters from phylogenetic analyses. This results justifies the use of geometric morphometric data as a further and equally useful proxy for addressing disparity.
- Early archosaur hatchlings share features of the skull shape, including short, pointed snouts, enlarged orbits and large postorbital regions. However, ontogenetic shape changes are only congruous in terms of a relative increase of the snout length and a relative decrease of the orbit size. The degree of these changes is not uniform, so that adult specimens of different species can vary substantially in snout length or orbit shape. Furthermore, archosaurs show a huge variability of changes in the snout depth, the length of the postorbital region as well as the relative size of the antorbital fenestra and the lateral temporal fenestra during ontogeny. This variability in ontogenetic trajectories probably causes the large skull shape diversity found in archosaurs.
- Due to the great variability in ontogenetic trajectories, cranial evolution of archosaurs is strongly affected by heterochronic events. Skull shape evolution of Crocodylomorpha, Sauropodomorpha, basal theropods, Tyrannosauroida as well as derived Oviraptoridae, Dromaeosauridae and Troodontidae was probably influenced by peramorphosis. However, within Crocodylia the short skull of *Osteolaemus* might result from a pedomorphic event. This is also likely for the short-snouted basal theropods *Daemonosaurus* and *Limusaurus*. The great similarity in the skull shapes of the juvenile megalosaurid *Sciurumimus* and basal coelurosaurs reveals that the skull shapes of the latter might be also caused by pedomorphosis. Further pedomorphic trends are suspected for the skull

evolution of basal Maniraptora and Avialae. The heterochronic events found seem to correlate with body size evolution.

Kurzfassung der Dissertation

Die Archosaurier repräsentieren die erfolgreichste Gruppe unter den Tetrapoden, die durch eine große Diversität an Arten, Nahrungsspektren, Bewegungsformen und im Körperbau gekennzeichnet ist. Dies gilt auch für die Schädelmorphologie, die durch eine große Variation in Größe und Formen sowie der häufigen Ausbildung von Schnäbeln, Hörnern, Hauben und Kämmen gekennzeichnet ist. Die Schädel der Archosaurier wurden in der Vergangenheit intensiv hinsichtlich ihrer Morphologie, Ontogenese, Funktion, Ökologie und Verhalten untersucht, jedoch beschränken sich die meisten Arbeiten auf Fallstudien zu einzelnen Arten bzw. einer kleinen Auswahl von Taxa. In der vorliegenden Arbeit soll die Diversität der Schädelmorphologie innerhalb der Archosaurier mit Hilfe von zwei-dimensionalen geometrischen Morphometrie auf breiterer Ebene untersucht werden. Dabei sollen sowohl ontogenetische als auch makroevolutionäre Muster und ihre Beziehung zu Funktion und Ökologie näher betrachtet werden. Eine Quantifizierung der Schädelform erfolgte für Crocodylomorpha (inklusive einer ontogenetischen Serie des rezenten Alligatoriden *Melanosuchus niger*), Pterosauria, Sauropodomorpha und Theropoda. Als Grundlage dienten publizierte Schädelrekonstruktionen aus der wissenschaftlichen Literatur sowie Fotos von Schädelmaterial. Die wichtigsten Ergebnisse der Arbeit sind wie folgt zusammengefasst:

- Die Verwendung von verschiedenen Schädelrekonstruktionen desselben Individuums aus der wissenschaftlichen Literatur hat keinen signifikanten Einfluss auf die Ergebnisse von morphometrischen Analysen. Die Ergebnisse können jedoch durch die Verwendung von Rekonstruktionen verfälscht werden,

die auf unvollständigem, stark verformtem oder pathologisch verändertem Material basieren.

- In einigen Fällen kann das Maß der innerartlichen Variation vergleichbar sein mit der zwischenartlichen Variation von nah-verwandten Arten mit ähnlichen ökologischen Nischen. Daher können Arten mit großer innerartlichen Variation die Ergebnisse von morphometrischen Analysen beeinträchtigen.
- Die Schädelform der Archosaurier korreliert stark mit der Funktion. Eine detaillierte Untersuchung an Theropoden-Schädeln zeigt, dass die Form des Hinterhaupts stärker durch Funktion beeinflusst wird als die Form der Schnauze. Die größte Korrelation zwischen Form und Funktion findet sich in der Augenhöhle, was die Ergebnisse früherer Arbeiten zur Biomechanik von Theropoden-Schädeln unterstützt. Ein Vergleich der ontogenetischen Beißkraftleistung mit dem Schädelwachstum bei *Melanosuchus* mit biomechanischen Studien an Krokodilschädeln zeigt, dass ontogenetische Veränderungen der Schädelform, speziell im Augen- und Hinterhauptsbereich, funktional beeinträchtigt sind.
- Sowohl ontogenetische als auch interspezifische Variation der Schädelform korrelieren bei Archosauriern mit Nahrungspräferenzen und Fressverhalten. Ein Vergleich zwischen karnivoren und nicht-karnivoren (d.h. omnivoren und herbivoren) Theropoden zeigt, dass beide ökologischen Gruppen große Bereiche im „Morphospace“ einnehmen, jedoch nicht signifikant miteinander überlappen. Kleinere Theropoden besitzen hier ein breiteres Nahrungsspektrum, so dass Präferenzen in der Nahrung wahrscheinlich größenabhängig sind.
- Die Verteilung der Taxa im „Morphospace“ der Crocodylomorpha, Pterosauria, Sauropodomorpha und Theropoda korreliert stark mit dem phylogenetischen

Verwandtschaft dieser Gruppen, d.h. das näher verwandte Taxa im „Morphospace“ näher beieinander liegen als entfernt verwandte Taxa. Dieses Ergebnis zeigt weiterhin, dass die Schädelform der Archosaurier auch durch die phylogenetische Verwandtschaft beeinträchtigt ist.

- Übereinstimmungen in den Ergebnissen von Disparitätsanalysen basierend auf geometrischer Morphometrie mit solchen basierend auf Längenmessungen und diskreten Merkmalen aus phylogenetischen Analysen zeigen, dass Disparität über mehrere Proxies gemessen werden kann, inklusive geometrisch morphometrischer Daten.
- Die Schädelformen von verschiedenen Archosaurier-Schlüpflingen ähneln einander durch das Vorhandensein einer kurzen Schnauze, großen Augenhöhlen und einer vergrößerten Hinterhauptsregion. Allgemeine ontogenetische Veränderungen betreffen die relative Verlängerung der Schnauze und die relative Verkleinerung der Augenhöhle. Diese Veränderungen sind allerdings nicht einheitlich in ihrer Intensität, so dass ausgewachsene Individuen verschiedener Arten sich deutlich in der Länge der Schnauze und der Form der Augen unterscheiden können. Des Weiteren besitzen Archosaurier eine große ontogenetische Variabilität hinsichtlich der Höhe der Schnauze, der Länge des Hinterhaupts sowie der relativen Größe des Antorbitalfensters und des lateralen Temporalfensters. Die große Variabilität der ontogenetischen Trajektorien ist wahrscheinlich für die große Diversität an Schädelformen innerhalb der Archosaurier verantwortlich.
- Aufgrund der großen Variabilität ontogenetischer Trajektorien ist die Schädelevolution der Archosaurier sehr stark durch heterochronische Ereignisse geprägt. Die Schädelevolution von Crocodylomorpha, Sauropodomorpha,

basalen Theropoden, Tyrannosauroiden sowie abgeleiteten Oviraptoridae, Dromaeosauridae und Troodontidae ist wahrscheinlich durch Peramorphose beeinflusst. Innerhalb der Crocodylia resultiert der kurze Schädel von *Osteolaemus* wahrscheinlich aus einer Pädomorphose. Das ist wahrscheinlich auch der Fall für die beiden kurzschnauzigen basalen Theropoden *Daemonosaurus* und *Limusaurus*. Die große Übereinstimmung der Schädelform des juvenilen Megalosauriden *Sciurumimus* mit dem von basalen Coelurosauriern könnte ebenfalls ein Hinweis sein, dass die Schädelform der basalen Coelurosaurier das Resultat einer Pädomorphose ist. Weitere pädomorphe Ereignisse könnten in der Schädelevolution der Maniraptora und Avialae aufgetreten sein. Die heterochronischen Ereignisse scheinen in enger Beziehung zur Evolution der Körpergröße zu stehen.

Acknowledgements

Finally, it is done and I feel really happy that I can start soon to enjoy the joy of regular unemployment as a high profile academic. But before I accept my fate, I would like to thank my supervisor Oliver Rauhut, who supported my scientific work over the last three years and gave me the possibility to work on one of the coolest dinosaur fossils ever found on this planet, in the history of man. Furthermore, I would like to thank Oliver for giving me an all-inclusive freedom in terms of working, and for making jokes worse than I could ever do. However, without his tireless dedication to hold me on the carpet, I would now probably stand on a floor made of oak wood or cobblestones. I further thank Adriana López-Arbarello and Richard Butler for their support, many careful advices and fruitful discussions. Especially Richard helped me a lot with correcting drafts, introducing statistical methods and developing own projects. Probably, he also thinks that my jokes are at least as bad as Oliver's, but this is just a single opinion. Furthermore, I would like to thank Johannes Müller for his willingness to review my thesis.

Another thanks goes to my co-authors Paula Bona, Julia Desojo, Steve Brusatte, Helmut Tischlinger, Mark Norell as well as Richard and Oliver. The quality of the single chapters presented in this thesis benefited substantially from your scientific input. I further thank Roger Benson, Steve Brusatte, Manubo Sakamoto, Michel Laurin, Mike Benton, Andrew Farke, Xu Xing, Gareth Dyke and Abby Drake for constructive and helpful reviews and comments on the single chapters. Another thanks goes to Martín Ezcurra, Roland Sookias, Christine Böhmer, Kerstin Schröder, Felix Quade, Melissa Tallman, Serjoscha Evers and Johannes Knebel for pleasurable discussions. Christine Böhmer and Melissa Tallman introduced me into geometric morphometric methods and

Roland Sookias spent hours of hours with proof-reading manuscripts on crocodylian skulls. Poor wretch!

During my PhD studies I had the possibility to visit a lot of wonderful zoological and palaeontological collections all over the world. These visits allowed me to study some of the most interesting dinosaur fossils ever found and to learn a lot about reptilian anatomy. Thus, I would like to thank all curators and collection managers who hosted me during my stays: Frank Glaw, Jakob Hallermann, Gunther Köhler, Linda Acker, Dennis Rödder, Ursula Bott, Mark Norell, Carl Mehling, Lindsay Zanno, Fernando Novas, Alejandro Kramarz, Eduardo Ruigómez, Hans-Jakob Siber, Ben Pabst, Thomas Bollinger, Martina Kölbl-Ebert, Xu Xing and Corwin Sullivan. Martin Dobritz is thanked for access to the X-ray facilities in the Klinikum rechts der Isar.

“Money, it's a gas, grab that cash with both hands and make a stash.“ (Roger Waters). In this sense, the current thesis was generously funded by the Deutsche Forschungsgemeinschaft (DFG project RA-1012/-12-1).

Finally, I would like to thank my parents, my brother and his wife, my grandparents and all my friends for being there and supporting me during my ontogeny so far. Furthermore, I thank the sweat reek of this evil plant for helping my neurons to feel happy and contented in times of media disinformation, collective cognitive dissonance and political corruption. But whatever, nothing helps more than lying in the arms of my only true love Julika. You keep me burning!

CHAPTER 1

Introduction and summary of the thesis

Keywords:

Archosauria; Saurischia; Crocodylomorpha; Pterosauria; Theropoda; *Melanosuchus*; ontogeny; skull shape; sexual dimorphism; feeding ecology; biomechanics; disparity; macroevolution; heterochrony; geometric morphometrics

Author contributions:

Research design: **Christian Foth**

Data collection: **Christian Foth**

Data analyses: **Christian Foth**

Preparation of figures and tables: **Christian Foth**

Wrote chapter: **Christian Foth**

Introduction and summary of the thesis

Christian Foth

INTRODUCTION

Within reptiles, the clade Archosauria Cope, 1869 is defined as the monophyletic group composed of recent crocodylians and birds, and all fossil taxa that share their last common ancestor (Gauthier & Padian 1985). Within recent tetrapods, archosaurs represents the most successful clade with approximately 10 000 living species described (Westheide & Rieger 2004). Based on the fossil record, the origin of Archosauria goes back at least to the Early Triassic (Nesbitt et al. 2011), whereas stem-line representatives were already present in the Late Permian (Tatarinov 1960; Borsuk-Białynicka & Evans 2009). The two main clades of Archosauria are the Pseudosuchia Zittel, 1887-1890, which are defined as clade including recent crocodylians and all other archosaurs closer to crocodylians than to birds (Gauthier & Padian 1985), and Ornithodira Gauthier, 1986, which are defined as the least inclusive clade containing the pterosaur *Pterodactylus* and the songbird *Passer* (Nesbitt 2011). During their cosmopolitan Mesozoic radiation, archosaurs became extremely diverse in terms of number of species, diet spectra and body plans, including different forms and manners of locomotion (Weishampel et al. 2004; Brusatte et al. 2008; Nesbitt 2011), and mastered not only terrestrial (most archosaur groups), but also aquatic and semi-aquatic (e.g. Phytosauria, Neosuchia) as well as aerial and arboreal habitats (e.g. Pterosauria, Avialae).

CHARACTERISTICS AND DIVERSITY OF ARCHOSAUR SKULLS

The skulls of recent archosaurs possess several characteristics unique amongst tetrapods including e.g. the presence of an antorbital fenestra, a laterosphenoid, a mandibular fenestra, a strongly pneumatized ear and braincase region, thecodont teeth as well as the absence of a parietal foramen, a supratemporal, a postparietal, a tabular, a postfrontal, an epipterygoid and palatal teeth (Mickoleit 2004). However, these characteristics do not represent ‘true’ apomorphic characters of the clade Archosauria. The pneumatization of the middle ear and the braincase as well as the reduction of the postfrontal and epipterygoid for example are characters evolved independently within the stem-line of both crocodylians and birds (Gower & Weber 1998; Gower 2002; Rauhut et al. 2003a; Holliday & Witmer 2008, 2009; Nesbitt et al. 2011), whereas the other character mentioned above were already evolved within the stem-line of archosaurs (Nesbitt 2011). Skull characters found as apomorphic for Archosauria are palatal processes of the maxilla meeting at the midline, an elongated and tubular cochlear recess, an external foramen for abducens nerves within the prootic, an antorbital fossa presented on the lacrimal, the dorsal process of the maxilla and the dorsolateral margin of the posterior process of the maxilla as well as probably the presence of foramina for entrance of cerebral branches of internal carotid artery into the braincase positioned on the anterolateral surface of the parasphenoid (Nesbitt 2011).

Despite these uniting characteristics archosaurs show a high diversity of shape, which includes the convergent formation of keratinous beaks (e.g. Hadrosauria, Ornithomimosauria, Oviraptoridae, Neornithes, Shuvosauridae, Tapajaridae), the reduction of the antorbital fenestra (e.g. Ankylosauria, Ceratopidae, Crocodylia, Hadrosauridae), the formation of premaxillary, nasal, frontal or postorbital crests and

domes (e.g. Bucerotidae, *Casuarius*, Ceratopsidae, Lambeosaurinae, Oviraptoridae, Pachycephalosauria, Tapajaridae) or the formation of nasal, lacrimal or frontal horns and knobs (e.g. *Allosaurus*, Ankylosauria, *Carnotaurus*, Ceratopsidae, *Ceratosaurus*) (Romer 1956; Starck 1979; Witmer 1997; Rauhut 2003a; Weishampel et al. 2004; Nesbitt 2007; Hieronymus & Witmer 2010; Pinheiro et al. 2011; Fig. 1.1).

PREVIOUS WORK ON ARCHOSAUR SKULL DIVERSITY, ECOLOGY AND FUNCTION

Since Georges Cuvier established the scientific fields of comparative anatomy, palaeontology and osteology, the skulls of archosaurs have been studied intensively in terms of their morphology, ontogeny, function, ecology and behavior (e.g. Romer 1956; Starck 1979; Weishampel 1981; 1984; Crompton & Attridge 1986; Zusi 1993; Witmer 1997; Zanno & Makovicky 2011; Brusatte 2012). In the last 20 years, such studies have been revolutionized due to the use of many new methods such as cladistics, including the concept of the extant phylogenetic bracket (Witmer 1995), computed tomography and digital modeling (e.g. Alonso et al. 2004), finite element analysis (e.g. Rayfield 2007), evolutionary developmental biology (e.g. Abzhanov et al. 2004) and geometric morphometrics (e.g. Chapman 1990).

Ontogenetic studies on the skull anatomy of archosaurs have been performed for example for extant crocodylians (e.g. Kunderát 2009; Piras et al. 2010), pterosaurs (e.g. Bennett 2006), ceratopsians (e.g. Chapman 1990; Horner & Godwin 2006), hadrosaurids (Evans 2010; Campione & Evans 2011), sauropodomorphs (Sues et al. 2004; Whitlock et al. 2010), basal tetanurans (e.g. Rauhut & Fechner 2005), tyrannosaurids (e.g. Carr 1999, Carr & Williamson 2004) and maniraptorans (e.g. Kunderát et al. 2008; Bever & Norell 2009).

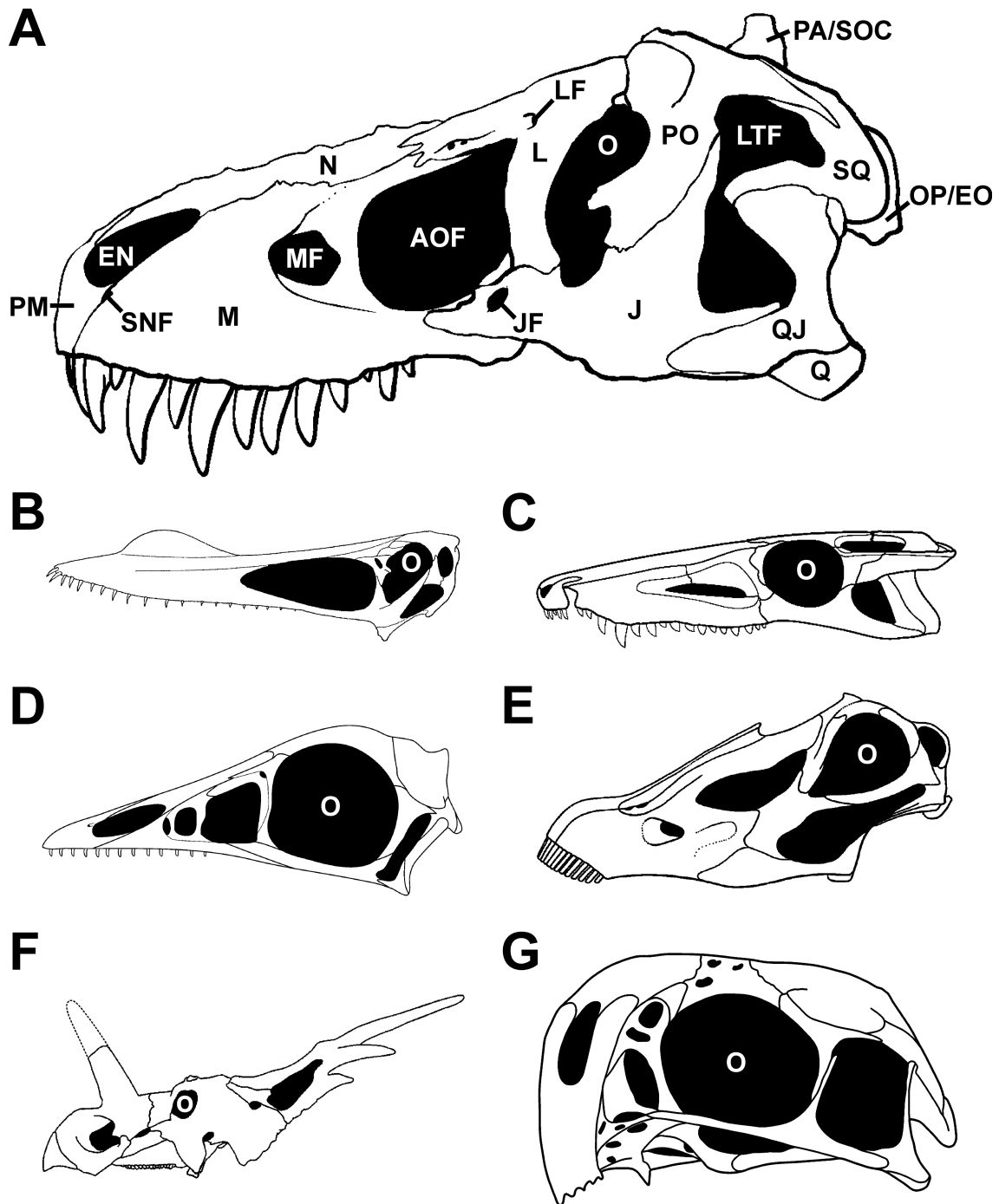


Fig. 1.1. A. A typical archosaur skull represented by *Tyrannosaurus* (modified after Carr & Williamson 2004). B-G. Examples of cranial diversity in archosaurs. B. The pterosaur *Anhanguera* (modified after Maisey 1991). C. The crocodylomorph *Domicosuchus* (modified after Nesbitt 2011). D. The avialian *Archaeopteryx* (modified after Rauhut in press). E. The sauropod *Diplodocus* (modified after Wilson & Sereno 1998). F. The ceratopsid *Styracosaurus* (modified after Ryan et al. 2007). G. The oviraptorid *Conchoraptor* (after Osmólska et al. 2004). AOF, antorbital fenestra; BOC, basioccipital; EN, nares; EO, exoccipital; J, jugal; JF, jugal foramen; L, lacrimal; LF, lacrimal fenestra; LTF, lateral temporal fenestra;

M, maxilla; MF, maxillary fenestra; N, nasal; O, orbit; OP, opisthotic; PA, parietal; PM, premaxilla; PO, postorbital; Q, quadrate; QJ, quadratojugal; SNF, subnarial foramen; SOC, supraoccipital; SQ, squamosal.

As mentioned, great advances have been made with respect to cranial function in archosaurs. These studies have drawn from classical morphological and experimental approaches as well as geometric studies (e.g. Weishampel 1984; Henderson 2002; Henderson & Weishampel 2002; Erickson et al. 2003, 2012; Holliday & Witmer 2008; Lautenschlager 2013) and, increasingly, from finite element methods (e.g. Rayfield et al. 2001; Rayfield 2004, 2005, 2011; Witzel & Preuschoft 2005; McHenry 2006; Pierce et al. 2008; Young et al. 2010; Witzel et al. 2011).

However, most of these studies have largely been restricted to case studies of single species or only a small number of taxa. Compared to the great number of large phylogenetic datasets existing for archosaurs (e.g. Wilson 2002; Mayr & Clarke 2003; Rauhut 2003a; Butler et al. 2007; Brusatte et al. 2010a; Prieto-Márquez 2010; Nesbitt 2011; Carrano et al. 2012; Turner et al. 2012; Pol et al. in press), broad-scale studies investigating the relationships between cranial diversity, ontogenetic modifications, functional constraints, and evolutionary processes are still rather rare. One means to integrate these concepts into one large scheme is via the use of geometric morphometrics. This method quantifies shape variation of objects in a multivariate morphospace. This morphospace can be compared thereafter with phylogenetic relationships, ecological and functional proxies or analysed to assess morphological disparity, ontogenetic or biogeographical patterns (e.g. Zelditch et al. 2004). Geometric

morphometric studies regarding cranial shape of archosaurs have been carried out to date for Crocodylomorpha (e.g. Pierce et al. 2008; Piras et al. 2009, 2010; Young et al. 2010), ornithischian dinosaurs (Chapman et al. 1981, Chapman 1990, Chapman & Brett-Surman 1990, Goodwin 1990), sauropodomorphs (Young & Larvan 2010) and non-avian theropod dinosaurs and extant birds (e.g. Chapman 1990; Mazzetta et al. 1998; Marugán-Lobón & Buscalioni 2004, 2006; Kulemeyer et al. 2009; Brusatte et al. 2012a; Bhullar et al. 2012). The relationship between shape and function was specifically investigated by, for example, Pierce et al. (2008), Young et al. (2010) and Brusatte et al. (2012a), whereas Piras et al. (2010) and Bhullar et al. (2012) for example examined the relationship between shape and ontogeny.

OBJECTIVE OF THE THESIS

As mentioned above, archosaurs possess enormous skull diversity, but only a small numbers of studies to date have investigated the correlation of shape diversity with function, ecology, ontogeny and evolution. Thus, the aim of this thesis is to obtain better insight into the ontogenetic and macroevolutionary patterns of archosaur skulls, and their relation to function and ecology by using two-dimensional geometric morphometrics and further statistical methods. The material used for the analyses consists of a) skull reconstructions published in the scientific literature, and b) photographs of skull material. The following main questions will be addressed:

1. How large is the impact of differing skull reconstructions from the same specimen or the same species on the results of morphometric studies?
2. What are the main patterns of shape variation in archosaur skulls?
3. How is skull shape influenced by functional constrains and feeding ecology?

4. Is skull shape correlated with phylogeny?
5. How are ontogenetic shape changes reflected in evolution?

The influence of skull reconstructions in geometric morphometric analyses is investigated for basal Saurischia, basal Tetanurae and Cretaceous Tyrannosauroida (Chapter 2). Skull shape variation and its relationship to function, ecology and/or phylogeny are investigated in detail for the recent caimanine alligatorid *Melanosuchus niger* (Chapter 3), Pterosauria (Chapter 4) and theropod dinosaurs (Chapter 5). In order to investigate the interrelation between ontogenetic and macroevolutionary patterns of skull shape variation within archosaurs a) ontogenetic patterns documented in the skull of *Melanosuchus* are compared to skull shape variation/evolution seen in Crocodylomorpha, and b) ontogenetic patterns of *Allosaurus*, Titanosauridae, *Diplodocus* *Massospondylus*, Megalosauridae (see Chapter 6), Oviraptoridae, *Tarbosaurus* and *Tyrannosaurus* are compared to skull shape variation and evolution in Saurischia.

INTRODUCTION TO RESULTS OF CHAPTER 2 TO CHAPTER 6

THE INFLUENCE OF DIFFERENT SKULL RECONSTRUCTIONS FROM THE SAME SPECIMEN OR SPECIES ON MORPHOMETRIC STUDIES

The geometric morphometric analyses of fossil archosaurs carried out in the current thesis as well as in other recently published studies on theropod skulls (e.g. Brusatte et al. 2012a; Bhullar et al. 2012) is mainly based on two-dimensional skull reconstruction from the scientific literature. Because skull reconstructions may differ greatly due to incompleteness and/or deformation of the material, this approach may be potentially problematic. Furthermore, macroevolutionary approaches generally consider only one

representative specimen per species, meaning that the influence of intraspecific variation is ignored. To test the influence of different skull reconstructions of the same specimen in morphometric analyses, three datasets for basal Saurischia, basal Tetanurae and Late Cretaceous Tyrannosauroida were created (see Chapter 2). The degree of shape variation (as a measure of disparity) was estimated for skull reconstructions based on the same specimen and compared to shape variation occurring in skull reconstructions based on different specimens of the same species and skulls of closely related species, in order to examine whether this potential source of variation may be comparable to taxonomically or even phylogenetically significant variation.

The results indicate that the effects of shape variation between different skull reconstructions based on the same specimen are negligible in geometric morphometric studies. Thus, if the skull reconstruction is based on rather complete, little deformed material, the impact of the author's drawing ability and style should not affect results of morphometric analyses. However, some skull regions are somewhat more problematic for the plotting of landmarks than most (e.g. the ventral contact between jugal and quadratojugal, the contact between the premaxilla and nasal on the dorsal margin of the skull, the most anterior point of the lacrimal along the dorsal margin of the antorbital fenestra and the contact between postorbital and squamosal on the dorsal margin of the lateral temporal fenestra) and their morphology should be verified with photographs or first hand observations. In contrast, skull shape variation found between different specimens and species is higher compared to shape variation between different skull reconstructions of the same specimen, because they further contain intraspecific or interspecific variation. Interestingly, for closely related species with similar ecological niche, the degree of interspecific variation can partly overlap with that of intraspecific

variation. Such overlap is well documented in recent animals and can be found at both the morphological and molecular level (e.g. Czechura & Wombey 1982; Lockwood 2005; Meyer 2005, Meier 2006, 2008). Thus, in some cases it could be possible that species with great intraspecific diversity potentially influence the results of morphometric analyses. Furthermore, the results could be affected by those species with unresolved taxonomy.

MAIN PATTERNS OF SHAPE VARIATION IN ARCHOSAUR SKULLS

Besides functional constraints (which will be discussed separately), skull shape in vertebrates is influenced by intraspecific variation (e.g. ontogenetic variation, sexual dimorphism) (e.g. Emerson & Bramble 1993; O'Higgins & Collard 2002; Bruner et al. 2005) and evolutionary processes (e.g. natural selection, heterochrony, genetic drift, adaptive radiation) (e.g. Rieppel 1993; Burns et al. 2002; Abzhanov et al. 2006; Smith 2011; Bhullar 2012), which can be captured in both intraspecific and interspecific morphospaces. In the current thesis an intraspecific morphospace was estimated for the recent caimanine alligatorid *Melanosuchus niger* as an example (see Chapter 3), whereas an interspecific morphospace was estimated for both Pterosauria (see Chapter 4) and Theropoda (see Chapter 5).

Intraspecific skull shape variation in Melanosuchus niger

The skull shape of *Melanosuchus* varies mainly in terms of the relative length of the snout, the depth of the tip of the rostrum, the relative size of the subnarial gap between premaxilla and maxilla, the shape of the ventral margin of the maxilla, the relative size and position of the orbit, the relative shape of the jugal region, the overall depth of the orbital and postorbital region, the relative length and width of the skull roof table and

the position of the jaw angle in both an anterolateral-posteromedial direction and an anteroventral-posterodorsal direction (Fig. 3.2, 3.3). This variation, which is summarized by the first principal component, describes over 70 % of total skull shape variation.

For both dorsal and lateral views the first PC axis is strongly correlated with centroid size (Fig. 3.4, Table 3.1), indicating that the shape variation mentioned above contains information of allometric variation related to ontogenetic growth. Thus, based on the relationship found, it is possible to reconstruct major shape changes in skull shape of *Melanosuchus* during ontogeny. The skulls of early juvenile individuals possess a very short snout, which is wide in dorsal view, but dorsoventrally pointed in lateral view. The ventral margin of the snout is straight and no subnarial gap is present. The orbit is very large and the jugal region is slender in both dorsal and lateral view. The postorbital region is elongated in an anteroposterior direction, and the broad skull roof table is posteriorly inclined in lateral view. The posterior end of the skull is relatively narrow and the jaw joint lies substantially anterior to the posterior end of the skull roof table. During ontogeny the snout becomes relatively elongated. In dorsal view, the snout becomes more slender, but deeper in lateral view, and the snout tip becomes blunter. Between premaxilla and maxilla a subnarial gap is formed, and the ventral margin of the maxilla becomes anteriorly convex in lateral view. The relative size of the orbit decreases, whereas the jugal region becomes broader and deeper. Due to the overall decrease in size of the orbit, the postrostrum becomes generally flattened in lateral view resulting in a horizontally aligned skull roof table. The postorbital region becomes shorter, but expands posterolaterally, and the jaw joint moves substantially posteriorly to the posterior end of the skull roof table (Fig. 3.2, 3.3). Most crocodylian

taxa share similar ontogenetic patterns in skull shape change, including, for example, relative elongation of the snout, decrease of the relative orbit size and increase of the interorbital width, as well as relative decrease in length of the postorbital skull roof (Table 3.2). The only exception is the long-snouted *Gavialis gangeticus*, in which skull growth is almost isometric (excepting the orbits) during ontogeny (see Piras *et al.* 2010).

Skull shape variation was further tested to attempt to detect presence of cranial sexual dimorphism in adult individuals of *Melanosuchus*. The results show that distinct sexual dimorphism is present, which is mainly size-related. This relationship to size is not surprising as males grow to about 30 % larger than females. Size-related sexual dimorphism is also described for other crocodylians (e.g. Webb & Messel 1978; Hall & Portier 1994; Verdade 2000, 2003; Platt *et al.* 2009), and caused by a generally faster and longer growth in males (e.g. Chabreck & Joanen 1979; Rootes *et al.* 1991; Wilkinson & Rhodes 1997). Statistical support for sexual dimorphism remained after excluding the effects of allometry with help of an pooled within-group regression from the dataset, indicating that differences between females and males may be not only size-related. Non-size related sexual dimorphism has only been described so far for the crocodylid *Crocodylus porosus* (Webb & Messel 1978), the gavialid *Gavialis gangeticus* (Hall & Portier 1994) and the alligatorid *Caiman latirostris* (Verdade 2000). However, differences in the sample size of males and females as well as the large numbers of landmarks and semi-landmarks compared to the sample size could lead to false positive signals in the statistical test. Therefore, the current result should be verified with larger sample sizes, different landmark configurations as well as for other crocodylian taxa.

Due to the diversity of crests and horns present (see above), cranial sexual dimorphism has been hypothesized for a large number of pterosaurs (e.g. Bennett 1992; Lü et al. 2011) and dinosaurs, e.g. Ceratopsia (e.g. Kurzanov 1972; Chapman 1990; Lehman 1990, 1998; Chapman et al. 1997), basal Sauropodomorpha (e.g. Gow et al. 1990), Pachycephalosauria (e.g. Chapman et al. 1997), Hadrosauria (e.g. Chapman et al. 1997), non-avian Theropoda (e.g. Colbert 1989, 1990; Carpenter 1990) and recent birds (e.g. Selander 1966). However, such interpretations in fossil taxa have been treated with great caution due to generally low sample sizes of single individuals for each species, making statistical verification problematic (see Molnar 1990; Padian & Horner 2011a, in press). Differences seen in cranial shape could be alternatively related to intraspecific variation (e.g. allometric shape variation due to size differences between different specimens) (e.g. Ryan et al. 2001), taphonomic deformation (e.g. Forster 1990) or even taxonomic misidentification (e.g. Evans & Reisz 2007). A further difficulty is that the determination of sex within extinct archosaurs usually cannot be based on single osteological characters (e.g. Erickson et al. 2005; Prieto-Márquez 2007). A possible reliable character for sex determination was found for ornithomirans in the form of presence of medullary bone in the long bones of several dinosaurs and one pterosaur species (Schweitzer et al. 2005; Lee & Werning 2008; Chinsamy et al. 2009, 2013; Hübner 2012). Within recent archosaurs this bone structure is only documented for female birds during their reproductive periods (e.g. Miller & Bowman 1981; Dacke et al. 1993), but not in crocodylians (Schweitzer et al. 2007). However, as medullary bone is only formed during reproductive periods, sex determination based on this character is seasonally restricted and thus unsuitable for broad-scale sexing of extinct ornithomirans.

The best-supported example of sexual dimorphism in the fossil record of Archosauria may be in the pterosaur *Darwinopterus*. Here, a female specimen was identified by the preservation of an egg in the pelvic region (Lü et al. 2011). In contrast to other specimens referred to this taxon (see Lü et al. 2010a), this particular female specimen lacks a sagittal crest on the head. If preservation artefacts can be ruled out and the taxonomic classification is correct, the interpretation of the presence of sexual dimorphism in the crest morphology of *Darwinopterus* hypothesized by Lü et al. (2011) could be valid. However, the expression of cranial sexual dimorphism in archosaurs must be viewed as an open question, may with such dimorphism varying from species to species and potentially being expressed in the form of size differences, soft tissue, colour patterns and/or behaviour rather than in the form of osteological structures (e.g. Cooper & Vitt 1993; Sampson 1997). Alternatively, it is possible that some species used cranial ornaments for species recognition (see Padian & Horner 2011b). For some recent birds it is further documented that both males and females develop ornamental structures, which are selected for via mate choice in both sexes (Jones & Hunter 1993, 1999; Amundsen 2000; Kraaijeveld et al. 2004). In contrast to common sexual selection this so-called mutual sexual selection does not result in sexually dimorphic display structures. Thus, it is further possible that the development of cranial ornaments in some extinct archosaurs resulted from mutual sexual selection (see Hone et al. 2012) and thus that such ornamentation was not sexually dimorphic.

Interspecific skull shape variation in Pterosauria

The majority of shape variation in pterosaur skulls occurs in the relative length of the snout, the relative size of the orbit and postorbital region, the relative size and shape of the naris-antorbital fenestra region and the position of the jaw joint relative to the orbit

(Fig. 4.1B). This shape variation is summarized by the first principal component, which describes over 50 % of total shape variation. The most extreme species affected by this shape variation are the short-snouted *Anurognathus* and the long-snouted *Pterodaustro*. However, the chosen landmark configuration does not capture the total shape of cranial crests known in pterosaurs. Thus, it is likely that the variation summarized by the first principal component is overestimated, and that the distribution of taxa within the morphospace should in fact be more widely spread. Variation related to crest formation is partly summarized by the second, third and fourth principal components. Here, shape variation captured by PC 2 includes a large frontal crest as present in pteranodontids, that of PC 3 includes the large rostral crests present in tapajarids, and that of PC 4 includes the premaxillary crest present in ornithocheirids (Fig. 4.1B).

Based on the data generated by the Principal Component Analysis, temporal and taxonomic disparity was estimated. Despite small sample sizes for each time bin as well as for particular taxonomic groups, some trends can be observed. Over time, cranial shape disparity increased within pterosaurs from the Late Triassic to the Early Cretaceous, but then declined in the Late Cretaceous. Due to small sample sizes, this result was confirmed by rarefaction analysis, which reduces the error for sample size differences (Fig. 4.3A, B). This temporal pattern of cranial disparity is consistent with previous studies based on limb measurements and discrete character data (Dyke et al. 2006, 2009; Prentice et al. 2011; Butler et al. 2012). Thus, if this pattern is correct, the disparity peak occurs relatively late in pterosaur evolution compared to other animal groups (see Erwin 2007), probably with the radiation of Monofenestrata. To test the results and to get a better insight into temporal disparity in pterosaurs it would be advisable to correct the measures of disparity used in the current study by adding

information of shape from hypothetical ancestors into the analyses. This can be done by mapping principal components as continuous characters on time-calibrated trees. As the origin of the hypothetical ancestors for each clade is sometimes shifted back into earlier time bins (see Brusatte et al. 2011) it is possible that this could affect the present disparity pattern in relation to the temporal radiation of Monofenestrata.

Cranial disparity of non-monofenestratan pterosaurs is lower than that of Monofenestrata, but this difference is not statistically significant. Here, the overlap of error bars is mainly caused due to the short-snouted *Anurognathus*. The exclusion of this taxon from the non-monofenestratan disparity sample results in a significantly more disparate Monofenestrata. Within Monofenestrata, the highest disparity is present in azhdarchoids and ornithocheiroids. Ctenochasmatooids show lower disparity than the former clades, whereas dsungaripteroids possess the lowest disparity in the cranium (Fig. 4.3C). These results largely coincide with those published by Prentice et al. (2011) based on discrete character data from the entire pterosaur skeleton.

Interspecific skull shape variation in Theropoda

For theropod dinosaurs, most variation summarized by the first principal component occurs in the relative length and depth of the snout, the length of the antorbital fenestra and the size of the lateral temporal fenestra affecting the length of the postorbital region. The second PC axis describes the shape of the snout tip, the relative depth of the antorbital fenestra, the size and shape of the orbit mainly influenced by the length and the depth of the suborbital body of the jugal, the relative depth of the postorbital region, and the position of the jaw joint. The third PC axis describes the shape and size of the antorbital fenestra and the orbit mainly influenced by the inclination of the lacrimal. All

three PC axes are correlated with centroid size, and thus contain allometric shape information. Interestingly, the length of the snout is inversely related to the length of the postorbital region (see Marugán-Lobón & Buscalioni 2003), whereas the depths of both skull regions seems to be more variable and unrelated to one another.

The skulls of *Plateosaurus* (outgroup), *Herrerasaurus*, *Eoraptor*, *Compsognathus* and *Erlikosaurus* resemble most the centroid shape for the whole morphospace (Fig. 5.2). By contrast, the most aberrant skulls within theropods occur in Oviraptorosauria, which possess an extremely short and deep snout and enlarged, round orbit as well as a huge lateral temporal fenestra. Based on Brusatte et al. (2012a), this group also possesses the highest within-group variation in skull shape. Another extreme in cranial shape is the abelisaurid *Carnotaurus*, which possesses a very short and deep snout, but with extremely short, oval orbits (Fig. 5.2). Extremes of cranial morphology are also represented by spinosaurids and *Gallimimus*, which both possess low skulls with elongated snouts, and short postorbital regions. Within basal birds, the most aberrant skull was found in *Confuciusornis*. Brusatte et al. (2012a) found the toothless ceratosaur *Limusaurus* to be yet more extreme, but in the current analyses this taxon plotted close to the centre of the morphospace. Compared to other ceratosaurs in which the skull is well known (e.g. *Ceratops*, several *Abelisauridae*), the skull shape of *Limusaurus* is divergent. However, incomplete skull material from the small-bodied noasaurid *Masiakasaurus* shows that some representatives of the group also possess skulls with low, elongated snouts and enlarged, round orbits (Carrano et al. 2011), indicating a huge skull shape diversity within ceratosaurs. This is supported by disparity analyses, performed by Brusatte et al. (2012a), which show that Ceratosauria possess higher within-group variation in skull shape than, for example, basal Tetanurae,

Tyrannosauroidae or Dromaeosauridae.

THE INFLUENCE OF FUNCTIONAL CONSTRAINTS AND FEEDING ECOLOGY ON SKULL SHAPE

Besides evolutionary processes, the shape of a biological structure is further influenced by functional constraints, in which function is understood as *mechanical role* or *physical role*, i.e. how a phenotypic feature is used (see Bock & Wahlert 1965; Lauder 1995).

Here, a strong correlation between functional loading and shape of a biological structure implies that a particular structure is selected for ‘optimal’ shape, defined as maximal strength with minimal material (e.g. Witzel et al. 2011). In the current thesis, the relationship between skull shape and function was tested for *Melanosuchus* (see Chapter 3) and theropods dinosaurs (see Chapter 5).

Ontogenetic shape variation vs. function and feeding ecology in Melanosuchus niger

To test the relationship between form and function in *Melanosuchus*, bite forces were used as a functional proxy. The bite force for each skull was computed with help of an equation originally estimated for *Alligator mississippiensis* (Erickson et al. 2003). These values were tested against skull shape variation using regression and two-block Partial Least Square analysis (2B-PLS) (see Rohlf & Corti 2000). Overall skull shape variation was found to be significantly correlated with bite forces (Table 3.1). This correlation is primarily influenced by shape captured by the first principal component. As previously stated, this component contains information on ontogenetic shape variation implying that these changes could be primarily functionally constrained. However, in adult crocodylians most mechanical stress during biting is concentrated in the posterior half of the skull, especially in the jugal region and around the orbits (Pierce et al. 2008). Thus, especially the shape changes observed in the orbital and postorbital region of

Melanosuchus skull ontogeny (e.g. flattening of the skull, expansion of the jugal depth and the lateral expansion of the postorbital region) can be seen as adaptations for generating higher bite forces and for minimizing mechanical stress (e.g. Schumacher 1973; Busbey 1989; Bona & Desojo 2011). By contrast, shape variation seen in the rostrum of crocodylians is highly variable and seems to be less strongly related to function and rather to prey selection and food processing (McHenry et al. 2006; Pierce et al. 2008; Erickson et al. 2012). Therefore, it is likely that ontogenetic changes of the rostral shape of *Melanosuchus* are correlated with changes of culinary preferences during life. The enormous increase in skull size seen during ontogeny will necessarily result in a change of dietary spectrum, which is well documented for other crocodylians (e.g. Cott 1961; Webb & Messel 1978; Hutton 1987; Webb et al. 1991; Cleuren & de Vree 2000; Horna et al. 2001, 2003). Here, the short and pointed snout seen in early juveniles of *Melanosuchus* is well adapted for hunting small invertebrates. The elongation and dorsoventral expansion of the snout seen during ontogeny and the formation of a subnarial gap, which go hand in hand with the postorbital adaptations to generate higher bite force, facilitate consumption of larger fish, birds and mammals.

Interspecific shape variation vs. function and feeding ecology in Theropoda

Skull shape variation for theropods was tested against two functional proxies, a) the skull strength indicator (SSI) based on beam models of different theropod skulls (see Henderson 2002) and b) the average maximum stress (AMS) based on finite element models (see Rayfield 2011) with help of 2B-PLS and a regression test wherein the functional and shape parameters were mapped on an informal supertree phylogeny (Butler & Goswami 2008) and transformed into phylogenetic independent contrasts (PICs) (see Felsenstein 1985). The relationship between skull shape and feeding

ecology was tested using 2B-PLS and NPMANOVA (see Hammer & Harper 2006).

Skull shape in theropods is significantly correlated with both functional proxies used, in which the SSI correlates best with the second and third PC axes, whereas the AMS correlates with the first and third PC axes (Table 5.2). All three PC axes contain information on allometric shape variation, which could be related to function. By excluding allometric shape variation from skull shape variation using non-allometric residuals, shape and function are no longer correlated. As in crocodylians (see Pierce et al. 2008; Erickson et al. 2012), the postorbital region in theropods seems to be more strongly related to function than the rostrum (Table 5.1), a conclusion that is also supported by finite element models (e.g. Rayfield 2011). These congruent results for crocodylians and theropod dinosaurs may indicate that the postorbital region of archosaur skulls is generally more important for understanding skull biomechanics than the snout. The strongest correlation to function within theropod skulls however was found for the orbital shape (Table 5.1), which tends to change from rounded to oval (in concert with a relative decrease of orbit size in relation to the whole skull) with the increase of mechanical stress. These findings support previous results from Henderson (2002).

As in crocodylians, the shape of the rostrum may be more related to feeding ecology than to function (Table 5.1). However, the ecological proxy used for feeding ecology correlates still better with the shape variation seen in the postorbital region. This may be because the ecological proxy also contains information on biting behaviour (i.e. information related to function), which was found to have a stronger effect on the posterior than the anterior part of the skull (see above). Furthermore, dietary preferences

are related to tooth morphology (e.g. Smith 1993), which was not taken into account in the geometric morphometric analyses. However, non-carnivorous theropods occupy a large area within the morphospace (Fig. 5.5), indicated by huge skull shape diversity (see also Brusatte et al. 2012a). Both carnivorous and non-carnivorous theropods are well separated within the morphospace with only a small area of overlap. In contrast, herbivorous and omnivorous theropods could not be distinguished from each other based on the morphometric data (Fig. 5.5, Table 5.3). Based on the Procrustes consensus shapes, carnivorous theropods tend to have a skull with a deep rostrum due to maxillary shape, a large antorbital fenestra, a deep suborbital region, and a relatively small, oval orbit, whereas non-carnivorous theropods (excluding aberrant oviraptorids) tend to have a tapering rostrum with a small antorbital fenestra, a shallow jugal region, an enlarged, round orbit, a shortened postorbital region, and a jaw joint significantly anterior to the quadrate head (by including oviraptorids the rostrum of the non-carnivorous theropods becomes shorter and deeper, and the postorbital region longer) (Fig. 1.2). Thus, the differences in the consensus skull shapes of carnivorous and non-carnivorous theropods correspond to the allometric trends seen in theropod skulls, indicating that feeding ecology in theropods may also be influenced by body and/or relative skull size, in which small-bodied theropods tend to adapt to a broader dietary spectrum. In this context, the indistinguishability of skull shape of omnivorous and herbivorous theropods may result from a gradual transition between both feeding strategies (see Zanno & Makovicky 2011).

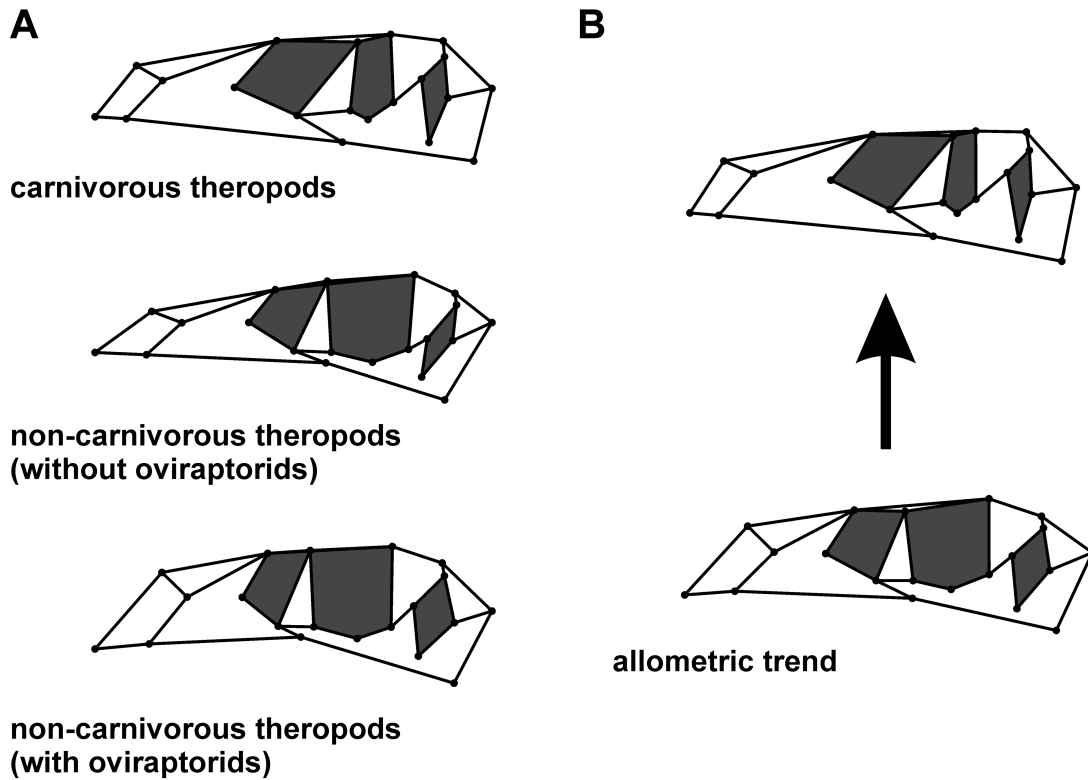


Fig. 1.2. **A.** Consensus shape of carnivorous and non-carnivorous theropods. **B.** Allometric trend from small-bodied to large-bodied theropods.

THE RELATIONSHIP BETWEEN SKULL SHAPE AND PHYLOGENY

Due to its complexity, the vertebrate skull provides a large number of potential characters for use in phylogenetic analyses. The number of skull characters (including tooth characters) used for phylogenetic analyses investigating the interrelationship of several archosaur groups varies between c. 40 to over 90 % of total number of characters (e.g. Rauhut 2003a; Butler et al. 2007; Lü et al. 2010a; Sereno & Brusatte 2009; Brusatte et al. 2010a; Prieto-Márquez 2010; Brochu 2011; Nesbitt 2011). Due to its huge impact on phylogenetic analyses one can assume that the shape of archosaur skulls is determined by phylogeny. By mapping phylogenetic hypotheses within the morphospace (see Stone 2003; Klingenberg & Gidaszewski 2010) this relationship can

be tested with help of a permutation test. If a strong phylogenetic signal is present, closely related taxa should appear closer to one another within morphospace than more distantly related taxa, in which the tree length of the original topology should be shorter than 95 % of all randomly generated trees (see Laurin 2004; Klingenberg & Gidaszewski 2010). As the geometric morphometric data are treated as continuous characters and optimized with help of e.g. square change parsimony (Maddison 1991) this approach can be further used to estimate the skull shape of hypothetical ancestors for each node of the phylogeny, and to comprehend skull shape variation during evolution (see below for Crocodylomorpha and Saurischia, see Chapter 4 for Pterosauria). In this thesis, the relationship between shape and phylogeny was tested for both Pterosauria (Chapter 4) and Theropoda (Chapter 5).

For both groups skull shape is significantly correlated with phylogeny, i.e. closely related taxa are more similar in skull shape to each other than more distantly related taxa. A similar result was also found for theropod dinosaurs by Brusatte et al. (2012a). According to these authors, phylogeny is even the primary determinant for skull shape variation seen in theropods, but other macroevolutionary analysis using different samples and landmark configurations found that skull shape evolution in theropods was further influenced by function and diet (see Chapter 5 for discussion) and heterochronic events (e.g. Bhullar et al. 2012, see below).

ONTOGENETIC AND HETEROCHRONIC PATTERNS IN ARCHOSAUR SKULLS

One of the key processes in evolution is heterochrony, which is defined as an evolutionary change of a phenotype due to a change in the timing of developmental processes (Wiesemüller et al. 2003; Futuyama 2007). Thus, heterochronic events could

lead to significant evolutionary changes in body plans within short periods of time. Evidence for heterochronic events occurring in evolutionary history could be potentially detected with the help of comparative ontogenetic studies between different taxa, taking into account their phylogenetic relationships. Here, skull shape variation of both Crocodylomorpha and saurischian dinosaurs are studied in lateral view in terms of heterochrony by combining interspecific and ontogenetic skull shape variation into one analysis for each group respectively. The data were analysed with help of Principal Component Analysis (PCA), regression methods, WARD cluster and character mapping, in which ontogenetic patterns in skull shape were compared to evolutionary patterns. A more detailed summary of material and methods is given in the supplementary information of the current chapter.

ONTOGENETIC AND HETEROCHRONIC PATTERNS IN CROCODYLOMORPHA

The ontogenetic patterns used as reference for heterochronic events within Crocodylomorpha are mainly based on *Melanosuchus* (see above, Chapter 3). However, comparison with other recent crocodylians shows that some ontogenetic patterns seem to be relatively similar, e.g. the relative increase of snout length and depth, relative decrease of the orbit size and relative decrease in the length of the postorbital region (Table 3.2). Additionally, based on the current dataset, the lateral temporal fenestra decreases in its relative size during ontogeny.

Within the PCA plot the ontogenetic series of *Melanosuchus* clusters closely together with the crocodyline *Osteolaemus* and the alligatorid *Alligator*. All three taxa differ from the other crocodylomorphs in their possession of a relatively flat skull, a strongly convex ventral margin of the snout, and a relatively large orbit, which is

summarized by the second PC axis. The WARD cluster analyses further shows that the skull shape of *Osteolaemus* is more similar to that of juvenile and subadult *Melanosuchus* individuals. In contrast, the skull shape of *Alligator* resembles that of adult *Melanosuchus* individuals (Fig. 1.3). The position of the short-snouted crocodyline *Osteolaemus* to juvenile *Melanosuchus* within the cluster could be an evidence for a paedomorphic event in the stem-line of *Osteolaemus*, i.e. a development of a juvenile morphology in an adult taxon, due to an earlier onset of sexual maturity (progenesis), the delay of the growth rate (neoteny) or the delay of the onset of time of growth (postdisplacement) compared to its ancestors (see McNamara 1982; Long & McNamara 1997). However, this should be tested in a more comprehensive dataset, which includes the ontogenetic series of several recent crocodylians including *Osteolaemus*.

Interestingly, several changes described in the skull shape of *Melanosuchus* (as well as other crocodylians) during ontogeny are also present in crocodylomorph evolution. Like early juvenile *Melanosuchus*, basal crocodylomorphs possess a relatively short snout, a large orbit, a relatively long postorbital region with a large temporal fenestra and a jaw joint, positioned anterior to or below the posterior end of the skull roof table. However, in contrast to early juvenile *Melanosuchus*, the snout of basal crocodylomorphs was distinctly deeper with a straight dorsal margin of the snout and a large antorbital fenestra. During evolution, the skull of crocodylomorphs became more and more elongate due to a relative increase of the snout length, the relative size of the orbit and the lateral temporal fenestra decreased successively, the length of the postorbital regions decreased and the jaw joint shifted more posterior relative to the posterior end of the skull roof table (Fig. 1.4). The coincidences between

crocodylomorph evolution and *Melanosuchus* ontogeny previously described could be an evidence for a peramorphic trend within crocodylomorph evolution, i.e. the evolvement of a more “developed” taxon due to a delayed onset of sexual maturity (hypermorphosis), an increase of growth rate (acceleration) or an early onset of growth (predisplacement) compared to its ancestor (see McNamara 1982; Long & McNamara 1997).

Unfortunately, no study on the body size evolution within Crocodylomorpha has been conducted to test this hypothesis in detail. Based on the fossil record, basal crocodylomorphs tend to be relatively small (e.g. Colbert & Mook 1951; Walker 1990; Wu & Chatterjee 1993; Clark et al. 2004), whereas some neosuchians reached enormous body size (e.g. Erickson & Brochu 1999; Sereno et al. 2001; Sereno & Larsson 2009; Brochu & Storrs 2012). After mapping the centroid size of the aligned skulls onto the phylogenetic tree used in the current study, it can be seen that skull size increased successively from the hypothetical ancestor of Crocodylomorpha to that of Crocodylia (Fig. 1.5), supporting the hypothesized peramorphic trend within crocodylomorph evolution. Nevertheless, because of missing data on the bone histology of crocodylomorphs, it is currently not well understood, which growth strategy led to this supposed peramorphosis. Small basal crocodylomorphs like *Terrestrisuchus* for instance grew relatively fast (de Ricqlès et al. 2003), whereas recent crocodylians possess a more ‘reptile’-like slowed growth pattern (e.g. Hutton 1987). However, histological data for the giant crocodylian *Deinosuchus* reveal that peramorphic events within crown-crocodylians could be caused at least by hypermorphosis, resulting from a prolongation of growth with juvenile growth rates (see Erickson & Brochu 1999).

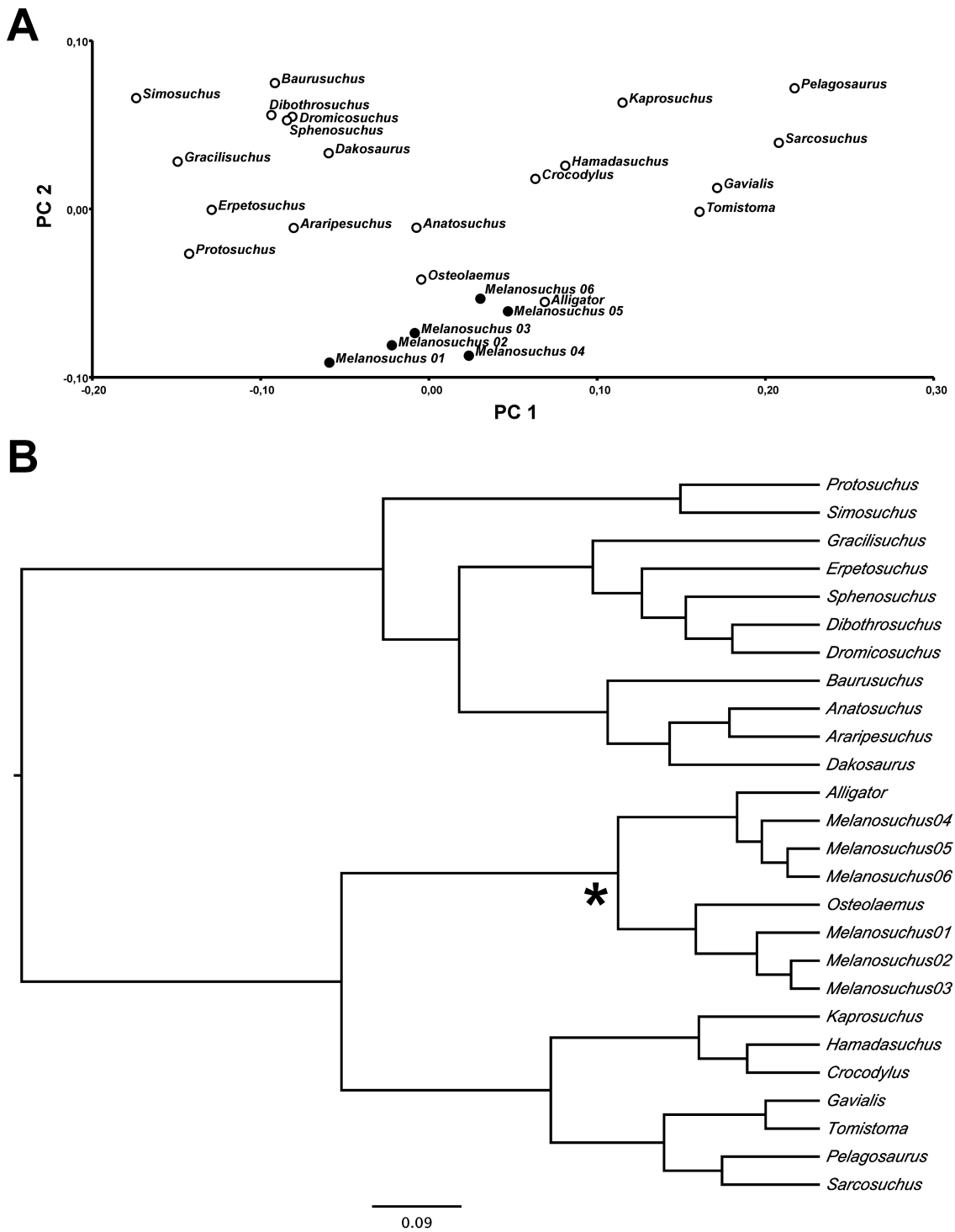


Fig. 1.3. A. Two-dimensional morphospace of the crocodylomorph skull shape based on the first two PC axes. The ontogenetic series of *Melanosuchus* is shown with black dots. **B.** Ward cluster showing the similarity in the skull shape of Crocodylomorpha (including an ontogenetic series of *Melanosuchus*) based on the Procrustes coordinates. The asterisk shows the cluster containing the ontogenetic series of *Melanosuchus*.

Nevertheless, as long no ontogenetic series of the skulls of crocodylian stem-line representatives are described and analysed for ontogenetic shape changes, this hypothesis must be regarded as unverified. Furthermore, some shape changes seen in crocodylomorph evolution, e.g. the flattening of the skull and the loss of the antorbital fenestra, may not be explicable in terms of heterochronic events, but rather as a adaptation for processing agile prey in aquatic habitats (McHenry et al. 2006; Pierce et al. 2008), in which the reduction of the antorbital fenestra was a biomechanical consequence of rostral flattening to minimize stress during biting and lateral motions of the head (Witmer 1997).

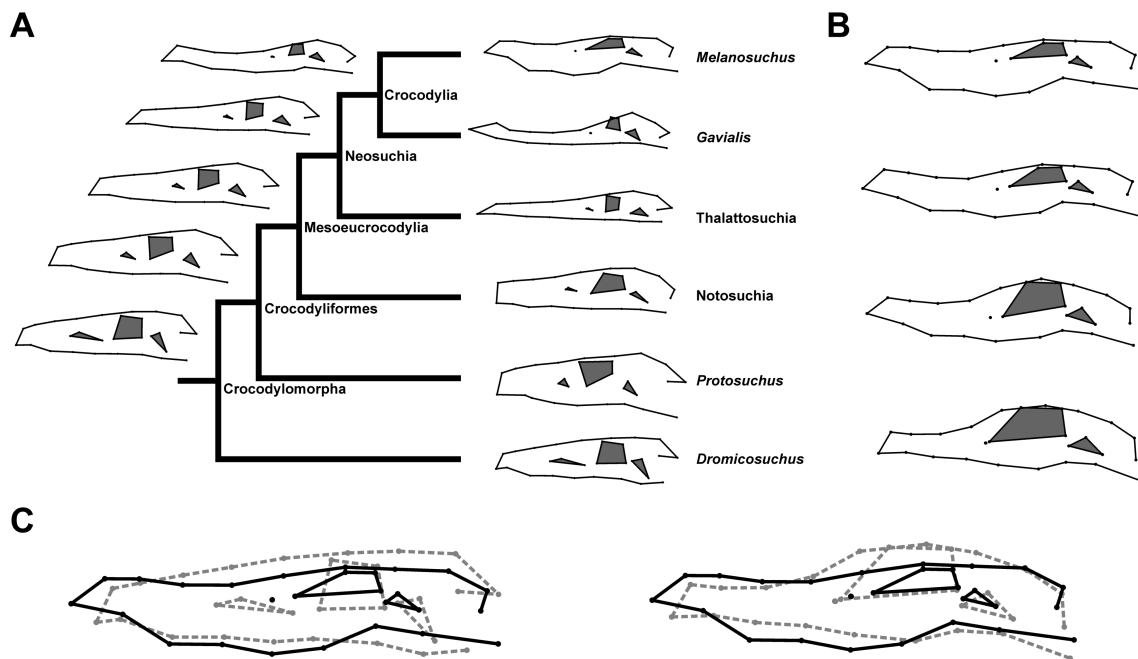


Fig. 1.4. **A.** Optimisation of ancestral skull shapes in Crocodylomorpha using squared-change parsimony reconstruction. **B.** Ontogenetic series of *Melanosuchus*. **C.** Visualization of the shape differences between *Dromicosuchus* (grey dashed lines) and an adult *Melanosuchus* (black solid lines) (left) and a juvenile (grey dashed lines) and an adult *Melanosuchus* (black solid lines) (right).

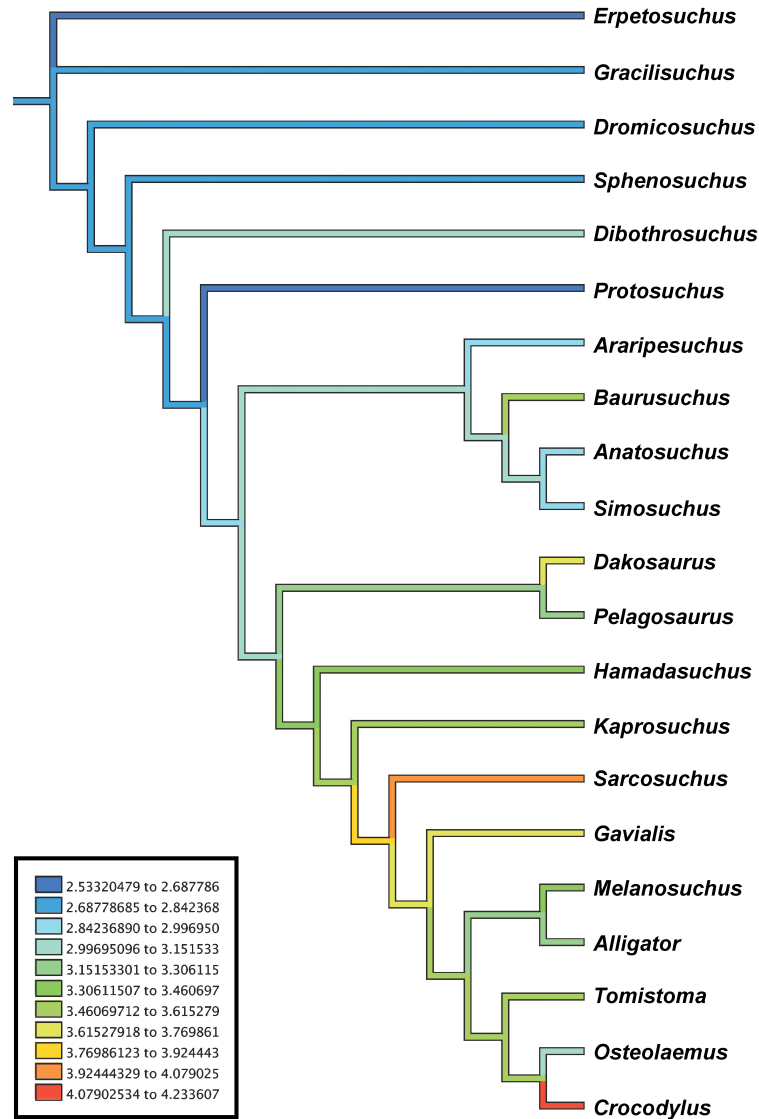


Fig. 1.5. Optimisation of skull size based on centroid sizes (log-transformed) of the Procrustes coordinates (see legend) in Crocodylomorpha using squared-change parsimony reconstruction.

ONTOGENETIC AND HETEROCHRONIC PATTERNS IN SAURISCHIA

Due to a more complete fossil record it is possible to describe and compare ontogenetic trends within saurischian dinosaurs in more detail than for Crocodylomorpha in respect of heterochronic events. Previous studies for example suggested that the rostral shape of derived Sauropoda as well as the skull shape of derived Tyrannosauridae are the result

of peramorphic events (Long & McNamara 1997), whereas the skull shape of birds may have been caused by paedomorphosis (Bhullar et al. 2012). The current study, which is based on a broad-scale sample of both Sauropodomorpha and Theropoda, attempts to detect more examples of heterochronic events within saurischian evolution, especially in more basal members of both saurischian clades. In this context, a comparison of the skull shape of the juvenile megalosaurid *Sciurumimus* (see Chapter 6) with that of basal coelurosaurs such as *Compsognathus* and *Dilong* could be of interest due to similarities such as an elongate skull with a triangular shape and a tapering snout, a large round orbit, a slender jugal or a jaw joint straight below the quadrate head.

For this study, ontogenetic series of basal sauropodomorphs (*Massospondylus*), sauropods (*Diplodocus* and Titanosauridae), basal tetanurans (*Allosaurus* and Megalosauridae), tyrannosaurids (*Tyrannosaurus* and *Tarbosaurus*) and oviraptorids were analysed. Furthermore, the skulls of the juvenile theropods *Juravenator* and *Scipionyx* were included into the dataset. The ontogenetic series for titanosaurids based on the reconstruction of embryonic sauropod skulls found in Patagonia (Chiappe et al. 1998) and the skull of *Antarctosaurus*. The ontogenetic series for megalosaurids is based on the skull of *Sciurumimus* and that of *Dubreuillosaurus*, whereas the ontogenetic series of oviraptorids is based on the skull of *Yulong* and the consensus shape of *Citipati*, *Conchoraptor* and *Nemegtomaia*. A more detailed discussion on taxonomic validity of some ontogenetic series used in the current analysis is given in the supplementary information of Chapter 1. The samples for *Allosaurus*, *Tyrannosaurus*, *Tarbosaurus*, oviraptorids and *Diplodocus* represent rather late ontogenetic series as the juveniles sampled represent late juvenile and subadult individuals. All ontogenetic shape changes presented are shown in Fig. 1.6.

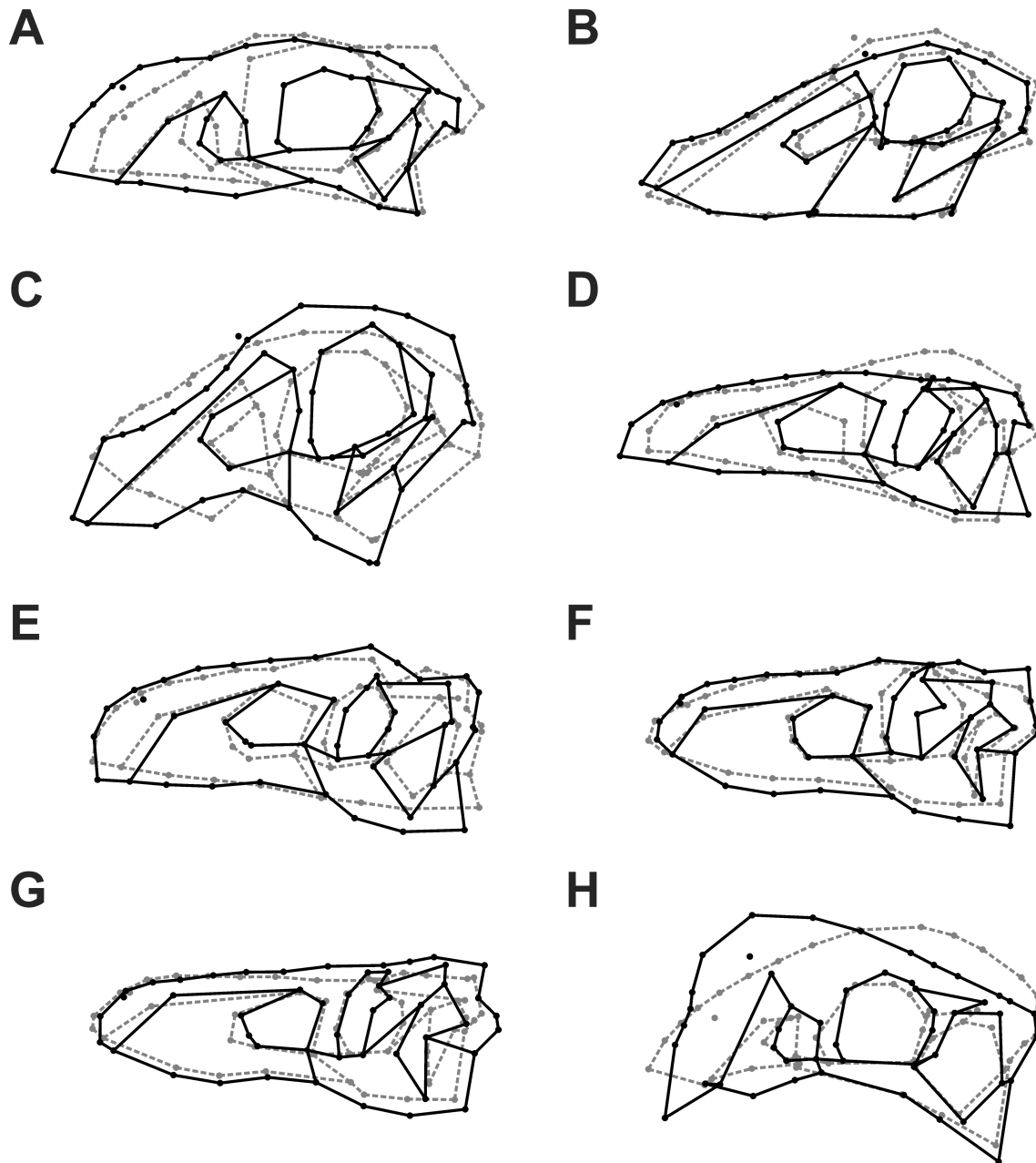


Fig. 1.6. Visualization of ontogenetic shape changes within different saurischian taxa. **A.** The basal sauropodomorph *Massospondylus*. **B.** The sauropod *Diplodocus*. **C.** A hypothetical titanosaurid sauropod. **D.** A hypothetical megalosaurid theropod. **E.** The basal tetanurans theropod *Allosaurus*. **F.** The tyrannosaurid *Tarbosaurus*. **G.** The tyrannosaurid *Tyrannosaurus*. **H.** An hypothetical oviraptorid. Juvenile skull shapes are shown in grey dashed lines and adult skull shapes are shown in black solid lines.

Ontogenetic patterns in Sauropodomorpha

Early juveniles of *Massospondylus* possess a short, tapering snout with a straight ventral margin, an anteroposteriorly compressed antorbital fenestra, an enlarged orbit and relatively deep postorbital region. Similar skulls shapes are also present from juvenile specimens of the basal sauropodomorph *Mussasaurus* (Pol & Powell 2007). During ontogeny the skull of *Massospondylus* become more elongate due to a relative increase of the overall snout length and a decrease of the orbit. The maxilla expands ventrally forming a convex margin. The relative size of antorbital fenestra increased slightly in anteroposterior direction. Furthermore, the depth of the postorbital region decrease relative in size.

The skull of the juvenile *Diplodocus* possesses a short snout with a straight ventral margin, a small antorbital fenestra, a relatively large orbit and a relatively deep orbital and postorbital region. During ontogeny, the snout becomes more elongate due to an anterior expansion of the maxilla. This change goes hand in hand with a bowing of the ventral margin of the anterior part of the maxilla in a dorsal direction. Furthermore, the relative size of the antorbital fenestra increases in an anteroposterior direction, whereas both the relative size of the orbit and the depth of the postrostral region decrease. The skull shape of early juvenile titanosaurids resembles that of a juvenile *Massospondylus* in terms of presence of a short snout with a small antorbital fenestra and a large orbit. In contrast to the *Massospondylus* hatchlings, the ventral margin of the maxilla of early juvenile titanosaurids is inverted Z-shaped. During ontogeny, both the premaxilla and the anterior part of the maxilla expand ventrally, and thereby the ventral margin of the maxilla becomes smoother to form an S-shape. The antorbital fenestra increases in dorsal and posterior directions. The orbit decreases in relative length, but

increases in relative depth. This process goes hand in hand with an increase of the orbital depth. The postorbital region decreases in relative length, but increases in its relative depth due a ventral expansion of the jugal and quadratojugal. Despite the decrease of the postorbital length, the lateral temporal fenestra shows a relative increase in its length.

Ontogenetic patterns in Theropoda

The skull of the juvenile megalosaurid possesses a relatively long snout, a large and rounded antorbital fenestra, and an anteriorly inclined lacrimal. The orbital region is deeper than the rostral and postorbital region. Furthermore, the jaw joint lies ventral to the squamosal body. During ontogeny, the snout becomes more elongated due to increase of the premaxilla length. Furthermore, the snout tip becomes deeper due to a ventral expansion of the premaxilla and the anterior part of the maxilla. The antorbital fenestra increases in dorsal and posterior direction and the lacrimal becomes more vertically orientated. This process goes hand in hand with a relative decrease of the orbital length leading to an oval orbital shape. In the adult specimen the orbital depth is as deep as the depth of the snout and the postorbital. The postorbital region increases in its relative length, which occurs in concert with an increase of the depth of the lateral temporal fenestra and a shift of the jaw joint posterior to the squamosal body.

The skull of a juvenile *Allosaurus* resembles that of a juvenile megalosaurid possessing an elongated snout and a rounded orbit. In contrast to the megalosaurid juvenile, the snout is relatively deeper and the lacrimal is already vertically orientated. This difference could be the result of the later ontogenetic stage of the juvenile specimen sampled for *Allosaurus*. The discovery of a single maxilla identified as that of

an allosauroid hatchling indicates that the snout of early juveniles was probably rather short (Rauhut & Fechner 2005). During ontogeny, the snout of *Allosaurus* becomes deeper due to a ventral expansion of the premaxilla and the anterior part of the maxilla. The antorbital fenestra decreases in its relative depth due to a dorsal expansion of the jugal process of the maxilla, but becomes relatively longer. The lacrimal develops a dorsal horn. The orbit decreases in its relative length and becomes oval in shape. The postorbital becomes more massive. Finally, the orbital and postorbital regions become deeper due a ventral expansion of the jugal (leading to an increase of the contribution of the jugal to the suborbital region) and the quadratojugal shifting the jaw joint in a ventral direction.

Juvenile tyrannosaurids resemble juvenile allosaurids by possessing a long snout and a rounded orbit. However, during ontogeny the snout becomes deeper due to ventral expansion of the maxilla. The antorbital fenestra decreases only slightly in size. As in *Allosaurus* and megalosaurids the orbit becomes oval in shape due to a relative decrease of the orbital length. In contrast to basal tetanurans, the postrostral region expands in both dorsal (parietal and squamosal) and ventral (jugal and quadratojugal) direction. As in *Allosaurus* the ventral expansion of the jugal and quadratojugal leads to a relative increase of the suborbital depth and a ventral shift of the jaw joint. Furthermore, the postorbital region increases in its relative length. This process goes hand in hand with an increase of the anterior-posterior dimension of the postorbital and the postorbital process of the jugal as well as the squamosal process of the quadratojugal. The latter also leads to a shift of the jaw joint in posterior direction.

The juvenile skull of oviraptorids possesses a relatively short, tapering snout with a prominent premaxilla, but very short maxilla, a small antorbital fenestra, an enlarged rounded orbit, an enlarged lateral temporal fenestra as well as a relatively deep orbital region. During ontogeny the depth of the snout increases due to a dorsal expansion of the premaxilla, with the nasal and the nasal process of the maxilla forming a rostral crest. The antorbital fenestra increases slightly in relative size, which goes hand in hand with a slight decrease of the relative orbit size. Both the orbital and postorbital region decrease in their relative depth.

Comparison of ontogenetic patterns in Saurischia

Based on this comparison one can conclude that early juvenile saurischian dinosaurs tend to have short, tapering snouts with a small antorbital fenestra, enlarged round orbits and a deep orbital and postorbital region relative to the snout depth (which is related to a relative large braincase in early juveniles, see Emerson & Bramble 1993) and a jaw joint anterior to the posterior end of the squamosal. Similar skull shapes can be found in early juveniles of basal sauropodomorphs (e.g. Pol & Powell 2007, Reisz et al. 2010), several theropods including basal birds (e.g. Sanz et al. 1997; Zhou & Zhang 2004; Rauhut & Fechner 2005; Chiappe et al. 2007; Bever & Norell 2009; Kundrát et al. 2008; Dal Sasso & Maganuco 2011), basal ornithischians (e.g. Butler et al. 2008), ornithomimids (e.g. Carpenter 1994; Evans 2010; Hübner & Rauhut 2010) and marginocephalians (e.g. Maryańska & Osmólska 1975; Coombs 1982; Goodwin et al. 2006), but also in recent alligatorids (e.g. Piña et al. 2007; see Chapter 3). Thus, one can conclude that this skull shape pattern is plesiomorphic for dinosaurs (Varricchio 1997), for archosaurs, and even for tetrapod hatchlings in general (Emerson & Bramble 1993). The skull of the *Massospondylus* hatchlings shows the greatest similarity with the skulls

of the juvenile theropods *Scipionyx* (which is currently described as a juvenile compsognathid; see Dal Sasso & Maganuco 2011) and *Yulong*, and less similarity with the titanosaurid hatchling (Fig. 1.7A-C, Table 1.1).

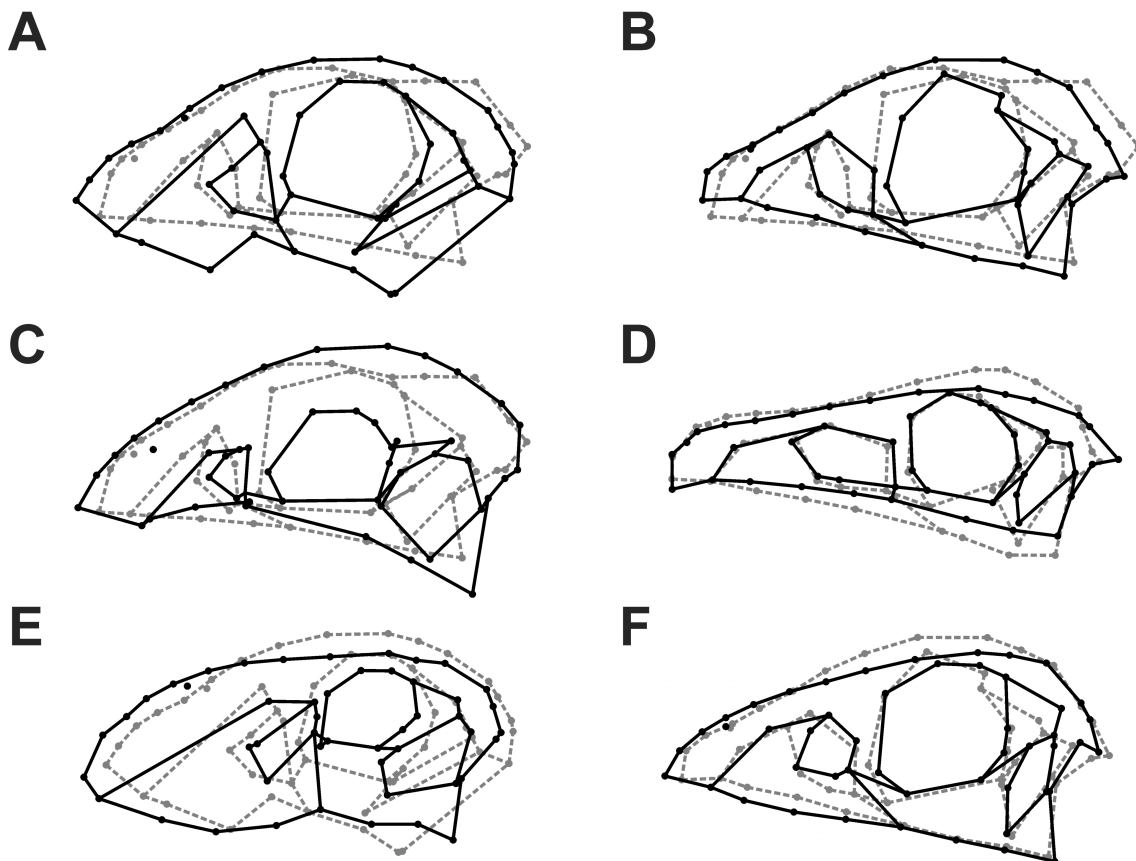


Fig. 1.7. Visualization of shape differences between different juvenile taxa and some juvenile and adult taxa. **A.** Hatchling of the basal sauropodomorph *Massospondylus* (grey dashed line) and a hatchling of a titanosaurid (black solid line). **B.** Hatchling of *Massospondylus* (grey dashed line) and a hatchling of the theropod *Scipionyx* (black solid line). **C.** Hatchling of *Massospondylus* (grey dashed line) and the juvenile oviraptorids *Yulong* (black solid line). **D.** Juvenile of the megalosaurid theropod *Sciurumimus* (grey dashed line) and the juvenile theropod *Juravenator* (black solid line). **E.** Hatchling of a titanosaurid (grey dashed line) and the juvenile theropod *Juravenator* (black solid line). **F.** Hatchling of the theropod *Scipionyx* (grey dashed line) and the skull of the adult theropod *Daemonosaurus* (black solid line).

Table 1.1. Euclidean distances between different juvenile taxa (grey fields), different adult taxa (white fields) and between juvenile and adult individuals of the same taxa (bold) based on the Procrustes coordinates.

	<i>Massospondylus</i>	<i>Diplodocus</i>	Titanosauridae	<i>Allosaurus</i>	Megalosauridae	<i>Tyrannosaurus</i>	<i>Tarbosaurus</i>	Oviraptoridae	<i>Juravenator</i>	<i>Scipionyx</i>
<i>Massospondylus</i>	0.188	0.405	0.245	0.254	0.226	0.323	0.260	0.183	0.237	0.131
<i>Diplodocus</i>	0.404	0.119	0.298	0.430	0.438	0.478	0.441	0.402	0.471	0.416
Titanosauridae	0.389	0.256	0.293	0.295	0.271	0.346	0.302	0.245	0.312	0.242
<i>Allosaurus</i>	0.164	0.407	0.393	0.113	0.131	0.148	0.120	0.248	0.147	0.208
Megalosauridae	0.195	0.450	0.459	0.130	0.168	0.168	0.116	0.242	0.121	0.149
<i>Tyrannosaurus</i>	0.194	0.433	0.439	0.150	0.127	0.140	0.113	0.326	0.171	0.267
<i>Tarbosaurus</i>	0.175	0.450	0.442	0.144	0.137	0.078	0.106	0.283	0.134	0.194
Oviraptoridae	0.243	0.428	0.393	0.283	0.342	0.320	0.319	0.215	0.253	0.192
<i>Juravenator</i>	-	-	-	-	-	-	-	-	-	0.186

Long-snouted crocodylians (e.g. *Gavialis*, *Tomistoma*) are an exception to the pattern mentioned above, as the hatchlings already possess a relatively long snout (see Piras et al. 2010). Relatively long snouts are also present in the *Sciurumimus* and *Juravenator* (see Fig. 1.7D). Thus, like these crocodylian species, both juvenile theropods could represent exceptions to the general morphology described above. On the other hand, as the known specimens of both taxa are early juveniles but not true hatchlings, it is possible that the relatively elongated snout results from a strong positive allometric growth of the facial region in early ontogeny. A similar pattern can be observed in the skull ontogeny of *Melanosuchus*, which shows a strong allometric shift in early ontogeny followed by moderate shape changes after reaching sexual maturity (Fig. 1.8). This interpretation is further supported by the discovery of a maxilla of an allosauroid hatchling mentioned above, indicating that hatchlings of basal tetanurans

probably possess short snouts (Rauhut & Fechner 2005).

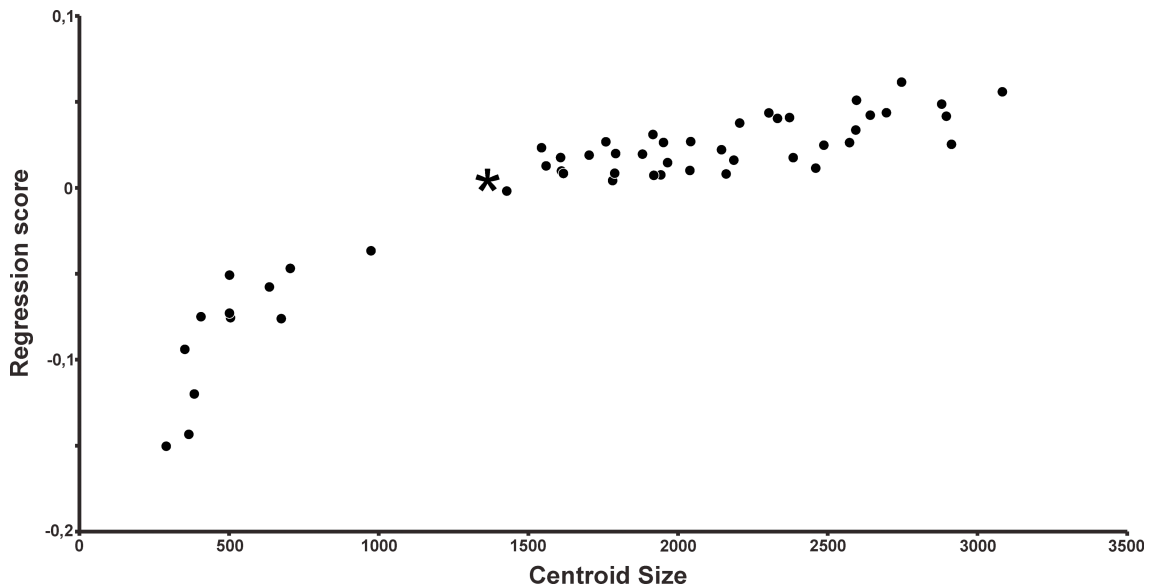


Fig. 1.8. Ontogenetic shape changes in the cranium of *Melanosuchus* in relationship to the centroid size.

In early ontogeny skull shape shows strong allometric shape changes until onset of sexual maturity (asterisk).

A common pattern of ontogenetic change within saurischians is the elongation of the snout, the increase of the relative size of the antorbital fenestra and the decrease of the relative orbit size. These patterns (apart the changes in the antorbital region) are also common in crocodylians (see Chapter 3) and tetrapods in general (Emerson & Bramble 1993). Elongation of the snout and increase of antorbital fenestra are not observed within Tyrannosauridae, but this probably results from the fact that the juveniles sampled represent subadults and not hatchlings or early juveniles. As hypothesized for *Sciurumimus* and *Juravenator* (see above) it could be possible that the elongation of the snout occurs in relatively early ontogeny.

Although sharing these common patterns, the skulls of saurischian dinosaurs develop along three main ontogenetic trajectories. The cranial shape changes observed in *Tyrannosaurus* and oviraptorids are primarily captured by the first principal component ($\approx 42\%$ of total variation), which describes the relative depth of the snout (mainly influenced by the relative depth of the maxilla) and the postrostral region (mainly influenced by the relative depth of the orbit, jugal and quadratojugal). Changes observed in *Massospondylus*, *Diplodocus* and megalosaurids are primarily captured by the second principal component ($\approx 15\%$ of total variation), which describes the relative length of the snout, the antorbital fenestra and the orbit; thus, the ontogenetic changes seen in these taxa follows the common pattern for Saurischia described above. The skulls of the titanosaurid and *Allosaurus* change along both first and second axes equally (Fig. 1.9A, Table 1.2). The most pronounced ontogenetic shape changes in relation to centroid size can be seen in *Diplodocus*, megalosaurids and *Massospondylus*, whereas changes to the skull shape of *Tyrannosaurus* are only minor during ontogeny (Fig. 1.9B, Table 1.2). However, as stated above, the latter result is probably due to the late ontogenetic stage of the juvenile *Tyrannosaurus* used.

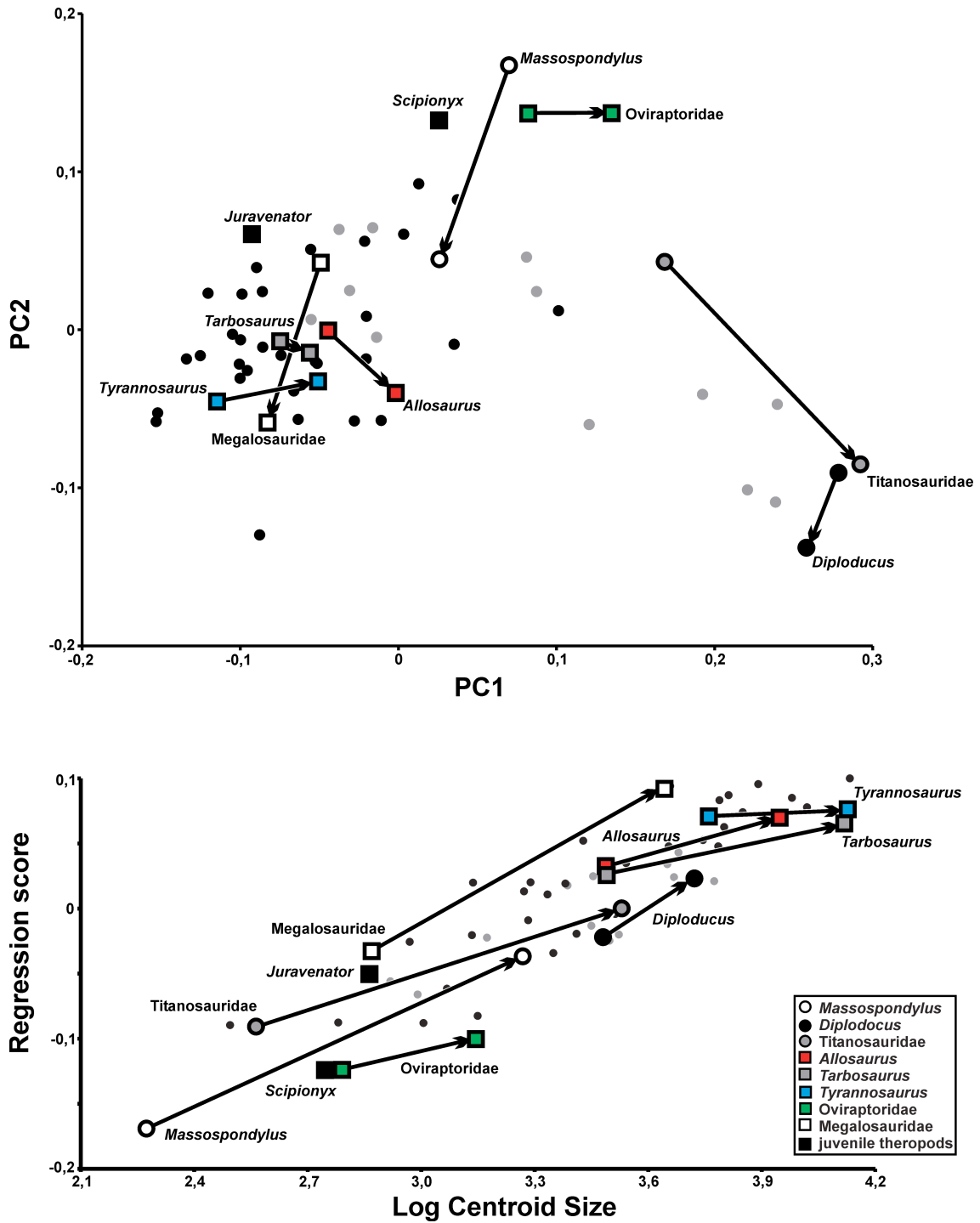


Fig. 1.9. A. Two-dimensional morphospace of saurischian dinosaurs based on the first two PC axes showing the ontogenetic trajectories of different saurischian taxa. B. Ontogenetic shape changes in different saurischian taxa in relationship to the centroid size (log-transformed). In both plots theropod taxa are shown as small black dots and sauropodomorph taxa as small grey dots.

Table 1.2. Angles of ontogenetic trajectories in saurischian taxa in relationship to centroid size (logCS) (bold) and different ontogenetic trajectories based on the first two axes of the Principal Component Analysis.

	Log CS	<i>Allosaurus</i>	Megalosauridae	<i>Tarbosaurus</i>	<i>Tyrannosaurus</i>	Oviraptoridae	<i>Massospondylus</i>	<i>Diplodocus</i>	Titanosauridae
<i>Allosaurus</i>	4.70	-	65.56	21.73	54.08	42.83	66.78	70.29	3.11
Megalosauridae	9.15		-	87.29	119.64	108.39	1.22	4.73	62.46
<i>Tarbosaurus</i>	3.57			-	32.36	21.10	91.50	92.01	24.83
<i>Tyrannosaurus</i>	0.96				-	11.26	120.86	124.37	57.19
Oviraptoridae	4.25					-	109.60	113.11	45.93
<i>Massospondylus</i>	7.59						-	3.51	63.67
<i>Diplodocus</i>	10.72							-	67.18
Titanosauridae	5.38								-

Heterochronic patterns in Saurischia

Based on the results of the cluster analyses (Fig. 1.10), the skull shape of the titanosaurid hatchling shows the greatest similarity with that of an adult *Shunosaurus* (see Fig. 1.7E), which is greater than between the *Massospondylus* hatchling and *Shunosaurus* and between an adult Titanosaurid and *Shunosaurus* (Table 1.3). As titanosaurids probably represent descendants of a *Shunosaurus*-like form, this find could be evidence for a peramorphic trend within sauropod evolution (the evolution of a more “developed” taxon compared to the ancestor), i.e. the skull shape of more derived sauropods hatchlings resembles that of basal adult sauropods, but due to ontogenetic changes (see above) adult skulls of derived sauropods appear more derived than those of basal ones. Peramorphosis of the skull was previously hypothesized by Long & McNamara (1997), as the skulls of sauropodomorphs show an evolutionary trend

towards development of a deeper maxilla, a dorsally shifted naris and expansion of the lateral temporal fenestra in a ventral direction. Due to these changes the skulls of sauropodomorphs become relatively deeper during their evolution, the antorbital fenestra becomes relatively shorter but deeper, and the relative size of the orbit and lateral temporal fenestra increases (Fig. 1.11). Furthermore, in the clade Macronaria the relative size of the external naris increases (Wilson & Sereno 1998). Interestingly, sauropodomorphs show a peramorphic trend in their overall body size (Sander et al. 2004, 2011; Rauhut et al. 2011), which is primarily caused by acceleration of growth (i.e. increase of the growth rate) during their evolution (Sander et al. 2004). Both trends are probably linked to an increasing specialization from an omnivorous towards a herbivorous diet (Rauhut et al. 2011), in which changes in the rostral shape of the skull are most likely adaptations for plant cropping and bulk feeding behavior, whereas the relative enlargement of the skull fenestrae may be correlated to a reduction of bite forces (Rauhut et al. 2011).

Based on Procrustes distances, the skull shape of the short-snouted *Daemonosaurus* and *Limusaurus* most resembles that of the early juvenile theropod *Scipionyx* and the hatchling of *Massospondylus* (Fig. 1.7F, Table 1.3). The similarity of the skull shape of *Daemonosaurus* and *Limusaurus* with that of basal saurischian hatchlings could provide evidence for a paedomorphic event (i.e. the development of a juvenile morphology in an adult taxon compared to an ancestor) in the stem-line of these short-snouted taxa. This is further supported by the fact that the hypothetical ancestors of Theropoda, Neotheropoda and Averostra possess rather long snouts with a relatively large antorbital fenestra in comparison to *Daemonosaurus* and *Limusaurus* (Fig 1.12). Other ceratosaurs like *Ceratops*, *Genyodectes*, and Abelisauridae also

possess relatively short snouts, but in contrast with *Limusaurus*, the overall shape of the skulls is deep with a massive maxilla and jugal, whereas the orbit is oval in shape (e.g. Bonaparte et al. 1990; Rauhut 2004; Sampson & Witmer 2007). Thus, pedomorphic skulls are not typical for ceratosaurs, but were probably also present in short-snouted noosaurids such as *Masiakasaurus* (Carrano et al. 2011).

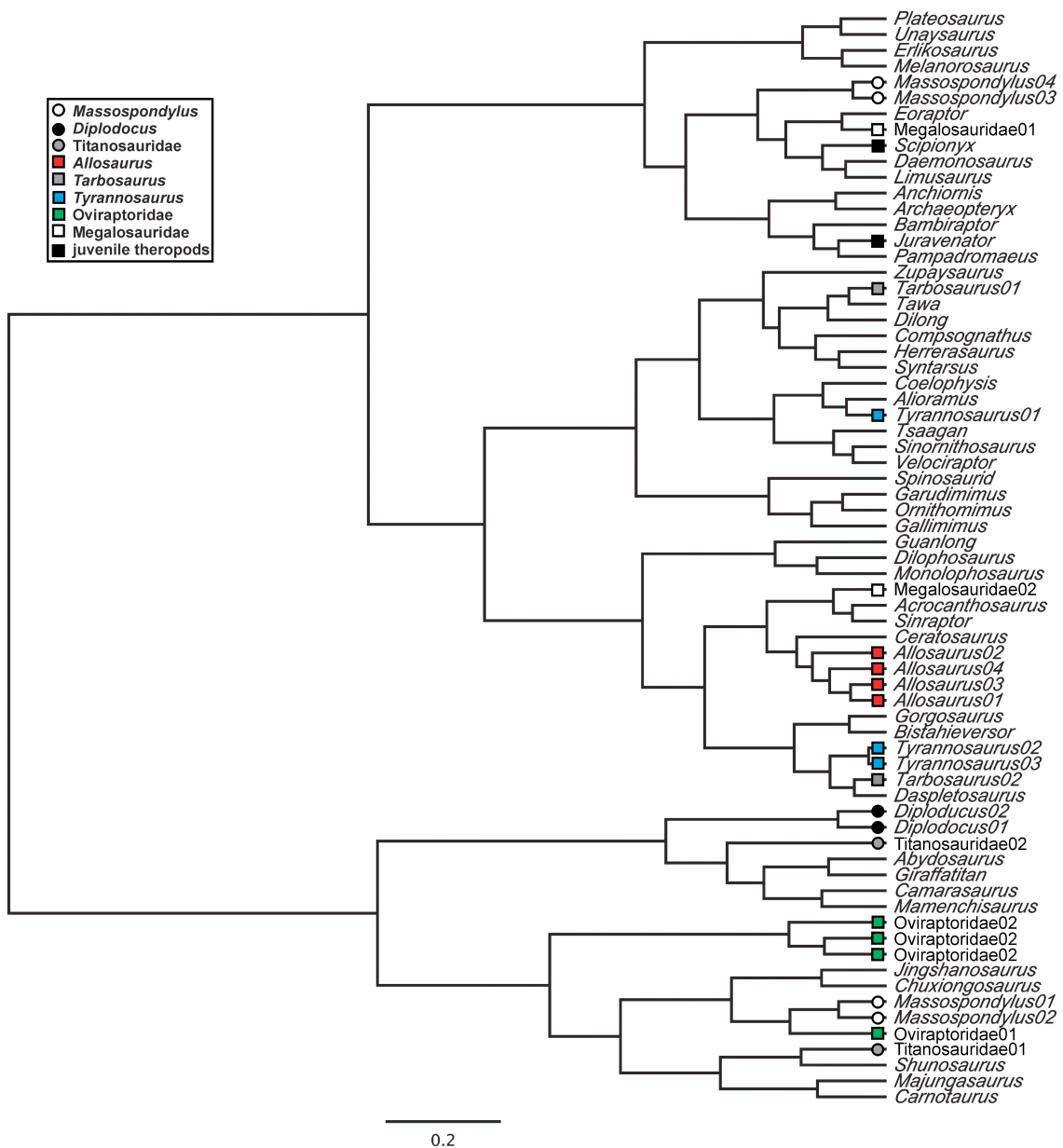


Fig. 1.10. Ward cluster showing the similarity in the skull shape of Saurischia (including juvenile and adult specimens) based on the Procrustes coordinates.

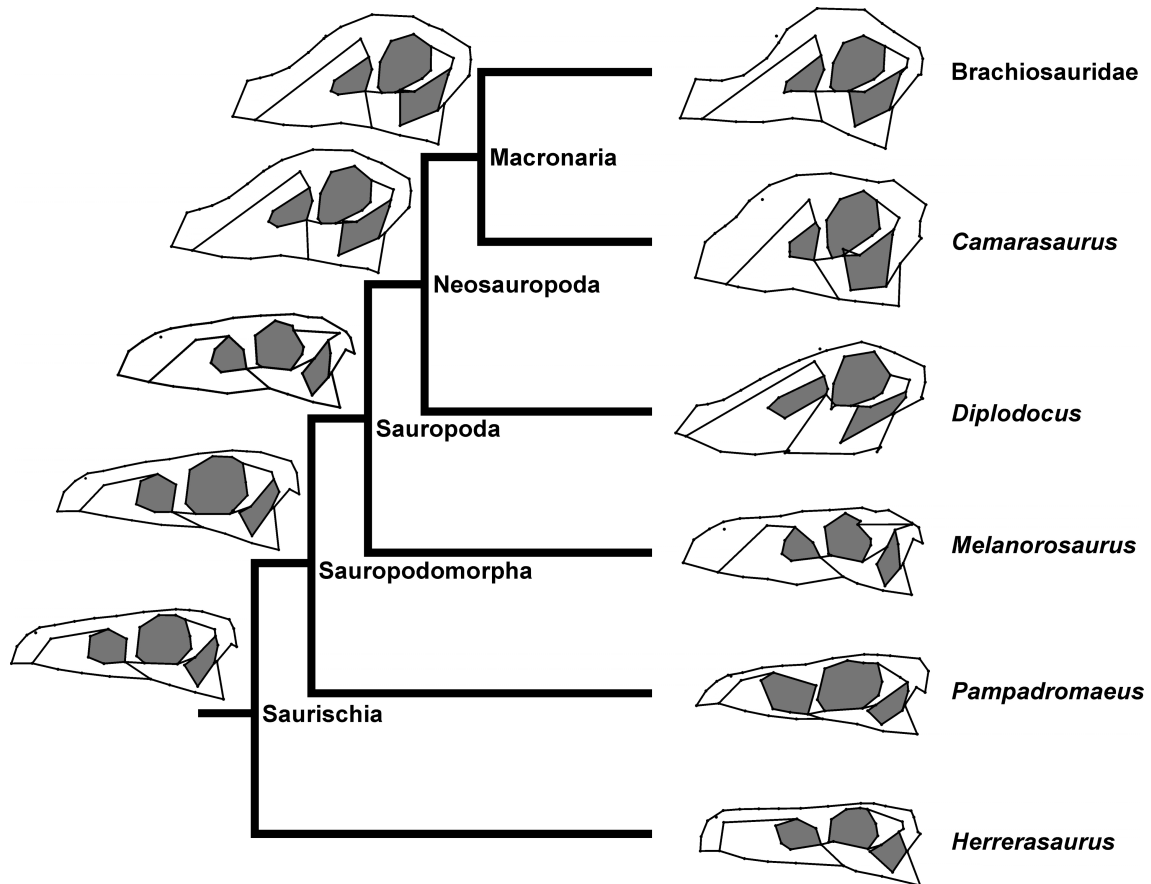


Fig. 1.11. Optimisation of ancestral skull shapes in Sauropodomorpha using squared-change parsimony reconstruction.

In contrast, the skull shapes of *Juravenator*, the juvenile megalosaurid *Sciurumimus*, and juvenile *Tarbosaurus* resemble those of adult basal Saurischia (i.e. *Eoraptor*, *Pampadromaeus* and *Tawa*) (Fig. 1.13A, B, C. Table 1.3). These similarities could provide evidence for a peramorphic trend in the stem-line of Coelurosauria, which is further supported by the evolutionary trend computed with help of skull shape mapping. Comparing the skull shape of the hypothetical ancestor of Theropoda with that of Tetanurae and Orionides (see Carrano et al. 2012), the snout becomes relatively longer but also deeper, the antorbital fenestra increases in relative length, and the orbit decreases in anteroposterior length during evolution becoming more oval in shape (Fig

1.12, 1.13E). As mentioned above, these evolutionary shape changes resemble the common ontogenetic trend described for saurischian dinosaurs. As in sauropodomorphs, this peramorphic trend in skull shape goes hand in hand with an increase in body size in basal theropods (Irmis 2011).

Table 1.3. Euclidean distances between taxa represented as ontogenetic series (including *Juravenator* and *Scipionyx*) and other selected saurischian taxa (adult) based on the Procrustes coordinates.

Taxa I	Taxa II	Euclidean distance (juvenile)	Euclidean distance (adult)
<i>Massospondylus</i>	<i>Shunosaurus</i>	0.279	0.188
	<i>Daemonosaurus</i>	0.144	0.120
	<i>Limusaurus</i>	0.166	0.130
Titanosauridae	<i>Shunosaurus</i>	0.209	0.306
Megalosauridae	<i>Eoraptor</i>	0.109	0.185
	<i>Compsognathus</i>	0.113	0.171
	<i>Dilong</i>	0.137	0.142
<i>Tyrannosaurus</i>	<i>Alioramus</i>	0.098	0.164
	<i>Dilong</i>	0.131	0.169
<i>Tarbosaurus</i>	<i>Tawa</i>	0.092	0.144
	<i>Alioramus</i>	0.131	0.164
	<i>Dilong</i>	0.102	0.164
<i>Juravenator</i>	<i>Pampadromaeus</i>	0.118	-
	<i>Eoraptor</i>	0.143	-
	<i>Compsognathus</i>	0.120	-
	<i>Dilong</i>	0.116	-
<i>Scipionyx</i>	<i>Daemonosaurus</i>	0.110	-
	<i>Limusaurus</i>	0.121	-
	<i>Compsognathus</i>	0.189	-
	<i>Dilong</i>	0.224	-

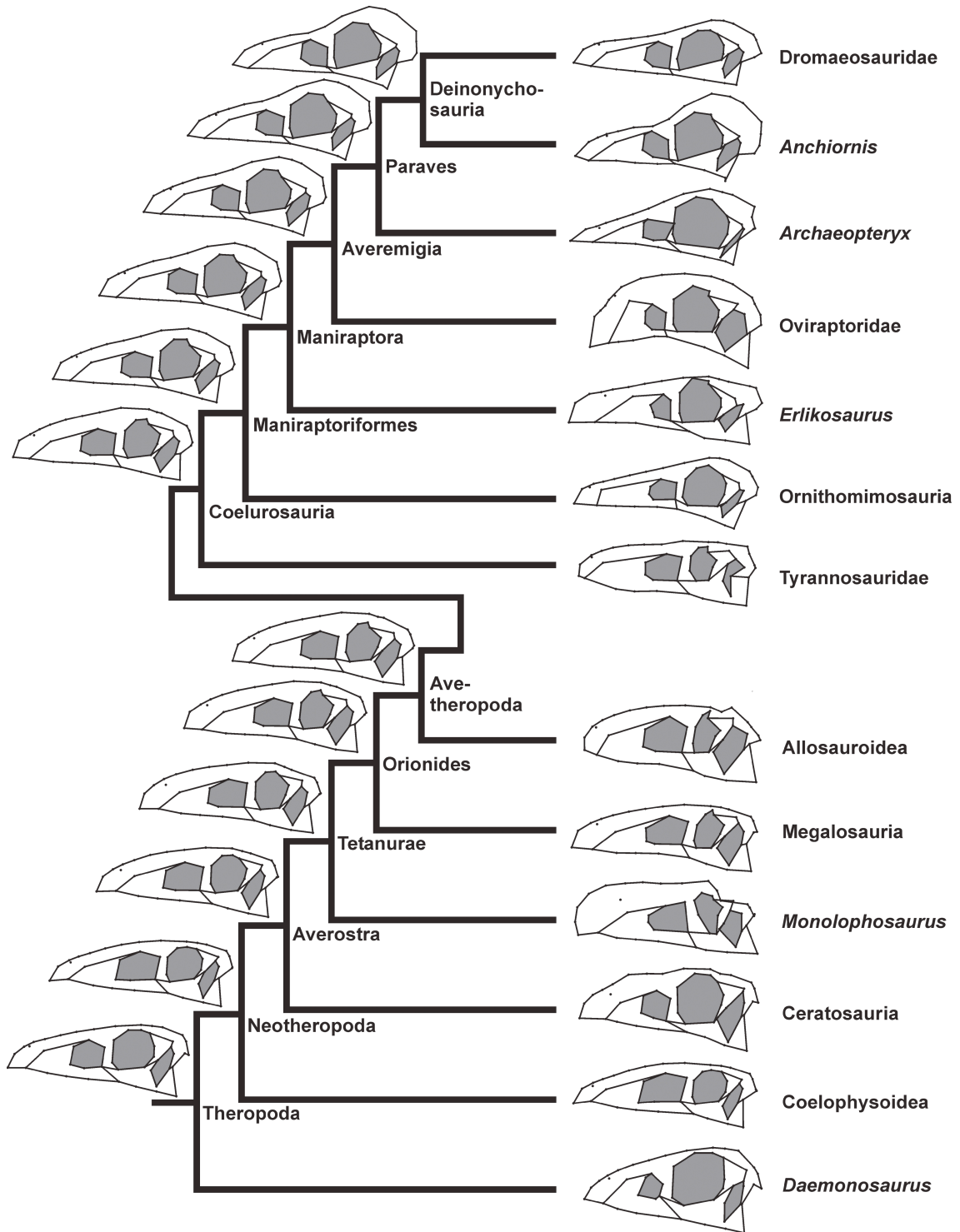


Fig. 1.12. Optimisation of ancestral skull shapes in Theropoda using squared-change parsimony reconstruction.

As hypothesized above, the skull shape of the juvenile megalosaurid *Sciurumimus* shows similarity with that of basal coelurosaurs such as *Compsognathus* or *Dilong* (Fig. 1.13.E, Table 1.3). This result may reflect an opposing trend (i.e. paedomorphosis) in the skull evolution of Orionides leading to Coelurosauria and Maniraptora, meaning that basal small-bodied coelurosaurs such as compsognathids and basal tyrannosaurids represent cute, adult versions of juvenile tetanurans. Shape changes related to this paedomorphic trend include a relative shortening and tapering of the snout, which goes hand in hand with a decrease of the snout depth and a shortening of the antorbital fenestra, and a relative increase of the orbit size (Fig. 1.12, 1.13F). Such an event is further supported by the dental morphology of *Sciurumimus*, which differs significantly from those of subadult and adult basal tetanurans, instead resembling that of compsognathids (e.g. Currie & Chen 2001) and dromaeosaurids (e.g. Xu & Wu 2001). This similarity in dental morphology may reflect convergence resulting from similar prey preferences in juvenile tetanurans and small-bodied coelurosaurs (see Chapter 6). Unfortunately, bone histological data are rather rare for basal theropod groups, meaning that the physiological underpinnings of skull and body size evolution are not well understood to date.

Within basal coelurosaurs the skull shape of the juvenile *Tyrannosaurus* resembles that of the medium-sized, long-snouted tyrannosaurid *Alioramus*. This is further supported by the close similarity of juvenile tyrannosaurids with the basal tyrannosauroid *Dilong* in terms of Procrustes distance (Table 1.3). These relationships may reflect a peramorphic trend within Tyrannosauroidea, as already hypothesized by Long & McNamara (1997). Bone histological data reveal that, as in sauropodomorphs, this peramorphic trends may be correlated with an increase of body size caused by an

acceleration of growth (Erickson et al. 2004a).

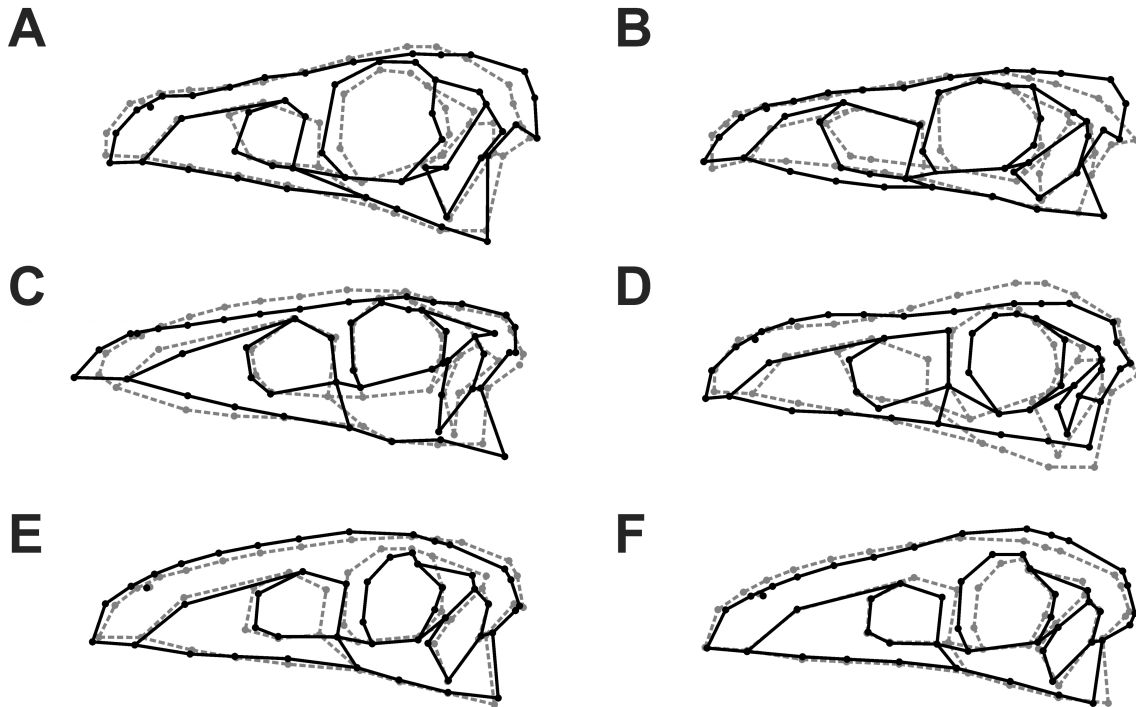


Fig. 1.13. A-C. Visualization of shape differences between different juvenile theropod taxa and basal Saurischia. **A.** The juvenile megalosaurid theropod *Sciurumimus* (grey dashed line) and *Eoraptor* (black solid line). **B.** The juvenile theropod *Juravenator* (grey dashed line) and *Pampadromaeus* (black solid line). **C.** The juvenile *Tarbosaurus* (grey dashed line) and *Tawa* (black solid line). **D.** Visualization of the shape difference between *Sciurumimus* (grey dashed line) and the basal tyrannosauroid *Dilong*. **E.** Evolutionary shape changes from the hypothetical ancestor of Theropoda (grey dashed lines) to that of Orionides (black solid lines). **F.** Evolutionary shape changes from the hypothetical ancestor of Orionides (grey dashed lines) to that of Maniraptoriformes (black solid lines).

Within Maniraptora, Bhullar et al. (2012) found evidence for a pedomorphic event on the stem-line of Avialae. The hypothetical ancestors of Dromaeosauridae, Troodontidae and Avialae possess skulls with short, tapering snouts and relatively enlarged orbital and postorbital regions, which is characteristic for juvenile archosaurs

(see above). This paedomorphic event is correlated with a decrease of body size within Maniraptora (Turner et al. 2007; Benson et al. 2012). Furthermore, Bhullar et al. (2012) hypothesized that the more theropod-typical skull shape seen in derived Dromaeosauridae and Troodontidae results from two separate peramorphic events happening within these groups leading to convergent elongation of the snout. This result is supported by the skull shape mapping of the current analyses (Fig. 1.12). As in sauropodomorphs and basal theropods, the peramorphic events in Dromaeosauridae and Troodontidae go hand in hand with a convergent body size increase within both groups (Turner et al. 2007). Additional to the described heterochronic events within Maniraptora, the skull shape mapping shows that the skulls of derived oviraptorids are also the results of a peramorphic event, which is expressed by a dorsal expansion of the premaxilla and a relative increase in size of the lateral temporal fenestra. However, the skulls of basal Oviraptorosauria such as *Caudipteryx* and *Similicaudipteryx* possess a more triangular skull shape with a short tapering snout (Zhou et al. 2000; Xu et al. 2010) resembling the skull shape of the juvenile oviraptorid *Yulong* (Lü et al. in press) and basal Paraves (Wellnhofer 2008; Zhang et al. 2008; Hu et al. 2009; Bhullar et al. 2012; Godefroit et al. 2013, in press). This indicates that the peramorphic deepening of the snout may not be plesiomorphic for Oviraptorosauria, but occurred within the stem-line of Oviraptoridae. All heterochronic events found within Saurischia are summarized in Fig. 1.14.

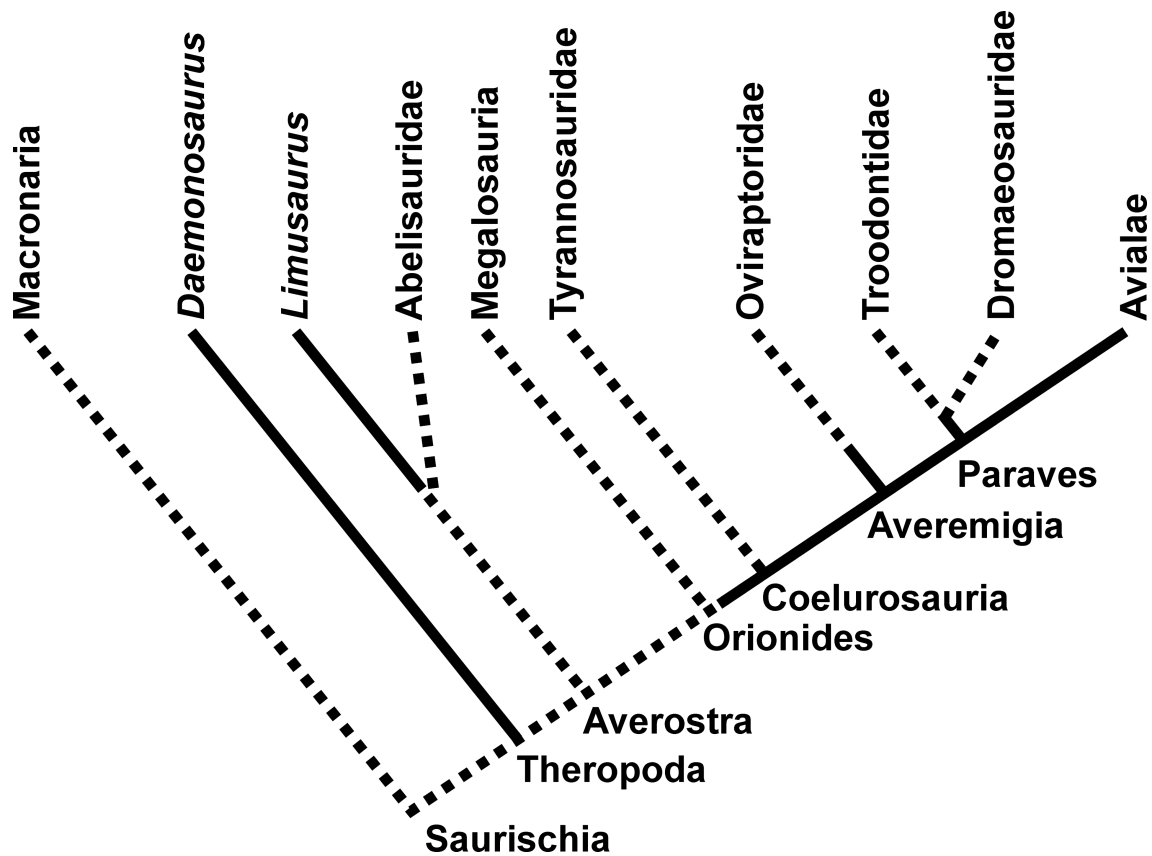


Fig. 1.14. Summary of possible heterochronic events found within Saurischia. Peramorphic events are shown in dashed lines and pedomorphic events in solid lines.

CONCLUSION

As presented for Pterosauria, Theropoda, and partially for sauropodomorphs and crocodylomorphs, skull shapes of archosaurs are extremely diverse. Skull shape is correlated with phylogeny, but also with function and dietary preferences. This diversity is also expressed in terms of ontogenetic patterns, which were investigated in more detail in the current chapter. Excepting some similar trends affecting snout shape and orbit size, skull shape change during ontogeny is not uniform within Archosauria, and the large differences in ontogenetic trajectories may underpin the huge diversity found in archosaur cranial morphology. A detailed comparison of ontogenetic and

evolutionary skulls shape changes in Crocodylomorpha and Saurischia reveal that archosaur skull evolution is strongly affected by heterochronic events. Evidence for peramorphosis was found in the stem-line of Crocodylomorpha, within Sauropodomorpha, basal theropods, Tyrannosauroida as well as within Dromaeosauridae, Troodontidae and within the stem-line of Oviraptoridae. In contrast, paedomorphic events may have occurred in the crocodylian *Osteolaemus*, in the basal theropods *Daemonosaurus* and *Limusaurus* as well as in basal Coelurosaurs including basal Maniraptora and Avialae. These heterochronic events appear to be correlated with body size evolution, but this must be tested in more detail in future analyses. Due to the close correlation between ontogeny and dietary preferences, heterochronic events often go hand in hand with evolutionary changes in diet and feeding behaviour, as exemplarily documented in the juvenile megalosaurid *Sciurumimus*. Thus, juveniles of basal tetanurans are of special interest to understand the evolution but also the ecology of basal coelurosaurs.

CHAPTER 2

The good, the bad, and the ugly: the influence of skull reconstructions and intraspecific variability in studies of cranial morphometrics in theropods and basal saurischians

Keywords:

Theropoda; Saurischia; morphospace; intraspecific variation; geometric morphometrics; skull reconstructions

The chapter was accepted as:

Foth C^{1,2} & Rauhut OWM^{1,2,3}. In press. The good, the bad, and the ugly: the influence of skull reconstructions and intraspecific variability in studies of cranial morphometrics in theropods and basal saurischians. *PloS ONE*.

¹*Bayerische Staatssammlung für Paläontologie und Geologie, Richard-Wagner-Str. 10, D-80333 München, Germany,*

²*Department of Earth and Environmental Sciences, Ludwig-Maximilians-University, Richard-Wagner-Str. 10, D-80333 München, Germany,*

³*GeoBioCenter, Ludwig-Maximilians-University; Richard-Wagner-Str. 10, D-80333 München, Germany*

Received 22 February 2013; revised 28 June 2013; accepted 09 July 2013

Author contribution:

Research design: **Christian Foth**, Oliver Rauhut

Data collection: **Christian Foth**

Data analyses: **Christian Foth**

Preparation of figures and tables: **Christian Foth**

Wrote paper: **Christian Foth**, Oliver Rauhut

***All figures of Chapter 2 are modified after Foth & Rauhut (in press)**

The good, the bad, and the ugly: the influence of skull reconstructions and intraspecific variability in studies of cranial morphometrics in theropods and basal saurischians

Christian Foth & Oliver W. M. Rauhut

ABSTRACT

Several studies investigating macroevolutionary skull shape variation in fossil reptiles were published recently, often using skull reconstructions taken from the scientific literature. However, this approach could be potentially problematic, because skull reconstructions might differ notably due to incompleteness and/or deformation of the material. Furthermore, the influence of intraspecific variation has usually not been explored in these studies. Both points could influence the results of morphometric analyses by affecting the relative position of species to each other within the morphospace. The aim of the current study is to investigate the variation in morphometric data between skull reconstructions based on the same specimen, and to compare the results to shape variation occurring in skull reconstructions based on different specimens of the same species (intraspecific variation) and skulls of closely related species (intraspecific variation). Based on the current results, shape variation of different skull reconstructions based on the same specimen seems to have generally little influence on the results of a geometric morphometric analysis, although it cannot be excluded that some erroneous reconstructions of poorly preserved specimens might cause problems occasionally. In contrast, for different specimens of the same species the variation is generally higher than between different reconstructions based on the same specimen. For closely related species, at least with similar ecological preferences

in respect to the dietary spectrum, the degree of interspecific variation can overlap with that of intraspecific variation, most probably due to similar biomechanical constraints.

INTRODUCTION

Recent years have seen an increase in studies on macroevolutionary patterns of skull shape in fossil reptiles using geometric morphometrics (e.g. Jones 2008; Brusatte et al. 2012a; Bhullar et al. 2012; Foth et al. 2012; Meloro & Jones 2012; Foth & Rauhut 2013). However, undistorted, complete, and three-dimensionally preserved skulls are an exception in fossil taxa. Thus, in all of these studies the sampling of skulls was based mainly on reconstructed skulls and at least partly on reconstructions taken from the scientific literature. However, this approach could be potentially problematic as a) skull reconstructions might differ considerably due to incompleteness and/or deformation of the material, and b) the influence of intraspecific variation is partly ignored in these macroevolutionary approaches, as is ontogenetic variation in most cases (with the exception of the study of Bhullar et al. 2012). The quality of the reconstructions is crucial, because the position of landmarks on reconstructed skulls as well as the position of species within the morphospace depends on the shape of the whole cranium and the precise relations between its individual bones. Furthermore, the position of species within the morphospace may also vary due to intraspecific variation. In the past some studies have tried to quantify intraspecific variation in dinosaur skulls with the help of morphometric and geometric morphometric methods (e.g. Carpenter 1990, 2010; Chapman 1990; Larson 2008; Campione et al. 2011; Mallon et al. 2011), whereas variation caused by taphonomic deformation was well-documented by Carpenter (1990) and Chapman (1990). However, a comprehensive review of the variability of

morphometric data due to differential reconstructions or as a result of intraspecific variation for any dinosaur lineage has not been published yet.

The aim of the current study is to investigate the variation in morphometric data between skull reconstructions based on the same specimen with the help of geometric morphometric methods. We furthermore analysed which skull regions might particularly be affected by high variation within these reconstructions. The results are compared to shape variation occurring in skull reconstructions based on different specimens of the same species and skulls of closely related species, in order to investigate whether this potential source of variation in geometric morphometric data might be comparable to taxonomically or even phylogenetically significant variation.

MATERIAL AND METHODS

Three different datasets for basal Saurischia, basal Tetanurae, and Tyrannosauroida were created, by collecting skull reconstructions in lateral view (Table S2.1, see supplementary information of Chapter 2). The taxon sample was, of course, limited to taxa for which several skulls are known and for which various reconstructions based on the same specimen could be found in the literature. All datasets include a) skull reconstructions based on the same specimen, b) skull reconstructions of different specimens of the same species and c) skull reconstruction of closely related species.

Plateosaurus and *Allosaurus* were treated as each being represented by a single species, following Weishampel & Chapman (1990), Moser (2003) and Carpenter (2010). The specimen FMNH PR308, which was originally described as *Gorgosaurus* (Russell 1970), is placed in *Daspletosaurus*, following Carr (1999).

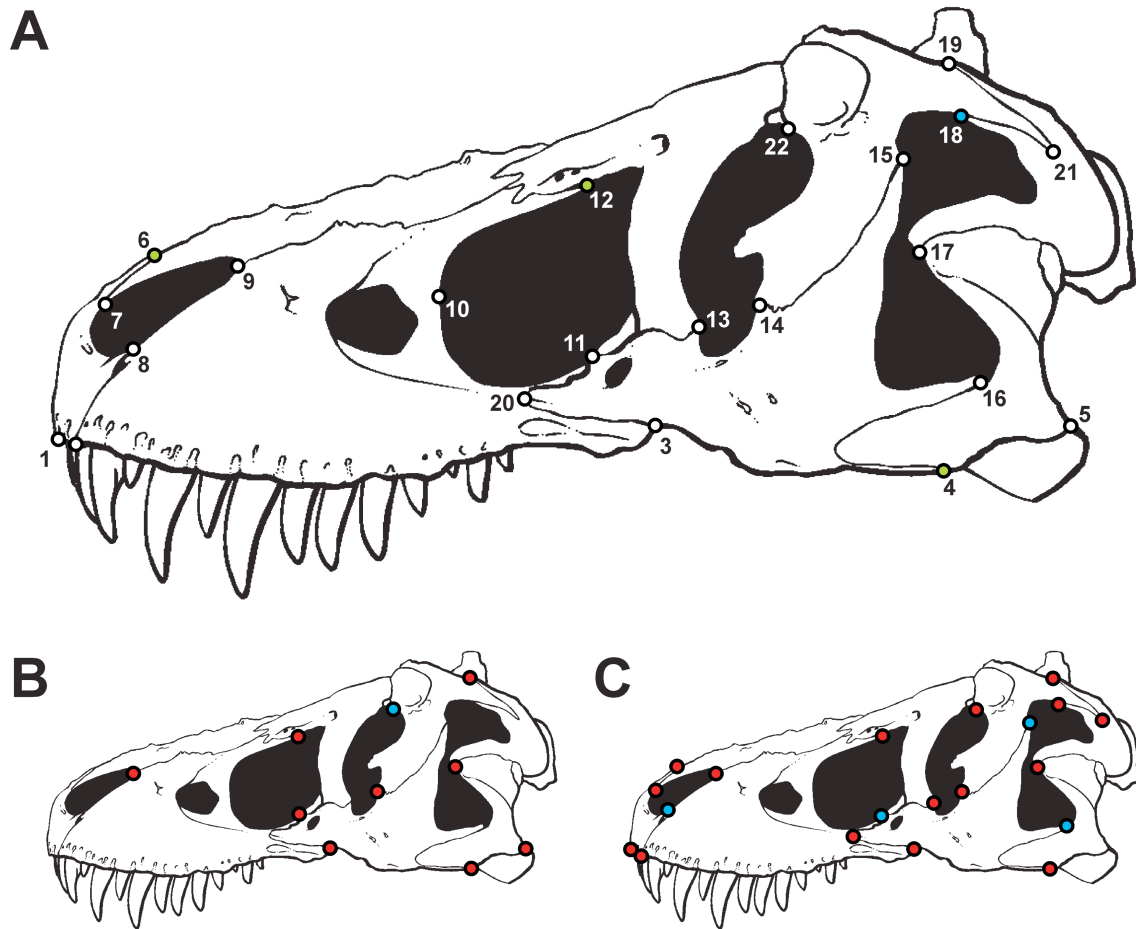


Fig. 2.1. Position of landmarks used in the study and variation of skull regions. **A.** Landmarks used in the study plotted on a skull reconstruction of *Tyrannosaurus* specimen of AMNH 5027 (modified after Carr & Williamson 2004). The green landmarks show skull regions that show most variation between different reconstructions based on the same specimen in both the original and the randomized dataset. The blue landmark LM 18 shows additional variation found in the original dataset. **B.** Skull regions with distinct variation between reconstructions based on different specimens (intraspecific variation). Red landmarks show variation found in both the original and the randomized dataset, blue landmarks show variation found in the randomized dataset. **C.** Skull regions with distinct variation between reconstructions based on different, closely related species (interspecific variation). Red landmarks show variation found in both the original and the randomized dataset, blue landmarks show variation found in the randomized dataset.

The skull shape of all species/specimens was captured by 22 homologous landmarks, which are figured in Fig. 2.1 and listed in Table S2.2 (see supplementary information of Chapter 2), using the program tpsDig (Rohlf 2005). This program outputs a tps (thin plate spline) file with two-dimensional landmark coordinates and scale (size) data for each specimen. The tps file was loaded into MorphoJ (Klingenberg 2011) and superimposed using Generalized Procrustes Analyses GPA, which align landmarks from all specimens by minimizing non-shape variation like size, location, orientation and rotation (Zelditch et al. 2004).

Afterwards, the datasets were divided into different subgroups containing the Procrustes coordinates of a) single specimens, b) different specimens of the same species and c) different, closely related species, respectively. To estimate the degree of variation of skull shape within single specimens, species and between different species a method was used that was originally developed for estimating the methodological error for plotting landmarks on specimens by hand (Singleton 2002). On the basis of the Procrustes coordinates the mean Procrustes distances to the respective consensus coordinates of each landmark were calculated. Then, the relation of these distances to the mean distance of the consensus landmarks to the centroid of the consensus shape was calculated as a percentage of the former from the latter. A further tps file was created for each dataset including a single skull reconstruction of only one specimen ($n = 10$) to calculate the methodological error of plotting landmarks on the skull reconstruction as mentioned above. The mean error for plotting landmarks ($= 0.364 \%$) was computed and subtracted from the percentage errors for individual landmarks. Afterwards, the median of the percentage error of each landmark and its 25th and 75th percentiles (interquartile range) were computed in PAST 2.17b (Hammer et al. 2001)

and compared between the different subgroups. Using this method for the purpose mentioned above, the results do not represent methodological errors, but a measure for morphological variation of overall shape (disparity, see Foote 1991; Wills et al. 1994). If the median is more than 5.0 % skull shape, variation within a sample was considered as significant. Thus, skull reconstructions from sample with significant variation could potentially affect the results of a geometric morphometric analyses and should be treated with caution. To verify the results, Procrustes coordinates were additionally used to calculate the Euclidian distances for every sample within each group (Lockwood et al. 2005). As in the previous case, the median Euclidian distance and its 25th and 75th percentiles were calculated. Furthermore, we wanted to know, which skull regions are particularly affected by significant shape variation within reconstructions of the same specimen, the same species and closely related taxa, respectively. For this, the median and its 25th and 75th percentiles were calculated for each landmark within the different subgroups mentioned above.

Due to the generally small numbers of skull reconstructions for most samples, we tested the robustness of the ‘original’ results in relation to sample size by computing random samples in the program R (R Development Core Team 2011) with a standard number of ten ‘hypothetical reconstructions’ per sample on the basis of the Procrustes coordinates of the original data. The function used computed ten normal pseudorandom variates based on the mean and the standard deviation of all Procrustes coordinates related to a corresponding landmark within the original sample (Braun & Murdoch 2008). Afterwards, all methods described above were repeated with randomized samples and compared to the original data. If both kinds of data produce similar results

one can conclude that the results of the original data are robust in relation to sample size.

INSTITUTIONAL ABBREVIATIONS

AMNH, American Museum of Natural History, New York; MB, Museum für Naturkunde, Berlin; MOR, Museum of the Rockies, Bozeman; FMNH, The Field Museum, Chicago; MOR, Museum of the Rockies, Bozeman; NMC, National Museum of Canada, Ottawa; PIN, Paleontological Institute, Russian Academy of Sciences, Moscow; SMNS, Staatliches Museum für Naturkunde Stuttgart, Stuttgart; USNM, National Museum of Natural History (= formerly United States National Museum), Smithsonian Institution, Washington, D.C.; UUVP, Utah Museum of Natural History, Salt Lake City.

RESULTS

Both the values of the median of landmark variation (median of variation) and Euclidean distances show generally similar distributions between the single samples of the three subgroups. This is also true for the comparison between original and randomized data. However, for the Euclidean distances the interquartile range of the randomized data is usually smaller than for the original data (for all samples with more than two reconstructions) with exception of *Gorgosaurus*, *Tarbosaurus* and the *Daspletosaurus* specimen FMNH PR308. In contrast, the range of interquartiles are comparable for both kinds of data with the exception of *Eoraptor*, *Massospondylus* and *Tarbosaurus* (here the interquartile range of the randomized data is slightly bigger than in the original data) as well as *Plateosaurus*, *Acrocanthosaurus* and the *Tyrannosaurus*

specimen AMNH 5027 (here the interquartile range of the randomized data is slightly smaller than in the original data, Fig. 2.2, 2.3).

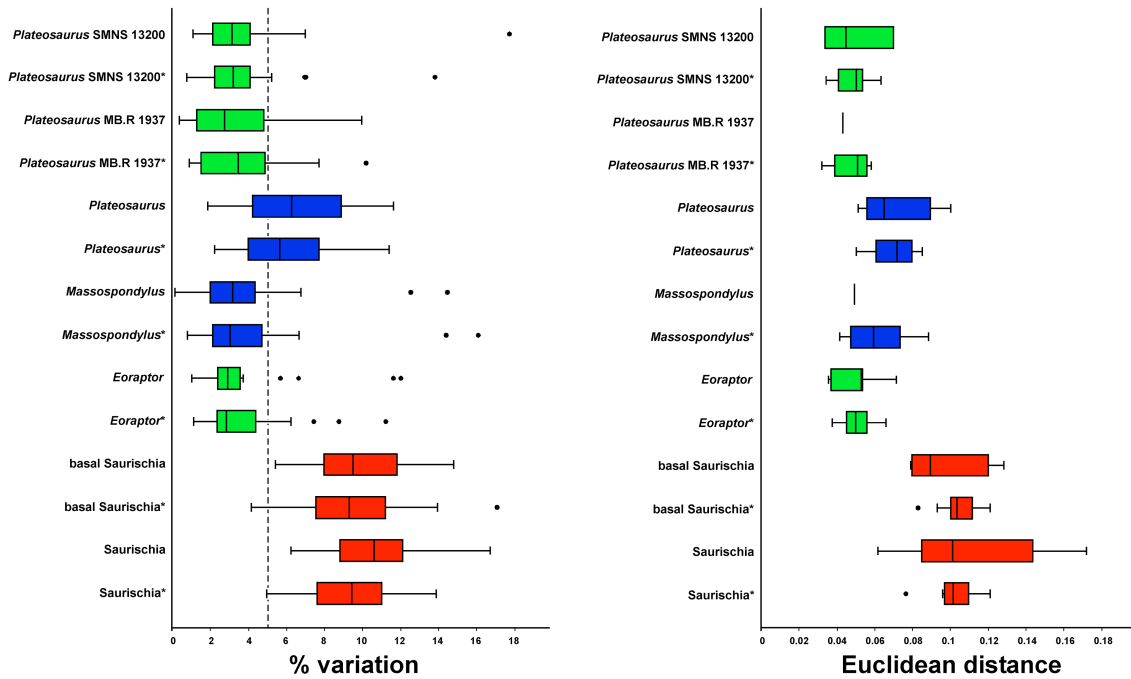


Fig. 2.2. Percentage variation and Euclidean distance for different skull reconstructions and randomized skull shapes of basal Saurischia. Shaded boxes show the interquartile range (defined by the 25th and 75th percentile) with the median marked as horizontal line. The whiskers mark the distance between the interquartile range and points up to 1.5 distances from the interquartile range. Outliers are represented as circles. Green boxes show shape variation between reconstructions based on the same specimen, blue boxes show shape variation between reconstructions based on different specimens (intraspecific variation), and red boxes show shape variation between reconstructions based on different, closely related species (interspecific variation). (*) Randomized samples.

In all sampled cases the median of the variation for reconstructions based on the same specimen is less than 5.0 %. In the *Allosaurus* specimen AMNH 600 (two reconstructions) and the *Daspletosaurus* specimens NMC 8506 (four reconstructions) and FMNH PR308 (three reconstructions) the median of variation is even less than 1.0

%. The mean for the median values of the original data is 2.08 % (and 2.27 % for the randomized data). Only in *Monolophosaurus* is the 75th percentile value higher than 5.0 % for both original and randomized data.

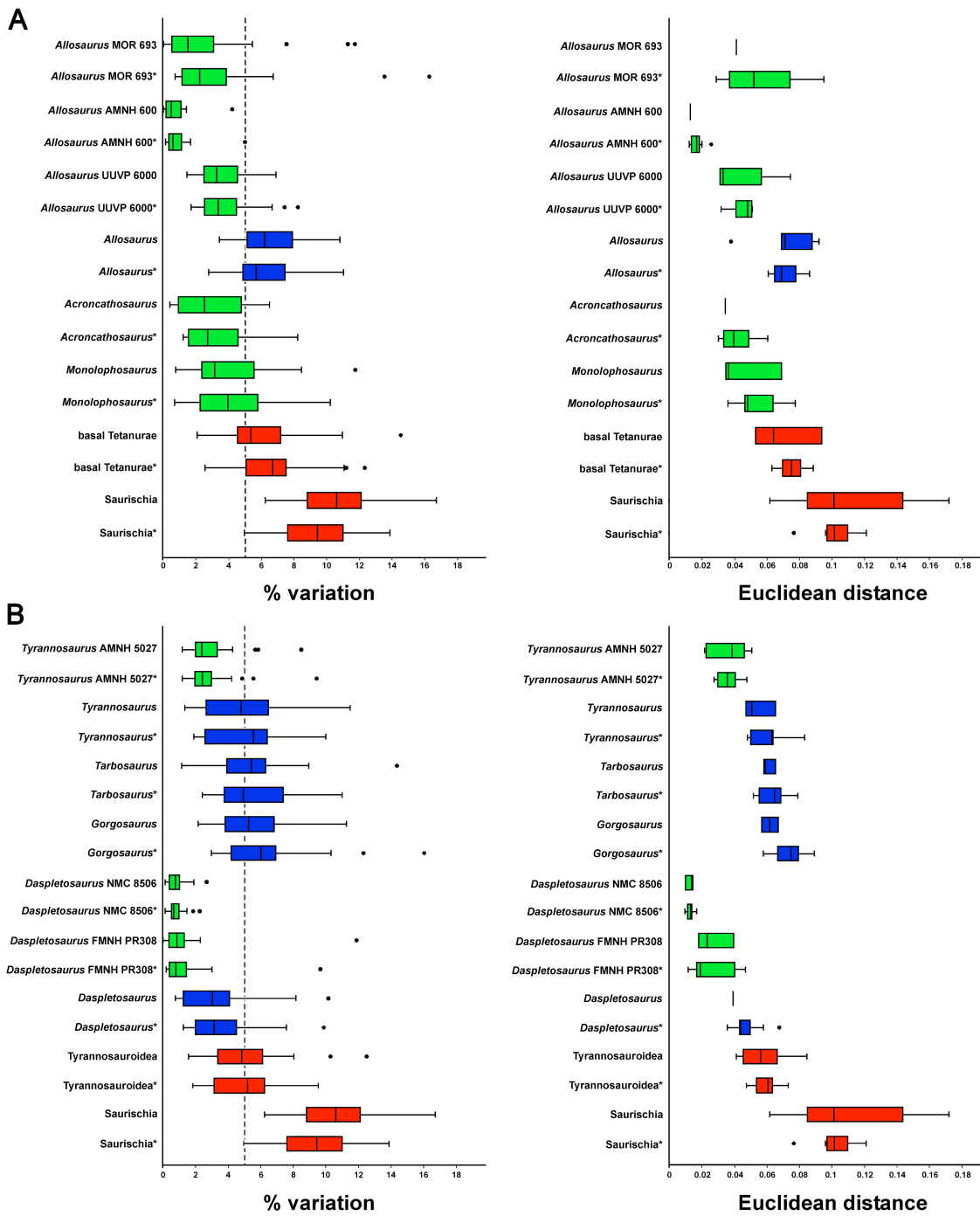


Fig. 2.3. Percentage variation and Euclidean distance for different skull reconstructions and randomized skull shapes of basal Tetanurae and Tyrannosauroidae. **A.** basal Tetanurae. **B.** Tyrannosauroidae. Shaded boxes show the interquartile range (defined by the 25th and 75th percentile) with the median marked as horizontal line. The whiskers mark the distance between the interquartile range and points up to 1.5 distances from the interquartile range. Outliers are represented as circles. Green boxes show shape variation between reconstructions based on the same specimen, blue boxes show shape variation between reconstructions based on different specimens (intraspecific variation), and red boxes show shape variation between reconstructions based on different, closely related species (interspecific variation). (*) Randomized samples.

The mean of the median values for skull reconstructions based on different specimens of the same species is 4.74 % for the original data (and 4.78 % for the randomized data), in which the median of the variation of the original data is less than 5.0 % for *Daspletosaurus*, *Massospondylus* and *Tyrannosaurus*. Here, the 75th percentile value is less than 5.0 % in the former two genera as well. Thus, the median of the variation of *Daspletosaurus* and *Massospondylus* strongly overlaps with that of reconstructions based on the same specimen for most taxa. In contrast, the median of the variation of the original data of *Allosaurus*, *Plateosaurus*, *Tarbosaurus* and *Gorgosaurus* is more than 5.0 %, but only for *Allosaurus* is the 25th percentile value higher than 5.0 %. In contrast, the median of the variation in the randomized datasets is less than 5.0 % for *Tarbosaurus*, but more than 5.0 % in *Allosaurus*, *Plateosaurus*, *Gorgosaurus* and *Tyrannosaurus* (Fig. 2.2, 2.3).

The mean of the median values for reconstructions of skulls of closely related taxa is 6.48 % for the original data (and 6.76 % for the randomized data). For the

original data of Tyrannosauroida only the 75th percentile value is more than 5.0 %, whereas median of the randomized data is more than 5.0 % as well. For basal Tetanurae the median of variation is more than 5.0 %. Thus, the degree of variation (in relation to the interquartile range) of both basal Tetanurae and Tyrannosauroida overlaps with that of reconstructions based on skulls of the same species. Only for basal Saurischia and all Saurischia sampled are the medians of the variation and their percentiles considerably higher than 5.0 %. In the latter cases the median of the variation is over 9.0 %, and thus, distinctly higher than that for basal Tetanurae and Tyrannosauroida (Fig. 2.2, 2.3).

For reconstructions based on the same specimen most variation can be seen in the ventral contact of the jugal and quadratojugal (LM 4), the contact between premaxilla and nasal along the dorsal margin of skull (LM 6), the position of the most anterior point of the lacrimal along the dorsal margin of the antorbital fenestra (LM 12), and the contact between postorbital and squamosum along the dorsal margin of the lateral temporal fenestra (LM 18, but only for the original data), as the 75th percentile of values the percentage variation is more than 5.0 % for these landmarks (Fig. 2.1, Table S2.6, S.2.7, see supplementary information of Chapter 2).

For reconstructions based on different specimens of the same species distinct variation occurs in the ventral margin of the jugal and its contacts with the maxilla and quadratojugal (LM 3, LM 4), the position of the posteroventral corner of the quadratojugal (LM 5), the length of tip of the maxillary process of the nasal (LM 9), in the position of the most ventral point of the lacrimal along the margin of the antorbital fenestra (LM 11), the position of the anteriormost contact of the lacrimal along the dorsal margin of the antorbital fenestra (LM 12), the contact between lacrimal and jugal

on the orbital margin (LM 14), the position of the anteroventral tip of the ventral process of the squamosal on the margin of the lateral temporal fenestra (LM 17), and in the dorsal contact between postorbital and squamosal (LM 19). For the randomized data the contact between frontal and postorbital on the dorsal margin of the orbit (LM 22) was found to be significant as well (Fig. 2.1, Table S2.6, S2.7, see supplementary information of Chapter 2).

In comparison, for skull reconstructions of closely related taxa, distinct landmark variation affects almost the entire skull, with the exception of the length of the anterior process of the maxillary body (LM 8), the position of the anteriormost point of the antorbital fenestra (LM 10), the contact of the jugal with both the squamosal and the quadratojugal on the margin of the lateral temporal fenestra (LM 15, LM 16). For the randomized data all landmarks except of LM 10 showed significant variation (Fig. 2.1, Table S2.6, S2.7, see supplementary information of Chapter 2).

DISCUSSION

Based on the results presented above, we can conclude that the shape variation of skull reconstruction (in relation to the median of variation and the interquartile range) based on the same specimen seems usually to be negligible in geometric morphometric studies (only in *Monolophosaurus* the 75th percentile is more than 5.0 %). The general consistency of the results between original and randomized data supports this result in spite of the small sample sizes of the original data. However, taxa for which only a single specimen and maybe even only a single reconstruction exist could introduce considerable error in geometric morphometric studies, if the particular specimen is incomplete or strongly taphonomically deformed. In *Allosaurus*, for example, the skull

reconstructed by Gilmore (1920) has figured prominently in both the scientific and the popular literature for a long time, until newly found, better preserved and complete specimens showed that this reconstruction, based on a disarticulated, partially deformed, and pathological skull, does not represent the “typical” skull shape of this taxon (Fig. 2.4).

Shape variation in reconstructions might be influenced, for instance, by the talent of the artists, their anatomical knowledge and their tendency to idealize structures, which are e.g., taphonomically deformed, damaged or missing (meaning to attempt a complete de-deformation of the skull). Differences in the skull shape of the holotype of *Monolophosaurus* or the *Plateosaurus* specimens MB.R 1937 and SNMS 13200 are probably partially caused by the latter factor, because Zhao & Currie (1993), Rauhut (2003a) and Yates (2003) idealized such deformations more completely than Galton (2001) (Fig. 2.4) or Brusatte et al. (2010b) (e.g. Brusatte et al. figured the disarticulation between jugal and postorbital on the right side of the skull). Furthermore, it might be important if the artist saw the specimen first hand, reconstructed the skull on the basis of photographs or simply redrew the skull from previously published reconstructions (as is the case e.g. with the reconstruction of *Monolophosaurus* in Rauhut 2003a). In order to minimize this source of error, a scientist analysing shape changes would be wise to not only take the reconstructed skull from the literature, but also look closely at the available data on the original material and how the skull was reconstructed from it.

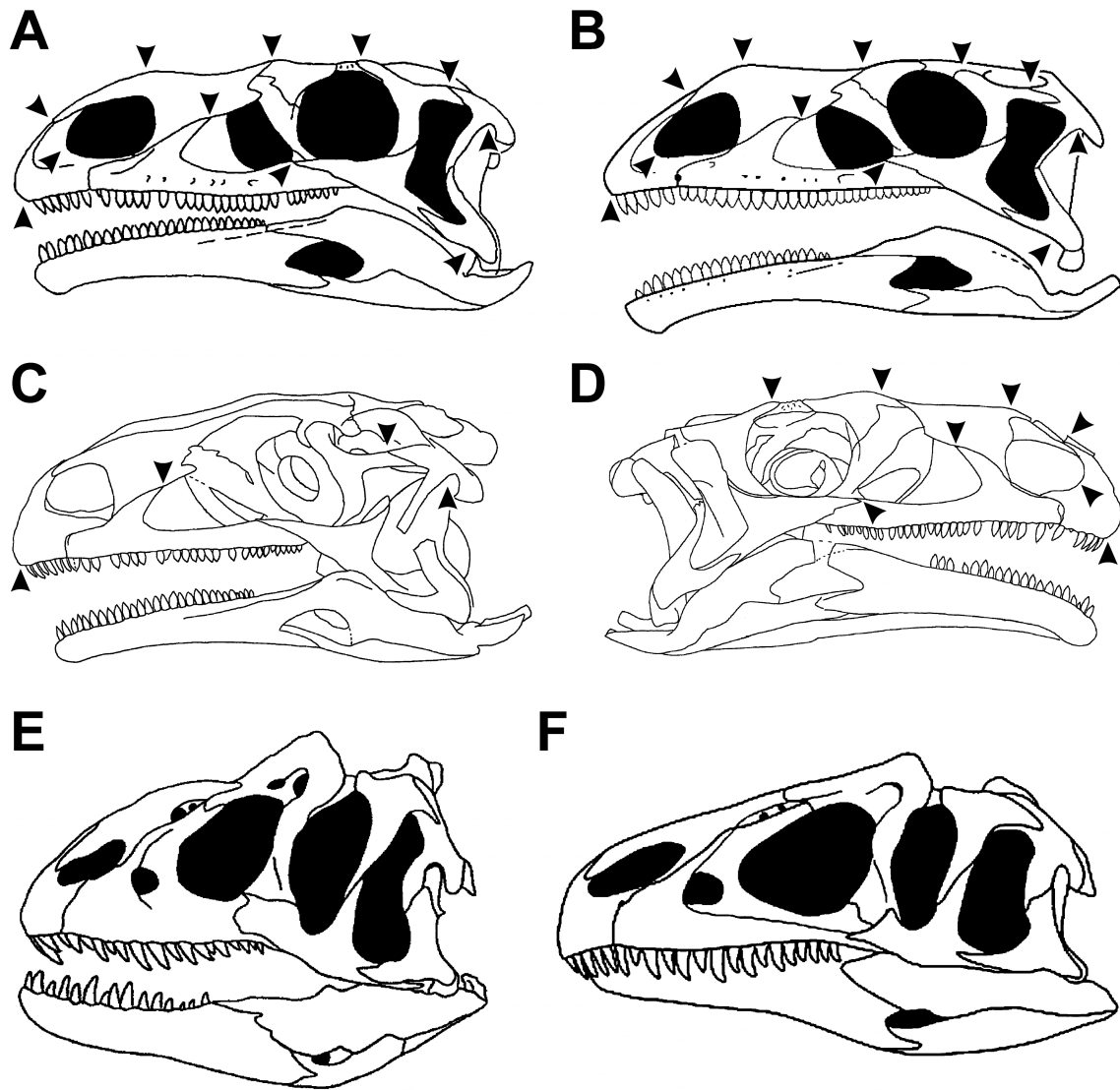


Fig. 2.4. Skull reconstructions of the *Plateosaurus* specimen SMNS 13200 and different *Allosaurus* specimens. **A.** Skull reconstruction of SMNS 13200 after Galton (2001). **B.** Skull reconstruction of the SMNS 13200 after Yates (2003) (modified after Nesbitt 2011). **C.** Line drawing of the left side of the original material of SMNS 13200 after Galton (1984). **D.** Line drawing of the right side of the original material of SMNS 13200 after Galton (1984). Arrows show shape differences in the reconstructions by Galton and Yates and the morphology of the respective structure of the original material of SMNS 13200. Here, the skull reconstruction of SMNS 13200 by Galton resembles the original material more in respect to the shape of the anterior margin of the premaxilla and its contact to the nasal, the shape of the anterior margin of the external naris, the contact between nasal and maxilla, the contact between maxilla, jugal and lacrimal, the shape of the dorsal margin of the skull, the shape of the postorbital and its contacts to the frontal and the squamosum, and the shape of the ventral margin of the quadratojugal. **E.** ‘Short-

snouted' *Allosaurus* specimen USNM 4735 described by Gilmore (1920), which was based on a disarticulated, partially deformed, and pathological skull (modified after Henderson 2000). F. 'Typical' *Allosaurus* skull based on MOR 693 (modified after Rauhut 2003a).

Within different reconstructions based on the same specimens the skull regions described by landmark 4, 6, 12 and 18 (i.e. the ventral contact of the jugal and quadratojugal, the contact premaxilla and nasal along the dorsal margin of skull, the position of the most anterior point of the lacrimal along the dorsal margin of the antorbital fenestra, and the contact between postorbital and squamosum along the dorsal margin of the lateral temporal fenestra) are more variable than other landmarks, although their variability is still less than that between landmarks in reconstructions of different specimens. Thus, these particular skull regions may contain a potential methodological error for plotting landmarks on dinosaur skulls and maybe also other reptiles, and should be verified carefully by photo material or first-hand observations.

The variation of skull reconstructions (in relation to the mean of the median values) based on different specimens of the same species is expected to be higher than that of different reconstructions of the same specimen as variation is further caused by intraspecific variation. However, the differences are not significant due to the strong overlap of the percentiles between both groups and also vary from species to species. For instance, the intraspecific skull variation found in *Massospondylus* is relatively low, challenging Gow et al. (1990), who hypothesized that the shape variation seen in the skulls of two *Massospondylus* specimens might be caused by sexual dimorphism. Based on the results of both the original and randomized samples this hypothesis cannot be

supported statistically. The variation might rather reflect allometric shape variation as both specimens slightly differ in skull size (Hinić 2002). Cranial sexual dimorphism was also hypothesized for *Allosaurus* (Molnar 2005), but also cannot be verified statistically.

On the other hand, the current results support previous studies on *Allosaurus* and *Plateosaurus*, which show a large intraspecific variation within these taxa (Weishampel & Chapman 1990; Smith 1998; Carpenter 2010). However, some of the variation presented in those studies reflects also ontogenetic variation, making a direct comparison of the studies difficult as this type of variation has only minor impact on the current results due to selective sampling of adult or nearly adult specimens.

Some of the variation found in the current results may also result from taphonomic deformation (e.g. the disarticulated contact of quadratojugal and squamosum in the holotype skull PIN 551-1 of *Tarbosaurus*, which is pictured in the reconstruction of Maleev 1974). Taphonomic deformation was also hypothesized as the major reason for the huge ‘morphological variation’ seen in the southern Germany *Plateosaurus* material (Moser 2003), and its influence on skull shape is well-documented for a *Plateosaurus* by Chapman (Chapman 1990). Furthermore, some variation in *Allosaurus* and *Plateosaurus* could be also explained by their controversial taxonomic status. As mentioned in the material and method section, reconstructed skulls of both genera were treated as belonging to one species, but some authors argued that there are at least two species for each genus (e.g. Chure 2000; Galton 2001; Yates 2003; Loewen 2009; Prieto-Márquez & Norell 2011). If the latter case is true, the variation is

partially covered by interspecific variation, and thus the actual intraspecific variation might be overestimated.

To minimize the ‘error’ of intraspecific variation in macroevolutionary approaches, taxa for which there are several good quality reconstructions of different specimens should be tested for intraspecific variation. This can be done in a separate small dataset with the same landmark configuration used in the macroevolutionary study by calculating the Procrustes coordinates for each specimen and estimating the respective Euclidean distances to the consensus shape of the small dataset. Subsequently, the specimen with the smallest distance to the consensus shape might be used for the study.

The examples of interspecific variation (in relation to the median of variation) presented in this study show all significant variation, except for the original sample of Tyrannosauroidae. However, the latter exception could be the result of a small sample size ($n = 5$). Interestingly, the interspecific shape variation (in relation to the interquartile range) of basal Tetanurae and Tyrannosauroidae strongly overlaps with the shape variation of the intraspecific variation of *Allosaurus*, *Tyrannosaurus*, *Tarbosaurus* and *Gorgosaurus*. The estimated intraspecific variation is even slightly higher than the estimated interspecific variation of the respective groups. At first glance this result is surprising, as one would expect that interspecific variation should be larger than intraspecific variation, as seen in basal Saurischia. Methodically, the overlap could be a false signal resulting from small sample sizes (see Molnar 1990). However, the differences between the numbers of reconstructions used for a single species and for different, closely related species are rather small, making this explanation rather

unlikely. Furthermore, because the results of the randomized data are similar to that of the original one, the sample size does not seem to influence the current result significantly. However, it is possible that the chosen landmark configuration does not capture skull regions that underlie strong interspecific variation in basal Tetanurae or Tyrannosauroida, like the dorsal margin of the nasal (e.g. *Monolophosaurus*) or the dorsal margin of the lacrimal horn (e.g. *Allosaurus*). Furthermore, semi-landmark analysis of overall skull shape, in combination with a landmark-based analysis, might capture variations in skull shape more completely and thus yield different results. Thus, it is possible that the present analyses underestimate the actual interspecific variation between those taxa. Furthermore, it is to be expected that interspecific skull variability increases with increasing the sample size of taxa analysed, as it is indeed demonstrated by the higher variation seen in the data set for basal saurischians or saurischians as a whole. By expanding the data set to species with more derived skull morphologies (e.g. long-snouted spinosaurids for basal Tetanurae), an increase of the interspecific variation even in rather closely related forms would also be expected. This is supported by several studies on crustacean, pterosaur and coelurosaur diversity for instance, which all show that disparity of larger taxonomic clades is higher than in the respective internal subclades (see Wills 1998; Prentice et al. 2011; Brusatte et al. 2012b; Foth et al. 2012). On the other hand, an overlap of intraspecific and interspecific variation in closely related taxa has also been demonstrated for instance in the cranial shape of recent Hominoidea (Lockwood et al. 2005), the osteology of skinks (Czechura & Wombey 1982) or in molecular sequences of different bilaterian clades (e.g. Meyer et al. 2005; Meier et al. 2006, 2008), and the phenomenon is therefore neither restricted to theropod dinosaurs, nor to skull shape.

In comparison with this rather small variation seen in closely related theropod taxa, basal Saurischia in total possess a very large interspecific variation. One reason for this could be the inclusion of *Eoraptor*, the taxonomic position of which is still debated (e.g. Martinez & Alcober 2009; Martinez et al. 2011; Nesbitt 2011). However, excluding *Eoraptor* from the data set does not change the result (median of variation = 9.66 %). Thus, the large variation seen in the skull shape might be due to diverging dietary preferences in basal saurischians, towards carnivory in many basal theropods, with omnivory and finally herbivory in sauropodomorphs (Barrett 2000; Galton & Upchurch 2004; Langer et al. 2009; Barrett et al. 2011). Indeed, this change in diet might lead to the evolutionary trend from slender and elongate skulls to short and broad skulls seen in the early evolution of Sauropodomorpha (Rauhut et al. 2011). A similar pattern regarding diet preferences was also found in theropods by Brusatte et al. (2012a) and Foth & Rauhut (2013), who have shown that both carnivorous and non-carnivorous taxa occupy large areas within the morphospace, but non-carnivorous taxa tend to develop more diverse, sometimes aberrant skull morphologies (e.g. Oviraptorosauria). In contrast, large-bodied carnivorous theropods tend to cluster closely together within morphospace (Brusatte et al. 2012a; Foth & Rauhut 2013), and show a smaller disparity in skull shape in comparison to smaller theropods with a broad dietary spectrum (Brusatte et al. 2012a). This might be due to a constrained biomechanical adaptation for high bite forces (Erickson et al. 1996; Henderson 2002; Sakamoto 2010), including an oval orbit, a deep jugal body and a short postorbital region (Henderson 2002; Foth & Rauhut 2013).

CONCLUSION

The median of variation of different skull reconstructions based on the same specimen seems to have generally little influence on the results of a geometric morphometric analysis of skull shape in theropods and basal saurischians. Shape differences seem to be mainly influenced by the talent of the artists, their anatomical knowledge, and their tendency to idealize structures that are damaged, missing or taphonomically deformed. In general, it is advisable to verify reconstructions used on the basis of the original material or photographs thereof. For different specimens of the same species the variation (in relation to the mean of the median values) is generally higher than in the previous example, indicating that intraspecific variation cannot be neglected, although this apparent variation might in some cases be overestimated due to uncertain taxonomy. For closely related species, at least with similar ecological preferences, the degree of interspecific variation (in relation to the median of variation and its percentiles) overlaps with that of intraspecific variation. This probably reflects considerable constraints in the skulls of theropods with similar feeding strategies. As would be expected, variation in morphometric data might increase with increased phylogenetic and/or ecological sampling, but this have to be tested in future studies in more detail. Given the nature of fossil data, our analysis is necessarily based on rather small sample sizes, and more investigations of the relation between intraspecific and interspecific variation in geometric morphometric data in recent animals, for which higher sample sizes are available, would be desirable.

ACKNOWLEDGMENTS

We would like to thank Martin Schwentner (University of Rostock), Serjoscha Evers and Richard Butler (both Ludwig-Maximilians-Universität, München) for discussion and two anonymous reviewers for critical comments, which helped to improve the manuscript. Furthermore, we want to thank Hans-Jakob Siber and Thomas Bollinger (Sauriermuseum Aathal) and Raimund Albersdörfer for access to *Allosaurus* material.

CHAPTER 3

Intraspecific variation in the skull morphology of the black caiman *Melanosuchus niger* (Alligatoridae, Caimaninae)

Keywords:

Melanosuchus; Crocodylia; ontogeny; sexual dimorphism; geometric morphometrics

The chapter was accepted as:

Foth C¹, Bona P^{2,3} & Desojo JB^{2,4}. In press. Intraspecific variation in the skull morphology of the black caiman *Melanosuchus niger* (Alligatoridae, Caimaninae). *Acta Zoologica*.

¹*Bayerische Staatssammlung für Paläontologie und Geologie, Richard-Wagner-Str. 10, D-80333 München, Germany*

²*CONICET, Consejo Nacional de Investigaciones Científicas y Técnicas*

³*División Paleontología Vertebrados, Museo de La Plata. Paseo del Bosque s/n. 1900, La Plata, Buenos Aires. Argentina*

⁴*Sección Paleontología de Vertebrados, Museo Argentino de Ciencias Naturales "Bernardino Rivadavia". Av. Angel Gallardo 470 C1405DRJ, Capital Federal. Argentina*

Received 28 January 2013; revised 04 July 2013; accepted 08 July 2013

Author contribution:

Research design: **Christian Foth**, Paula Bona, Julia Desojo

Data collection: **Christian Foth**, Julia Desjo

Data analyses: **Christian Foth**

Preparation of figures and tables: **Christian Foth**

Wrote paper: **Christian Foth**, Paula Bona, Julia Desojo

***All figures of Chapter 3 are modified after Foth et al. (in press)**

Intraspecific variation in the skull morphology of the black caiman *Melanosuchus niger* (Alligatoridae, Caimaninae)

Christian Foth, Paula Bona & Julia B. Desojo

ABSTRACT

Melanosuchus niger is a caimanine alligatorid widely distributed in the northern region of South America. This species has been the focus of several ecological, genetic and morphological studies. However, morphological studies have generally been limited to examination of interspecific variation among extant species of South American crocodylians. Here we present the first study of intraspecific variation in the skull of *Melanosuchus niger* using a two-dimensional geometric morphometric approach. The crania of 52 sexed individuals varying in size were analyzed to quantify shape variation and to assign observed shape changes to different types of intraspecific variation, i.e. ontogenetic variation and sexual dimorphism. Most of the variation in this species is ontogenetic variation in snout length, skull depth, orbit size and the width of the postorbital region. These changes are correlated with bite force performance and probably dietary changes. However, a comparison with previous functional studies reveal that functional adaptations during ontogeny seems to be primarily restricted to the postrostral region, whereas rostral shape changes are more related to dietary shifts. Furthermore, the skulls of *Melanosuchus niger* exhibit a sexual dimorphism, which is primarily size related. The presence of non-size related sexual dimorphism has to be tested in future examinations.

INTRODUCTION

Knowledge of vertebrate morphology and its intraspecific variation (e.g. ontogenetic variation, sexually dimorphic variation, polymorphisms) is crucial for accurate systematic, taxonomic, evolutionary, ecological, physiological and functional hypothesis of the different groups (e.g. Sudhaus & Rehfeld 1992; Wiesenmüller et al. 2003; Carpenter 2010; Porro et al. 2011). Among extant crocodylians, previous studies of skull anatomy and intraspecific variation (including ontogenetic variation), evolution and functional morphology include those of Mook (1921), Kälin (1933), Medem (1963), Iordansky (1973), Dodson (1975), Busbey (1989), Hall & Portier (1994), Monteiro & Soares (1997), Brochu (1999, 2001), Verdade (2000), Erickson et al. (2003, 2012), McHenry et al. (2006), Piña et al. (2007), Wu et al. (2006), Sadleir & Makovicky (2008), Platt et al. (2009) and Bona & Desojo (2011). Nevertheless, lack of morphological studies and data, especially for osteology, is common to all extant South American crocodylians. The main problem is that crocodylian skeletons are rare in South American herpetological collections. This is unfortunate because detailed knowledge of the osteology of extant species and its morphological variation become further relevant when reconstructing the evolutionary history of a group, especially given that most of fossil specimens are preserved only by skeletons (and generally as fragments).

Extant South American Alligatoridae are grouped in three genera of Caimaninae, *Paleosuchus* Cuvier 1807, *Caiman* Spix 1825 and *Melanosuchus* Spix 1825. Certain taxonomic controversies among caimanines are related to *Melanosuchus*. This genus is represented by two species: the extinct *Melanosuchus fisheri* Medina, 1976 from the Upper Miocene (Urumaco Formation) of Venezuela (Sánchez-Villagra & Aguilera

2006) and the extant *Melanosuchus niger* Spix, 1825, in which the taxonomic status of the synonym *Melanosuchus fisheri* has been questioned (e.g. Brochu 1999). The presence of prominent rostral ridges on the skull, shared with the extant *Caiman latirostris* Daudin, 1802 and the extinct *Caiman* cf. *lutescens* (Langston, 1965) from the Miocene of South America, supports a sister-group relationship of *Melanosuchus niger* with these two species in morphological cladistic analyses (Norell 1988; Poe 1997; Brochu 1999, 2003, 2010, 2011; Bona 2007; Aguilera et al. 2006). This result has generated differing taxonomic proposals with regard to the putative paraphyly of the genus *Caiman* (see Norell 1988; Poe 1997).

Melanosuchus niger is particularly interesting among Alligatoridae, because is one of the largest extant members of the group, with adult males sometimes exceeding 6 m in length (Cott 1926; Brazaitis 1974). It has been the focus of ecological (e.g. Otte 1974; Medem 1981; Plotkin et al. 1983; Herron 1991; Pacheco 1994; Villamarín-Jurado & Suárez 2007; Marioni et al. 2008; Horna et al. 2001) and genetic works (e.g. Farias et al. 2004; de Thoisy et al. 2006; Vasconcelos et al. 2008), as well as a limited number of morphological studies (Mook 1921; Kálin 1933; Medem 1963). Although there have been some qualitative studies on differently sized specimens of *Melanosuchus niger* (e.g. Mook 1921), its general intraspecific morphological variation is poorly understood. The purpose of the present study is to quantify, describe and interpret the intraspecific variation in the skull of *Melanosuchus niger* using a geometric morphometric approach. Geometric morphometrics is widely regarded as a powerful tool for taxonomic identification and functional interpretations (Rohlf & Marcus 1993; Zelditch et al. 2004), and has great potential to characterize developmental and genetic effects on morphological shape (see Klingenberg 2010). This method quantifies

differences in shape between objects from coordinates of homologous landmark locations, after the effects of non-shape variation (position, size and rotation) are mathematically held constant (Adams et al. 2004; Zelditch et al. 2004). Geometric landmark based analysis captures and retain more information about shape than traditional morphometric measurements (e.g. linear distances, ratios and measurements of angles), which often fail to capture the full geometry of the original object (Rohlf & Marcus 1993; Rohlf 2000; Hammer & Harper 2006). Geometric morphometrics has been used successfully to document intraspecific variation and to test specific taxonomic and ontogenetic biological hypotheses (e.g. Richtsmeier et al. 1993; O'Higgins & Collard 2002; Bookstein et al. 2003; Elewa 2004; Zelditch et al. 2004). However, only a few analyses of extant crocodylian skulls using a geometric morphometric approach have been previously conducted. Monteiro et al. (1997) studied ontogenetic changes in three *Caiman* species, and Pierce et al. (2008) described the cranial morphospace of extant crocodylians and its correlation with functional morphology based on finite element modeling (FEM). Piras et al. (2009) investigated the influence of phylogeny and ecological factors (climate change) on the skull shape of Alligatoroidea and Crocodyloidea, and Piras et al. (2010) compared allometric trajectories in different crocodylian taxa to test phylogenetic hypotheses about the relationships of gavials (*Gavialis gangeticus*) and false gavials (*Tomistoma schlegelii*).

In the context of quantifying skull shape variation within *Melanosuchus niger*, we want to classify ontogenetic variation and sexual dimorphism, and to test whether skull shape is correlated with bite force performance (which is used as a functional proxy) in this species. The results are compared with published data for other

crocodylian species to identify probable key patterns in intraspecific variation in cranial shape and how these patterns might be related to ecology and function.

MATERIAL AND METHODS

SPECIMEN SAMPLING

The crania of 52 individuals of *Melanosuchus niger* (Table S3.1, see supplementary information of Chapter 3) were analyzed using a two-dimensional geometric morphometric approach. Most of the specimens ($n = 40$) are deposited in the Zoologische Staatssammlung, Munich (Germany), which possesses one of oldest and largest collections of extant crocodylian skulls in the world. These specimens were collected mainly on Marajó Island (NE Brazil) between 1906 and 1925 during expeditions made by the Zoologische Staatssammlung. Additional material ($n = 12$) was examined in the Senckenberg Naturmuseum Frankfurt (Germany), Zoologisches Forschungsmuseum Alexander Koenig, Bonn (Germany), Zoologisches Museum Hamburg (Germany) and Naturhistorisches Museum Wien (Austria). The length of the skulls varies from approximately 5 to 50 cm (Table S3.1, see supplementary information of Chapter 3). All specimens, for which historical notes are available, represent wild individuals. This is crucial as skull shape can vary between wild and captive crocodylians (Erickson et al. 2004b), which could influence the results of shape analyses.

Determination of the sex of each specimen was based on original collection data. Unfortunately, most specimens were collected almost 100 years ago, so we were not able to ascertain how sex was originally determined (e.g. direct inspection of the cloaca, see Chabreck 1963; Ziegler & Olbort 2007) and no historical notes exist describing this

procedure (Frank Glaw, personal communication). Therefore, it is possible that the dataset includes some misidentifications of sex, especially between small males and females within the same size range. However, the skull of the largest male is approximately 14 cm (i.e. about 30 %) longer than that of the largest female (see Table S3.1, see supplementary information of Chapter 3), which represents a percentile size difference between the largest females and males similar to that documented for other crocodylian species (Chabreck & Joanen 1979; Wilkinson & Rhodes 1997, Platt et al. 2009). Based on this observation some specimens were classified as males by one of the authors (CF) based on their larger size (see Table S3.1, see supplementary information of Chapter 3).

Unfortunately, there is no information on the sex of the smallest specimens, and little is known about the reproduction biology of *Melanosuchus niger*. According to Herron (1991) it reaches sexual maturity at total body length of c. 2 m. Assuming isometric growth between body length and skull length (see Webb & Messel 1978; Verdade 2000; Wu et al. 2006) and a similar relation between body length at maturity and maximum body length as in *Alligator mississippiensis* (see Chabreck & Joanen 1979; Wilkinson & Rhodes 1997), the skull length of a *Melanosuchus niger* individual reaching sexual maturity is approximately 22 to 26 cm. Based on this estimation, specimens with skull lengths less than 22 cm were treated as immature juveniles in all analyses. Furthermore, the age and the place of capture of each specimen investigated in this study are unknown. Thus, it is not possible to test geographical variation in *Melanosuchus niger* with the current dataset.

GEOMETRIC MORPHOMETRICS

The majority of specimens were macerated skulls. Skulls were photographed in dorsal and lateral views. Because macerated skull material of juvenile *Melanosuchus niger* is rare, we additionally X-rayed the skulls of alcohol-preserved specimens in dorsal and lateral views (Table S3.1, see supplementary information of Chapter 3). The X-ray data were outputted as digital images. Skull shape was captured using eight (lateral view) and nine (dorsal view) homologous landmarks (Fig. 3.1, see supplementary information of Chapter 3 for full description of landmarks), which were digitized onto photographs/X-ray images using the program tpsDig2 (Rohlf 2005). We used landmarks of types 1 (good evidence for anatomical homology, such as points where two bone sutures meet) and 2 (good evidence for geometric homology, such as points of maximal curvature or extremities) following the terminology of Bookstein (1991). Because the detection of some bone sutures and the determination of the shape of the lateral temporal fenestra was difficult or unfeasible in the X-ray images, we additionally captured the outer shape of the skull and the shape of the orbit with help of six (dorsal view) and 13 (lateral view) semi-landmarks. For dorsal view we used a unilateral configuration for the right skull side, because a mirroring of the landmark and semi-landmarks would not add more information (see Young et al. 2010), but in contrast would inflate the degrees of freedom in the statistical analyses (see Pierce et al. 2008).

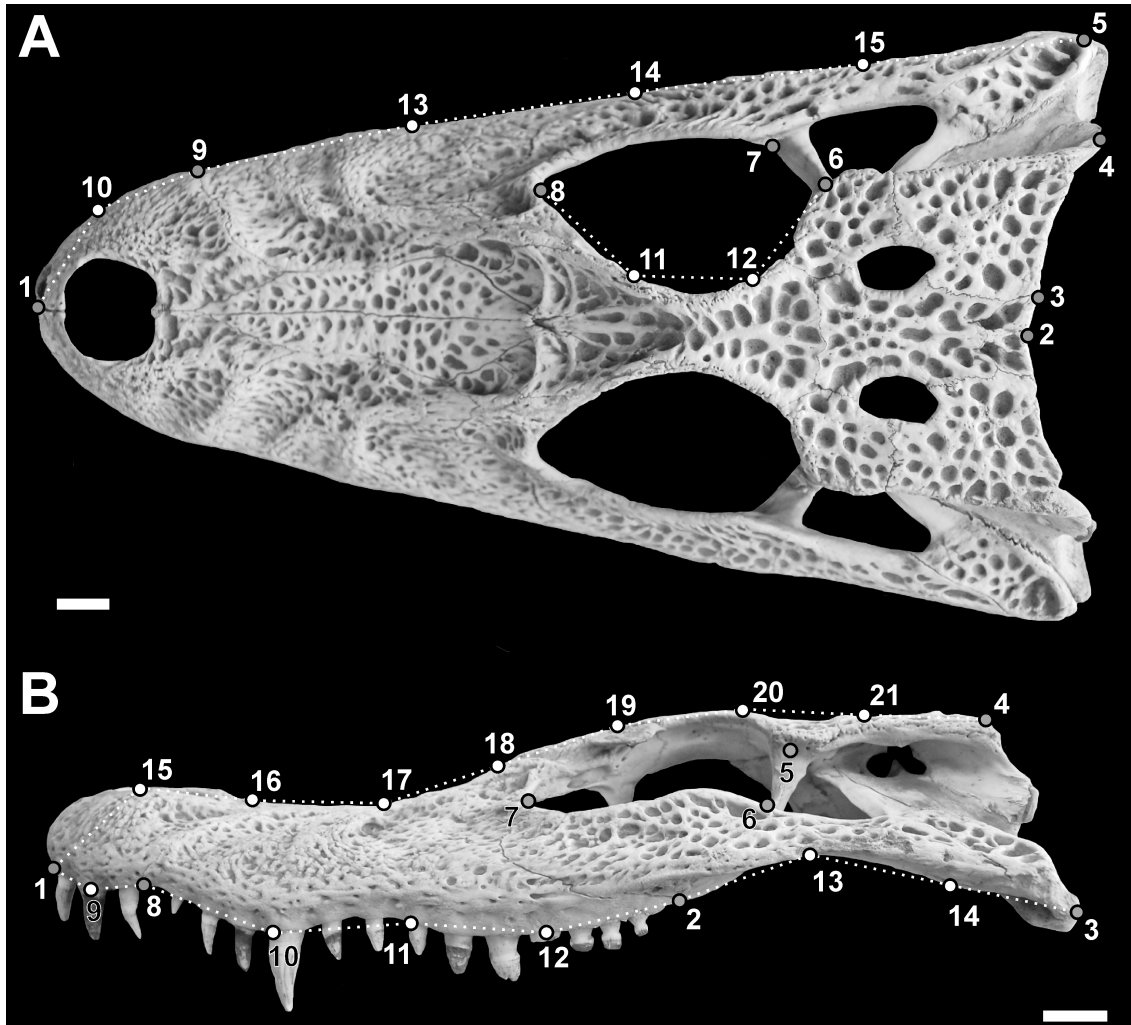


Fig. 3.1. Visualisation of the landmarks and semi-landmarks used for the geometric morphometric analyses. **A.** Specimen ZSM 86/1911 in dorsal view. **B.** Specimen ZSM 68/1911 in lateral view. Landmark points are shown in grey and semi-landmark points are shown in white. The shape described by semi-landmarks is shown as dotted line. Scale bar 2 cm.

The landmark and semi-landmark coordinates of both datasets were superimposed separately using Generalized Procrustes Analysis (GPA) in tpsrelw (Rohlf 2003), which serves to minimize non-shape variation between species, including that caused by size, location, orientation and rotation (Gower 1975; Rohlf & Slice 1990). To reduce the effects of variation due to the arbitrary spacing of the semi-

landmarks over the sampled curves, semi-landmarks were slid along their tangent to align with the perpendicular of corresponding semi-landmarks, minimizing the Procrustes distance. Thus, semi-landmarks capture primarily information about the bowing of the sampled curve (Bookstein 1997; Zelditch et al. 2004).

Before starting the analyses, the percentage error for each landmark and semi-landmark was computed for two specimens (one represented by a photograph and the other by a X-ray image; with $n = 10$ repetitions), each in dorsal and lateral view after the method of Singleton (2002) (Table S3.2, see supplementary information of Chapter 3). The methodological error for plotting landmarks by hand varies between 0.08 and 1.27 % and should have no significant impact on the shape analyses. Afterwards, the superimposed landmarks and semi-landmark data of each dataset were imported into MorphoJ 1.05d (Klingenberg 2011) and subjected to Principal Component Analysis (PCA) by generating a covariance matrix. This procedure assimilates data from all Procrustes coordinates and reduces them into a few dimensions with significant variance in a way that preserves as much variance as possible (see Hammer & Harper 2006).

ONTOGENETIC PATTERNS

In order to assign the observed shape changes to different types of intraspecific variation and to visualize ontogenetic changes in skull shape, we performed a multivariate regression in MorphoJ on the Procrustes coordinates as well as the scores of the first two PC axes against log-transformed centroid size. If an ontogenetic signal is present then a statistical correlation between size and shape should be detectable. The degree of correlation was estimated as a percentage of total shape variation, with a

corresponding p value computed by a permutation test with 10 000 permutations and a null hypothesis of independence (see Drake & Klingenberg 2008). Additionally, we tested the correlation between shape and size by performing a two-block partial least squares (2B-PLS) in MorphoJ using the Procrustes coordinates and centroid size. This method explores the pattern of covariation between two sets of variables by constructing pairs of variables that are linear combinations of the variables within each of the two sets, and it accounts for as much as possible of the covariation between the original datasets. In contrast to linear regression models (which casts one set of variables as dependent on the other), 2B-PLS treats the two sets of variables symmetrically in an attempt to find relationships between them without assuming that one is the cause on the other (Rohlf & Corti 2000; Zelditch et al. 2004). The strength of the correlation is given by the RV coefficient (see Robert & Escoufier 1976) and a p value generated by 10 000 permutations. In order to test if the results could be falsified by use of two different sources of samples (i.e. photographs and X-ray images) we repeated the analyses excluding all specimens represented by X-ray images and compared the results to the previous analyses.

SEXUAL DIMORPHISM

To determine whether skull shape is related to sex we created a second dataset including only mature males and females and performed a new generalized Procrustes fit. We assessed the statistical significance of differences between males and females based on the Procrustes coordinates using NPMANOVA (nonparametric multivariate analysis of variance) with 10 000 permutations and Euclidian distances using the software PAST 2.09 (Hammer et al. 2001). This approach tests for significant differences in the distribution of groups within the morphospace (Anderson 2001). One of the strengths of

this approach is that it does not assume or require normality from the multivariate data. The test generates F and p values, with a significant difference between the sexes indicated when the F value is high and the p value less than 0.05. Due to size differences between males and females it is possible that apparent sexual dimorphism is largely due to size. In order to detect evidence for non-size related sexual dimorphism we repeated the analysis mentioned above with the non-allometric residuals, which were separated from the Procrustes coordinates by a multivariate, pooled within-group regression against log-transformed centroid size. The resulting residuals contain the non-allometric component of shape variation within the dataset (Drake 2011). If a significant difference remains in the NPMANOVA, one can conclude that males and females show sexual dimorphism in cranial shape that is not related to size.

SHAPE VS. FUNCTION

In order to test if function is correlated with shape variation in the cranium we follow Erickson et al. (2003), who propose an allometric relationship between bite force and skull length. We used the bite force performance of *Alligator mississippiensis* in relation to skull length as functional proxy. The bite force was estimated for every specimen and log transformed. We performed a 2B-PLS in MorphoJ to determine the degree of covariation of bite force with cranial shape. Furthermore, we performed regression analyses between bite force and Procrustes coordinates. Both, the 2B-PLS and the regression analyses were performed as explained above (see Ontogenetic and allometric patterns section). To test if bite force is only correlated with allometric shape changes we additionally performed all analyses with non-allometric residuals. As described above, we excluded all specimens represented by X-ray images in further dataset to verify if the results are falsified by the usage of two different sources of samples.

RESULTS

In dorsal view the first two axes accounts for over 80 % of total variance (PC 1: 71.07 % and PC 2: 9.90 %). The first PC axis mainly accounts for the relative length of the snout, the relative size and position of the orbit influencing the relative width of the jugal region and the interorbital width, the relative length and width of the skull roof table and the position of the jaw angle in anterolateral-posteromedial direction. The second PC axis is primarily associated the shape of the snout tip, the position of the orbit influencing the length of the snout and the postorbital region inversely and the overall width of the postrostrum influencing the relative width of the occipital region and the position of the jaw joint in anteromedial-posterolateral direction (Fig. 3.2).

In lateral view the first two PC axes accounts for almost 80 % of total variance (PC 1: 74.96 % and PC 2: 5.97 %). The first PC accounts for mainly the depth of the tip of the rostrum, the relative size of the subnarial gap, the shape and length of the ventral margin of the maxilla, the relative size of the orbit influencing the overall depth of the jugal and the orbital and postorbital region and the relative position of the jaw joint in anteroventral-posterodorsal direction. The second PC accounts for the shape and the relative length of the premaxilla, the relative length of the maxilla and the length of the postorbital region (Fig. 3.3).

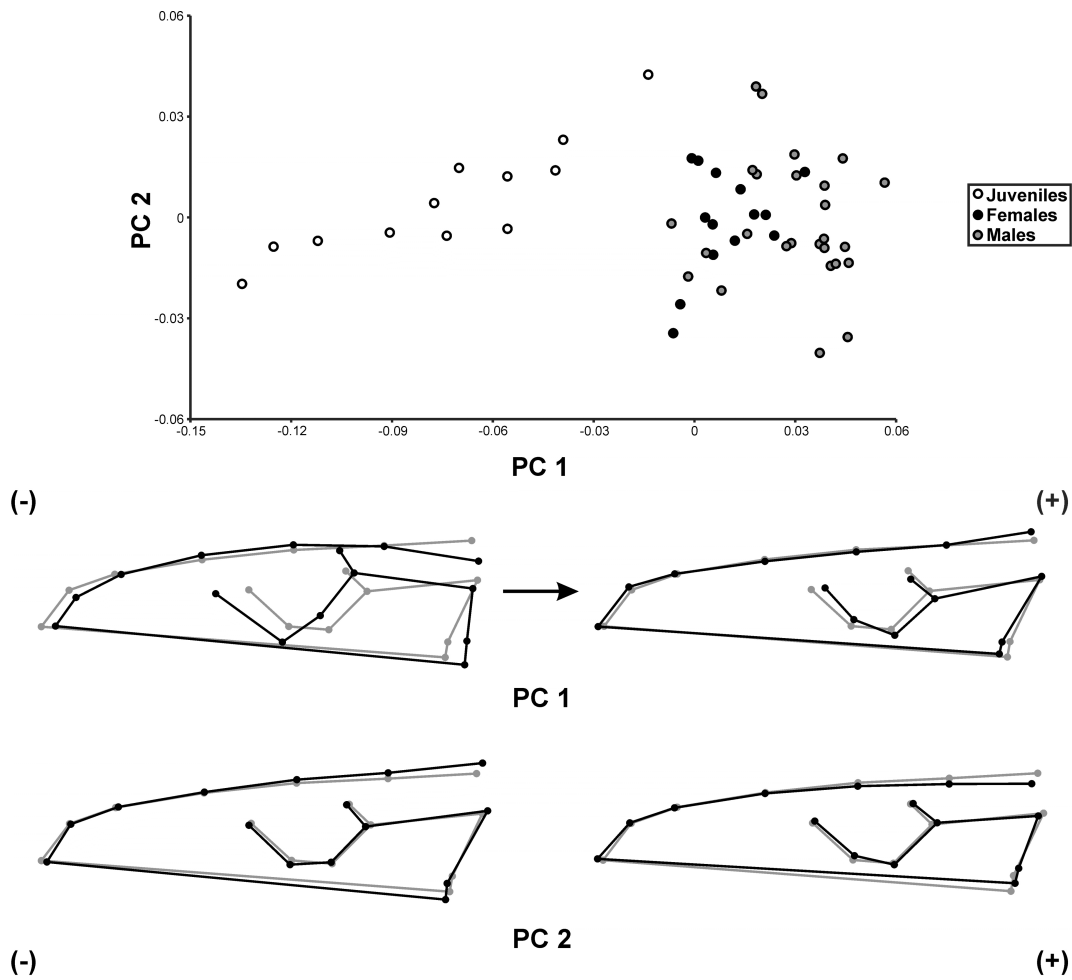


Fig. 3.2. Two-dimensional cranial morphospace and major shape changes (black outlines) of *Melanosuchus* in respect to the consensus shape (grey outline) for the dorsal view. The arrows indicate shape changes along the first principal component axis (PC1) that is highly correlated with centroid size (log-transformed).

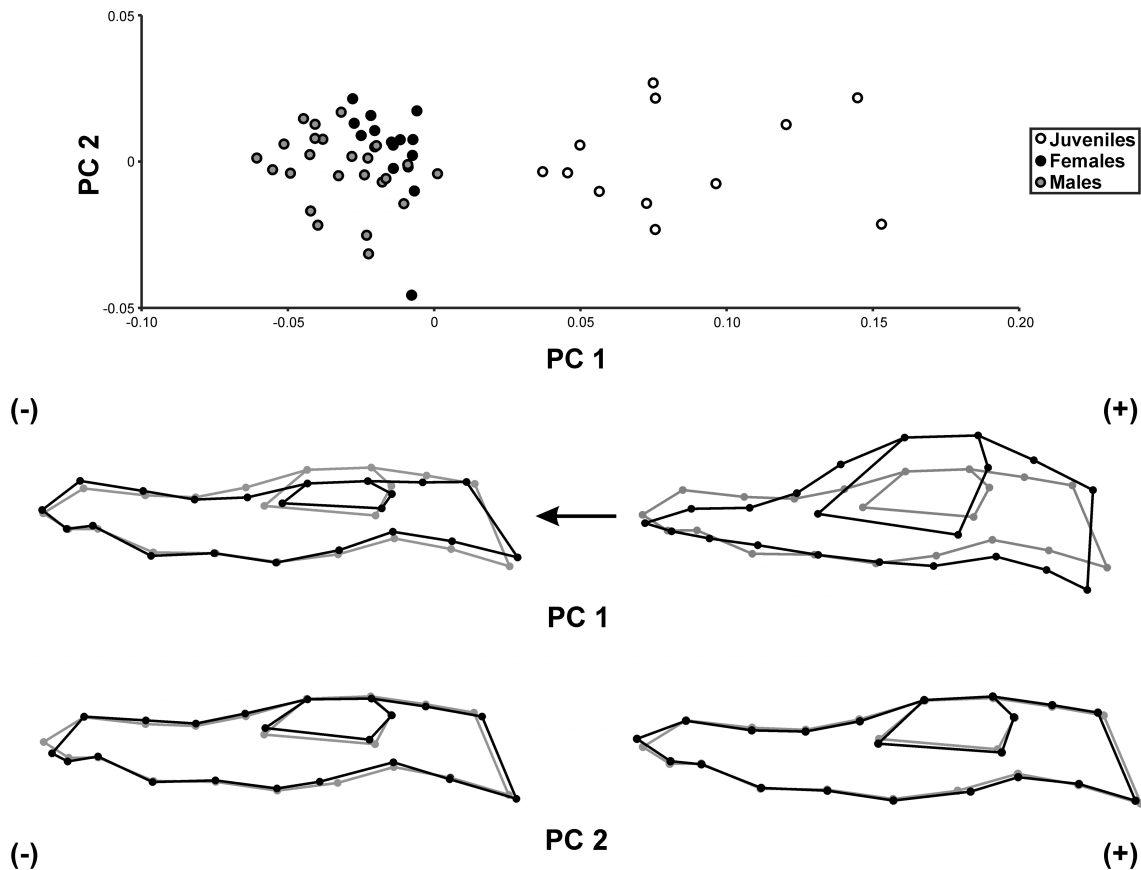


Fig. 3.3. Two-dimensional cranial morphospace and major shape changes (black outlines) of *Melanosuchus* in respect to the consensus shape (grey outline) for the lateral view. The arrows indicate shape changes along the first principal component axis (PC1) that is highly correlated with centroid size (log-transformed).

Based on the 2B-PLS and the regression test, skull shape (in both views) is strongly correlated with centroid size (log-transformed), indicating that the observed skull shape variation contains a linear allometric relationship between shape and size. This relationship only holds for the first PC however (Table 3.1), with the remaining PCs not correlated with centroid size. Males and females possessing similar centroid sizes are not separated from each other (Fig. 3.4A, B). The exclusion of those specimens represented by X-ray images from the datasets has no significant impact on

the general results, but the estimated correlations are slightly weaker. Skull shape is still correlated with centroid size (log-transformed) when only adult specimens are considered. However, these correlations are noticeably weaker than in the two previous cases.

Table 3.1. Relationship between skull shape, centroid size and bite force in *Melanosuchus niger* based on regression test (proportion of total variation in percent / p value) and the two block- partial least squares analysis (2B-PLS; RV coefficient / p value); (*) pooled analyses.

Centroid size	Dorsal view		Lateral view	
	Regression	2B-PLS	Regression	2B-PLS
Proc. coordinates (all)	65.28/<0.001	0.905/<0.001	68.97/<0.001	0.913/<0.001
PC 1 (all)	91.53/<0.001	0.955/<0.001	91.79/<0.001	0.918/<0.001
PC 2 (all)	1.25/0.437	0.013/0.430	0.90/0.510	0.009/0.500
Proc. coordinates (no X-ray)	48.44/<0.001	0.816/<0.001	51.58/<0.001	0.844/<0.001
PC 1 (no X-ray)	87.05/<0.001	0.871/<0.001	86.19/<0.001	0.862/<0.001
PC 2 (no X-ray)	0.92/0.527	0.009/0.533	5.82/0.108	0.058/0.109
Proc. coordinates (adults)*	15.83/<0.001	0.345/<0.001	16.83/<0.001	0.399/<0.001
Bite Force				
Proc. coordinates (all)	66.36/<0.001	0.920/<0.001	69.34/<0.001	0.918/<0.001
PC 1 (all)	93.07/<0.001	0.931/<0.001	92.27/<0.001	0.923/<0.001
PC 2 (all)	1.64/0.364	0.016/0.372	1.69/0.353	0.017/0.365
Proc. coordinates (no X-ray)	50.57/<0.001	0.852/<0.001	51.08/<0.001	0.836/<0.001
PC 1 (no X-ray)	91.15/<0.001	0.912/<0.001	84.93/<0.001	0.849/<0.001
PC 2 (no X-ray)	1.41/0.443	0.014/0.431	7.53/0.068	0.075/0.068
Res. coordinates (all)	0.08/1.000	0.002/1.000	0.09/1.000	0.002/1.000
Res. coordinates (no X-ray)	0.29/0.999	0.006/0.100	0.06/1.000	0.001/1.000

Based on the Procrustes coordinates a significant difference was found between males and females for both dorsal and lateral view (dorsal view: $F = 4.31$, $p = 0.002$; lateral view: $F = 4.62$, $p < 0.001$). The significant differences between both sexes still

remains by using the non-allometric residuals, but at a lower level (dorsal view: $F = 2.18$, $p = 0.020$; lateral view: $F = 2.33$, $p = 0.033$).

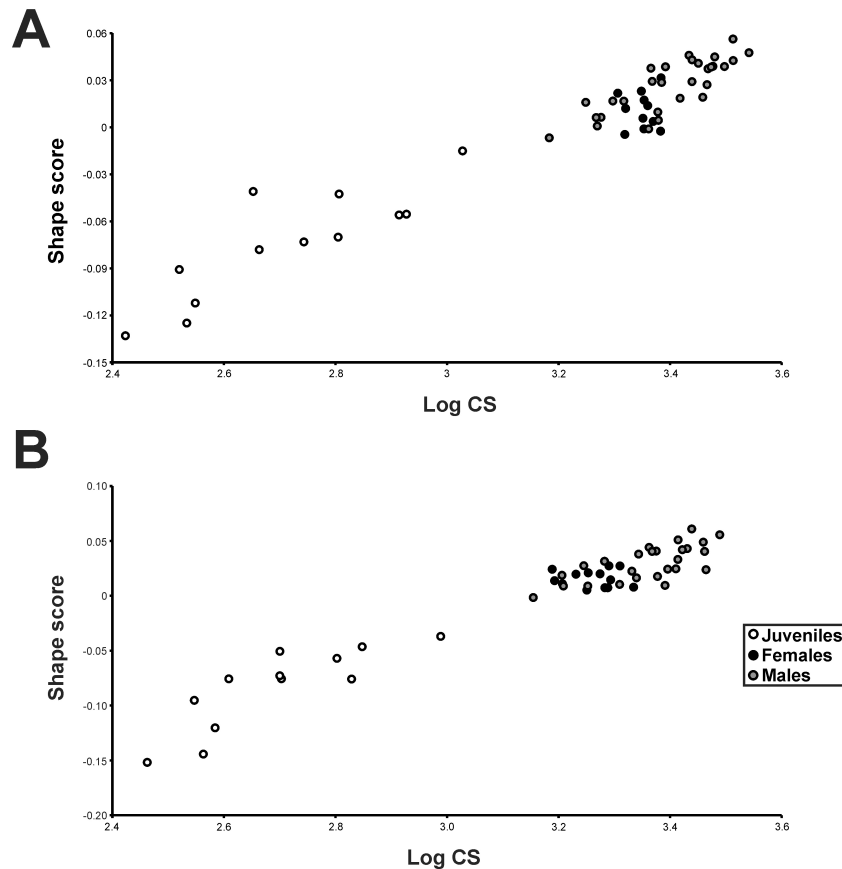


Fig. 3.4. Relationship between skull shape and centroid size. **A.** Regression between skull shape and centroid size in dorsal view. **B.** Regression between skull shape and centroid size in lateral view.

Both the 2B-PLS and the regression test indicate that Procrustes shape variation in *Melanosuchus niger* is significantly correlated with bite force (log-transformed) (Table 3.1). This relationship is mainly influenced by PC 1, which is also strongly correlated with centroid size (see above). By contrast, no significant correlation remains after the excluding allometric information from shape. These results remain if all specimens represented by X-ray images are excluded from the dataset.

DISCUSSION

ONTOGENETIC PATTERNS

The correlation between overall shape and centroid size (log-transformed) in *Melanosuchus niger* may represent an ontogenetic pattern, which is characterized by the shape change captured by the first PC. Skulls of young juveniles have a very short snout, which is wide in dorsal view, but dorsoventrally pointed, and the ventral margin is straight. The orbit is very large, the jugal region is slender in both dorsal and lateral view and the postorbital region is elongated in anterior-posterior direction. The broad skull roof table is posteriorly inclined in lateral view. The posterior end of the skull is relatively narrow and the jaw joint lies substantially anterior to the posterior end of the skull roof table. During ontogeny the snout becomes longer due to the elongation of the maxilla, but also narrower (in dorsal view) and deeper (in lateral view). The tip of the snout becomes blunter and a subnarial gap is developed between premaxilla and maxilla. The ventral margin of the maxilla becomes anteriorly convex in lateral view. The postrostrum becomes flattened and the relative size of the orbit decreases. In contrast, the jugal region becomes broader and deeper. The postorbital region becomes shorter, but expands posterolaterally. Due to the overall flattening of the postrostrum the skull roof table becomes straight in lateral view and the jaw joint moves substantially posterior to this.

As was mentioned in the introduction, the numbers of studies investigating the cranial shape variation of crocodylians using geometric morphometric is rare. This is especially true for ontogenetic studies (see Monteiro et al. 1997; Piras et al. 2010). On the other hand, in the past ontogenetic variation of crocodylian skulls was studied multiple times by traditional morphometrics (e.g. Dodson 1975; Webb & Messel 1978;

Hall & Portier 1994; Monteiro & Soares 1997; Wu et al. 2006). As no standardized samplings and analyses do exist so far, we compared the ontogenetic shape variation of *Melanosuchus niger* with that of other crocodylian species taken from literature (Table 3.2). However, due to differences in the sampling of skull measurements, landmark configurations and statistical analyses in the studies mentioned above, the current comparison is limited to whether certain skull regions growth allometric (positive or negative) or isometric during ontogeny.

Melanosuchus niger shares a relative increase of snout length with all extant crocodylians except *Tomistoma schlegelii* and *Gavialis gangeticus* (Piras et al. 2010). A relative increase of the width of the snout during ontogeny occurs also in *Alligator sinensis* (Wu et al. 2006), *Crocodylus acutus*, *Mecistops cataphractus* and *Tomistoma schlegelii* (Piras et al. 2010), whereas *Caiman crocodilus* and *Caiman yacare* (Monteiro & Soares 1997) show a relative narrowing of the rostral width. In *Alligator mississippiensis* the posterior part of the snout grows isometrically, but the snout tip increases in width (Dodson 1975), whereas in *Crocodylus novaeguineae* snout width decreases from early juveniles to small adults, but increases again in later ontogenetic stages (Hall & Portier 1994). In *Caiman latirostris* snout width grows isometrically (Monteiro & Soares 1997). A relative ontogenetic increase of the depth of the snout occurs in *Crocodylus acutus*, *Mecistops cataphractus* and *Tomistoma schlegelii*. The relative decrease of the orbit size is the only common ontogenetic pattern that is present in all taxa used for comparison. A further common ontogenetic pattern in crocodylians is the relative increase of the interorbital width, which is only absent in *Alligator sinensis*. Another common pattern is the relative decrease in length of the postorbital skull roof, which is probably related to the relative increase of the snout length

mentioned above (see Marugán-Lobón & Buscalioni 2003). However, in *Tomistoma schlegelii* and *Gavialis gangeticus* the postorbital skull roof grows almost isometrically. Finally, most taxa show a relative increase of the posterior width of the postorbital region during ontogeny with the exception of *Alligator mississippiensis*, *Alligator sinensis*, *Caiman crocodilus*, *Caiman yacare* and *Gavialis gangeticus*, which show isometric growth.

Based on this simplified comparison, most crocodylian taxa share similar ontogenetic patterns in skull shape and some ontogenetic trajectories seem to be relatively constrained (e.g. the relative increase of the snout length together with relative decrease of the postorbital length, the relative decrease of the orbit size together with the relative increase of the interorbital width). The only exception is the long-snouted *Gavialis gangeticus*, which shows an almost isometric growth of the skull during ontogeny (see also Piras et al. 2010). However, the current comparison of ontogenetic trends in crocodylian skulls is very limited, as the available ontogenetic studies on crocodylian skulls are not standardized in sampling and methods. Thus, with the data on hand it is not possible to compare how strong certain skull regions growth relative to others and how ontogenetic patterns in the cranium differ within different taxa in detail. To improve our understanding of cranial ontogeny in crocodylians also with respect to heterochronic events within their evolution, it would be worthwhile to investigate ontogenetic shape variation in the future with broader taxon and specimen sampling and with standardized methods.

Table 3.2. Ontogenetic patterns in the skull of *Melanosuchus* and other extant crocodylian species. (+) Positive allometric growth, (-) negative allometric growth, (=) isometric growth; (1) Monteiro & Soares (1997); (2) Dodson (1975); (3) Wu et al. (2006); (4) Piras et al. (2010); (5) Hall & Portier (1994); (6) Monteiro et al. (1997); (7) Webb & Messel (1978).

Species	Ref.	Snout (= rostrum)			Orbital region		Postorbital region	
		length	width	depth	orbit size	interorbital width	length (skull roof)	posterior width
<i>Melanosuchus niger</i>		+	+	+	-	+	-	+
<i>Caiman crocodilus</i>	1, 6	+	-	?	-	+	-	=
<i>Caiman latirostris</i>	1, 6	+	=	?	-	+	-	+
<i>Caiman yacare</i>	1, 6	+	-	?	-	+	-	=
<i>Alligator mississippiensis</i>	2	+	+/=	?	-	+	?	=
<i>Alligator sinensis</i>	3	+	+	?	-	-	-	=
<i>Crocodylus acutus</i>	4	+	+	+	-	?	-	+
<i>Crocodylus novaeguineae</i>	5	+	+/-	?	-	+	+	+
<i>Crocodylus porosus</i>	7	+	?	?	-	+	?	+
<i>Mecistops cataphractus</i>	4	+	+	+	-	?	-	+
<i>Tomistoma schlegelii</i>	4	=	+	+	-	?	=	+
<i>Gavialis gangeticus</i>	4	=	=	=	-	?	=	=

SEXUAL DIMORPHISM

Sexual dimorphism in crocodylians is described for both Caimaninae (Verdade 2000, 2003) and Crocodylinae (Hall & Portier 1994; Platt et al. 2009) and mainly size related. The larger size in male crocodylians has been found to be the result of generally faster and longer growth (e.g. Chabreck & Joanen 1979; Rootes et al. 1991; Wilkinson & Rhodes 1997), probably resulting from different selective pressures faced by females and males (see Shine 1989; Platt et al. 2009). Female growth trajectories probably slow upon reaching sexual maturity as energy is shifted from growth to reproduction (see Andrews 1982), whereas males are subject to sexual selection favouring large body size in male-to-male interactions (see Anderson & Vitt 1990; Cooper & Vitt 1993). A size related sexual dimorphism is also present in *Melanosuchus niger*, in which the skull length of the largest males is about 30 % longer than that of the largest females.

In contrast, non-size related sexual variation seems to be less common in crocodylians. It is only documented for the shape of the external naris in *Gavialis gangeticus* (Hall & Portier 1994) and *Caiman latirostris* (Verdade 2000). Furthermore, Webb & Messel (1978) describe a non-size related sexual dimorphism in the interorbital width and width of the skull roof table in *Crocodylus porosus*. Thus, non-size related sexual dimorphism documented in these crocodylian taxa is only restricted to certain skull regions. Based on the results of the NPMANOVA the overall skull shape of males and females in *Melanosuchus niger* shows a non-size related sexual dimorphism. As mentioned in the *Material and methods* section, no information is known about how sex was determined for the single specimens and misidentification cannot be ruled out. However, a wrong identification of sex would rather result in a non-significant signal. Nevertheless, at this stage the current findings should be still seen with caution, as the sample size of females

($n = 14$) is distinctively smaller than that of males ($n = 26$). Furthermore, it is possible that the large number of landmarks and semi-landmarks compared to the sample size of both males and females could lead to wrong positive signals due an overestimation of the true degrees of freedom (Zelditch et al. 2004). Thus, the current findings should be tested in future examinations in greater detail with larger datasets for *Melanosuchus niger*, different landmark configurations (also with a three-dimensional approach) as well as for other crocodylians.

SHAPE VS. FUNCTION

That allometric skull shape variation in *Melanosuchus niger* is significantly correlated with bite force performance (log-transformed) is not surprising because the functional proxy used in this study is correlated with skull size (see Erickson et al. 2003, 2004b, 2012). Deleting allometric information from shape leads to a non-significant signal, showing that this correlation seems to be primarily related to allometric shape changes caused by ontogenetic growth (see above). However, in recent crocodylians, stress distributions during biting do not distribute over the whole skull uniformly, but are largely concentrated in the postrostrum, peaking around the orbits and the temporal fenestrae during bilateral and unilateral biting, and laterally at the level of the jugal during lateral loading to the snout (Pierce et al. 2008). Thus, the strong correlation found between bite force performance and ontogenetic shape variation is probably an artefact of the allometric dependency of both parameters. Based on the biomechanical results of Pierce et al. (2008) only the shape changes seen in the postrostral region (including the expansion of the jugal, the relative decrease of the orbit size and the posterolateral expansion of the postorbital region) seems to be functionally related. In this context, the posterolateral expansion of the postorbital region might further

correlate with the increase of the muscle system in the postorbital region to achieve higher bite performance (see Schumacher 1973; van Drongelen & Dullemeijer 1982; Busbey 1989; Erickson et al. 2003, 2012; Bona & Desojo 2011).

Based on the results of recent studies on cranial function in several crocodylian species with different snout morphologies, snout shape is not strongly correlated with function but instead with prey selection (McHenry et al. 2006; Pierce et al. 2008; Erickson et al. 2012). Thus, it is likely that the shape changes seen in the snout of *Melanosuchus niger* (including the relative increase of the snout length and depth, the formation of a subnarial gap and the shape changes of the ventral margin of the maxilla) are rather related to changes in diet preferences and feeding behavior through ontogeny. Hatchlings and small *Melanosuchus niger* possessing skulls with a short pointed snout feed predominantly on aquatic and shoreline invertebrates (e.g. insects, beetles and snails) (Da Silveira & Magnusson 1999; Horna et al. 2001, 2003), whereas adults possessing deep and elongated snouts with a subnarial gap feed on medium-sized prey, such as capybaras (*Hydrochoerus hydrochaeris*), white-lipped peccaries (*Tayassu pecari*), long-whiskered catfishes (Pimelodidae) and piranhas (Trutnau 1994; Horna et al. 2001). Similar dietary shifts from small invertebrates to medium-sized vertebrates during ontogeny are also documented for other crocodylian species (Cott 1961; Webb & Messel 1978; Hutton 1987; Webb et al. 1991; Cleuren & de Vree 2000). Especially, the development of a convex shape of the anterior part of the ventral margin of the maxilla could be related to the development of a prominent upper caniniform tooth, which is used primarily for seizing larger prey (Erickson et al. 2012). In this context, the ontogenetic shape changes in the jugal and postorbital region (see above) provide the mechanical background for handling larger prey.

Finally, the usage of two different sample sources (i.e. photographs and X-ray images) affected only the selection of landmarks in order to capture skull shape, as many skull structures (e.g. bone sutures or the lateral temporal fenestra) were not visible in the X-ray images. However, the similar results regarding the relation between shape, centroid size and bite forces for both datasets with and without X-ray images (Table 3.1) as well as the minor error for plotting landmarks on both sample sources (Table S3.2, see supplementary information of Chapter 3) indicate that the usage of photographs and X-ray images together did not falsify the current results.

CONCLUSIONS

The present study represents the first assessment of intraspecific variation of the skull of the caimanine crocodylian *Melanosuchus niger* using a geometric morphometric approach. Skull shape variation is concentrated in the width and height of the postorbital region, the length and depth of the snout, the size of the orbit, and the relative position of jaw joint. Similar patterns can be observed in the cranial ontogeny of other crocodylian taxa, but due to the lack of broad-scale examinations with standardized landmark configurations and statistical methods the results of the current comparison is limited regarding the quality of change. The ontogenetic shape changes in *Melanosuchus niger* seems to be correlated with increased bite force performance, but are primarily restricted to the postrostral region. In contrast, shape variation seen in the snout is probably rather related to the changes in diet through ontogeny. Based on the current results the skull shape of females and males differ on a significant level, even when allometric shape variation is reduced. However, the presence of a non-size related sexual dimorphism in *Melanosuchus niger* should be seen as preliminary result due to the small sample sizes in relation to the number of landmarks and semi-landmarks and

differences of sample size between males and females, and thus, has to be tested in future examinations in more detail. Because knowledge of intraspecific variation is important for the systematics of extant, but also extinct taxa, it would be worthwhile investigating ontogenetic patterns in different crocodylian taxa with help of standardized methods (see e.g. Piras et al. 2010) to capture broad-scale patterns of intraspecific variation and specific trajectories in crocodylian ontogeny more precisely. This may in turn allow us to resolve the taxonomic status of problematic extinct species such as *Melanosuchus fisheri*.

ACKNOWLEDGEMENTS

We thank Frank Glaw (Zoologische Staatssammlung München) who allowed two of us (JBD, CF) to study the specimens under his care, and for providing helpful information concerning historical collection data. We further thanks Martin Dobritz (Institut für Radiologie, Klinikum rechts der Isar, Technische Universität München), Jakob Hallermann (Zoologisches Museum Hamburg, Universität Hamburg), Heinz Grillitsch and Richard Gemel (Naturhistorisches Museum Wien), Gunther Köhler and Linda Acker (Senckenberg Naturmuseum Frankfurt) and Dennis Rödder and Ursula Bott (Zoologisches Forschungsmuseum Alexander Koenig, Bonn) for additional photo material, access to collections and technical support for the production of the X-ray images. We further thank Richard Butler, Roland Sookias (GeoBio-Center, Ludwig-Maximilians-University, München), Oliver Rauhut (Bayerische Staatssammlung für Paläontologie und Geologie, München), Melissa Tallman (Department of Biomedical Sciences, Grand Valley State University, Allendale), David Gower (Life Sciences Department, Natural History Museum, London) and Abby Drake (Department of Biology, Dana Science Center, Skidmore College, Saratoga Springs) for comments and

suggestions on an early version of the manuscript. This research was partially funded by the Agencia Nacional de Promoción Científica y Técnica PICT 2010 N°207, Alexander von Humboldt Foundation (to JBD) and Deutsche Forschungsgemeinschaft (Project RA 1012/12-1) (to CF).

CHAPTER 4

Do different disparity proxies converge on a common signal? Insights from the cranial morphometrics and evolutionary history of Pterosauria (Diapsida: Archosauria)

Keywords:

Disparity; macroevolution; skull shape; Pterosauria; Monofenestrata; geometric morphometrics; phylogeny; phylogenetic comparative methods; Mesozoic

The chapter was published as:

Foth C^{1,2}, Brusatte SL^{3,4} & Butler RJ^{2,5}. 2012. Do different disparity proxies converge on a common signal? Insights from the cranial morphometrics and evolutionary history of Pterosauria (Diapsida: Archosauria). *Journal of Evolutionary Biology* 25: 904-915.

¹*Bayerische Staatssammlung für Paläontologie und Geologie, Richard-Wagner-Str. 10, D-80333 München, Germany*

²*Department of Earth and Environmental Sciences, Ludwig-Maximilians-University, Richard-Wagner-Str. 10, D-80333 München, Germany*

³*Division of Paleontology, American Museum of Natural History, Central Park West at 79th Street, New York, NY 10024, USA*

⁴*Department of Earth and Environmental Sciences, Columbia University, New York, NY, USA*

⁵*GeoBioCenter, Ludwig-Maximilians-University; Richard-Wagner-Str. 10, D-80333 München, Germany*

Received 11 January 2012; revised 26 January 2012; accepted 27 January 2012

Author contribution:

Research design: **Christian Foth**, Stephen Brusatte, Richard Butler

Data collection: **Christian Foth**, Richard Butler

Data analyses: **Christian Foth**, Stephen Brusatte

Preparation of figures and tables: **Christian Foth**

Wrote paper: **Christian Foth**, Stephen Brusatte, Richard Butler

***All figures of Chapter 4 are modified after Foth et al. (2012)**

Do different disparity proxies converge on a common signal? Insights from the cranial morphometrics and evolutionary history of Pterosauria (Diapsida: Archosauria)

Christian Foth, Stephen L. Brusatte & Richard J. Butler

ABSTRACT

Disparity, or morphological diversity, is often quantified by evolutionary biologists investigating the macroevolutionary history of clades over geological timescales. Disparity is typically quantified using proxies for morphology, such as measurements, discrete anatomical characters, or geometric morphometrics. If different proxies produce differing results, then the accurate quantification of disparity in deep time may be problematic. However, despite this, few studies have attempted to examine disparity of a single clade using multiple morphological proxies. Here, as a case study for this question, we examine the disparity of the volant Mesozoic fossil reptile clade Pterosauria, an intensively studied group that achieved substantial morphological, ecological, and taxonomic diversity during their 145+ million year evolutionary history. We characterise broadscale patterns of cranial morphological disparity for pterosaurs for the first time using landmark-based geometric morphometrics, and make comparisons to calculations of pterosaur disparity based on alternative metrics. Landmark-based disparity calculations suggest that monofenestratan pterosaurs were more diverse cranially than basal non-monofenestratan pterosaurs (at least when the aberrant anurognathids are excluded), and that peak cranial disparity may have occurred in the Early Cretaceous, relatively late in pterosaur evolution. Significantly, our cranial disparity results are broadly congruent with those based on whole skeleton discrete

character and limb proportion datasets, indicating that these divergent approaches document a consistent pattern of pterosaur morphological evolution. Therefore, pterosaurs provide an exemplar case demonstrating that different proxies for morphological form can converge on the same disparity signal, which is encouraging because often only one such proxy is available for extinct clades represented by fossils. Furthermore, mapping phylogeny into cranial morphospace demonstrates that pterosaur cranial morphology is significantly correlated with, and potentially constrained by, phylogenetic relationships.

INTRODUCTION

Evolutionary biologists often calculate measures of morphological disparity to help understand the macroevolutionary history of clades over long time scales (Gould 1991; Wills et al. 1994; Erwin 2007). Disparity is essentially a morphological equivalent of taxonomic diversity: it measures the variety of anatomical features expressed by a group. By tracking disparity over time and among taxa, biologists can assess the pace at which clades developed novel morphologies, determine how morphological variability was affected by evolutionary radiations and mass extinctions, and test whether certain groups were more morphologically variable than others (perhaps due to key innovations or differential niche exploitation). Disparity studies also allow taxa to be plotted into a morphospace: a visual representation of the range of morphological form expressed by the species in question.

Studies of disparity are predicated on a straightforward but difficult issue: how best to quantify the morphology of organisms using manageable proxies. Three general

proxies are often used, each of which is compiled for every species in an analysis so that morphology can be measured equivalently: measurements (e.g. Foote 1993; Lefebvre et al. 2006; Dyke et al. 2009), geometric morphometric landmarks (e.g. Foote 1993; Smith & Lieberman 1999; Friedman 2010; Brusatte et al. 2012a), and discrete characters (e.g. Foote 1994; Wills et al. 1994; Lupia 1999; Brusatte et al. 2008; Ruta 2009; Butler et al. 2012). Because the accuracy of disparity studies hinges on the choice of proxies, it is desirable that different proxies converge on the same signals. For instance, if discrete characters indicate that there was a rapid rise in disparity during the early history of a group, it is hoped that measurements or geometric landmarks would show the same result. Surprisingly, this has not been widely tested with empirical case studies. Villier & Eble (2004) used multiple proxies to quantify the disparity of echinoids, which generally gave consistent results. It is currently unknown, however, whether measurements, landmarks, and discrete characters give concordant or discordant results in any vertebrate clades, which recently have become more frequent subjects of disparity study than non-vertebrate groups (e.g. Brusatte et al. 2008; Ruta 2009; Friedman 2010; Prentice et al. 2011; Butler et al. 2012).

Pterosaurs, the familiar Mesozoic flying reptiles, are an excellent case study for assessing this question. Pterosaurs were the earliest vertebrates to evolve active flapping flight (Padian 1983, 1985). The oldest pterosaur fossils date from the Late Triassic (c. 210 Ma), and the clade formed an important component of terrestrial vertebrate diversity for nearly 150 million years, prior to their extinction at the end of the Cretaceous (65.5 Ma) (Wellnhofer 1991; Unwin 2006; Butler et al. 2009a). During their evolutionary history pterosaurs evolved considerable taxonomic (> 140 species currently recognised: Barrett et al. 2008; Butler et al. 2009a, 2011a) and morphological

diversity (Butler et al. 2011a, 2012; Prentice et al. 2011). Body size estimates range from a mere 5-35 g for the frogmouth-like aerial insectivore *Anurognathus* up to 259–544 kg for the giant stork-like *Quetzalcoatlus*, whose wingspan is estimated at 10–12 m (Witton 2008; Henderson 2010; Witton & Habib 2010). Ecologically, skeletal morphology has been used to suggest a diverse range of feeding strategies within the clade, including piscivory, filter-feeding, insectivory, molluscivory, frugivory, aerial predation, vulture-like scavenging, and stork-like stalking and scavenging (e.g. Bonaparte 1970; Wellnhofer 1991; Ősi et al. 2005; Unwin 2006; Bennett 2007; Witton & Naish 2008; Lü et al. 2010a). In short, pterosaurs were a remarkable radiation of extinct reptiles, and understanding their evolutionary history promises to unlock more general insights into the development of novel body plans, locomotion styles (flight) and ecological behaviours over deep time.

Recent years have seen an explosion of scientific interest in pterosaurs, with the discovery of spectacular new fossils and fossil assemblages (e.g. Wang et al. 2005; Lü et al. 2010a, 2011), new insights into palaeobiology (e.g. Wilkinson et al. 2006; Butler et al. 2009b; Claessens et al. 2009; Palmer & Dyke 2010), the development of new phylogenetic hypotheses (e.g. Andres & Ji 2008; Andres 2010; Andres et al. 2010; Lü et al. 2010a) and synthetic work focusing on the macroevolutionary history and diversity of the group (e.g. Dyke et al. 2006, 2009; McGowan & Dyke 2007; Butler et al. 2009a, 2011a, 2012; Prentice et al. 2011). A particularly vigorous research program has developed concerning the temporal and phylogenetic patterns of morphological and taxonomic diversity amongst pterosaurs, and the impact of variable fossil record quality on our understanding of these patterns (Dyke et al. 2009; Butler et al. 2009a, 2011a, 2012; Andres 2009; Benton et al. 2011; Prentice et al. 2011). Among the most

interesting topics of debate is whether the morphological diversity of pterosaurs peaked early or late in the Mesozoic history of the group, and whether different clades of pterosaurs were more or less morphologically diverse than others, perhaps due to the development of novel diets and ecologies (e.g. Dyke et al. 2006, 2009; Prentice et al. 2011; Butler et al. 2011a, 2012). Previous authors have assessed these questions by using both discrete characters (Prentice et al. 2011; Butler et al. 2011a, 2012) and measurements (Dyke et al. 2009) to quantify disparity.

Here, we characterise broadscale patterns of cranial morphological diversity for pterosaurs for the first time using geometric morphometrics, a common technique (but one infrequently used to study Mesozoic reptile clades) that models a series of specimens using homologous landmarks, allows these specimens to be plotted into a morphospace, and then utilises multivariate statistics to tease out major patterns of shape variation (O'Higgins 2000; Zelditch et al. 2004). The purposes of this project are two-fold. First, the availability of cranial morphometric data allows us to assess whether disparity results based on this proxy (both temporal and clade-by-clade comparisons) are congruent with published results based on measurements and discrete characters. Second, we use cranial morphometrics to assess large-scale patterns in pterosaur morphological evolution. Our focus is on a handful of explicit questions. Did pterosaurs exhibit constant or variable disparity across their history? If the latter is true, did disparity peak early or late in the history of pterosaur evolution? Did certain pterosaur subgroups have significantly higher disparity than others? Is pterosaur cranial morphology significantly correlated with phylogeny, as would be indicative of phylogenetic constraint in pterosaur cranial shape evolution? Were there any major trends in cranial shape across pterosaur phylogeny? Taken together, the various

quantitative analyses have broad implications for our understanding of pterosaur evolutionary history and large-scale patterns of pterosaur cranial evolution during the Mesozoic.

METHODS

TAXON SELECTION

The taxonomy of pterosaurs used here is based primarily on Unwin (2006). Because the great majority of preserved pterosaur skull material is crushed or incomplete, we focused our analyses on cranial reconstructions in lateral view (supplemented by some photographs of complete, undistorted skulls). Unfortunately, such reconstructions and complete skulls are available for only a small fraction (~20%) of the known pterosaur species (see supplementary information of Chapter 4 for details of cranial reconstructions/photographs used). However, useable reconstructions were available for at least one species from nearly all significant ‘family’-level clades of pterosaurs, with the exception of the Early Cretaceous Istiodactylidae and the late Early-early Late Cretaceous Lonchodectidae. Thus, it is likely that we can successfully capture broadscale phylogenetic and temporal patterns of cranial morphological diversity across Pterosauria, even if it is not possible for us capture detailed variation within ‘family’-level clades.

GEOMETRIC MORPHOMETRICS

We analysed morphological variation in the skull (excluding the lower jaw) of pterosaurs using two-dimensional geometric morphometrics. The advantage of this approach is that it has high statistical power to detect shape differences, because landmark coordinates capture more information about shape than can be obtained from

traditional morphometric measurements (linear distances, ratios and angular measures), which are generally insufficient to capture the whole geometry of the original object (Rohlf 2000; Hammer & Harper 2006). Geometric morphometric approaches have been reviewed and discussed by many authors (e.g. Bookstein 1991; Elewa 2004; Zelditch et al. 2004), and the methods we use here are similar to those used in the recent morphometric study of Brusatte et al. (2012a).

We encapsulated the cranial geometry of 31 pterosaur species using 21 homologous landmarks (Fig. 4.1A, see supplementary information of Chapter 4 for full description), which were plotted onto published cranial reconstructions and photographs in lateral view (one image per species) using the program tpsDig2 (Rohlf 2005). We used landmarks of types 2 (good evidence for geometric homology, such as points of maximal curvature or extremities) and 3 (points constructed between two clearly homologous landmarks, which mainly define the shape of the skull or skull openings rather than the position of exact homologous points), following the terminology of Bookstein (1991). The usage of Type 3 landmarks is necessary because some reconstructions do not show the patterns of articulation for individual bones (because of poor preservation and crushing on the fossil specimens), and because in many species a number of elements are fused or reduced (see supplementary information of Chapter 4).

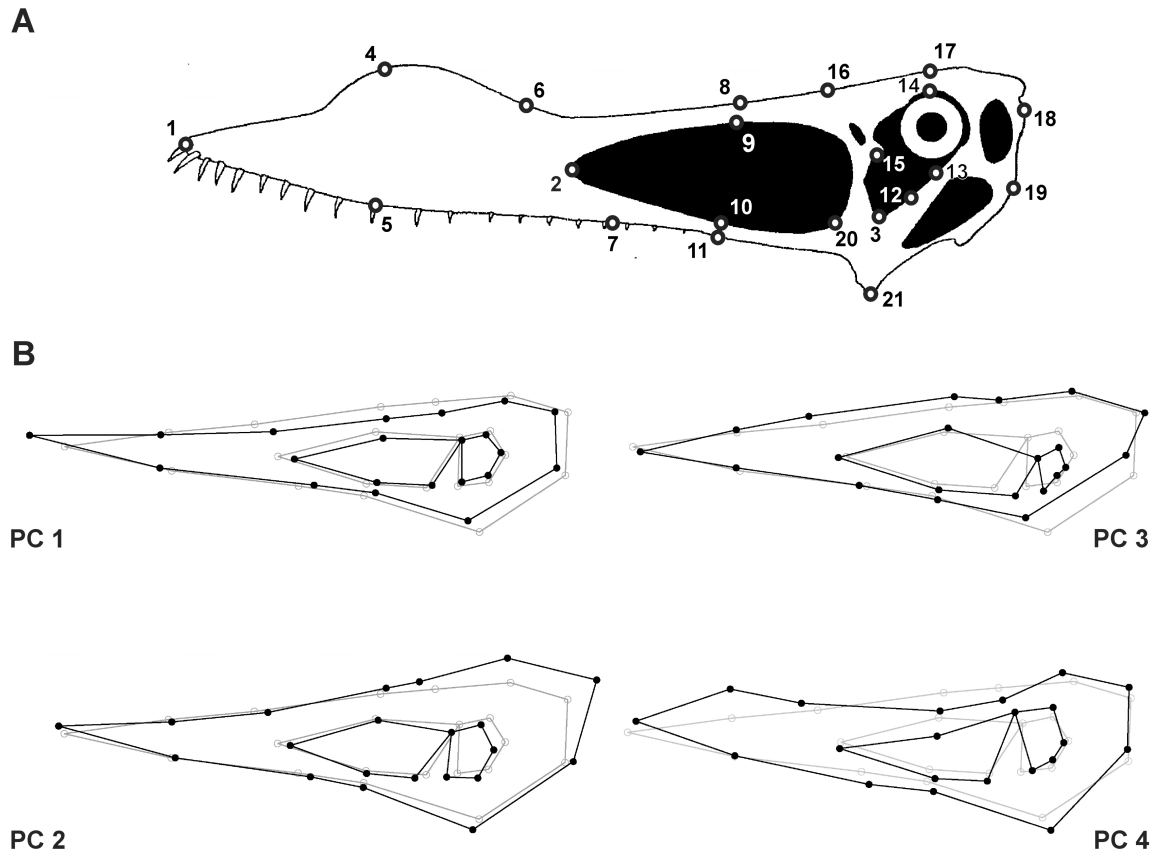


Fig. 4.1. Pterosaur skull shape analyzed using geometric morphometrics. **A.** Homologous landmarks used in the study plotted on a skull reconstruction of *Anhanguera santanae* (modified from Maisey 1991; see supplementary information of chapter 4 for further details, including lines used to reconstruct type 3 landmarks). **B.** Major changes in skull shape (black outlines) occurring on the first four principal component (PC) axes in respect to the calculated consensus shape (grey outlines) of the whole data set.

Thus, the dataset is focused primarily on the external shape of the skull, the dimensions of the naris + antorbital fenestra, and the size of the orbit. Unfortunately, we were not able to capture shape variation of the naris and the antorbital fenestra independently from each other, because in derived pterodactyloid pterosaurs the naris and the antorbital fenestra are conjoined into a single opening (the so called nasopreorbital fenestra). Therefore, both fenestrae are here treated together as a single

unit. Furthermore, our landmarks do not, in general, capture overall variation in the form of cranial crests (although some small degree of variation in these structures is likely incorporated due to the usage of type 3 landmarks), which are difficult to describe by homologous landmarks, often incompletely preserved, and are liable to swamp the dataset with characters related more to extravagant variation in display structures (see e.g. Bennett 2003; Martill & Naish 2006; Elgin et al. 2008; Tomkins et al. 2010; Hone et al. 2012) than to features related to underlying skull architecture and function (e.g. feeding).

The landmark coordinates were superimposed using Generalized Procrustes Analyses (GPA) in MorphoJ (Klingenberg 2011) which serves to minimise non-shape variation between species, such as that caused by size, location, orientation, and rotation (Zelditch et al. 2004). Next, the “corrected” landmarks were converted into a covariance matrix and subjected to Principal Component Analyses (PCA), also using MorphoJ. This procedure gathers together data from all landmarks and reduces it into a set of PC scores that summarise the skull shape of each taxon and describe maximal shape variation in a morphospace (Hammer & Harper 2006).

DISPARITY ANALYSES

Morphological disparity measures the anatomical diversity (variety) exhibited by a group of organisms (Foote 1993; Wills et al. 1994; Ciampaglio et al. 2001). Disparity calculations require a measure of morphological form for each organism being assessed, and as a proxy for pterosaur skull shape we used PC scores from the morphometric PCA. We examined temporal trends in cranial disparity by binning pterosaur taxa into four broad temporal bins (Late Triassic-Early Jurassic, Middle Jurassic-Late Jurassic,

Early Cretaceous, Late Cretaceous; see supplementary information of Chapter 4). Our assignment of species to temporal bins was based upon information taken from the *Paleobiology Database*. Large temporal bins were necessary because using finer-scale (shorter) bins would, in most cases, render sample sizes too small for meaningful statistical comparison. Coarse bins of similar (and sometimes identical) length have been used in previous studies of pterosaur morphological and taxonomic diversity (e.g. Dyke et al. 2006, 2009; Prentice et al. 2011; but see Butler et al. 2012).

Additionally, we examined taxonomic variation in disparity by measuring disparity for seven different groupings: non-monofenestratan pterosaurs ('rhamphorhynchoids'); non-monofenestratan pterosaurs excluding the aberrant Anurognathidae (which plot as outliers in morphospace and which have a highly unusual cranial morphology with an extremely short snout and an enlarged orbit. In that respect, anurognathids differs substantially from all other pterosaurs: e.g. Bennett 2007); Monofenestrata; Dsungaripteroidea; Azhdarchoidea; Ctenochasmatoidea; Ornithocheiroidea (see supplementary information of Chapter 4). The major clades of monofenestratan pterosaurs are all inferred to have originated at approximately the same time (by the Late Jurassic), and have traditionally been given equivalent rank-based names. Assignment of species to taxonomic groupings was based primarily on Unwin (2006), and we note that the first two of our bins are paraphyletic (they exclude monofenestratan pterosaurs). As an alternative, we also grouped monofenestratan pterosaurs in several different ways according to the topology of Andres & Ji (2008): Archaeopterodactyloidea; Ornithocheiroidea; Pteranodontoidea + *Nyctosaurus*; clade consisting of *Zhejiangopterus* + Tapejaridae + Dsungaripteridae + Azhdarchidae (see supplementary information of Chapter 4).

Four disparity metrics were calculated for each temporal or taxonomic grouping: the sum and product of the ranges and variances on the first six PC axes of the 31-taxon morphometric dataset, which together comprise more than 90% of total variance. The program RARE was used to perform these calculations (Wills 1998). Range measures summarise the total spread of morphospace occupied by the taxa in question, whereas variance denotes mean dissimilarity among the taxa (roughly equivalent to their spread in morphospace). Range metrics can be strongly biased by sample size differences, including those caused by uneven fossil sampling over time, but variance metrics are more robust (Wills et al. 1994; Butler et al. 2012). Statistical significance of disparity comparisons was assessed by the overlap or non-overlap of 95% confidence intervals, generated by bootstrapping, and rarefaction was used to assess whether disparity differences between groups are robust to sample size differences (both were also performed in RARE).

PHYLOGENETIC COMPARATIVE METHODS

An interesting question that has not previously been quantitatively addressed is whether trends in pterosaur morphological evolution are strongly related to (and perhaps constrained by) phylogeny. In the current case, the main question is: is pterosaur skull shape significantly correlated with phylogeny? A strong phylogenetic signal means that closely related species tend to fall out closer in morphospace than more distantly related species (Klingenberg & Gidaszewski 2010). One way to assess the degree of this correlation is to map the phylogeny into the morphospace. This requires an ancestral state reconstruction of the morphometric data (PC scores) for each internal node on the tree, which is accomplished in MorphoJ using squared change parsimony (Maddison 1991; Klingenberg 2011). This algorithm collates the sum of square changes of the PC

scores (which are continuous characters) along all branches of the tree and calculates the most parsimonious ancestral states for each node by minimising the total sum of squared change across the phylogeny. The optimal configuration is mathematically described by a tree length (= squared length) value, which can be used to determine the strength of the correlation between shape and phylogeny (if there is a strong correlation then the tree length value should be small).

The statistical significance of the tree length is calculated by a permutation test performed in MorphoJ in which the topology of an input phylogeny (assumed to be the “true” phylogeny of the group in question) including branch lengths is held constant and the PC scores for each taxon are randomly permuted across the tree 10 000 times (Laurin 2004; Klingenberg & Gidaszewski 2010). If the tree length of the “true” phylogeny is less than that in at least 95% of the randomly generated trees then there is said to be statistically significant correlation at a 5% threshold between phylogeny and PC scores (skull shape).

For our pterosaur dataset, we calculated the tree length and its significance value by using two different topologies: a) a pruned consensus tree (which includes all species used in this study) from Lü et al. (2010a) and b) an informal pterosaur supertree (*sensu* Butler & Goswami 2008), based upon Andres & Ji (2008) and Andres et al. (2010). Because the phylogenetic position of *Feilongus* is uncertain (e.g. Wang et al. 2005; Lü & Ji 2006; Andres & Ji 2008) we placed this taxon at the base of Ornithocheiroidea for the Lü et al. topology (Lü & Ji 2006; see supplementary information of Chapter 4). Because *Raeticodactylus*, *Darwinopterus* and *Shenzhoupterus* are not included in the phylogenies of Andres & Ji (2008) and Andres et al. (2010), we placed *Raeticodactylus*

in a polytomy with *Eudimorphodon*, *Darwinopterus* as sister taxon to Pterodactyloidea, and *Shenzhoupterus* in a polytomy with Tapejarinae and Thalassodrominae (after Lü et al. 2010a).

For both trees branch lengths were assigned based upon first appearances of species, and zero branch lengths were adjusted by sharing out the time equally between branches (see Ruta et al. 2006; Brusatte et al. 2008; Brusatte 2011). An arbitrary length of 10 million years was added to the root. The assignment of branch lengths was performed in the program R (R Development Core Team 2011) using the APE package (version 2.7-2; Paradis et al. 2004) and a function written by Graeme Lloyd (see <http://www.graemelloyd.com/methdpf.html>).

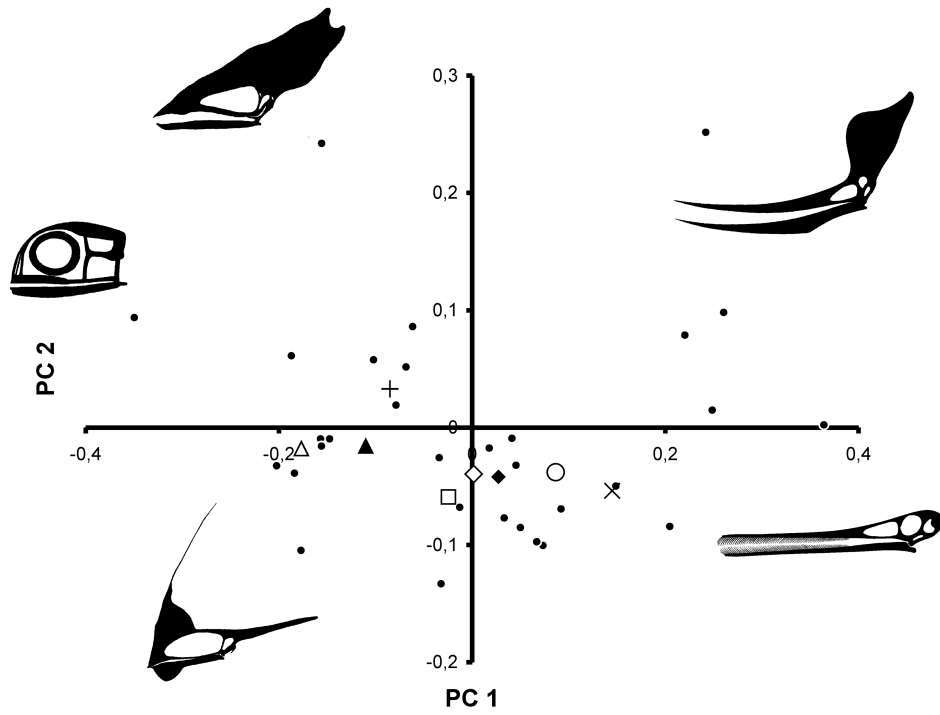
To better understand and visualise how skull shape changed during pterosaur evolution, which may reveal major evolutionary trends, we further mapped the PC scores as continuous characters onto the time calibrated topology from Lü et al. (2010a) using squared change parsimony in Mesquite 2.72 (Maddison & Maddison 2009). In the supplementary information of this chapter an equivalent description is given for the supertree topology.

RESULTS

MORPHOSPACE OCCUPATION AND MAJOR SHAPE CHANGES

The whole data set is summarised by 30 PC axes. The majority of shape variation in pterosaur skulls is summarised by the first four PC axes (51.7 %, 15.3 %, 13.2 % and 5.1 % of total variance), which together describe over 85 % of total variance. The main shape changes of the first four principal component axes (PC) are shown in Fig. 4.1B. The first PC axis describes the relative length of the snout, the relative size of the orbit and postorbital region, the size and dorsoventral depth of the naris–antorbital fenestra region and the position of the jaw joint relative to the orbit. The second PC axis describes the relative position of the orbit, the depth of the anterior part of the skull roof posterodorsal to the orbit and the position of the jaw joint relative to the orbit along the dorsoventral axis. The third PC axis describes the relative size and location of the orbit, the depth of the skull roof and dorsal part of the snout in the naris-antorbital fenestra region and the relative size of the jaw joint region (i.e. the distance between the ventral margin of the orbit and the jaw joint), including the position of the jaw joint relative to the orbit along the anteroposterior axis. Finally, the fourth PC axis describes the depth of the tip of the snout, the overall shape of the naris-antorbital fenestra region (triangular to trapezoidal), the inflection of the snout and the location of the jaw joint along the dorsoventral axis. The cranial morphospace of the first four PC axes described above is visualised in Fig. 4.2.

A



B

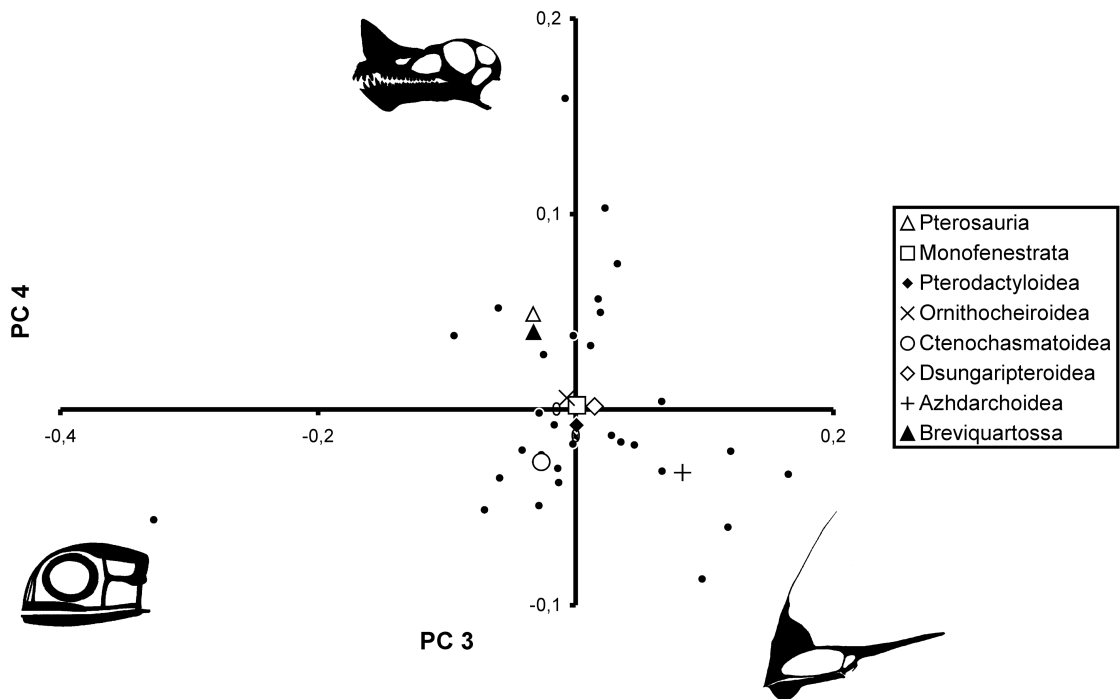


Fig. 4.2. Two-dimensional plots of pterosaur skull shape morphospace, based on the first four PC axes. Positions of hypothetical ancestors are plotted based upon squared-change parsimony optimisation. Silhouettes represent mostly extreme cranial morphologies plotting close to the edge of morphospace. The sources of the silhouettes are given in table S4.1 (see supplementary information of Chapter 4).

MORPHOLOGICAL DISPARITY

Based on all four metrics, cranial disparity is lowest in the Late Triassic-Early Jurassic, increases from the Middle Jurassic-Late Jurassic, reaches a peak in the Early Cretaceous (although only slightly exceeding the Middle Jurassic-Late Jurassic value), and then declines in the Late Cretaceous. With that being said, however, almost none of the bin-to-bin changes are significant, with the exception that Early Cretaceous range-based disparity (both sum and product) is significantly higher than that in the Late Triassic-Early Jurassic (the sum of variances also approaches significance). Rarefaction demonstrates that Early Cretaceous cranial disparity is higher than for all other time bins, and that Late Triassic-Early Jurassic cranial disparity is lower than for all other time bins, at all sample sizes and for all disparity metrics (Fig. 4.3A, B).

The disparity of non-monofenestratan pterosaurs ('rhamphorhynchoids') is lower than that of Monofenestrata for three of the disparity metrics (sum and product of ranges, sum of variances), but in no case is the difference significant. When the highly aberrant Anurognathidae are excluded from the non-monofenestratan disparity sample, non-monofenestratan pterosaurs are significantly less disparate than Monofenestrata for all metrics except product of variances. Within Monofenestrata, the highest disparity for all four metrics is shown by Azhdarchoidea and Ornithocheiroidea. Ctenochasmatoidea

exhibit lower disparity for all four metrics than these two aforementioned clades, but the difference is not significant. Dsungaripteroidea has the lowest disparity of the monofenestratan clades for all four metrics, and is significantly lower than the disparity of Azhdarchoidea and Ornithocheiroidea for both range metrics and sum of variances (but marginally non-significant for product of variances). On no metric is Dsungaripteroidea significantly less disparate than Ctenochasmatoidea (Fig. 4.3C).

When the monofenestratan clades of Andres & Ji (2008) were used, Ornithocheiroidea was found to be significantly more disparate than Archaeopterodactyloidea for three metrics (all except sum of variances), whereas the disparity values of the two major subclades within Ornithocheiroidea (Pteranodontoidea + *Nyctosaurus*; Tapejaridae + Dsungaripteridae + Azhdarchidae) are not significantly different from one another (see Fig. S4.6, supplementary information of Chapter 4).

PHYLOGENETIC COMPARATIVE METHODS AND EVOLUTION OF SKULL SHAPE IN PTEROSAURS

For all phylogenies that we tested, the permutation test in MorphoJ demonstrates a significant correlation between skull shape and phylogeny ($p < 0.0001$). The tree lengths of the time-calibrated phylogenies are 0.642 for the Lü et al. (2010a) topology and 0.626 for the supertree.

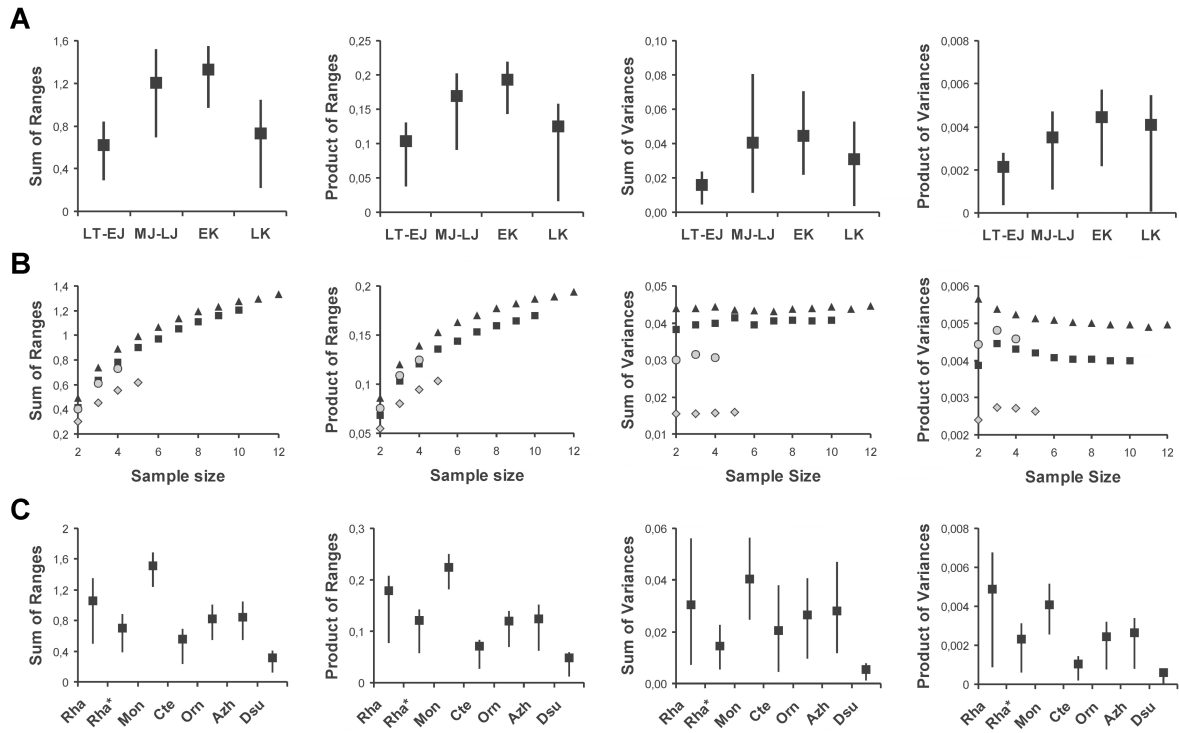


Fig. 4.3. Temporal and taxonomic disparity of pterosaur skull shape calculated for four disparity metrics (from left to right: sum of ranges, product of ranges, sum of variances, product of variances). **A.** Temporal patterns in Late Triassic-Early Jurassic (LT-EJ), Middle Jurassic-Late Jurassic (MJ-LJ), Early Cretaceous (EK) and Late Cretaceous (LK) time bins. **B.** Rarefaction profiles for Late Triassic-Early Jurassic (grey diamonds), Middle Jurassic-Late Jurassic (black squares), Early Cretaceous (black triangles) and Late Cretaceous (grey circles) time bins. **C.** Disparity for the taxonomic groupings Azhdarchoidea (Azh), Ctenochasmatoidea (Cte), Dsungaripteridae (Dsu), Monofenestrata (Mon), Ornithocheiridae (Orn), ‘Rhamphorhynchoidea’ (Rha) and ‘Rhamphorhynchoidea’ without Anurognathidae (Rha*).

Mapping the PC scores onto the phylogeny of Lü et al. (2010a; differences with the results from the supertree are discussed in the supplementary information of Chapter 4) demonstrates that the skull of the hypothetical pterosaur ancestor (i.e., the node at the base of pterosaur phylogeny) had a short, stout snout (negative position of PC 1, positive position of PC 4), triangular naris-antorbital fenestra region (positive position of PC 4), relatively large orbit (negative position of PC 3) and a relatively large

postorbital region. In the hypothetical ancestor of the clade Breviquartossa the tip of the snout is more pointed. Compared to the hypothetical pterosaur ancestor, the hypothetical ancestor of Monofenestrata and Pterodactyloidea had a more elongated skull with a long snout (more positive position of PC 1), a more trapezoidal naris-antorbital fenestra region (negative position of PC 4) and a relatively smaller orbit and postorbital region (positive position of PC 1). In the hypothetical ancestor of Ornithocheiroidea the snout became more elongated (positive position of PC 1) than that of Monofenestrata and Pterodactyloidea. Compared to the hypothetical ancestor of Pterodactyloidea and Ornithocheiroidea, the hypothetical ancestor of Pteranodontidae showed an expansion of the dorsal skull roof (positive position of PC 2), whereas in the hypothetical ancestor of Ornithocheiridae the premaxillary region was dorsally expanded (positive position of PC 4). The skull of the hypothetical ancestor of Ctenochasmatoidea did not differ substantially from that of the hypothetical ancestor of Pterodactyloidea. This is also true for the hypothetical ancestor of Dsungaripteroidea, whereas the hypothetical ancestor of Dsungaripteridae had a skull with an enlarged naris-antorbital fenestra region, a decreased orbit size, a deep snout (positive position of PC 1, positive position of PC 3) with a pointed tip and a small postorbital region (negative position of PC 2). Compared to that of the hypothetical ancestor of Pterodactyloidea, the skull of the hypothetical ancestor of Azhdarchoidea was extremely deep with an enlarged naris-antorbital fenestra, a decreased orbit size (positive position of PC 3), a shortened snout length (negative position of PC 1) and an enlarged postorbital region (positive position of PC 2) (Fig. 4.4).

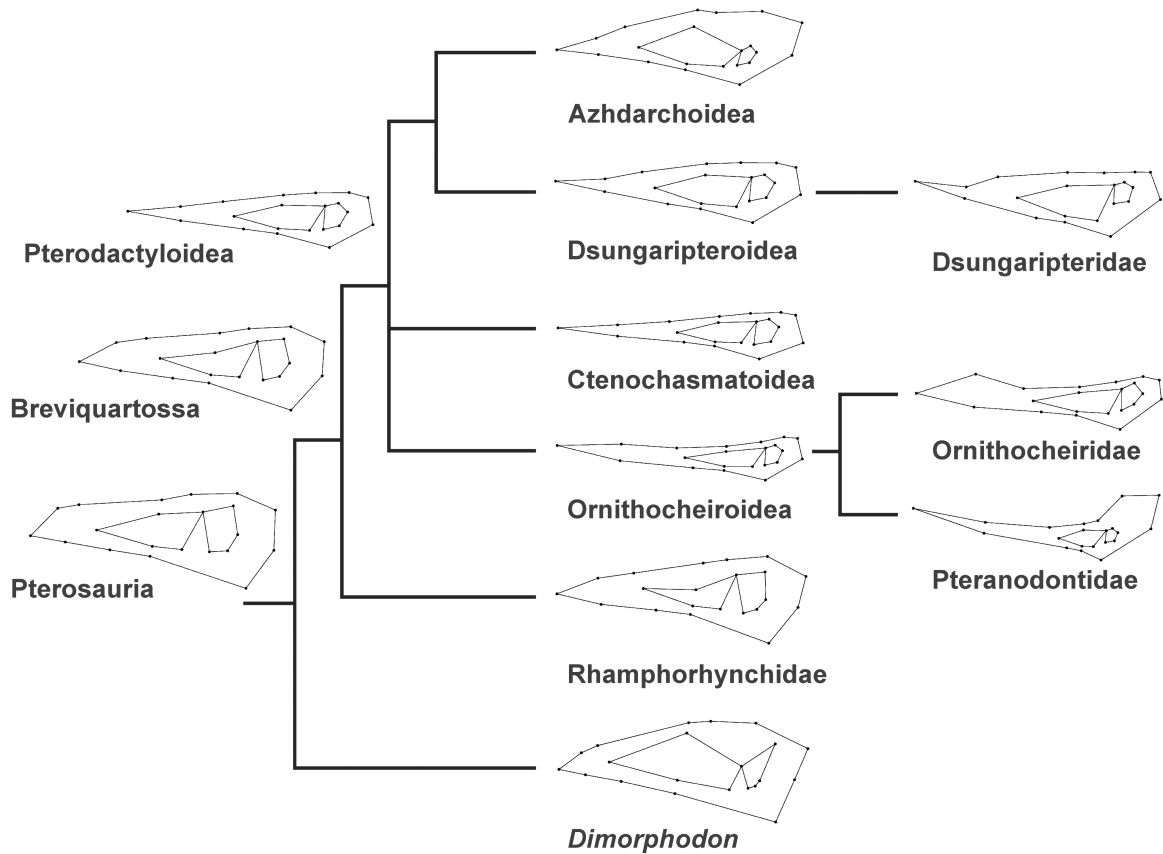


Fig. 4.4. Optimisation of ancestral skull shapes using squared-change parsimony reconstruction based on the phylogenetic hypothesis of Lü et al. (2010a). The pterosaur hypothetical ancestor had a short, stout skull with relatively large orbit size. During the evolution of the clade the snout became elongated and the orbital and postorbital regions decreased in relative size. The hypothetical ancestor of Pteranodontidae showed an expansion of the dorsal skull roof, whereas in the hypothetical ancestor of Ornithocheiridae the premaxillary region was dorsally expanded. The skull of the hypothetical ancestor of Azhdarchoidea and Dsungaripteridae had an enlarged naris-antorbital fenestra and a decreased orbit size which developed convergently in both lines. However, the hypothetical ancestor of Azhdarchoidea had in addition a much deeper snout and a posterodorsal expansion of the skull roof.

DISCUSSION

MAJOR PATTERNS IN PTEROSAUR CRANIAL SHAPE

Most pterosaurs bunch fairly close together in the cranial morphospace, in the vicinity of the origin. The taxa that are most broadly separated are: *Anurognathus* due to its extremely short rostrum, large orbit and postorbital region; *Pterodaustro* due its extreme elongated rostrum; *Thalassodromeus* probably due to its enlarged premaxillary crest (which may be partly captured with our landmark construction approach); and pteranodontids probably due to their enlarged frontal crests (which may be partly captured as well: see Fig. 4.2A). The general bunching of the majority of taxa means that skull shape as captured by the chosen landmarks is, in general terms, fairly uniform among pterosaurs. It seems, therefore, that despite their long evolutionary history and great diversity of body size, pterosaurs exhibited a restricted range of skull shape. Most variation occurs in the length of the snout and size of the postorbital region (PC 1). The former is probably related with feeding ecology (Witton & Naish 2008; Ősi 2010). A comparison of the different PC axes demonstrates further that variation in the length of the snout (PC 1) is greater than variation in the depth of the snout (PC 3). Within the postorbital region, variation in the shape and size of the skull roof (PC 2) is probably not strongly linked to the position of the jaw joint (PC 3), as the two are summarised by different PC axes. The depth of the snout tip (PC 4) seems to be independent from variation in snout length (PC1) and the depth of the snout (PC 3) in general.

It is important to remember that because we did not include landmarks relative to entire shape of the cranial crests (see the diversity of crest types in e.g. *Nyctosaurus*, *Tapejara*, *Tupuxuara*, Pteranodontidae), it is likely that a morphospace based on a dataset including such landmarks would appear quite different. In particular, because

there is such a diversity of crest morphologies among pterosaurs we suspect that the first PC axes (and perhaps the first several PC axes) would largely characterise features relating to the crest. Furthermore, it is likely that there would be a greater spread of taxa in morphospace (i.e., taxa would not be so closely bunched together, which would indicate more total morphological diversity). As we are primarily focused on the shape of the snout and postorbital regions (regions that are more likely to have mechanical significance), we leave landmark or outlined-based analyses of pterosaur crest shape to future studies. In particular, such studies may provide evidence relevant to long-standing debate over the function of cranial crests in pterosaurs, especially the question of whether they may have provided aerodynamic utility during flight (Frey et al. 2003; Elgin et al. 2008) or were mostly, or entirely, display structures (Bennett 2003; Martill & Naish 2006; Elgin et al. 2008; Tomkins et al. 2010; Hone et al. 2012).

TEMPORAL AND TAXONOMIC DISPARITY

The peak disparity observed for all four metrics in the Early Cretaceous is consistent with other studies that also suggest peak disparity in this time interval, based on measurements and discrete character data (Dyke et al. 2009; Prentice et al. 2011; Butler et al. 2012). However, although the Early Cretaceous pterosaur sample is significantly or nearly significantly more disparate than that of the Late Triassic-Early Jurassic for three of the disparity metrics, it is not significantly different to that of the Middle Jurassic-Late Jurassic or the Late Cretaceous. Therefore, there is currently not enough evidence to conclusively identify true variation in cranial disparity through time (a problem that may be caused by the low sample size of our study, as there are over 100 additional pterosaurs that cannot be included because they are not known from adequate skull material). With that said, rarefaction results do support the existence of a disparity

peak during the Early Cretaceous, occurring at all sample sizes and in all metrics, including variance-based metrics, which have been demonstrated to be less susceptible than range-based metrics to sampling biases (e.g. Wills et al. 1994; Butler et al. 2012). If accurate, this disparity peak coincides with the major Early Cretaceous radiation of monofenestratan pterosaurs, and is unusual in occurring relatively late in pterosaur evolutionary history (most clades show disparity peaks early in their evolutionary history e.g. see Erwin 2007).

Our taxonomic disparity results are similar to those obtained by Prentice et al. (2011) using a discrete character dataset that includes information from the entire pterosaur skeleton. Our results follow those of Prentice et al. (2011) in recovering Monofenestrata (approximately equivalent to Pterodactyloidea of their analysis) as significantly more disparate than non-monofenestratan pterosaurs (=“Rhamphorhynchoidea” in their analysis), but only when the highly divergent Anurognathidae are excluded from the non-monofenestratan sample. Because this result is recovered using sum of variances it seems plausible that it is not simply related to differences in sample sizes (Wills et al. 1994; Butler et al. 2012), despite the fact that our sampling of non-monofenestratans is substantially smaller than that of monofenestratans. Prentice et al. (2011) also found disparity to be lower for Dsungaripteroidea than other pterosaur ‘superfamilies’, but not significantly so. Moreover, our results also recover higher disparity for Azhdarchoidea and Ornithocheiroidea compared to Ctenochasmatoidea (although not significantly so, so it is possible that these differences relate to taxonomic sampling) when the controversial taxon *Feilongus* is assigned to Ornithocheiroidea. Prentice et al. (2011) found no significant difference in disparity between Ornithocheiroidea and Ctenochasmatoidea

when *Feilongus* was assigned to Ctenochasmatoidea, but a significant difference (higher disparity in Ornithocheiroidea) when it was assigned to Ornithocheiroidea.

DIFFERENT DISPARITY PROXIES: A COMMON THEME

As summarised above, our disparity results (both temporal and taxonomic) based upon cranial morphometrics broadly agree with those based upon discrete characters from the entire skeleton (Prentice et al. 2011; Butler et al. 2012) and on limb measurements and ratios (Dyke et al. 2009). This is an encouraging finding, as it demonstrates that different proxies for morphological form in pterosaurs, a group with complex three-dimensional skeletons that are difficult to represent in disparity studies, converge on the same disparity signal. A similar finding was reported by Villier & Eble (2004) in a study of echinoid morphological evolution, as several proxies for morphological form (e.g. discrete characters, landmark morphometrics, traditional measurement morphometrics) produced generally congruent temporal disparity curves for the clade. Whether this is also true of disparity studies of other groups deserves further study. At the very least, the echinoid and pterosaur data show that, for exemplar non-vertebrate (echinodermatan) and vertebrate clades, disparity can be consistently measured based on several different proxies. This justifies the use of discrete characters [including those generated for phylogenetic analyses, as were the characters used by Prentice et al. (2011) and Butler et al. (2012)] when morphometric data may not be available, or vice versa.

THE EVOLUTION OF SKULL SHAPE IN PTEROSAURS

Because no morphofunctional data are available for pterosaur skulls so far (e.g. skull strength estimates generated by FEA or beam theory, mechanical advantage bite profiles), it is not possible to judge how, and to what extent, skull shape was influenced by functional constraints. This is also the case for comparing skull shape to feeding or other ecological data. However, the results of all permutation tests clearly show that pterosaur skull shape is strongly correlated with phylogeny. In other words, closely related taxa have more similar skull shapes than distantly related taxa (or than predicted by chance alone) despite the well-known incompleteness of the pterosaur record (e.g. Butler et al. 2009a). This means that general patterns of cranial shape evolved sufficiently slowly for the sampled taxa to reveal the phylogenetic signal. One potential explanation of this pattern is that pterosaur cranial shape evolution was subject to strong phylogenetic constraint. Because this study is a broad scale analysis that examines the range of skull shape across Mesozoic pterosaurs, the results must be interpreted carefully: they indicate that the most general patterns of cranial shape variation in pterosaurs are closely related to the most general, higher-level phylogenetic relationships. As more pterosaur fossils are found and morphometric datasets can be expanded, it will be important to revisit this comparison and assess whether the correlation between skull shape and phylogeny may be weaker at lower taxonomic levels, due to more subtle differences between many individual species within individual pterosaur subclades (see Jones & Goswami [2010] for a similar finding in an extant mammal clade).

Based on the optimisation of PC scores onto pterosaur phylogeny, basal pterosaur taxa (with exception of anurognathids) had a conservative skull shape,

highlighted by a short snout, a triangular nares-antorbital fenestra region, a large orbit and a large postorbital region. However, in the clade Monofenestrata snouts became extremely elongated relative to the rest of the skull, leading to a relatively small orbit and postorbital region. The shape of the nares-antorbital fenestra region thus became trapezoidal. We interpret this shift of shape as related to the fusion of the nares and the antorbital fenestra into a single large opening, which occurred in this clade. Because these events apparently occur simultaneously, it is possible that the fusion of the preorbital skull openings could be functionally linked to elongation of the snout. However, due to the lack of FEA and other biomechanical data it is not possible to test this hypothesis at present. The skull shape of the hypothetical ancestors of Ornithocheiroidea, Dsungaripteroidea and Ctenochasmatoidea more-or-less resembles that of the hypothetical ancestor of Pterodactyloidea, whereas the ancestors of Dsungaripteridae, Pteranodontidae and Azhdarchoidea show more variation in shape compared to the hypothetical ancestor of Pterodactyloidea due to their development of different kinds of cranial crests.

CONCLUSIONS

In summary, our morphometric analysis of pterosaur skull shape (31 taxa, 21 landmarks) identifies the greatest sources of cranial variation within the clade and documents morphological changes occurring during pterosaur evolution. Pterosaur skull shape was apparently subject to strong and statistically significant phylogenetic constraint, with closely related taxa having more similar skull shapes than distantly related taxa (or than predicted by chance alone). Cranial disparity of Pterosauria may have reached a peak in the Early Cretaceous, which occurs relatively late in the clade's evolutionary history. With the exclusion of the highly aberrant anurognathids, basal

non-monofenestratan pterosaurs appear to have been less disparate cranially than monofenestratan pterosaurs, consistent with their apparently more restricted range of ecological adaptations and body sizes. From a broader evolutionary and methodological standpoint, one of the most salient results of our study is that temporal and taxonomic patterns in cranial shape disparity closely match disparity patterns generated from discrete characters and limb measurements. Therefore, based on a well-studied exemplar clade (pterosaurs), different sources of morphological data give broadly congruent disparity results. This is a promising finding because often only one such data source is available for extinct clades represented by fossils, which are often poorly and incompletely preserved.

ACKNOWLEDGEMENTS

We thank Gareth Dyke and Michel Laurin for their helpful reviews and Brian Andres, Roger Benson and Oliver Rauhut for discussion. RJB was funded by the DFG Emmy Noether Programme (BU 2587/3-1), CF by the DFG (RA 1012/12-1) and SJB by a NSF Graduate Research Fellowship, Doctoral Dissertation Improvement Grant (DEB 1110357) and the American Museum of Natural History and Columbia University.

CHAPTER 5

Macroevolutionary and morphofunctional patterns in theropod skulls: a morphometric approach

Keywords:

Theropoda; geometric morphometrics; Mesozoic; macroevolution; feeding ecology; biomechanics; avian evolution

The chapter was published as:

Foth C^{1,2} & Rauhut OWM^{1,2,3}. 2013. Macroevolutionary and morphofunctional patterns in theropod skulls: a morphometric approach. *Acta Palaeontologica Polonica* 58: 1-16.

¹*Bayerische Staatssammlung für Paläontologie und Geologie, Richard-Wagner-Str. 10, D-80333 München, Germany*

²*Department of Earth and Environmental Sciences, Ludwig-Maximilians-University, Richard-Wagner-Str. 10, D-80333 München, Germany*

³*GeoBioCenter, Ludwig-Maximilians-University; Richard-Wagner-Str. 10, D-80333 München, Germany*

Received 16 December 2011, accepted 19 April 2012, available online 20 April 2012.

Author contribution:

Research design: **Christian Foth**, Oliver Rauhut

Data collection: **Christian Foth**

Data analyses: **Christian Foth**

Preparation of figures and tables: **Christian Foth**

Wrote paper: **Christian Foth**, Oliver Rauhut

***All figures of Chapter 5 are modified after Foth & Rauhut (2013)**

Macroevolutionary and morphofunctional patterns in theropod skulls: a morphometric approach

Christian Foth & Oliver W. M. Rauhut

ABSTRACT

Theropod dinosaurs are one of the most remarkable lineages of terrestrial vertebrates in the Mesozoic, showing high taxonomic and ecological diversity. We investigate the cranial diversity of non-avian theropods and some basal birds, using geometric morphometrics to obtain insights into the evolutionary modifications of the skull.

Theropod skulls mostly vary in the shape of the snout and length of the postorbital region (principal component, PC 1), with further variation in orbit shape, depth of the postorbital region, and position of the jaw joint (PC 2 and PC 3). These results indicate that the cranial shape of theropods is closely correlated with phylogeny and dietary preference. Skull shapes of non-carnivorous taxa differ significantly from carnivorous taxa, suggesting that dietary preference affects skull shape. Furthermore, we found a significant correlation between the first three PC axes and functional proxies (average maximum stress and an indicator of skull strength). Interestingly, basal birds occupy a large area within the morphospace, indicating a high cranial, and thus also ecological, diversity. However, we could include only a small number of basal avialan species, because their skulls are fragile and there are few good skull reconstructions. Taking the known diversity of basal birds from the Jehol biota into account, the present result might even underestimate the morphological diversity of basal avialans.

INTRODUCTION

Theropod dinosaurs were one of the most remarkable lineages of terrestrial vertebrates in the Mesozoic Era. They attained a high level of taxonomic and ecological diversity (Weishampel et al. 2004), and represent the only dinosaur clade that survived the mass extinction event at the end of the Cretaceous, in the form of birds (Dingus & Rowe 1997). Mesozoic theropod species occupied the mass spectrum from a few hundred grams to more than six tonnes (Christiansen & Fariña 2004; Turner et al. 2007), and showed a huge diversity in skull morphologies (Fig. 5.1; Weishampel et al. 2004) and feeding strategies (Barrett 2005; Zanno & Makovicky 2011). Numerous papers have been published on the phylogenetic relationships of non-avian theropods and basal birds (e.g. Gauthier 1986; Sereno 1999; Clark et al. 2002a; Rauhut 2003a; Smith et al. 2007; Choiniere et al. 2010). These analyses largely agree in the general interrelationships of major groups, but the phylogenetic position and validity of several clades (e.g. Alvarezsauridae, Ceratosauria, Compsognathidae, Therizinosauridae) and the detailed positions of many species are still controversial (see Rauhut 2003a; Choiniere et al. 2010; Zanno 2010; Xu et al. 2011). In contrast to this rather high number of phylogenetic analyses, relatively few studies have investigated the morphofunctional evolution of theropod character complexes, or have addressed macroevolutionary questions, such as the importance of heterochrony or biomechanical constraints in theropod evolution. Those studies that have addressed such questions have overwhelmingly concentrated on the evolution of the limbs (e.g. Gatesy 1990; Wagner & Gauthier 1999; Middleton & Gatesy 2000; Hutchinson 2001a, b; Dececchi & Larsson 2011), growth patterns as indicated by bone histology (e.g. Erickson et al. 2001, 2009; Padian et al. 2001), body size, breathing and physiology (e.g. Schweitzer & Marshall 2001; Turner et al. 2007; Benson et al. 2012) or, most recently, the evolution of feathers

(e.g. Xu & Guo 2009) and the variety of diets (Barrett et al. 2011; Zanno & Makovicky 2011). However, apart from the works of Rayfield (2005, 2011), Barrett (2005), Barrett & Rayfield (2006), Sakamoto (2010), Zanno & Makovicky (2011), and Brusatte et al. (2012a), the relationships between cranial diversity, functional constraints, diet, and evolutionary processes have received surprisingly little attention so far.

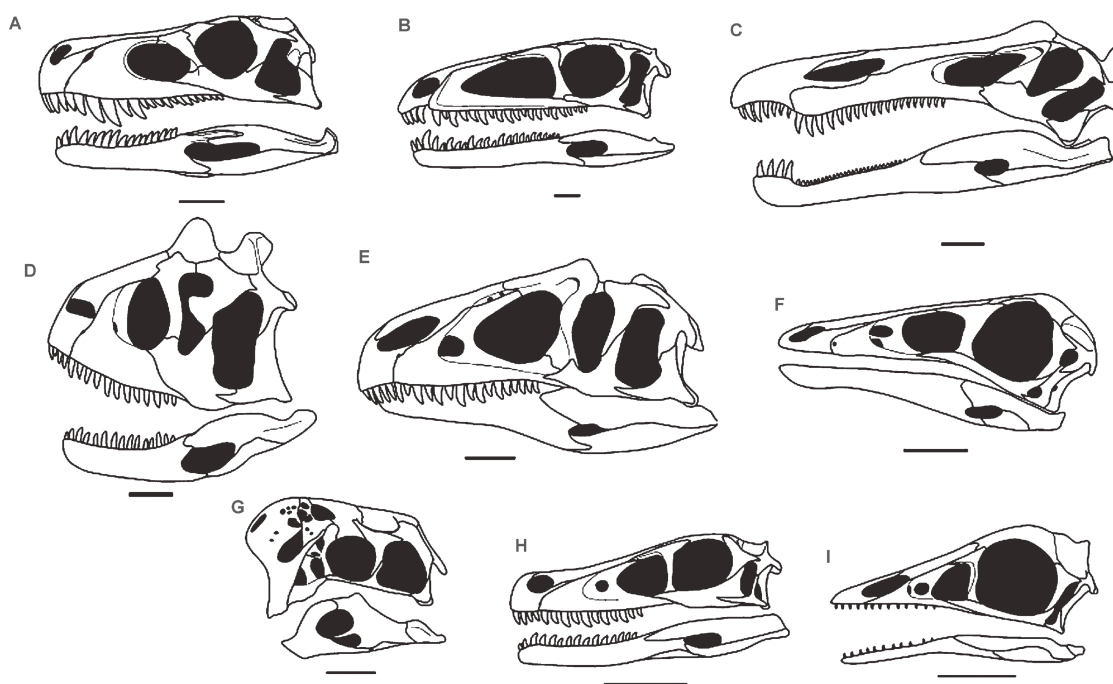


Fig. 5.1. Diversity of skull shapes in theropod dinosaurs. **A.** basal theropod *Herrerasaurus*; **B.** coelophysid *Syntarsus*; **C.** generalized spinosaurid; **D.** abelisaurid *Carnotaurus*; **E.** allosaurid *Allosaurus*; **F.** ornithomimosaur *Ornithomimus*; **G.** unnamed oviraptorid (originally referred to *Oviraptor*); **H.** dromaeosaurid *Velociraptor*; **I.** basal bird (avialian) *Archaeopteryx*. Scale bars represent 10 mm (B, I), 50 mm (a, f-h) and 100 (c-e). Modified from Rauhut (2003a).

In recent years, geometric morphometrics has been used increasingly in palaeontology. The most comprehensive study focusing on the morphometrics of archosaurian skulls is Marugán-Lobón & Buscalioni (2003), though this investigation

was based on simple distance measurements for three homologous units of the skull (braincase, orbit and rostrum). Geometric morphometric studies have often been carried out for ornithischian dinosaurs (Chapman et al. 1981; Chapman 1990; Chapman & Brett-Surman 1990; Goodwin 1990; Dodson 1993), where they were mainly used for taxonomic purposes. Further studies deal with geometric morphometrics of the skulls of sauropods (Young & Larvan 2010) and of single or small numbers of taxa of theropods, such as *Allosaurus* and *Tyrannosaurus* (Chapman 1990), and *Carnotaurus* and *Ceratosaurus* (Mazzetta et al. 2000), as well as with isolated theropod teeth (D'Amore 2009). More comprehensive analyses were published by Marugán-Lobón & Buscalioni (2004, 2006) for extant birds. Recently, Brusatte et al. (2012a) investigated the cranial diversity of non-avian theropods, using two datasets (small data set: 26 taxa and 24 landmarks; large data set: 36 taxa and 13 landmarks). These authors concluded that cranial shape of theropods is highly correlated with phylogeny, but only weakly with functional biting behaviour and thus that phylogeny was the major determinant of theropod skull shape. Their result challenges previous studies, which suggested marked functional constraints on the evolution of theropod skull shape (Henderson 2002; Rayfield 2005).

The goal of this study, which was initiated in parallel with that of Brusatte et al. (2012a), is therefore to evaluate theropod cranial diversity and its relation to phylogeny, ecology and function, using geometric morphometrics. We used an independent subsample of taxa and a different combination of landmarks, as well as different proxies for cranial function. Thus, this study helps to test the results obtained by Brusatte et al. (2012a), using a different set of data. Further, we investigated how shape variation of

different skull regions is correlated with function, and how different dietary patterns affect skull shape.

MATERIAL AND METHODS

TAXON SAMPLING

The cranium of 35 non-avian theropod species (+ four outgroup species and two Avialae) was analysed, using a two-dimensional geometric morphometric approach. The dataset is based on published reconstructions of adult (or nearly adult) fossil material in lateral view (see supplementary information of Chapter 5). For the majority of the ~270 valid non-avian theropods described so far (see Butler et al. 2011b), skull material is incomplete, juvenile or missing; therefore, the present dataset includes only a small fraction (~ 13 %) of ‘real’ theropod cranial diversity. However, usable reconstructions were available for at least one species from all major ‘family’-level clades of theropods. Thus, it is likely that the present dataset successfully captures broad phylogenetic and functional patterns of cranial morphological diversity across theropods, even if it is not possible for us to document detailed variation within ‘family’-level clades.

Because the skulls of basal birds are extremely fragile, their preservation is usually poor. Furthermore, the vast majority of basal avialan taxa come from Konservat-Lagerstätten, such as the Solnhofen limestones of southern Germany or the famous Jehol beds of China, in which specimens are usually rather two-dimensionally preserved. Thus, good reconstructions of the skulls of basal avialan taxa are extremely rare. Because of the highly derived morphology of some taxa we were not able to place all landmarks on all specimens, so we created a second, smaller data set, including

Pengornis and *Shenquiornis*. In addition to the paravian taxa from the larger data set, we included only a few non-paravian coelurosaurs (*Compsognathus*, *Dilong*, *Ornithomimus*, *Erlikosaurus*, *Shuvuuia* and *Conchoraptor*) as outgroup taxa. We were able to include the alvarezsaurid *Shuvuuia* only in the small dataset because of its bird-like skull shape, which includes the loss of the postorbital process of the jugal. All taxa are listed in table S5.1 (see supplementary information of Chapter 5).

GEOMETRIC MORPHOMETRICS

Geometric morphometric approaches are commonly used to quantify and study interspecific or intraspecific shape variation across a number of specimens based on outline or landmark data that capture the shape of the specimens in question (Adams et al. 2004; Zelditch et al. 2004). The advantage of this approach is that landmark coordinates capture more information about shape than can be obtained from traditional morphometric measurements (linear distances, ratios and angular measures), which are often insufficient to capture the whole geometry of the original object (Hammer & Harper 2006). Geometric morphometric approaches have been reviewed and discussed by many authors including Bookstein (1991), Elewa (2004), Zelditch et al. (2004), and Adam et al. (2004).

In the large data set, cranial geometry was captured using 20 homologous landmarks, which were plotted on the reconstructed skulls using the program tpsDig2 (Rohlf 2005), which outputs a tps (thin plate spline) file with two-dimensional landmark coordinates and scale (size) data for each specimen. The chosen landmarks are of type 1 (good evidence for anatomical homology, such as points where two bone sutures meet) and type 2 (good evidence for geometric homology, such as points of maximal

curvature or extremities) in the terminology of Bookstein (1991). The landmark dataset includes the outer shape of the whole cranium (excluding nasal crests or horns on the skull roof), maxilla, antorbital fenestra, orbit, lateral temporal fenestra, jugal, quadratojugal, postorbital and the posterior part of the skull roof (parietal and squamosal). For comparison, the dataset shares eleven landmarks (55 %) with the 26-taxon dataset of Brusatte et al. (2012a) and only five (25 %) with the 36-taxon data set. In the smaller dataset we used only 15 landmarks, owing to the fusion or loss of various skull elements in some taxa (Fig. 5.2, see supplementary information of Chapter 5 for the anatomical description of the landmarks).

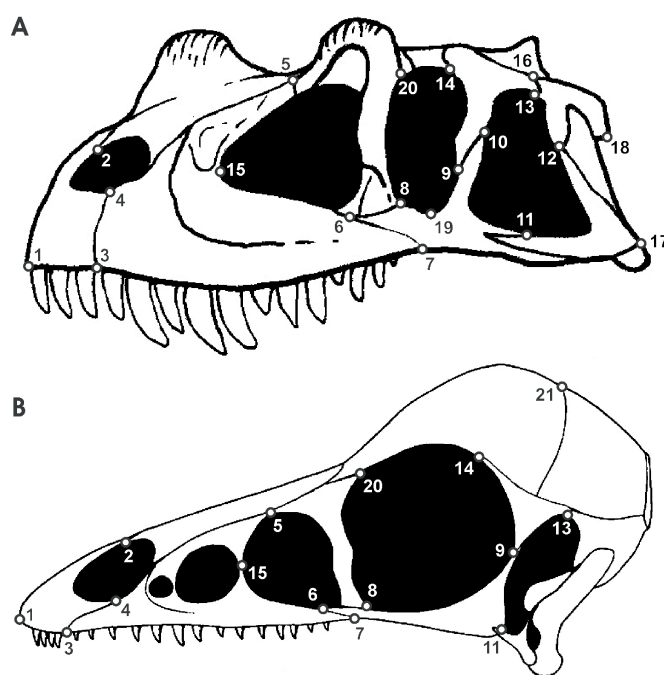


Fig. 5.2. Position of the landmarks on theropod skulls. **A.** 20 landmarks used for the large dataset plotted on the skull of *Ceratosaurus* (modified from Sampson & Witmer 2007). **B.** 15 landmarks used for the small dataset plotted on the skull of *Anchiornis* (modified from Hu et al. 2009). The description of landmark positions is given in the supplementary information of Chapter 5.

The landmark coordinates were superimposed using Generalized Procrustes Analyses (GPA) in tpsRelW (Rohlf 2003) and PAST 2.09 (Hammer et al. 2001), which serves to minimize non-shape variation between species, such as that caused by size, location, orientation, and rotation (Zelditch et al. 2004). Afterwards, the Procrustes coordinates were subjected to Principal Component Analysis (PCA) using PAST and tpsRelW. This procedure assimilates data from all landmarks and reduces it to a set of PC scores that summarize the skull shape of each taxon and describe maximal shape variation in a morphospace (Hammer & Harper 2006).

CHARACTER EVOLUTION

One main question is how far is theropod skull shape correlated with phylogeny? This is important for reconstructing skull shape changes using character-mapping approaches. If a strong phylogenetic signal is present, closely related taxa should occur closer to one another in morphospace than more distantly related taxa (Klingenberg & Gidaszewski, 2010). The degree of this correlation can be calculated by mapping the phylogeny into the morphospace. This requires an ancestral state reconstruction of the morphometric data for each internal node on the tree using squared change parsimony (Maddison 1991; Klingenberg 2011). This algorithm collates the sum of squared changes of continuous characters (here PC scores) along all branches of the tree and calculates parsimonious ancestral states by minimizing the total sum of squared change across the phylogeny. The most optimal configuration of ancestral PC scores is mathematically described by a squared length value, which can be used to determine the strength of the correlation between shape and phylogeny (see below).

For this approach an informal supertree (*sensu* Butler & Goswami 2008) was created. The tree is based on several of the most recent phylogenetic analyses of theropods: basal theropods, including coelophysoids (Sues et al. 2011), Ceratosauria (*sensu* Rauhut 2003a; Smith et al. 2007; Xu et al. 2009a), basal tetanurans (Benson et al. 2010), Coelurosauria (Hu et al. 2009), Tyrannosauroida (Brusatte et al. 2010a), and Dromaeosauridae (Csiki et al. 2010). In general, most trees show strong similarities with regard to the higher-level relationships of theropod dinosaurs, but may disagree on the positions of individual lineages. *Euparkeria*, *Lesothosaurus*, *Massospondylus* and *Plateosaurus* were taken as outgroup taxa (Fig. S5.3, see supplementary information of Chapter 5; the topology showing the interrelationships of the coelurosaurian taxa used in the small dataset is shown in Fig. S5.4). As discussed by Hunt & Carrano (2010), models of phenotypic evolution require information about time. To include this information, branch lengths were scaled to the present topology, using stratigraphic ages of taxa obtained from Weishampel et al. (2004) or from original literature (Table S5.1, see supplementary information of Chapter 5).

In the next step, the original landmark data from the tps file and supertree were imported into MorphoJ (Klingenberg 2011). The landmark data were superimposed (GPA) and converted into a covariance matrix and subjected to Principal Component Analysis (PCA). Subsequently, the tree was mapped into the morphospace (see above). Furthermore, a permutation test was performed in MorphoJ in which the topology is held constant and the PC scores for each taxon are randomly permuted across the tree 10 000 times (Laurin 2004; Klingenberg & Gidaszewski 2010). For this approach both the tps file and the supertree were imported into MorphoJ. If the squared length of the

supertree is less than occurs in at least 95 % of the randomly generated trees then the phylogenetic signal may be deemed significant.

For a more detailed description of cranial shape changes through time, a similar character mapping approach was performed using the software package Mesquite 2.72 (Maddison & Maddison 2009). For this approach, a Nexus file containing the PC scores taken from PAST was produced. The data were used as continuous characters and mapped on the supertree using squared change parsimony (see above). The shape changes along the tree were visualised by plotting the ancestral state values in the morphospace within the visualization window of tpsRelW.

SHAPE VS. FUNCTION

Another main question is whether cranial shape is correlated with skull function? As proxies for function we used the skull strength indicator (SSI; after Henderson 2002) and the average maximum stress (after Rayfield 2011) (Table S5.2, see supplementary information of Chapter 5), which are both size-related parameters. Originally, Henderson (2002) calculated the skull strength at the longitudinal position of the orbital midpoint by treating the skull as a cantilevered beam, with the posterior region held immobile while a vertical force was applied at a point on the ventral edge of the snout. In the first step, we tested the correlation between SSI and shape using only those taxa that were also used by Henderson (2002). However, because SSI is strongly correlated with skull depth in the orbital region (Fig. S5.1, Table S5.2, see supplementary information of Chapter 5), this distance was measured in order to estimate SSI for all taxa included in this study. As a second proxy, we used the average maximum stress (AMS). The estimation of ASM is based on a two-dimensional finite element approach

by calculating the value of maximum stress per element, which was carried out for the crania of various allosauroids and megalosauroids (Rayfield 2011). For those taxa, AMS shows a significant correlation with the skull length (see Rayfield 2011). We therefore used this relationship to estimate AMS for all taxa in this study (Fig. S5.2, Table S5.2, see supplementary information of Chapter 5).

The estimated values of SSI and AMS were logarithmically transformed to normalize for data distribution (Freckleton et al. 2002). To evaluate the correlation between shape and function we performed a two-block partial least squares analysis (2B-PLS; see Rohlf & Corti 2000) in MorphoJ using the Procrustes coordinates from the GPA (shape) and both functional proxies (functional coefficients). This method explores the pattern of covariation between two sets of variables by constructing pairs of variables that are linear combinations of the variables within each of the two data sets, and accounts for as much as possible of the covariation between the two original data sets. The strength of correlation is given by the RV coefficient and a p value, generated by 10 000 permutations. Additionally, we divided the landmark dataset into several modules (preorbital region, postorbital region, antorbital fenestra, orbit, and lateral temporal fenestra; see supplementary information of Chapter 5), and reran the analyses. Using this approach, we were able to test how the shape variation of specific skull regions and skull openings is correlated with functional proxies. If different skull regions show different degrees of correlation with the functional proxies it is also possible that shape variations that occur in these regions are independent of each other. To test this we performed 2B-PLS for the preorbital and postorbital regions, as well as PLS in one configuration. The difference between both approaches is that the former is based on a separate Procrustes fit, testing the covariation between the shapes of the parts

of each considered separately, whereas the latter is based on a joint Procrustes fit, testing the covariation between parts within the context of the structure as a whole (see Klingenberg 2009).

We performed phylogenetic independent contrast (PICs) analyses on the first three PC axes and both functional proxies including the small data set, which was based on the original data from Henderson (2002). First, the correlation of SSI and AMS with phylogeny was tested, by loading both proxies into Mesquite as continuous characters and mapping them on the supertree using squared change parsimony. Then, a permutation test was performed as outlined above. Assuming that a correlation of shape and function with phylogeny is present, and the terminal scores of both factors are non-independent, the scores have to be transformed into PICs (Felsenstein 1985). This was done using the PDTREE package for Mesquite (Midford et al. 2005). This procedure considers the relationships of species to each other and calculates contrasts that are statistically independent by assuming that character evolution can be modelled as a random walk (brownian motion model) and that characters change at a uniform rate per unit branch length across all branches. To produce ‘standardised’ branch lengths, the original branch lengths were \log_e -transformed prior to analysis, as recommended by Garland et al. (1992). To test if the data fulfil these assumptions the absolute values of the standardized PICs were plotted against: a) their standard deviations (Garland et al. 1992); b) their estimated nodal values (ancestral PIC values); and c) the corrected age of their base nodes (Purvis & Rambaut 1995). Finally, the estimated nodal values were plotted against the corrected node ages. The assumption is justified if no significant correlation is present in all plots (Garland et al. 1992; Purvis & Rambaut 1995; Midford et al. 2005). Finally, if all quantities fulfil the four criteria, the resulting contrasts of PC

scores were plotted against the contrasts of SSI and AMS. If any signal is present between shape and function then a statistical correlation should be detectable. This relationship was evaluated by calculating the coefficient of determination (R^2) and the corresponding p value.

Because both functional parameters were originally size related, we tested if the shape variation (after the landmarks were superimposed) is correlated with centroid size (log-transformed) as a proxy for total size, which is defined as the square root of the sum of squared differences between landmark coordinates and centroid coordinates for any dimension. Because original size was previously removed from the data by performing GPA, a significant correlation between centroid size and shape variation could indicate an allometric trend (see e.g. Piras et al. 2011). The test was performed for all Procrustes coordinates and for the first three PC axes.

SHAPE VS. ECOLOGY

To test if feeding ecology is correlated with skull shape we categorized taxa based on dietary preference and feeding style, using the following characters: character 1, carnivorous vs. non-carnivorous; character 2, carnivorous vs. omnivorous vs. herbivorous; and character 3, weak biting vs. medium biting vs. strong biting. The subdivision of the second character is based on Barrett & Rayfield (2006), supplemented by data from Zanno & Makovicky (2011). In addition, *Euparkeria*, *Daemonosaurus* and *Zupaysaurus* were coded as carnivorous, *Eoraptor*, *Archaeopteryx*, *Anchiornis*, *Confuciusornis* and oviraptorids as omnivorous and *Limusaurus* as herbivorous. The subdivision of the third character is based on Sakamoto (2010) (Table S5.2, see supplementary information of Chapter 5). The characters were originally

coded as discrete characters. To test the correlation between shape and diet, we performed 2B-PLS in MorphoJ. Scorings of characters 2 and 3 (see above) were transformed into covariates via a Principal Coordinates Analysis (PCO) with Euclidean distances and the transformation exponent $c = 2$. This analysis was repeated for the preorbital and postorbital data sets, to test whether dietary patterns have an influence on the shape variation of different skull regions, and for the small data set, which was mainly focused on skull variation in basal birds.

To test whether taxa with different dietary preferences (carnivorous vs. non-carnivorous and carnivory vs. omnivory vs. herbivory) occupied different regions within the morphospace, we additionally performed a NPMANOVA test (nonparametric multivariate analysis of variance) in PAST with 10 000 permutations, Euclidean distances and a Canonical Variate Analyses (CVA), using the first six PC axes (large data set), which describe over 75 % of the total variance in theropod cranial shape (all outgroup taxa were excluded from the analysis, to avoid false-positive or negative signals). The NPMANOVA estimates whether the distribution of the three groups shows significant differences in morphospace (see Anderson 2001). One of the strengths of this approach is that it does not assume or require normality of the multivariate data. The test computes an F statistic and a p value, pointing to a significant difference between dietary preferences if the F value is high and p value less than 0.05. The p values were Bonferroni corrected, which set the significance level lower than the overall significance to avoid false positive signals in a dataset comparing more than two groups (Hammer & Harper 2006). In a second approach we excluded the oviraptorid taxa from the data set, to evaluate the influence of their aberrant skull morphology on previous results.

SHAPE VS. PHYLOGENY, FUNCTION AND ECOLOGY

Finally, as already addressed by Brusatte et al. (2012a), we wanted to evaluate whether skull shape in theropods is better explained by function, ecology or phylogeny. To evaluate this, we calculated various agglomerative, hierarchical cluster topologies based on the Procrustes coordinates, the SSI, ASM, SSI and ASM, as well as feeding ecology. In the latter case we combined the covariates from the PCO (see above) with SSI and ASM values, which therefore represent a diet-function cluster. The cluster analyses (UPGMA and Ward's method) were performed in PAST. In general, these kinds of cluster algorithms search for the two most similar objects and join them into a cluster. Then, the next most similar object is identified and joined and this continues until all objects are joined into one supercluster (Hammer & Harper 2006). In UPGMA, the clusters are joined based on the average distance between all members in the two groups, and in Ward's method the clusters are joined such that increase in within-group variance is minimized (Hammer 2009). Subsequently, we loaded all topologies into MorphoJ, mapped them onto the tree, and performed a permutation test. By comparing the squared length and the p value with that of the supertree topology, we were able to estimate which of the parameters best explained skull shape, based on a parsimony criterion. All topologies are shown in the supplementary information of Chapter 5 (Fig. S5.5-S5.14).

RESULTS

MORPHOSPACE AND EVOLUTIONARY TRENDS IN SKULL SHAPE

The whole dataset (large data set) is summarized by 40 PC axes. Most shape variation in theropod skulls (including outgroup taxa) is captured by the first three PC axes (34.4%, 17.1% and 11.4% of total variance), describing over 60% of total variance in all.

The first PC describes the relative length and depth of the snout (premaxilla and maxilla) and the anteroposterior dimensions of the antorbital fenestra and lateral temporal fenestra. The second PC describes the angle of the premaxillary body, the relative length and depth of the anterior extension of the jugal, the dorsoventral dimension of the antorbital fenestra, the anteroposterior dimension of the orbit, as indicated by the length of the suborbital body of the jugal, the depth of the postorbital region, and the position of the jaw joint. The third PC describes the relative length of the posterior extension of the maxilla, the inclination and depth of the lacrimal and the influence that this has on the relative size and shape of the antorbital fenestra and orbit, and the relative height of the quadratojugal. Most taxa plotted on the positive side of the first PC axis and are equally distributed along the second PC axis. Oviraptorids plot far from the other taxa because of high negative PC 1 scores, reflecting a shortened snout but enlarged lateral temporal fenestrae (Fig. 5.3).

The permutation test indicates that theropod cranial form is significantly correlated with phylogeny (tree length weighted by branch lengths = 0.78293449, $p < 0.0001$). Based on the ancestral state reconstruction, PC 1 remains almost constant from the hypothetical ancestor of basal archosauriforms to that of basal deinonychosaurs, indicating that this component was very uniform and close to the consensus shape (Fig. 5.4A). A significant deviation in this value is seen in the hypothetical ancestor of Neotheropoda, with a rapid shift to extreme snout elongation in the hypothetical ancestor of Coelophysidae. Similar deviations, and thus trends of snout elongation, can be seen in the hypothetical ancestors of Spinosauridae, Tyrannosauroidae, Ornithomimosauria, and Dromaeosauridae. Opposite deviations are present in the hypothetical ancestors of ceratosaurs and oviraptorids, which have markedly shorter

snouts; this trend is especially pronounced in oviraptorids. In contrast, according to this component (PC 1) the skull shape of the hypothetical ancestor of basal birds does not differ greatly from that of basal deinonychosaurs (Fig. 5.4A). Principal Component 2 (Fig. 5.4B) shows a continuous decrease from the hypothetical ancestor of Archosauriformes to that of Theropoda, thus demonstrating a trend of relative increase of the anteroposterior length of the orbit (in relation to orbit height) and decrease of the dorsoventral depth of the infratemporal fenestra. From the hypothetical ancestor of theropods to that of neotetanurans the value is relatively constant, but decreases again from this point to the hypothetical ancestor of deinonychosaurs. However, this value shows a number of deviations along the main phylogenetic axis of theropods. Whereas the hypothetical ancestors of Ceratosauria, Tyrannosauroidae, Ornithomimosauria and Avialae show a further decrease of PC 2, values increase in the hypothetical ancestor of Abelisauridae, Allosauroidae, Megalosauroidae, and Tyrannosauridae, indicating a shift to a skull shape with a deep temporal fenestra, a dorsoventrally elongated orbit and a deep suborbital body of the jugal. In all of these taxa, these changes are related to a marked increase in body size (Fig. 5.4B). The third PC (Fig. 5.4C) shows a continuous increase from the hypothetical ancestor of archosauriforms to that of coelurosaurs, indicating a shift in the orientation of the lacrimal, resulting in an increase of the relative size of the antorbital fenestra and a decrease of the orbit. From the hypothetical ancestor of coelurosaurians to that of deinonychosaurs the component decreases only slightly. However, with the exceptions of the hypothetical ancestors of coelophysids, basal ceratosaurs and avialans, all other groups show a further increase in their respective lines. The skull shape of the hypothetical ancestor of Avialae fits with that of basal Deinonychosauria (Fig. 5.4C).

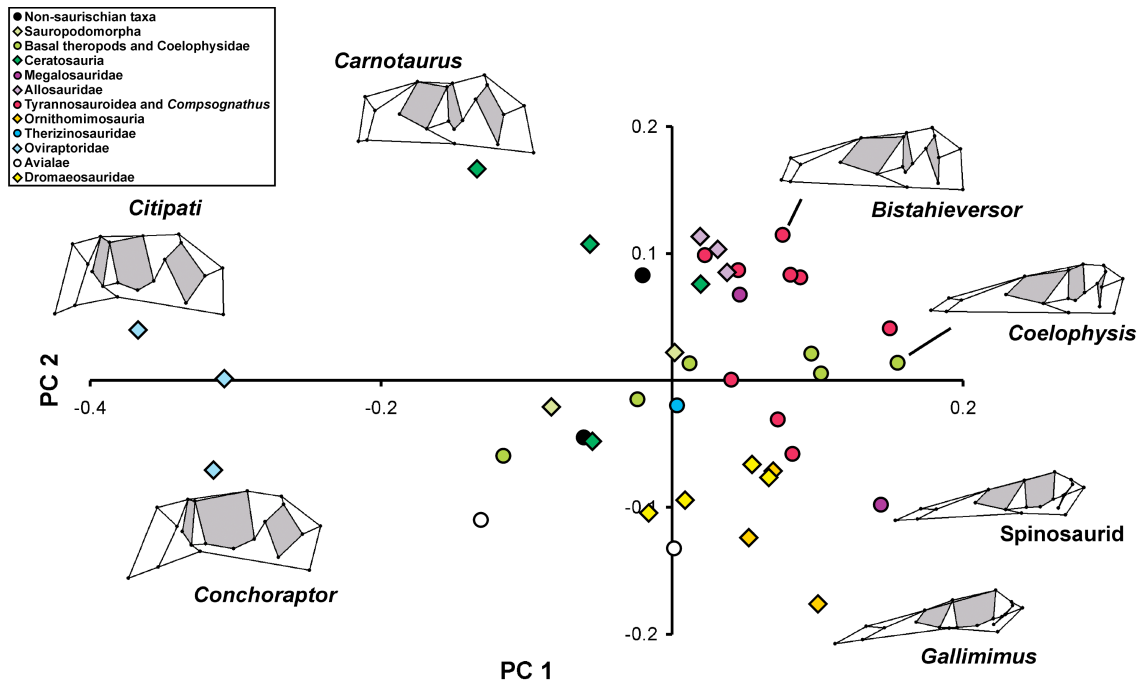


Fig. 5.3. Two-dimensional morphospace of the theropod skull shape (large data set) with distribution of the different theropod clades, based on the first two PC axes. The most derived taxa with respect to the first two components are visualized with relative warps. Shape changes along PC 1 reflect changes in the length and height of the snout and the anteroposterior dimensions of the lateral temporal fenestra. Changes along PC 2 reflect the height of the postorbital region, the size of the orbit and the position of the jaw joint.

The morphospace of the second, smaller dataset is summarized with 13 PC axes. Here, the first three PC axes describe more than 70% of total variation (PC 1 = 34.6%, PC 2 = 21.9%, PC 3 = 14.1%). The paravian taxa are well separated from other coelurosaurian taxa, in which the close paravian outgroup taxa *Velociraptor* and *Sinornithosaurus* plot in the same morphospace as the more basal coelurosaurs *Compsognathus*, *Dilong* and *Ornithomimus*. This is also true for the alvarezsaurid *Shuvuuia*. However, *Erlikosaurus* and *Anchiornis* lie closer to *Archaeopteryx*. *Confuciusornis* represents the greatest outlier within Avialae, whereas the skull shape of

enantiornithine birds plots close to *Archaeopteryx* (Fig. 5.4D). Performing the permutation test for the smaller data set, the tree length is 0.45221156 ($p = 0.0124$), indicating a significant phylogenetic signal. The following trends of shape changes can be described within the avialan lineage: a decrease in the angle of the anterior margin of the premaxillary body accompanied by an elongation of the nasal process of the premaxilla, both leading to a markedly triangular skull shape, a decrease in the height of the maxillary body, a decrease in the size of the antorbital fenestra, a decrease in the depth of the jugal body, and a decrease in the size of the temporal fenestra.

SHAPE VS. FUNCTION

The 2B-PLS reveals significant correlation between Procrustes coordinates (shape) and both functional parameters (SSI and AMS). Interestingly, this correlation is stronger in the postorbital than in the preorbital region (Table 5.1), which indicates that skull function has a stronger influence on shape variation in the postorbital region than in the preorbital region. Despite this difference, shape variation in both regions is significantly correlated (2B-PLS: RV coefficient=0.261, $p < 0.0001$; PLS: RV coefficient=0.494; $p < 0.0001$). Comparing the results of the shape variation for the three lateral skull openings, the orbit showed the strongest correlation with both functional proxies. The lateral temporal fenestra, as part of the postorbital region, also shows a significant correlation, whereas the shape of the antorbital fenestra does not. This result supports Henderson's (2002) proposal that orbit shape is an important indicator of the mechanical performance of a theropod skull (see below).

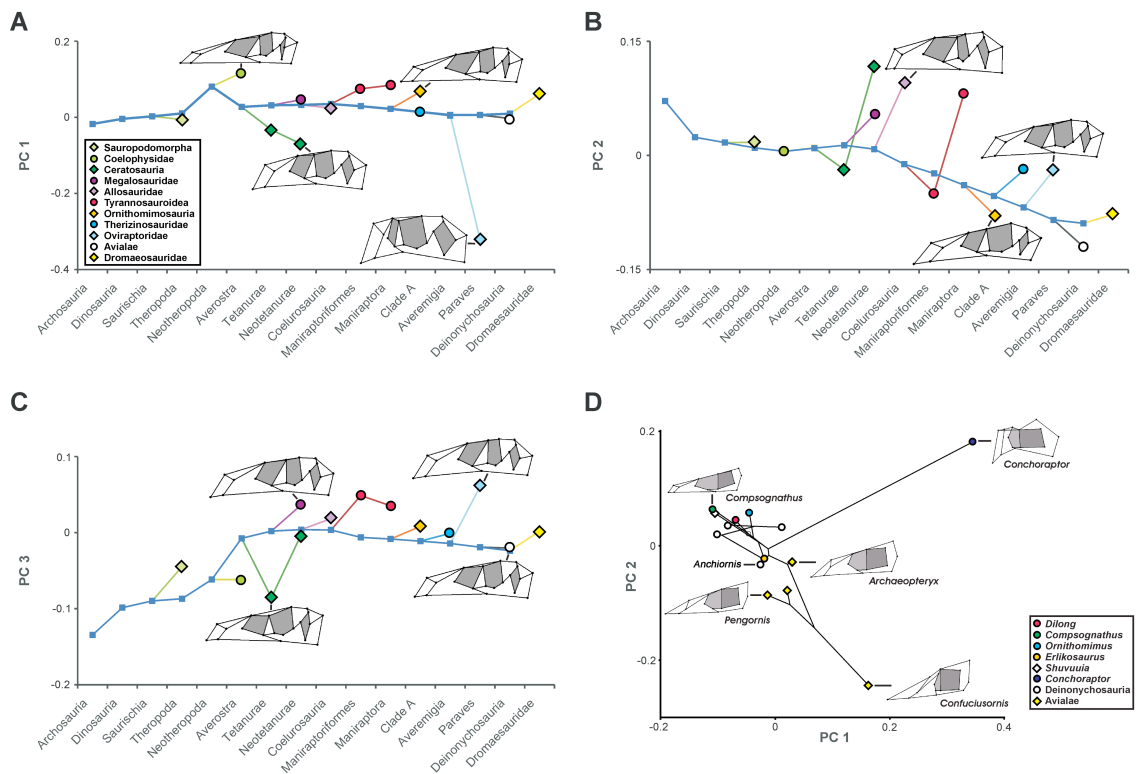


Fig. 5.4. A-C. One-dimensional morphospaces of the most important theropod groups based on the ancestral state reconstruction of the first three principal components illustrating the major shape changes of the respective principal components. The X-axis represents the clade rank. **D.** Morphospace of the smaller dataset showing the cranial diversity of paravians. Deinonychosaurs and basal coelurosaurs (with the exception of *Conchoraptor*) plot in a small area possessing skulls with a rectangular shape and large antorbital fenestrae, whereas basal birds occupy a large area possessing skulls with a more triangular shape, but with great variation in the beak shape and the relative size of the antorbital fenestra (Note that the symbols in D differ from that of A-C).

Based on the PIC analyses of the large data set, the skull strength indicator is significantly correlated with PC 2 and 3, whereas the average maximum stress is significantly correlated with PC 1 and 3 (Table 5.2). Thus, shape variation described by the first three PC axes seems to include morphofunctional information in respect to average maximum stress and skull strength. All three components at least partially

describe the shape of the postorbital region (PC 1 – anteroposterior dimension of lateral temporal fenestra; PC 2 – depth of postorbital region and relative position of jaw joint; PC 3 – relative height of quadratojugal), which, given the strong correlation between the shape variation in this region and functional indicators, might explain this correlation. Furthermore, PC 2 and 3 both concern the shape of the orbit and surrounding structures, supporting the result described above. In contrast, the PIC analysis based on the original dataset from Henderson (2002) shows no significant correlation between shape and function (Table 5.2). However, this contradictory outcome could be the result of the small sample size of the original data set, and fails to be a diagnostic test for the PIC analysis (Table S5.4, see supplementary information of Chapter 5).

Table 5.1. Results of the two-block partial least squares, showing the degree of correlation of Procrustes coordinates with biomechanical coefficients (skull strength indicator and average maximum stress, both log-transformed) and the diet (RV coefficient and *p* value) with the whole skull, the preorbital and the postorbital region.

	Log Centroid Size	SSI	AMS	AMS+SSI	Diet
Whole skull	0.38/<0.001	0.33/<0.001	0.39/<0.001	0.35/<0.001	0.41/<0.001
Preorbital region	0.23/<0.001	0.15/0.019	0.19/0.004	0.16/0.012	0.26/0.001
Postorbital region	0.39/<0.001	0.32/0.0002	0.33/<0.001	0.32/<0.001	0.43/<0.001
Antorbital fenestra	0.12/0.03	0.06/0.234	0.01/0.067	0.07/0.167	-
Orbit	0.59/<0.001	0.63/<0.001	0.60/<0.001	0.63/<0.001	-
Lateral temporal fenestra	0.28/<0.001	0.21/0.002	0.24/<0.001	0.22/0.001	-
Small data set (bird skulls)	0.31/0.04	-	-	-	0.32/0.114

The overall skull shape represented by the Procrustes coordinates is strongly correlated with centroid size in the large data set. Furthermore, all three PC axes show a significant correlation, with the second axis showing the best fit (Table S5.3, see supplementary information of Chapter 5). This result differs from that of Brusatte et al. (2012a), where only the second PC axis showed a significant relationship with centroid size. This indicates that all three PC axes still retain some information on size. A correlation between centroid size and Procrustes coordinates is also found for the small data set, thus also indicating a correlation between skull shape and skull size. However, in contrast to the results for the large data set, there is no significant correlation of centroid size with each of the first three PC axes.

Table 5.2. Results of the PIC analyses, showing the degree of correlation between PC scores and biomechanical coefficients (R^2 and p value). SSI* represents the small dataset which includes only the original data from Henderson et al. (2002).

	R^2	p value
PC 1 contrasts vs. SSI contrasts	0.011	0.521
PC 2 contrasts vs. SSI contrasts	0.327	<0.001
PC 3 contrasts vs. SSI contrasts	0.341	<0.001
PC 1 contrasts vs. AMS contrasts	0.141	0.015
PC2 contrasts vs. AMS contrasts	0.082	0.070
PC 3 contrasts vs. AMS contrasts	0.154	0.011
PC 1 contrasts vs. SSI* contrasts	0.203	0.122
PC 2 contrasts vs. SSI* contrasts	0.296	0.054
PC 3 contrasts vs. SSI* contrasts	0.069	0.386

SHAPE VS. ECOLOGY

The 2B-PLS analysis reveals a significant correlation between overall skull shape and dietary parameters. As was the case for the functional proxies, this correlation is

stronger in the postorbital region (Table 5.1). A comparison between only carnivorous and non-carnivorous taxa shows a significant difference between both groups. When looking at non-carnivorous taxa in more detail (i.e. distinguishing between omnivorous and herbivorous forms), we find that, within the morphospace of the first three PC axes, herbivorous and omnivorous taxa overlap in a large area, but only slightly with the carnivorous taxa (Fig. 5.5A, B). This is also supported by the distribution of taxa in the CVA plot (Fig. 5.5C, D). A pairwise comparison of all three groups after performing a NPMANOVA test supports this observation, i.e. carnivorous taxa differ significantly from omnivorous and herbivorous taxa, whereas omnivores do not differ significantly from herbivores (Table 5.3). The exclusion of the highly aberrant oviraptorid taxa in both analyses does not affect these results. Performing the 2B-PLS analysis for the small dataset recovers no significant signal, which might, however, be a result of the significantly smaller sample size.

SHAPE VS. PHYLOGENY, FUNCTION AND ECOLOGY

Based on the squared length, the topologies of both diet-function clusters are the most parsimonious explanation for the distribution of taxa within the morphospace, followed by the Ward's Cluster that combines the values of the average maximum stress and the skull strength indicator, and the supertree topology. The other functional clusters are less parsimonious than the supertree phylogeny (Table 5.4). Based on this result it seems that feeding ecology (as a combination of diet and biting performance) explains skull shape in theropod dinosaurs better than phylogeny. However, similar to the results of Brusatte et al. (2012a), phylogeny seems to have a larger influence on skull shape variance than any single functional proxy.

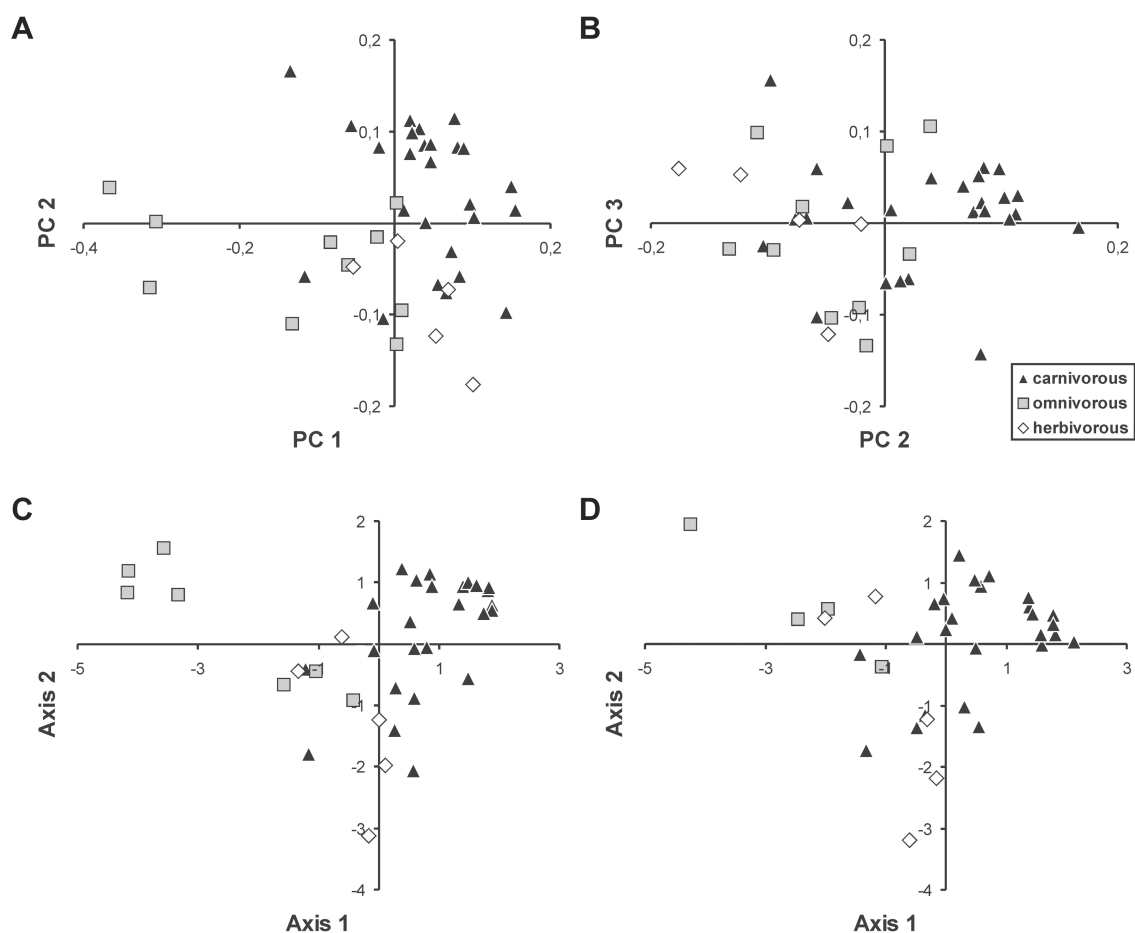


Fig. 5.5. Two-dimensional morphospace of the theropod skull shape and CVA plot with distribution of the carnivorous (black triangle), omnivorous (grey squares) and herbivorous (white diamonds) taxa (non-theropod taxa are not shown). **A.** PC 1 vs. PC 2. **B.** PC 2 vs. PC 3. In both diagrams herbivorous and omnivorous taxa overlap one another strongly, whereas carnivorous taxa overlap only marginally with herbivorous forms, but moderately with omnivorous forms. **C.** CVA plot with oviraptorids. **D.** CVA plot with oviraptorids excluded.

DISCUSSION

MAJOR PATTERNS IN THEROPOD CRANIAL MORPHOSPACE

Analysing theropod cranial diversity via geometric morphometrics helps to quantify variation in shape. The data show that snout length and the length of the postorbital

region are inversely correlated with each other (as already found by Marugán-Lobón & Buscalioni 2003), whereas snout length is weakly positively correlated with orbit size (PC 1). The depth of the postorbital region is correlated with the relative position of the jaw joint (PC 2). In contrast, snout depth (PC 1, 3) is not correlated with the depth of the postorbital region (PC 2). The size of the orbit is mainly correlated with the length of the jugal body and inversely correlated with the depth of the postorbital region (PC 2). These findings might indicate that total snout shape is not directly associated with the shape of the postorbital region, as previously hypothesized by Marugán-Lobón & Buscalioni (2004) and Brusatte et al. (2012a). However, based on the results of the PLS tests, shape variations in both regions do not seem to be completely independent of one another.

Table 5.3. Results of the NPMANOVA (with and without oviraptorids) verifying the differences of the skull shape based on different diets (*F* value - white fields / *p* value - grey fields).

	non-carnivorous	carnivorous	
non-carnivorous	-	7.430	
carnivorous	<0.001	-	
non-carnivorous (no oviraptorids)	-	5.626	
carnivorous (no oviraptorids)	<0.001	-	
	herbivorous	omnivorous	carnivorous
herbivorous	-	3.129	3.324
omnivorous	0.161	-	10.780
carnivorous	0.051	<0.001	-
herbivorous (no oviraptorids)	-	1.498	3.324
omnivorous (no oviraptorids)	0.533	-	4.992
carnivorous (no oviraptorids)	0.051	0.006	-

The theropod group with the most aberrant skull morphology is the Oviraptoridae, which shows an extreme negative PC 1, indicating a short and high snout and large postorbital region (see also Clark et al. 2002b; Osmólska et al. 2004). This conclusion is supported by the cluster analyses (Fig S5.5, S5.6, see supplementary information of Chapter 5) where all three oviraptorid taxa cluster together, but form a branch to the exclusion of all other theropods. Brusatte et al. (2012a) also found oviraptorids to have the most unusual skull shape within theropods. Further outliers are the abelisaurid *Carnotaurus* (high positive PC 2), which has an extremely high skull with a small, dorsoventrally elongated orbit, and the ornithomimosaur *Gallimimus* (high negative PC 2), which has a flat skull with an enlarged orbit.

Table 5.4. Results of the permutation test showing the correlation of the morphospace with the supertree and various cluster topologies (squared length and *p* value).

	Squared length / <i>p</i> value
Supertree	0.783/<0.001
UPGMA (PCA)	(0.585/<0.001)
Ward (PCA)	(0.476/<0.001)
UPGMA (AMS)	0.806/0.002
Ward (AMS)	0.816/0.003
UPGMA (SSI)	0.838/0.081
Ward (SSI)	0.836/0.044
UPGMA (AMS+SSI)	0.792/<0.001
Ward (AMS+SSI)	0.726/<0.001
UPGMA (Diet+ AMS+SSI)	0.587/<0.001
Ward (Diet+ AMS+SSI)	0.602/<0.001

Previous studies on recent birds demonstrated that the greatest morphological variation is also found in the rostrum (primarily in the shape of the premaxilla; Marugán-Lobón & Buscalioni 2006), which is correlated with a great variety of feeding

strategies (Zusi 1993; Smith 1993). In birds, the length of the rostrum is independent from that of the orbital and postorbital region, whereas the orientation of the rostrum has an influence on the shape of the posterior skull parts (Marugán-Lobón & Buscalioni 2006). However, this morphological variation seems to be controlled by only a small set of signal molecules (β -catenin, BMP, calmodulin, Dkk3, TGF β IIr; Abzhanov et al. 2004, 2006; Wu et al. 2004, 2006; Mallarino et al. 2011). At this stage, it is of course speculative to hypothesize similar gene regulatory networks in theropods. However, by investigating the molecular control of the development of the rostrum shape in different bird and crocodile groups, it might be possible to create an extant phylogenetic bracket (*sensu* Witmer 1995) for cranial development in Archosauria. If it is possible to correlate different expression patterns of signal molecules with the morphological variation of the rostrum in birds and crocodiles in a mathematical way (see Johnson & O'Higgins 1996; Campàs et al. 2010), it might be possible to use geometric morphometric methods to investigate the genetic control of cranial diversity in fossil archosaurs (see also Klingenberg 2010).

SHAPE VS. PHYLOGENY

The skull shape of theropods is significantly correlated with higher-level phylogeny in both data sets. A similar result was found by Brusatte et al. (2012a). However, the correlation in the smaller dataset was weaker at a lower taxonomic level (see Jones & Goswami 2010), which could be the result of incomplete sampling.

A problem with this correlation is certainly the highly incomplete sampling of theropod phylogeny, because of incompleteness of the fossil record, most importantly the lack of good cranial material for most taxa. Thus, only 13% of known global

theropod diversity could be included in the analyses. Cranial data from Megalosauridae (e.g. *Eustreptospondylus*, *Torvosaurus*), Alvarezsauridae (included in the small data set), basal Oviraptorosauria (e.g. *Caudipteryx*, *Incisivosaurus*), basal Therizinosauridae (e.g. *Beipiaosaurus*) and some basal birds are missing in the current analysis. Furthermore, many data are derived from skull reconstructions, the accuracy of which might be questionable. This problem is exemplified by the spinosaurid skull used, which is based on a combination of information on skull morphology from three different taxa (see supplementary information of Chapter 5 and Rauhut 2003a for details). Additionally, there are large time gaps, especially in the Early and Middle Jurassic as well as in the late Early Cretaceous to early Late Cretaceous, which might influence the results of the squared changed parsimony and PIC analyses. The time gaps mainly concern the basal radiation of the clades Averostra, Abelisauridae, Tyrannosauridae, Ornithomimosauria, Therizinosauridae, Oviraptoridae, and Dromaeosauridae.

Interestingly, the skull shape of basal birds does not differ significantly from that of basal deinonychosaurians, which are represented by *Anchiornis*. On the one hand this might mean that the skulls of basal birds and troodontids were very similar, from close relationship or similar diet preference. Alternatively, this observation might reflect phylogenetic uncertainty, and it is possible that *Anchiornis* was instead a basal member of Avialae, as originally described (see Xu et al. 2009b). This has to be tested in future phylogenetic analyses, as is the case with the currently published hypothesis that *Anchiornis* forms a clade with *Archaeopteryx* at the base of Deinonychosauria, outside of Avialae (Xu et al. 2011), in which case the similarities in shape between these two taxa might represent a low-level taxonomic signal. In contrast, the skull of the

alvarezsaurid *Shuvuuia* plots within the coelurosaurs, close to *Compsognathus*, but far away from the avialan taxa. This is surprising, because the skull of *Shuvuuia* is extremely bird-like and possesses several characters otherwise unknown in non-avian theropods, which was one of the factors that led to the original identification of this animal as a basal avialian (see e.g. Chiappe et al. 2002). However, in contrast to basal birds, *Shuvuuia* possesses an enlarged antorbital fenestra and an extremely elongated maxillary body, which is similar to basal coelurosaurs. Thus, the different positions of *Shuvuuia* and basal birds within the morphospace are mainly based upon the shape of the snout. However, the shape analysis might lend further support to the hypothesis that alvarezsaurids are more basal coelurosaurs outside Paraves (Clark et al. 2002a; Novas & Pol 2002; Choiniere et al. 2010). Within Avialae, the skull shapes of *Archaeopteryx*, *Confuciusornis* and Enantiornithes differ greatly from each other. Mapping the phylogeny onto the morphospace further demonstrates that the stem species of Avialae, Pygostylia and Enantiornithes are well separated from each other, indicating a rapid diversification of skull morphology, probably in connection with the phylogenetic and ecological radiation of this group in the Early Cretaceous (Zhou & Zhang 2003; You et al. 2006; Li et al. 2010; O'Connor & Chiappe 2011). This result is further supported by the cluster analyses carried out for the large dataset, which includes only two avialan species. However, here both *Archaeopteryx* and *Confuciusornis* plot in very different positions in the morphological clusters, indicating strong dissimilarities in cranial shape (Fig. S5.5, S5.6, see supplementary information of Chapter 5). Taking the skull morphology of the long-headed *Zhongjianornis* and Longipterygidae or the short-headed Sapeornithidae into account, the actual morphospace of basal birds is probably much greater than estimated.

SHAPE VS. FUNCTION

As mentioned above, the study presented by Brusatte et al. (2012a) attempted to correlate geometric morphometric data of the theropod cranium with biting performance, based on a mechanical advantage approach (see Sakamoto 2010). These authors found a significant, but weak correlation between shape and function and concluded that phylogeny was a more important determinant of skull shape than function. By comparing the RV coefficients of the 2B-PLS presented in both studies, the correlation between shape and function is about three times higher in the current data set, but the results of the PIC analyses are almost the same in both studies. The average maximum stress explains only about 6.6% and the skull strength indicator about 9.5% of total cranial shape variation in theropods. However, an interesting result of the present study is that the shape of the postorbital region is better correlated with function than that of the preorbital region, and that the shape of the orbit shows the strongest correlation, whereas the shape of the antorbital fenestra shows no significant correlation. These results are also supported by the correlation of the skull strength indicator with the second and third PC axes (see PIC analysis), which include aspects that describe the shape and depth of the orbital and postorbital regions (e.g. shape and size of the orbit, depth of the suborbital body of the jugal, the position of the jaw joint). These results support previous morphofunctional studies that demonstrated that the orbital and postorbital regions of theropod skulls seem to be more important for an understanding of skull biomechanics than the snout. According to Henderson (2002) there is an inverse relationship between the size of the theropod orbit and the resistance of the skull to bending in the sagittal plane, and the narrowness of the orbit shows a positive correlation with skull strength. Henderson (2002) interpreted the correspondence between orbit size and shape to relate to increases in the amount of bone comprising the

skull, and so its strength. He furthermore proposed that the shape of the orbit in theropods with strong skulls is governed by the requirements of the posterior half of the skull to resist muscle-generated forces associated with prey capture and/or dismemberment. Furthermore, based on a finite element approach, Rayfield (2005) demonstrated that high tensile and shear stresses especially affect the jugal bone, the shape of which in turn influences the anteroposterior dimension of the orbit. According to Rayfield (2011), the postorbital part of the skull (especially the squamosal, quadrate and quadratojugal) experiences most of the Von Mises stress associated with biting in theropods. It is thus to be expected that these stresses result in stronger mechanical constraints on the postorbital region of the skull than on the preorbital region, which is confirmed by the findings presented here. Furthermore, since overall stress acting on the skull (for which the functional data used here are a proxy) is necessarily correlated with skull size, it is not surprising that the shape of the postorbital region is also correlated with centroid size (as proxy for skull size). This is also in accordance with the finding of Rauhut (2007) that phylogenetic characters in the braincases of theropods seem to be influenced by size. Thus, the results of biomechanical studies (e.g. Rayfield 2011), phylogenetic data (Rauhut 2007) and morphometric analyses (present study) converge on the result that the postorbital region of the skull is particularly strongly influenced by biomechanical forces and related aspects of size. It might be worth noting, however, that the correlation between functional proxies and the preorbital region, found in both the 2B-PLS and in the PIC analysis (average maximum stress vs. PC 1), indicates that snout shape is also functionally constrained, but to a weaker degree.

The lack of correlation between the shape of the antorbital fenestra and the proxies for cranial mechanics used here might be surprising at first glance. Witmer

(1997) suggested that the size and shape of the antorbital fenestra were largely determined by biomechanical factors, in that bone was resorbed opportunistically by pneumatic diverticula if it was not biomechanically necessary. Thus, our results seem to contradict this hypothesis. However, it is necessary to keep in mind that the shape of the antorbital fenestra is only captured by three landmarks and that the proxies for cranial function used here are proxies for the overall stress acting on the skull, not for the stress distribution within the cranium. Thus, although the overall stress experienced by the skull during biting might be high, this does not contradict the idea that particular parts of the cranium experience stresses that are below the threshold for the formation of bone, as has been demonstrated by Finite Element Structural Synthesis for other dinosaurs (Witzel & Preuschoft 2005; Witzel et al. 2011). In this respect, the hypothesis that the antorbital fenestra is associated with a region of low stress might even be supported by the weaker correlation between the shape of the preorbital region with the functional proxies for overall stress in the cranium, since the latter indicates that there might be less overall stress acting on this part of the skull (which, in turn, is in accordance with the results obtained by Rayfield [2011]).

It must be emphasised that the current approach is much more simple than that used by Brusatte et al. (2012a), and both functional parameters used here are necessarily strongly correlated with size, since larger taxa are expected to experience higher total stresses than smaller taxa (see Henderson 2002; Rayfield 2011). In contrast, Brusatte et al. (2012a) used a metric of functional biting profiles, which are more complex and independent from size. However, the impact of both the functional parameters (AMS and SSI) on skull shape is rather small, as previously hypothesized by Brusatte et al. (2012a). Nevertheless, it would be worthwhile to test the results further by using other

functional parameters or metrics (e.g. finite element analyses) or by using a different landmark combination, different skull views, or a three-dimensional approach (see also Brusatte et al. 2012a).

SHAPE VS. ECOLOGY

As is the case with phylogeny and function, dietary patterns are also correlated with skull shape variation. Interestingly, we found a higher correlation for the postorbital region than for the preorbital region. This might be regarded as a surprising result, because one might expect that dietary preferences would have an equal or even stronger influence on the shape of the snout, the main organ used to obtain and process food. However, the result probably reflects the generalised subdivision in diet preference (carnivory vs. omnivory vs. herbivory) and that the dietary patterns also contain information on biting behaviour (see character 3), and thus biomechanical aspects (see above). Furthermore, different tooth morphologies, which are not captured in the current approach, might better reflect more specific dietary patterns than overall shape of snout (see also Smith 1993; Barrett et al. 2011; Zanno & Makovicky 2011).

Carnivorous, omnivorous and herbivorous theropods occupy large areas of morphospace. Based on disparity analyses, Brusatte et al. (2012a) demonstrated that non-carnivorous theropods (i.e. herbivores and omnivores) display a higher cranial disparity than carnivores. This result was largely influenced by the aberrant skull shape of oviraptorid dinosaurs, and their exclusion significantly reduced the difference in disparity between carnivorous and non-carnivorous forms. However, the current results indicate that both omnivorous and herbivorous taxa overlap strongly in morphospace, but only slightly with carnivorous theropod taxa (Fig. 5.5, Table 5.3). The exclusion of

oviraptorids does not affect this result. This might indicate that changes between omnivory and herbivory had only small effects on skull shape, whereas changes between carnivory and non-carnivory (i.e. omnivory or herbivory) affect skull shape more strongly. Alternatively, this result might also indicate that the classification of omnivorous and herbivorous taxa on the basis of skull shape in fossil taxa is rather poor, particularly because among extant vertebrates the boundary between herbivory and omnivory is gradual (Zanno & Makovicky 2011). Further information should be incorporated, such as pelvis morphology, fossilized gut contents and coprolites, or the presence of gastroliths (Zhou et al. 2004; Barrett & Rayfield 2006; Zanno & Makovicky 2011), i.e. evidence that is independent from cranial morphology. Subdividing the taxa into carnivorous and non-carnivorous forms leads to a significant difference as well, supporting the assumption that a change between carnivory and non-carnivory had a marked effect on cranial shape. However, the large area of morphospace occupied by non-carnivorous taxa indicates further that an omnivorous or herbivorous diet was an important resource for many small-bodied theropods and may have been a fundamental driver of theropod evolution, especially within the coelurosaurian (Zanno & Makovicky 2011; Brusatte et al. 2012a) and avialan clades (O'Connor & Chiappe 2011).

CONCLUSIONS

This study investigates the cranial shape variation of various non-avian theropod dinosaurs and some basal birds in a broad scale approach, using two-dimensional geometric morphometrics. The results indicate that most variation in the theropod cranium occurs in the shape of the snout (PC 1), the shape and size of the orbit and the shape of the postorbital region (PC 2 and PC 3). Interestingly, especially in the first principal component, there is surprisingly little change in the ancestral node

reconstructions from basal archosauriforms all the way to birds. This might indicate that, in respect to snout shape, there is a generalist archosauriform condition, from which different clades deviate when specializing for certain ecological niches. Oviraptorids had the most aberrant skull shape in the theropod data set, but we further found that the skull shapes of abelisaurids and spinosaurids, for instance, differ greatly from those of other large bodied predators, with the former being characterized by an unusually deep and short skull and the latter by the other extreme, a low and long skull. Skull shape is strongly correlated with phylogeny, but also feeding ecology. Interestingly, the skull shape of non-carnivorous taxa differs significantly from that of carnivorous forms, which might indicate that a change between both diet preferences strongly affected skull shape. In sum, non-carnivorous taxa occupy large areas of morphospace, indicating that a diverse diet might have been a fundamental driver of the evolution of the morphological diversity of theropod skulls. We further found that skull shape is also correlated with dietary patterns, average maximum stress and skull strength, indicating that the cranium of theropods (especially the shapes of the orbital and postorbital regions) was constrained by ecology and function, especially biomechanics.

Using a different subsample of taxa (including some outgroup taxa and basal birds) and landmarks, we were able to support most of the results found by Brusatte et al. (2012a) in their independently conducted study of cranial shape in theropods. These include major shape changes along the first two PC axes, i.e. the relative length of pre- and postorbital regions (PC 1), and the depth of the postorbital region and the size and shape of the orbit (PC 2), leading to a very similar distribution of taxa within the morphospace. We also found that skull shape is significantly correlated with phylogeny, but also with function. Comparing the squared lengths of the permutation tests, the

functional clusters of the average maximum stress and the skull strength indicator taken separately are less parsimonious, which might indicate that phylogeny has a stronger influence on skull shape than function, as already hypothesized by Brusatte et al. (2012a). However, a single Ward cluster, which includes both functional proxies, was found to be more parsimonious, challenging the previous result, whereas the best match was found for those clusters that include dietary patterns and both functional proxies. Nevertheless, given the consensus in several important points between Brusatte et al. (2012a) and the current study, the other results mentioned above can be considered as strongly supported.

Based on the current results, we prefer not to speculate about which factor had the largest influence on theropod skull shape, as this might vary within different groups and also depends on the different proxies used. Further investigations into the relationship between function and cranial shape are needed, preferably using more specific data not only on overall stress, but also on stress distribution within the cranium, such as data from finite element analyses. To further test the current results it would also be worthwhile to use other subsamples of landmarks, incorporating data from other views of the skull, broadening the taxonomic sample, and, as far as possible, using three-dimensional data. Furthermore, it would also be interesting to evaluate the variation of skull shape of one species based on different reconstructions or different specimens, or differences between closely related species, and how this might influence the results of the PCA.

ACKNOWLEDGEMENTS

We thank Roger Benson (University of Cambridge, UK), Steve Brusatte (American Museum of Natural History, New York, USA) and Manabu Sakamoto (University of Bristol, UK) for their critical and helpful reviews, Richard Butler (Ludwig Maximilians University, München, Germany) for proofreading and for discussion, and Michael Benton (University of Bristol, UK) for the final correction of the manuscript. Christine Böhmer (Die Bayerische Staatssammlung für Paläontologie und Geologie, München, Germany) is thanked for help with the introduction to the morphometric software. The study was funded by the German Research Foundation (DFG) under project RA 1012/12-1.

CHAPTER 6

An exceptionally preserved juvenile megalosauroid theropod dinosaur with filamentous integument from the Late Jurassic of Germany

Keywords:

feather evolution; Megalosauridae; Theropoda; Upper Jurassic

The chapter was published as:

Rauhut OWM^{1,2,3}, Foth C^{1,2}, Tischlinger³ & Norell MA⁴. 2012. An exceptionally preserved juvenile megalosauroid theropod dinosaur with filamentous integument from the Late Jurassic of Germany. *Proceedings of the National Academy of Sciences, U.S.A.* 109: 11746-11751.

¹*Bayerische Staatssammlung für Paläontologie und Geologie, Richard-Wagner-Str. 10, D-80333 München, Germany*

²*Department of Earth and Environmental Sciences, Ludwig-Maximilians-University, Richard-Wagner-Str. 10, D-80333 München, Germany*

³*GeoBioCenter, Ludwig-Maximilians-University; Richard-Wagner-Str. 10, D-80333 München, Germany*

⁴*Tannenweg 16, 85134 Stammham, Germany.*

⁵*Division of Paleontology, American Museum of Natural History, Central Park West at 79th Street, New York, NY 10024, USA*

Received 27 February 2012, accepted 29 May 2012.

Author contribution:

Research design: Oliver Rauhut, **Christian Foth**, Mark Norell

Data collection: Oliver Rauhut, **Christian Foth**, Helmut Tischlinger

Data analyses: Oliver Rauhut, **Christian Foth**

Preparation of figures and tables: Oliver Rauhut

Wrote paper: Oliver Rauhut, **Christian Foth**, Mark Norell

***All figures of Chapter 6 are modified after Rauhut et al. (2012)**

An exceptionally preserved juvenile megalosauroid theropod dinosaur with filamentous integument from the Late Jurassic of Germany

Oliver W. M. Rauhut, Christian Foth, Helmut Tischlinger & Mark A. Norell

ABSTRACT

Recent discoveries in Asia have greatly increased our understanding of the evolution of dinosaurs integumentary structures, revealing a previously unexpected diversity of ‘protofeathers’ and feathers. However, all theropod dinosaurs with preserved feathers reported so far are coelurosaurs. Evidence for filaments or feathers in non-coelurosaurian theropods is circumstantial and debated. Here we report an exceptionally preserved skeleton of a juvenile megalosauroid, *Sciurumimus albersdoerferi* n. gen. n. sp., from the Late Jurassic of Germany, which preserves a filamentous plumage at the tail base and on parts of the body. These structures are identical to the type 1 feathers that have been reported in some ornithischians, the basal tyrannosaur *Dilong*, the basal therizinosauroid *Beipiaosaurus*, and, probably in the basal coelurosaur *Sinosauropteryx*. The new taxon represents the phylogenetically most basal theropod that preserves direct evidence for feathers and helps to close the gap between feathers reported in coelurosaurian theropods and filaments in ornithischian dinosaurs, further supporting the homology of these structures. The specimen of *Sciurumimus* is the most complete megalosauroid yet discovered and helps clarifying significant anatomical details of this important basal theropod clade, such as the complete absence of the fourth digit of the manus. The probably early post-hatchling individual furthermore shows marked

similarity with basal coelurosaurian theropods in the dentition, indicating that coelurosaur occurrences based on isolated teeth should be used with caution.

INTRODUCTION

The discovery of *Archaeopteryx* in 1861 in Late Jurassic rocks in Southern Germany provided the first evidence of derived, avialan maniraptoran theropods with feathers (Wellnhofer 2008). These remains long remained the only skeletal specimens with preserved feathers from the Mesozoic. In recent years, however, Mesozoic birds that preserve feathers and even non-avian theropods with feathery body coverings have been found and are now phylogenetically and temporally widespread (Xu & Guo 2009). Nearly all of these come from the Middle Jurassic to Early Cretaceous of eastern Asia and all are coelurosaurs. Thus, there is a considerable phylogenetic gap between these animals and some basal ornithischians and pterosaurs, in which mono-filamentous integumentary structures have been reported (Mayr et al. 2002; Unwin 2006; Zheng et al. 2009). The specimen reported here is significantly more basal in the evolutionary tree of theropods and thus represents the phylogenetically most basal theropod yet discovered with direct fossil evidence of a filamentous body covering. It is furthermore noteworthy in that it represents the most complete basal tetanuran theropod known to date and one of very few complete early juvenile theropods known.

SYSTEMATIC PALEONTOLOGY

Dinosauria Owen, 1842; Theropoda Marsh, 1881; Tetanurae Gauthier, 1986; Megalosauroida (Fitzinger, 1843); *Sciurumimus albersdoerferi* gen. et sp. nov.

HOLOTYPE

BMMS (Bürgermeister Müller Museum Solnhofen) BK 11, a complete and exquisitely preserved skeleton of a juvenile individual preserved on a single slab.

ETYMOLOGY

Genus name from the scientific name of the tree squirrels, *Sciurus*, and *mimos* (Greek), meaning mimic, in reference to the bushy tail of the animal. The species epithet honours Raimund Albersdörfer, who made the specimen available for study.

TYPE LOCALITY AND HORIZON

Rygol quarry, near Painten, Bavaria, Germany. Thin-bedded to laminated micritic limestones that are equivalent to the upper part of the Rögling Formation (Zeiss 1977), Upper Kimmeridgian, *Beckeri* zone, Ulmense subzone, *rebouletianum* horizon (Link & Fürsich 2001; Schweigert 2007).

DIAGNOSIS

Megalosauroid theropod with the following apomorphic characters: Axial neural spine symmetrically “hatchet-shaped” in lateral view; posterior dorsal neural spines with rectangular edge anteriorly and lobe-shaped dorsal expansion posteriorly; anterior margin of ilium with semioval anterior process in its dorsal half.

DESCRIPTION AND COMPARISONS

The specimen is preserved in complete articulation, lying on its right side (Fig. 6.1A). The skull (Fig. 6.1B) is relatively large, longer than the cervical vertebral series and 156 % of the femur length. It is subtriangular in outline and slightly more than two times

longer than high. The nares are large, its length being approximately 13 % of the skull length. The orbit is the largest skull opening and encloses a complete scleral ring. The premaxillary body is considerably longer than high and meets a long anterior process of the maxilla below the naris. However, the latter bone is excluded from the narial margin by a robust posterior subnarial process of the premaxilla that contacts the nasal. The maxilla has a marked kink in the anterior margin of the ascending process dorsally and a large maxillary fenestra, which is closed medially (Fig. 6.1B, 6.2A), as in other megalosaurids (Benson 2008a, 2010). A small premaxillary fenestra seems to be present under the overhanging anterior rim of the antorbital fossa. The maxillary antorbital fossa anterior to the antorbital fenestra accounts for approximately 23 % of the total length of the antorbital fossa, and resembles the condition in other basal tetanurans, but is unlike the situation in coelurosaurs, where it typically accounts for 40 % or more (Rauhut 2003a). The lacrimal has a long, thin anterior process, which is laterally forms a large lacrimal antorbital fossa, which is continuous between the dorsal and ventral part of the vertical strut, in contrast to most theropods, but as in *Torvosaurus* (Britt 1991). The jugal seems to be excluded from the antorbital fenestra by a contact between the maxilla and lacrimal. The postorbital is slender and “T”-shaped, with the ventral process ending above the ventral margin of the orbit. The infratemporal fenestra was obviously high and narrow, though its borders are only partially preserved. In along the frontoparietal suture, a triangular area has been reconstructed as bone, occupying almost the same position and area as the open frontoparietal gap in the hatchling theropod *Scipionyx* (Dal Sasso & Maganuco 2011). Although partially obscured by reconstruction, the borders of the bones towards this gap do not show clear signs of breakage, making the interpretation of this area as a similar structure probable. However, a similar reconstructed area is present within the frontal and most probably

does not represent an unossified area, but rather a damaged one. The quadratojugal is considerably higher than long and has a broad dorsal contact with the broad ventral process of the squamosal. A large quadrate foramen is present in the quadratojugal-quadrate suture. A broad and deep longitudinal fossa is present on the posterior face of the basioccipital below the occipital condyle (Fig. 6.2B), as in other megalosaurids and spinosaurids (Benson 2010).

The anterior end of the dentary is slightly raised dorsally over the first three tooth positions; the medial side of the dentary shows two Meckelian foramina anteriorly, as in other basal theropods (Benson 2010). An anteroventrally opening mylohyoid foramen is present along the ventral margin of the splenial. A large mandibular fenestra is present and the retroarticular process is short and stout. The premaxilla bears four unserrated teeth, and the eleven maxillary and 12-14 dentary teeth are strongly recurved and bear serrations on the distal, but not the mesial carina (Fig. 6.2A).

There are ten cervical and thirteen dorsal vertebrae. As in many basal theropods, the axis lacks pleurocoels, but single, large pneumatic foramina are present in the remaining cervicals (Fig. 6.2B). Anterior cervical vertebrae might be slightly opisthocoelous, but the posterior cervicals seem amphiplatycoelous. Cervical neural arches have pronounced prezygoepipophyseal laminae and large, elongate epipophyses, which considerably overhang the postzygapophyses posteriorly (Fig. 6.2B). Anterior dorsal vertebrae have a well-developed ventral keel and bear pleurocoels, whereas posterior dorsals are apneumatic. Posterior dorsal vertebrae seem to have rather poorly developed neural arch lamination and backswept transverse processes. The neural

spines of the posterior dorsal vertebrae are unusual in being very low anteriorly, with a squared anterior end and a lobe-shaped posterodorsal expansion posteriorly (Fig. 6.2C, D). This expansion becomes more conspicuous in the posteriormost elements.

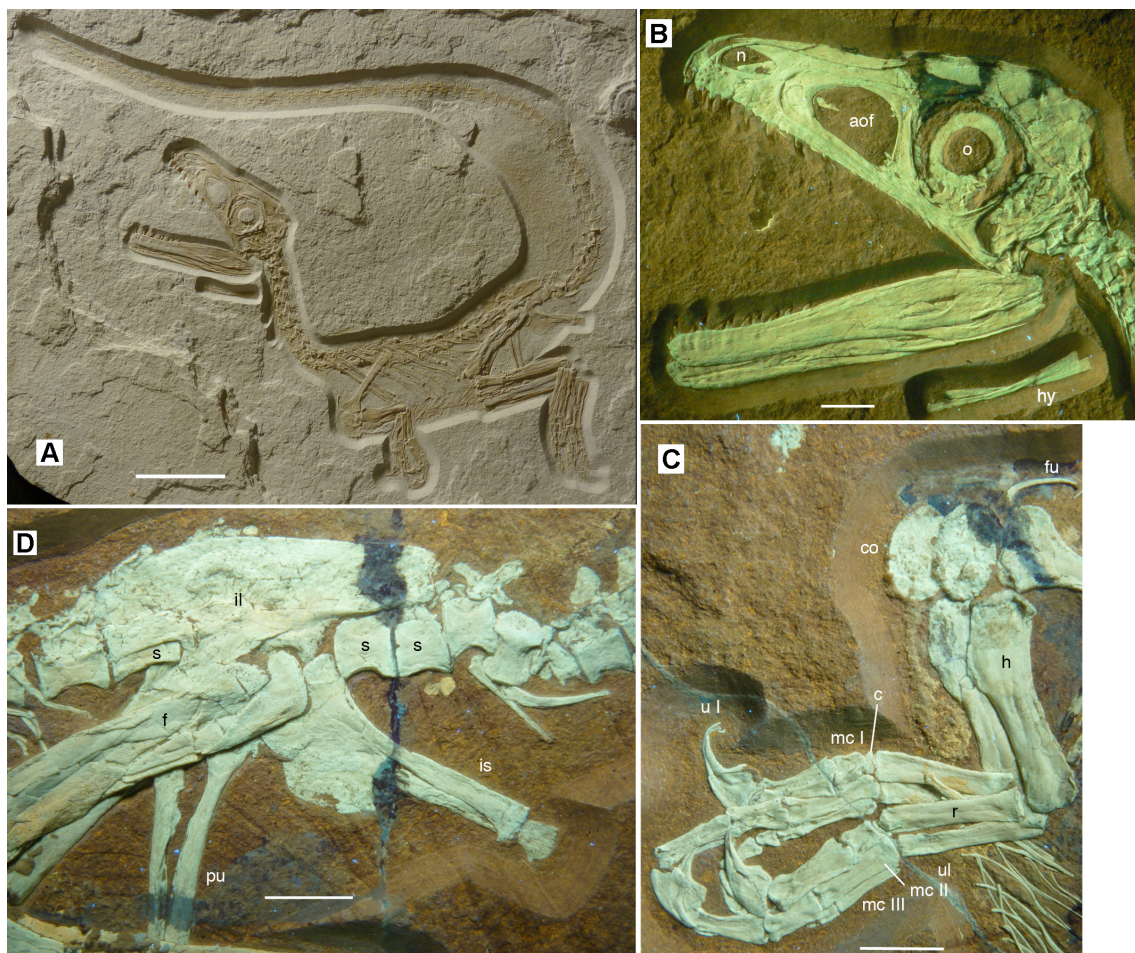


Fig. 6.1. Juvenile megalosaurid *Sciurumimus albersdoerferi* (BMMS BK 11). **A.** Overview of the limestone slab with the specimen as preserved. **B.** Skull and hemimandibles under ultraviolet light in left lateral view. **C.** Forelimbs under ultraviolet light. **D.** Pelvic girdle under ultraviolet light. aof, antorbital fenestra; c, carpal; co, coracoid; f, femur; fu, furcula; h, humerus; hy, hyoid; il, ilium; is, ischium; mc, metacarpal; n, nares; o, orbit; pu, pubis; r, radius; s, sacral vertebra; u, unguis; ul, ulna. (Scale bars are 50 mm for **A** and 10 mm for **B-D**.)

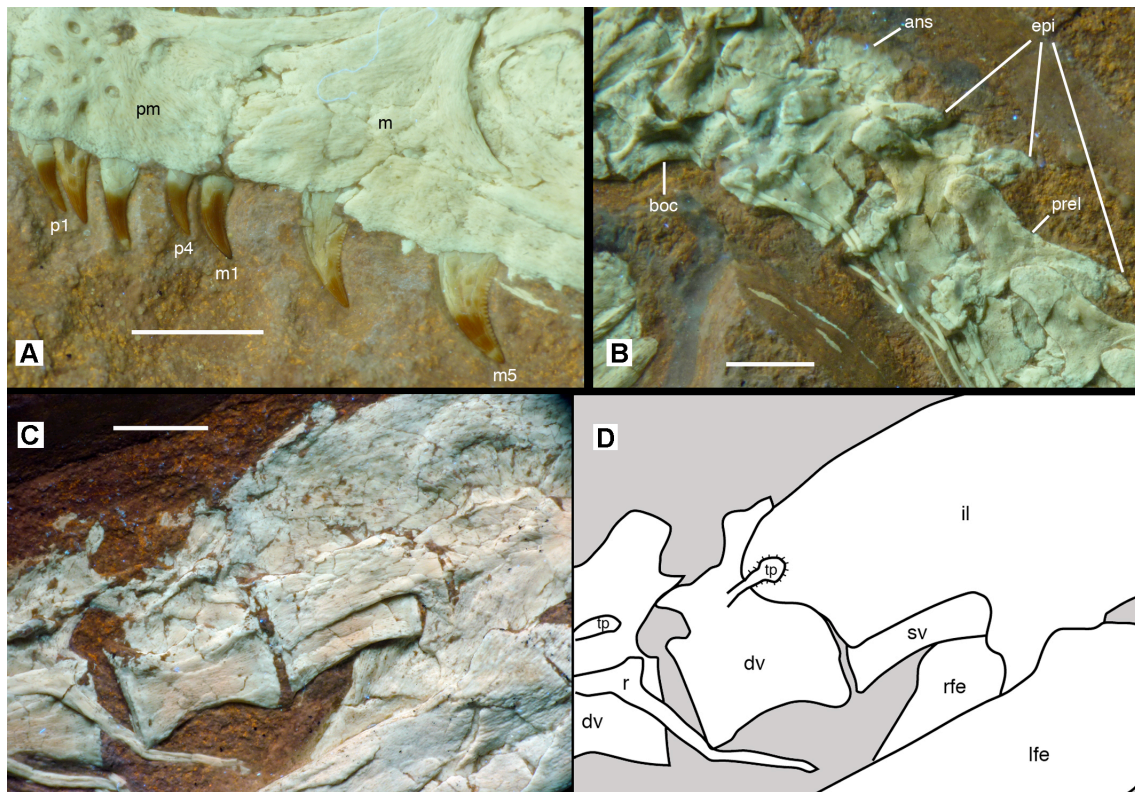


Fig. 6.2. Anatomical details of *Sciurumimus albersdoerferi*. **A.** Dentition of left premaxilla and anterior end of left maxilla. **B.** Disarticulated occiput, atlas, axis, and anterior cervical vertebrae. **C-D.** Posteriormost dorsal vertebrae and anterior part of ilium, photograph **C** and interpretative drawing **D**. All photographs under UV light. ans, axial neural spine; boc, basioccipital; dv, dorsal vertebrae; epi, epiphyses; il, ilium; lfe, left femur; m, maxilla; m1, m5, first and fifth maxillary tooth, respectively; p1, p4, first and fourth premaxillary tooth, respectively; pm, premaxilla; prel, prezygoepiphysal lamina; r, rib; rfe, right femur; sv, sacral vertebra; tp, transverse process. (Scale bars are 5 mm for **A** and 10 mm for **B-D**).

The sacrum consists of five vertebrae; the posterior ones being considerably shorter than the anterior sacrals. A total of 59 caudal vertebrae are preserved, with a few elements probably missing. Anterior caudal vertebrae lack ventral grooves or keels and have rather low, simple, posterodorsally directed neural spines. The exact position of the transition point cannot be established, but transverse processes are certainly absent

posterior to caudal twenty. Posterior caudals are elongate in shape and have short, bowed pre- and postzygapophyses, unlike the strongly elongate prezygapophyses in allosauroids and coelurosaurs. Chevrons are present in at least 36 vertebrae; they are simple rod-like structures in lateral view, without ventral anterior or posterior expansion. Slender gastralia are present, with the medial elements being longer and more robust than the lateral elements.

The scapula is more than ten times longer than wide at its narrowest point, unlike the broader scapula in basal theropods, including megalosauroids, but rather comparable to the situation in derived allosauroids and coelurosaurs (Rauhut 2003a; Benson 2010). It has a slight distal expansion that gradually arises from the shaft. The acromion process is only moderately and gradually expanded relative to the width of the shaft. The coracoid is oval in shape and shorter than high and lacks a subglenoid process and a biceps tubercle, as it is the case in megalosaurids and spinosaurids. The left ramus of a small, slender furcula is exposed.

The forelimbs (Fig. 6.1C) are short and robust, as it is the case in some other megalosaurids (Benson 2010), with a long manus accounting for ~ 45% of the length of the forelimb. The humerus is short and robust, with a triangular internal tuberosity and a well-developed deltopectoral crest. Radius and ulna are considerably shorter than the humerus and the ulna is anteroposteriorly expanded proximally to form a concave facet for the humerus anteriorly and a small, but stout olecranon process posteriorly. The ulna is slightly more slender than the radius. A poorly ossified carpal is present and covers the proximal end of metacarpal I. The manus has three digits, with metacarpal I being less than half the length of metacarpal II and metacarpal III being shorter and

considerably more slender than metacarpal II; there is no trace of a fourth metacarpal. Digit I is very robust, with phalanx I-1 exceeding the radius in width, as in compsognathids (Currie & Chen 2001), and the unguis is more than half the length of the radius.

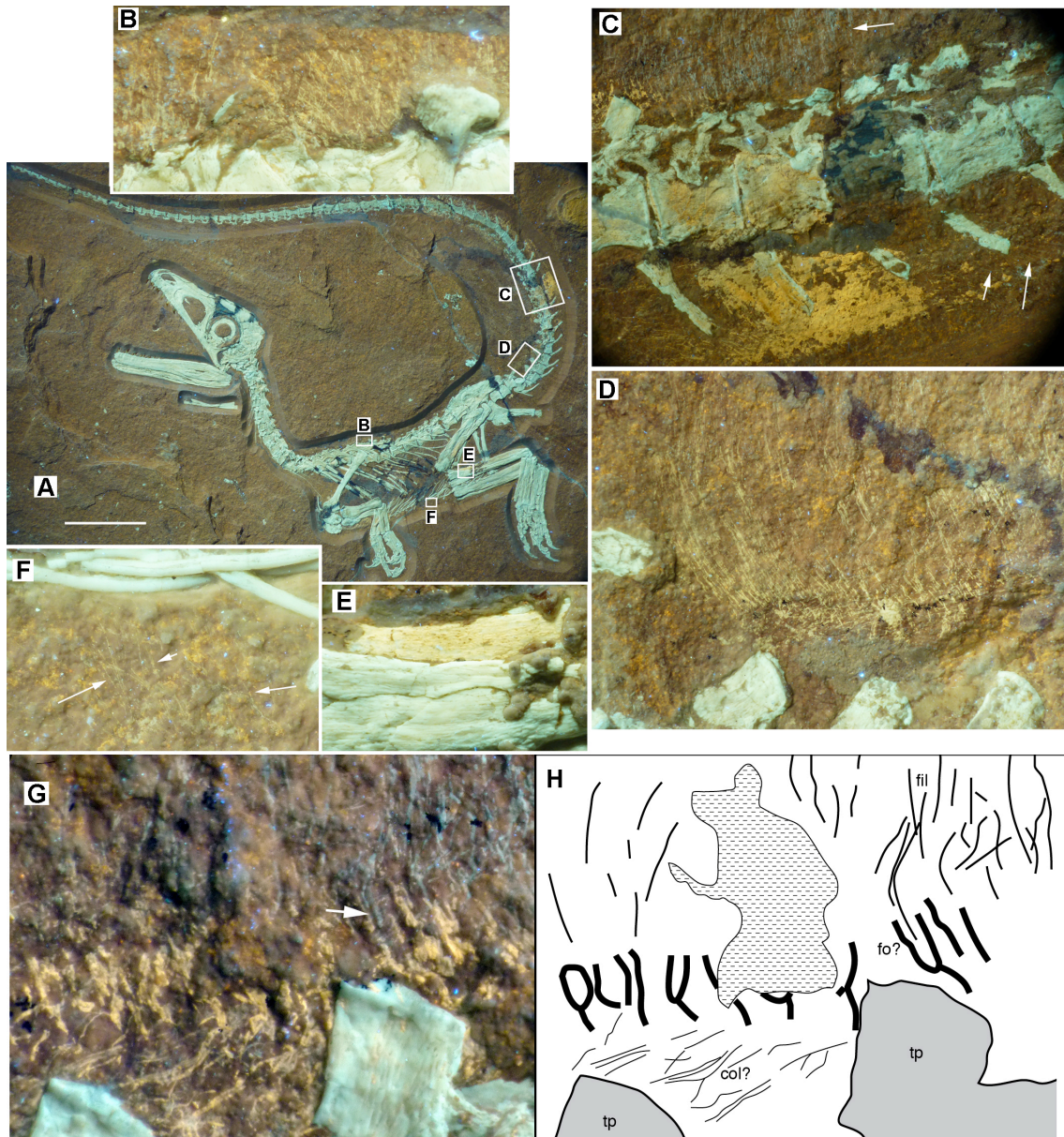


Fig. 6.3. Soft tissue preservation in *Sciurumimus*. **A.** Overview of skeleton under ultraviolet light, with position of magnifications B-F indicated. **B.** Fine filaments above the scapular region of the dorsal vertebral column. **C.** Anterior mid-caudal section, with long dorsal filaments (upper white arrow), preserved skin (yellow patch), and fine filaments at the ventral lateral tail flank (lower white arrows). **D.** Long filaments, anchored in the skin, at the dorsal tail base. **E.** Small section of possibly fossilized muscle tissue along the posterior edge of the tibia. **F.** Small, fine filaments ventral to the gastralia in the abdominal area (arrows point to individual filaments). **G-H.** Magnification of soft tissues dorsal to the 9th and 10th caudal vertebra **G** and interpretative drawing **H**, showing possible follicles. Greenish white structures are bone, fine greenish lines above the vertebrae are preserved filaments, and yellow parts represent skin structures. Arrow points to a filament entering one of the vertical skin structures that might represent follicles. Abbreviation: col, collagen fibres in the skin; fil, filaments; fo? possible follicles; tp, transverse process. All photographs under ultraviolet light. (Scale bar in **A** is 50 mm.).

The ilium is elongate, with a gently curved dorsal margin and an undulate posterior end (Fig. 6.1D). There is no ventral hook anteriorly, but the anterior end has an unusual anterior “lip” dorsally (Fig. 6.2C, D). The medial brevis shelf is not exposed in lateral view. The pubic peduncle is anteroposteriorly longer than the ischial peduncle, as in other tetanurans (Rauhut 2003a). The pubis is slender, longer than the ischium and the shaft is straight, with a moderately expanded distal boot. The ischium is slightly expanded anteriorly distally and the large, hatchet-shaped obturator process is not offset from the pubic peduncle. The femur is stout and has a wing-like lesser trochanter that reaches approximately half the height of the slender greater trochanter (Fig. 6.1D, 6.2C, D). Tibia and fibula are slightly longer than the femur and the fibula is distally expanded. The metatarsus is slender, metatarsals II and IV are of subequal length, and metatarsal V is transversely flat and anteriorly flexed. Metatarsal I is elongate and splint-

like, rather than short and triangular as is the case in most other tetanurans (Rauhut 2003a). In the foot, pedal unguis II is slightly larger than the other unguis.

Soft tissues are preserved in several areas of the skeleton (Fig. 6.3), and most seem to represent integumentary structures, with the possible exception of a short section of fossilized tissue along the posterior edge of the tibia, which might represent muscle tissue (Fig. 6.3E). The best soft tissue preservation is found on the tail, which preserves large patches of skin especially on the ventral, but also on the dorsal side, and very fine, long, hair like filaments that correspond to type 1 feathers (Xu & Guo 2009) dorsally in the anterior mid-section (Fig. 6.3C, D). The skin is smooth and does not show clear signs of scales, in contrast to the situation in *Juravenator* (Chiappe & Göhlich 2010). The feathers seem to be anchored in the skin and form a thick covering on the dorsal side of the tail and reach more than two and a half times the height of their respective caudal vertebrae. Shorter filaments are preserved on the ventral tail flank (Fig. 6.3D), above the mid-dorsal vertebrae (Fig. 6.3B), and in a small patch on the ventral part of the body (Fig. 6.3F).

The protofeathers are probably monofilaments, since no branching patterns are visible in the well-preserved, long filaments above the tail; apparent branching patterns in a few places are probably the result of compaction of these structures (Foth 2012). Due to the preservation, it cannot be established if these structures were hollow like the filaments found in other dinosaurs (Currie & Chen 2001; Mayr et al. 2002). The thickness of these filaments is approximately 0.2 mm in the long filaments in the dorsal tail region, and less in the shorter filaments at the tail flank, the back and the belly of the

animal, comparable to the size of the filamentous protofeathers found in *Sinosauropteryx* (Currie & Chen 2001).

DISCUSSION

To establish the phylogenetic position of *Sciurumimus*, we carried out several analyses, using three large recently published matrices (see supplementary information of Chapter 6). *Sciurumimus* was consistently found to be a basal tetanuran, and recovered as a basal megalosaurid within Megalosauroidea in the most detailed analysis of basal tetanuran interrelationships yet published (Benson et al. 2010; Fig. 6.4). Synapomorphies of megalosauroids and more restricted ingroups present in the new taxon include an elongate anterior process of the maxillary body, a medially closed maxillary fenestra, a very slender anterior process of the lacrimal, lateral blade of lacrimal does not overhang antorbital fenestra, presence of a deep fossa ventral to the basioccipital condyle, a splenial foramen that opens anteroventrally, a slightly dorsally expanded anterior end of the dentary, a pronounced ventral keel in the anterior dorsal vertebrae, absence of a posteroventral process of the coracoid, and an enlarged manual ungual I.

Interestingly, the inclusion of *Sciurumimus*, without changes to any other codings, resulted in the recovery of a monophyletic Carnosauria that includes Megalosauroidea and Allosauroidea and represents the sister group to Coelurosauria. This is in contrast to the vast majority of recent analysis, which depict the former two clades as successive sister taxa to coelurosaurs. Although this result should certainly be seen with caution, given the early ontogenetic stage of *Sciurumimus*, this rather severe change to the phylogeny by simple inclusion of an additional taxon highlights our still incomplete understanding of basal tetanuran evolution.

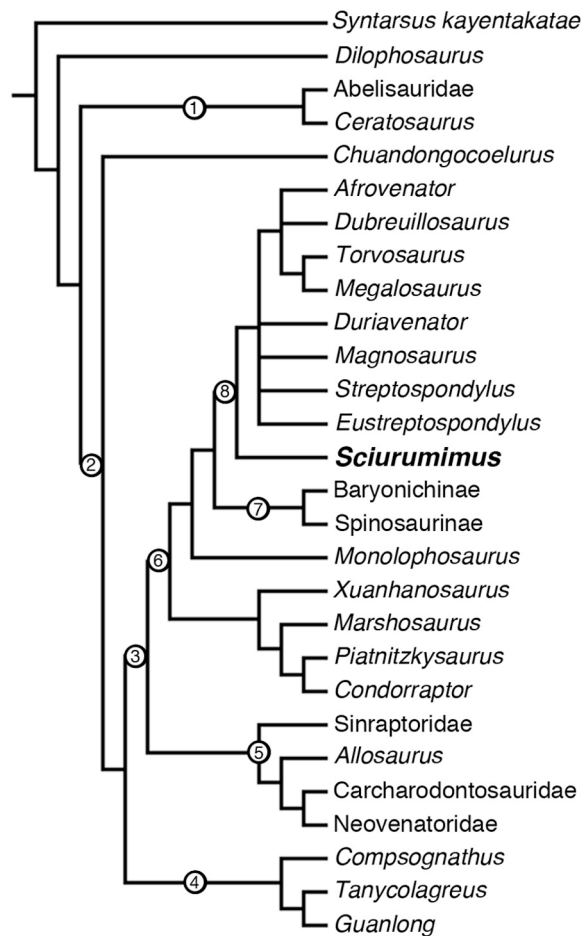


Fig. 6.4. Phylogenetic position of *Sciurumimus* in the analysis of Benson et al. (2010). Clade names: 1, Ceratosauria; 2, Tetanurae; 3, Carnosauria; 4, Coelurosauria; 5, Allosauroidae; 6, Megalosauroidae; 7, Spinosauridae; 8, Megalosauridae. Numbers on the stem indicate stem-based taxa, numbers on the node indicate node-based taxa.

Sciurumimus represents the only complete megalosauroid known and helps to clarify previously uncertain aspects of the anatomy of this group, such as the absence of a fourth digit in the manus. This highlights a surprisingly high level of homoplasy in this character, given that the basal allosauroid *Sinraptor* (Currie & Zhao 1993), the neovenatorid *Megaraptor* (Calvo et al. 2004), and the basal tyrannosaur *Guanlong* (Xu et al. 2006) retain a rudimentary fourth metacarpal, whereas most derived allosauroids

(Gilmore 1920; Currie & Carpenter 2000) and also coelurosaurs (e.g. Currie & Chen 2001) have only three metacarpals. This suggests that the fourth digit was either reduced several times independently, or a reduction of this structure at the base of tetanurans was reversed in some taxa, possibly atavistically.

Several characters indicate that the *Sciurumimus albersdoerferi* type specimen represents a very young, probably early posthatchling individual, including the body proportions, with a very large skull and rather short hindlimbs, lack of fusion in the skeleton (unfused neurocentral sutures in all of the vertebral column, unfused sacral vertebrae, lack of fusion between elements of the braincase) (Brochu 1996), coarsely striated bone surface texture in all skeletal elements (Tumarkin-Deratzian et al. 2006), and a very regular pattern of tooth development in the maxilla, possibly indicating that no teeth had been replaced (Dal Sasso & Signore 1998). This differs from the condition in perinates of more derived coelurosaurs where there is considerable heterogeneity in among the teeth (Bever & Norell 2009).

The dentition of *Sciurumimus* differs significantly from those of subadult or adult basal tetanurans in the slender and unserrated premaxillary teeth and strongly recurved maxillary teeth with distal serrations only. Given the rather uniform tooth morphology in most basal tetanurans (at least in respect to general morphology, such as tooth shape and presence and extent of serrations), these features are here regarded as juvenile characters. Thus, these differences support the assertion that juveniles of large theropod species fed on different prey items than adults (Farlow 1976). Conversely, this dentition is remarkably similar to that of basal coelurosaurs, which commonly have slender, more rounded premaxillary teeth that lack serrations (Stromer 1934; Rauhut

2003a) and often have strongly recurved lateral teeth, frequently without mesial serrations in at least some teeth (Stromer 1934; Currie & Chen 2001; Norell et al. 2006). This indicates that the dentition as seen in compsognathids (Stromer 1934; Currie & Chen 2001; Peyer 2006) and dromaeosaurids (Xu & Wu 2001; Norell et al. 2006) might have evolved by heterochronic processes, or it reflects convergence due to similar prey preferences. It also implies that the common practice of referring small, strongly recurved lateral teeth with reduced or no mesial serrations to dromaeosaurids or coelurosaurs in general (Maganuco et al. 2005; Knoll & Ruiz-Omeñaca 2009; van der Lubbe et al. 2009) should be done with caution, and coelurosaur occurrences based on these tooth characters alone are of no use for inferring biogeographic or evolutionary patterns.

Sciurumimus is comparable in size to and basically indistinguishable in proportions from the juvenile basal coelurosaur *Juravenator* (Göhlich & Chiappe 2006; Butler & Upchurch 2007; Chiappe & Göhlich 2010) (see supplementary information of Chapter 6). However, these taxa differ significantly in anatomical details (see supplementary information of Chapter 6). Thus, if this observation is indicative of the condition in early posthatchling theropods in general, these seem to have been remarkably similar in proportions, and differences in allometric growth might account for the different body plans seen in adult theropods (Carr 1999; Erickson et al. 2004a). However, data on juvenile theropods is still very limited, and more information is needed to test this hypothesis.

The presence of type 1 feathers along the dorsal side of the tail, the ventral tail flank and parts of the body in *Sciurumimus* show that the entire body of this animal was

plumaged, as it is the case in compsognathids (Xu & Guo 2009). As a megalosaurid, *Sciurumimus* is the most basal theropod taxon yet reported with such integumentary structures, and demonstrates that at least juveniles of basal tetanurans had protofeathers. *Sciurumimus* thus helps to bridge the considerable gap between basal ornithischians, for which monofilaments have been reported (Zheng et al. 2009) and coelurosaurs, where protofeathers [morphotype 1 (Prum 1999)] or feathers seem to be generally present (Norell & Xu 2005; Xu & Guo 2009; Chiappe & Göhlich 2010). As in tyrannosauroids (Xu & Guo 2009), the preservation of scaly skin in adult basal tetanurans (Glut 2003) is therefore no argument against the presence of feathers in this group in general, neither should the presence of scales in other dinosaur clades (Xu & Guo 2009) be taken as such. Large adult dinosaurs might have secondarily lost feathers, as in the case of hair loss in several groups of large mammals today. Furthermore, the joint presence of scales and filaments in some taxa (Mayr et al. 2002; Chiappe & Göhlich 2010) indicates that the apparent lack of filaments in animals that preserve impressions of scaly skin in more coarse-grained sediments could also be due to taphonomic processes. Given that filaments in ornithischian dinosaurs (Mayr et al. 2002; Zheng et al. 2009) are morphologically indistinguishable from protofeathers found in tetanurans and basal coelurosaurs, a filamentous body covering obviously represents the plesiomorphic state for dinosaurs in general, or, if one assumes that the hair-like structures of pterosaurs (Unwin 2006) are homologous structures, for ornithodiran archosaurs (Brusatte et al. 2010c).

In the anterior mid-section of the tail of *Sciurumimus*, the feathers seem to be anchored in the skin and are associated with dorsoventrally elongate skin structures (Fig. 6.3). Whereas collagen fibres in avian skin are usually oriented parallel to the body

surface, these structures are perpendicular to the long axis of the body, and several of them show an elongate-cup-shaped outline (Fig. 6.3). The only comparable structures in the avian skin are the follicles associated with the feathers (Lucas & Stettenheim 1972), so we tentatively suggest that these structures might represent follicles. Thus, whereas several recent papers have argued that the origin of follicles was linked with the evolution of a rachis or barb ridges (Sawyer & Knapp 2003; Alibardi & Toni 2008; Xu & Guo 2009), *Sciurumimus* might present evidence for the hypothesis that follicles were associated with the origin of feathers (Prum 1999). Furthermore, there is a meshwork of thin, elongate soft tissue structures below this outer layer (Fig. 6.3). These structures most probably represent collagen fibres within the stratum compactum of the dermis, which is characterized by a high density of collagen bundles in birds (Lucas & Stettenheim 1972). The fibres are clearly different from the filaments in their orientation and their luminescence under filtered UV light, and thus provide evidence against the interpretation of similarly arranged and oriented filaments in Chinese theropods as decaying collagen fibres (Feduccia et al. 2005; Lingham-Soliar et al. 2007).

ACKNOWLEDGEMENTS

We especially thank Raimund Albersdörfer, who financed the excavations during which the specimen was found and made it available for study. Special thanks are also due to Birgit Albersdörfer, the owner of the specimen. Joseph Schels and Wolfgang Häckel found and excavated the specimen, and the very delicate preparation was carried out by Jürgen Geppert, Wolfgang Häckel und Stefan Selzer. Wolfgang Rygol and the Kalkwerk Rygol GmbH & CoKG courteously permitted the excavations. Martin Röper and Monika Rothgaenger introduced Raimund Albersdörfer to the fossiliferous layers at Painten. Martina Köbl-Ebert is thanked for access to *Juravenator* for comparison, and

Adriana López-Arbarello and Richard Butler helped with many useful discussions. The paper greatly benefited from critical revisions by Xu Xing and Roger Benson. This research was funded by the Volkswagen Foundation under grant I/84 640 (OWMR) and the American Museum of Natural History (MAN).

References

- Abzhanov A, Protas M, Grant BR, Grant PR & Tabin CJ. 2004. Bmp4 and morphological variation of beaks in Darwin's finches. *Science* 305: 1462-1465.
- Abzhanov A, Kuo WP, Hartmann C, Grant BR, Grant PR & Tabin CJ. 2006. The calmodulin pathway and evolution of elongated beak morphology in Darwin's finches. *Nature* 442: 563-567.
- Adams DC, Rohlf FJ & Slice DE. 2004. Geometric morphometrics: ten years of progress following the 'revolution'. *Italian Journal of Zoology* 71: 5-16.
- Aguilera OA, Riff D & Bocquentin-Villanueva J. 2006. A new giant *Purusaurus* (Crocodyliformes, Alligatoridae) from the Upper Miocene Urumaco Formation, Venezuela. *Journal of Systematic Palaeontology* 4: 221-232.
- Alibardi L & Sawyer RH. 2006. Cell structure of developing downfeathers in the zebrafish with emphasis on barb ridge morphogenesis. *Journal of Anatomy* 208: 621-642.
- Alibardi L & Toni M. 2008. Cytochemical and molecular characteristics of the process of cornification during feather morphogenesis. *Progress in Histochemistry and Cytochemistry* 43: 1-69.
- Allain R. 2002. Discovery of megalosaur (Dinosauria, Theropoda) in the middle Bathonian of Normandy (France) and its implications for the phylogeny of basal Tetanurae. *Journal of Vertebrate Paleontology* 22: 548-563.
- Alonso PD, Milner AC, Ketcham RA, Cookson MJ, Rowe TB. 2004. The avian nature of the brain and inner ear of *Archaeopteryx*. *Nature* 430: 666-669.
- Amundsen T. 2000. Why are female birds ornamented? *Trends in Ecology and Evolution* 15: 149-155.

- Anderson BG, Barrick RE, Droser ML & Stadtman KL. 1999. Hadrosaur skin impressions from the Upper Cretaceous Neslen Formation, Book Cliffs, Utah: Morphology and paleoenvironmental context. *Vertebrate Paleontology in Utah 99*: 295-301.
- Anderson MJ. 2001. A new method for non-parametric multivariate analysis of variance. *Austral Ecology* 26:32-46.
- Anderson RA & Vitt LJ. 1990. Sexual selection versus alternative causes of sexual dimorphism in teiid lizards. *Oecologia* 84: 145-157.
- Andres B. 2009. The quality of the pterosaur fossil record. *Anniversary Meeting Society of Vertebrate Paleontology, Abstracts 2009*: 55A.
- Andres B. 2010. *Systematics of the Pterosauria*. PhD thesis, Yale University, New Haven.
- Andres B & Ji Q. 2008. A new pterosaur from the Liaoning Province of China, the phylogeny of Pterodactyloidea, and convergence in their cervical vertebrae. *Palaeontology*. 51: 453-469.
- Andres B, Clark J & Xu X. 2010. A new rhamphorhynchid pterosaur from the Upper Jurassic of Xinjiang, China, and the phylogenetic relationships of basal pterosaurs. *Journal of Vertebrate Paleontology* 30: 163-187.
- Andrews RM. 1982. Patterns of growth in reptiles. In: Gans C & Pough FH (eds). *Biology of the Reptilia*. Academic Press, New York: 273-320.
- Arratia G & Tischlinger H. 2010. The first record of Late Jurassic crossognathiform fishes from Europe and their phylogenetic importance for teleostean phylogeny. *Fossil Record* 13: 317-341.
- Averianov AO. 2004. New data on Cretaceous flying reptiles (Pterosauria) from Russia, Kazakhstan and Kyrgyzstan. *Paleontological Journal* 38: 426-436.

- Bakhurina NN & Unwin DM. 1995. A preliminary report on the evidence for “hair” in *Sordes pilosus*, an Upper Jurassic pterosaur from middle Asia. In: Sun A & Wang Y (eds). *Sixth symposium on mesozoic terrestrial ecosystems and biota*. China Ocean Press, Beijing: 79-82.
- Barrett PM. 2000. Prosauropod dinosaurs and iguanas: speculations on the diets of extinct reptiles. In: Sues H-D (ed). *Evolution of herbivory in terrestrial vertebrates*. Cambridge University Press, Cambridge: 42-78.
- Barrett PM. 2005. The diet of ostrich dinosaurs (Theropoda: Ornithomimosauria). *Palaeontology* 48: 347-358.
- Barrett PM & Rayfield EJ. 2006. Ecological and evolutionary implications of dinosaur feeding behaviour. *Trends in Ecology and Evolution* 21: 217-224.
- Barrett PM, Butler RJ, Edwards NP & Milner AR. 2008. Pterosaur distribution in time and space: an atlas. *Zitteliana B* 28: 61-107.
- Barrett, PM, Butler RJ & Nesbitt SJ. 2011. The roles of herbivory and omnivory in early dinosaur evolution. *Earth and Environmental Science Transactions of the Royal Society of Edinburgh* 101: 383-396.
- Barsbold R & Osmólska H. 1999. The skull of *Velociraptor* (Theropoda) from the Late Cretaceous of Mongolia. *Acta Palaeontologica Polonica* 44: 189-219.
- Bell PR. 2012. Standardized terminology and potential taxonomic utility for hadrosaurid skin impressions: a case study for *Saurolophus* from Canada and Mongolia. *PLoS ONE* 7: e31295.
- Bennett SC. 1992. Sexual dimorphism of *Pteranodon* and other pterosaurs, with comments on cranial crests. *Journal of Vertebrate Paleontology* 12: 422-434.
- Bennett SC. 2003. New crested specimens of the Late Cretaceous pterosaur *Nyctosaurus*. *Paläontologische Zeitschrift* 77: 61-75.

- Bennett SC. 2006. Juvenile specimens of the pterosaur *Germanodactylus cristatus*, with a review on the genus. *Journal of Vertebrate Paleontology* 26: 872-878.
- Bennett SC. 2007. A second specimen of the pterosaur *Anurognathus ammoni*. *Paläontologische Zeitschrift* 81: 376-398.
- Benson RBJ. 2008a. A redescription of '*Megalosaurus*' *hesperis* (Dinosauria, Theropoda) from the Inferior Oolite (Bajocian, Middle Jurassic) of Dorset, United Kingdom. *Zootaxa* 1931: 57-67.
- Benson RBJ. 2008b. New information on *Stokesosaurus*, a tyrannosauroid (Dinosauria: Theropoda) from North America and the United Kingdom. *Journal of Vertebrate Paleontology* 28: 732-750.
- Benson RBJ. 2010. A description of *Megalosaurus bucklandii* (Dinosauria: Theropoda) from the Bathonian of the UK and the relationships of Middle Jurassic theropods. *Zoological Journal of the Linnean Society* 158: 882-935.
- Benson RBJ, Carrano MT & Brusatte SL. 2010. A new clade of archaic large-bodied predatory dinosaurs (Theropoda: Allosauroida) that survived to the latest Mesozoic. *Naturwissenschaften* 97: 71-78.
- Benson RBJ, Butler RJ, Carrano MT & O'Connor PM. 2012. Air-filled postcranial bones in theropod dinosaurs: physiological implications and the “reptile”–bird transition. *Biological Reviews* 87: 168-193.
- Benton MJ & Walker AD. 2002. *Erpetosuchus*, a crocodile-like basal archosaur from the Late Triassic of Elgin, Scotland. *Zoological Journal of the Linnean Society* 136: 25-47.
- Benton MJ, Dunhill AM, Lloyd GT & Marx FG. 2011. Assessing the quality of the fossil record: insights from vertebrates. In: McGowan AJ & Smith AB (eds).

- Comparing the geological and fossil records: implications for biodiversity.*
Geological Society, London, Special Publication 358: 63-94.
- Bever GS & Norell MA. 2009. The perinate skull of *Byronosaurus* (Troodontidae) with observations on the cranial ontogeny of paravian theropods. *American Museum Novitates* 3657: 1-51.
- Bhullar B-A, Marugán-Lobón J, Racimo F, Bever GS, Rowe T, Norell MA & Abzhanov A. 2012. Birds have paedomorphic dinosaur skulls. *Nature* 487: 223-226.
- Bock WJ & v. Wahlert G. 1965. Adaption and the form-function complex. *Evolution* 19: 269-299.
- Bona P. 2007. Una nueva especie de *Eocaiman* Simpson (Crocodylia, Alligatoridae) del Paleoceno Inferior de Patagonia. *Ameghiniana* 44: 435-445.
- Bona P & Desojo JB. 2011. Osteology and cranial musculature of *Caiman latirostris* (Crocodylia: Alligatoridae). *Journal of Morphology* 272: 780-795.
- Bonaparte JF. 1970. *Pterodaustro guinazui* gen. et sp. nov. Pterosaurio de la Formación Lagarcito, Provincia de San Luis, Argentina y su significado en la geología regional (Pterodactylidae). *Acta Geologica Lilloana* 10: 207-226.
- Bonaparte JF, Novas FE & Coria RA. 1990. *Carnotaurus sastrei* Bonaparte, the horned, lightly built carnosaur from the Middle Cretaceous of Patagonia. *Contributions in Science* 416: 1-42.
- Bookstein FL. 1991. *Morphometric tools for landmark data*. Cambridge University Press, Cambridge.
- Bookstein FL. 1997. Landmark methods for forms without landmarks: morphometrics of group differences in outline shape. *Medical Image Analysis* 1: 225-243.

- Bookstein FL, Gunz P, Mitteroecker F, Prossinger H, Schaefer K & Seidler H. 2003. Cranial integration in *Homo*: singular warps analysis of the midsagittal plane in ontogeny and evolution. *Journal of Human Evolution* 44: 167-187.
- Borsuk-Białynicka M & Evans SE. 2009. A long-necked archosauromorph from the Early Triassic of Poland. *Palaeontologia Polonica* 65: 203-234.
- Braun WJ & Murdoch DJ. 2008. *A first course in statistical programming with R*. Cambridge University Press, Cambridge.
- Brazaitis P. 1974. The identification of living crocodiles. *Zoologica* 58: 59-105.
- Britt BB. 1991. Theropods of Dry Mesa Quarry (Morrison Formation, Late Jurassic), Colorado, with emphasis on the osteology of *Torvosaurus tanneri*. *Brigham Young University Geology Studies* 37: 1-72.
- Brochu CA. 1996. Closure of neurocentral sutures during crocodylian ontogeny: implications for maturity assessment in fossil archosaurs. *Journal of Vertebrate Paleontology* 16: 49-62.
- Brochu CA. 1999. Phylogenetic, taxonomy, and historical biogeography of Alligatoroidea. *Journal Vertebrate Paleontology* 19: 9-100.
- Brochu CA. 2001. Crocodylian snouts in space and time: phylogenetic approaches toward adaptive radiation. *American Zoologist* 41: 564-585.
- Brochu CA. 2003. Phylogenetic approaches toward crocodylian history. *Annual Review of Earth and Planetary Sciences* 31: 357-397.
- Brochu CA. 2010. A new alligatorid from the lower Eocene Green River Formation of Wyoming and the origin of caimans. *Journal Vertebrate Paleontology* 30: 1109-1126.

- Brochu CA. 2011. Phylogenetic relationships of *Necrosuchus ionensis* Simpson, 1937 and the early history of caimanines. *Zoological Journal of the Linnean Society* 163: S228-S256.
- Brochu CA & Storrs GW. 2012. A giant crocodile from the Plio-Pleistocene of Kenya, the phylogenetic relationships of Neogene African crocodylines, and the antiquity of *Crocodylus* in Africa. *Journal of Vertebrate Paleontology* 32: 587-602.
- Brochu CA, Parris DC, Grandstaff BS, Denton RK Jr. & Gallagher WB. 2012. A new species of *Borealosuchus* (Crocodyliformes, Eusuchia) from the Late Cretaceous-early Paleogene of New Jersey. *Journal of Vertebrate Paleontology* 32: 105-116.
- Bruner E, Costantini D, Fanfani A & Dell’Omo G. 2005. Morphological variation and sexual dimorphism of the cephalic scales in *Lacerta bilineata*. *Acta Zoologica (Stockholm)* 86: 245-254.
- Brusatte, S.L. 2011. Calculating the tempo of morphological evolution: rates of discrete character change in a phylogenetic context. In: Elewa AMT (ed). *Computational paleontology*. Springer-Verlag, Heidelberg: 53-74.
- Brusatte SL. 2012. *Dinosaur paleobiology*. Wiley-Blackwell, Oxford.
- Brusatte SL, Benton MJ, Ruta M & Lloyd GT. 2008. Superiority, competition, and opportunism in the evolutionary radiation of dinosaurs. *Science* 321: 1485-1488.
- Brusatte SL, Carr TD, Erickson GM, Bever GS & Norell MA. 2009. A long-snouted, multihorned tyrannosaurid from the Late Cretaceous of Mongolia. *Proceedings of the National Academy of Sciences, U.S.A.* 106: 17261-17266.
- Brusatte SL, Norell MA, Carr TD, Erickson GM, Hutchinson JR, Balanoff AM, Bever GS, Choiniere JN, Makovicky PJ & Xu X. 2010a. Tyrannosaur paleobiology: new research on ancient exemplar organisms. *Science* 329: 1481-1485.

- Brusatte SL, Benson RBJ, Currie PJ & Zhao X. 2010b. The skull of *Monolophosaurus jiangi* (Dinosauria: Theropoda) and its implications for early theropod phylogeny and evolution. *Zoological Journal of the Linnean Society* 158: 573-607.
- Brusatte SL, Nesbitt SJ, Irmis RB, Butler RJ, Benton MJ & Norell MA. 2010c. The origin and early radiation of dinosaurs. *Earth-Science Reviews* 101: 68-100.
- Brusatte SL, Montanari S, Yi H, Norell MA (2011) Phylogenetic corrections for morphological disparity analysis: new methodology and case studies. *Paleobiology* 37: 1-22.
- Brusatte SL, Sakamoto M, Montanari S & Harcourt Smith WEH. 2012a. The evolution of cranial form and function in theropod dinosaurs: insights from geometric morphometrics. *Journal of Evolutionary Biology* 25: 365-377.
- Brusatte SL, Butler RJ, Prieto-Márquez A & Norell MA. 2012b. Dinosaur morphological diversity and the end-Cretaceous extinction. *Nature Communications* 3 (804): 1-8. doi:10.1038/ncomms1815.
- Burnham DA. 2004. New information on *Bambiraptor feinbergi* (Theropoda: Dromaeosauridae) from the Late Cretaceous of Montana. In: Currie PJ, Koppelhus EB, Shugar MA & Wright JL (eds). *Feathered dragons*. Indiana University Press, Bloomington: 67-111.
- Burns KJ, Hackett SJ & Klein NK. 2002. Phylogenetic relationships and morphological diversity in Darwin's finches and their relatives. *Evolution* 56: 1240-1252.
- Busbey AB. 1989. Form and function of the feeding apparatus of *Alligator mississippiensis*. *Journal of Morphology* 202: 99-127.
- Butler RJ & Goswami A. 2008. Body size evolution in Mesozoic birds: little evidence for Cope's rule. *Journal of Evolutionary Biology* 21: 1673-1682.

- Butler RJ & Upchurch P. 2007. Highly incomplete taxa and the phylogenetic relationships of the theropod dinosaur *Juravenator starki*. *Journal of Vertebrate Paleontology* 27: 253-256.
- Butler RJ, Upchurch P & Norman DB. 2007. The phylogeny of the ornithischian dinosaurs. *Journal of Systematic Palaeontology* 6: 1-40.
- Butler RJ, Porro LB & Norman DB. 2008. A juvenil skull of the primitive ornithischian dinosaur *Heterodontosaurus tucki* from the “Stormberg” of southern Africa. *Journal of Vertebrate Paleontology* 28: 702-711.
- Butler RJ, Barrett PM, Nowbath S & Upchurch P. 2009a. Estimating the effects of the rock record on pterosaur diversity patterns: implications for hypotheses of bird/pterosaur competitive replacement. *Paleobiology* 35: 432-446.
- Butler RJ, Barrett, PM & Gower DJ. 2009b. Postcranial skeletal pneumaticity and air-sacs in the earliest pterosaurs. *Biology Letters* 5: 557-560.
- Butler RJ, Barrett PM, Benson RBJ, Brusatte SL & Andres B. 2011a. The taxonomic diversity and morphological disparity of pterosaurs: untangling sampling biases, the impact of Lagerstätten, and diversification trajectories. *Anniversary Meeting Society of Vertebrate Paleontology, Abstracts 2011*: 81A.
- Butler RJ, Benson RBJ, Carrano MT, Mannion PD & Upchurch P. 2011b. Sea-level, dinosaur diversity, and sampling biases: investigating the “common cause” hypothesis in the terrestrial realm. *Proceedings of the Royal Society of London B* 278: 1165-1170.
- Butler RJ, Brusatte SL, Andres B. & Benson RBJ. 2012. How do rock record biases affect studies of disparity in deep time? A case study of the Pterosauria (Reptilia: Archosauria). *Evolution* 66: 147-162.

- Cabreira SF, Schultz CL, Bittencourt JS, Soares MB, Fortier DC, Silva LR & Langer MC. 2011. New stem-sauropodomorph (Dinosauria, Saurischia) from the Triassic of Brazil. *Naturwissenschaften* 98: 1035-1040.
- Calvo JO, Porfiri JD, Veralli C, Novas FE & Poblete F. 2004. Phylogenetic status of *Megaraptor namunhuaiquii* Novas based on a new specimen from Neuquén, Patagonia, Argentina. *Ameghiniana* 41: 565-575.
- Campàs O, Mallarino R, Herrel A, Abzhanov A & Brenner MP. 2010. Scaling and shear transformations capture beak shape variation in Darwin's finches. *Proceedings of the National Academy of Sciences, U.S.A.* 107: 3356-3360.
- Campione NE & Evans DC. 2011. Cranial growth and variation in edmontosaurs (Dinosauria: Hadrosauridae): implications for Latest Cretaceous megaherbivore diversity in North America. *PLoS ONE* 6: e25186.
- Carballido JL, Rauhut OWM, Pol D & Salgado L. 2011. Osteology and phylogenetic relationships of *Tehuelchesaurus benitezii* (Dinosauria, Sauropoda) from the Upper Jurassic of Patagonia. *Zoological Journal of the Linnean Society* 163: 605-662.
- Carpenter K. 1990. Variation in *Tyrannosaurus rex*. In: Carpenter K & Currie PJ (eds). *Dinosaur systematics: approaches and perspectives*. Cambridge University Press, Cambridge: 141-145.
- Carpenter K. 1992. Tyrannosaurids (Dinosauria) of Asia and North America. In: Mather NJ & Chen P (eds). *Aspects of nonmarine Cretaceous geology*. China Ocean Press, Beijing: 250-268.
- Carpenter K. 1994. Baby *Dryosaurus* from the Upper Jurassic Morrison Formation of Dinosaur National Monument. In: Carpenter K, Hirsch KF & Horner JR (eds). *Dinosaur eggs and babies*. Cambridge University Press, Cambridge: 288-297.

- Carpenter K. 2010. Variation in a population of Theropoda (Dinosauria): *Allosaurus* from the Cleveland-Lloyd Quarry (Upper Jurassic), Utah, USA. *Paleontological Research* 14: 250-259.
- Carr TD. 1999. Craniofacial ontogeny in Tyrannosauridae (Dinosauria, Coelurosauria). *Journal of Vertebrate Paleontology* 19: 497-520.
- Carr TD & Williamson TE. 2004. Diversity of late Maastrichtian Tyrannosauridae (Dinosauria: Theropoda) from western North America. *Zoological Journal of the Linnean Society* 142: 479-523.
- Carr TD & Williamson TE. 2010. *Bistahieversor sealeyi*, gen. et sp. nov., a new tyrannosauroid from New Mexico and the origin of deep snouts in Tyrannosauroidea. *Journal of Vertebrate Paleontology* 30: 1-16.
- Carr TD, Williamson TE, Britt BB & Stadtman K. 2011. Evidence for high taxonomic and morphologic tyrannosauroid diversity in the Late Cretaceous (Late Campanian) of the American Southwest and a new short-skulled tyrannosaurid from the Kaiparowits formation of Utah. *Naturwissenschaften* 98: 241-246.
- Carrano MT, Loewen MA & Sertich JJW. 2011. New materials of *Masiakasaurus knopfleri* Sampson, Carrano, and Forster, 2001, and implications for the morphology of the Noasauridae (Theropoda: Ceratosauria). *Smithsonian Contributions of Paleobiology* 95: 1-53.
- Carrano MT, Benson RBJ & Sampson SD. 2012. The phylogeny of Tetanurae (Dinosauria: Theropoda). *Journal of Systematic Palaeontology* 10: 211-300.
- Carvalho IS, Campos ACA & Nobre PH. 2005. *Baurusuchus salgadoensis*, a new Crocodylomorpha from the Bauru Basin (Cretaceous), Brazil. *Gondwana Research* 8: 11-30.

- Chabreck RH. 1963. Methods of capturing, marking and sexing alligators. *Southeastern Association of Game and Fish Commissioners* 17: 47-50.
- Chabreck RH & Joanen T. 1979. Growth rates of American Alligators in Louisiana. *Herpetologica* 35: 51-57.
- Chapman RE 1990. Shape analysis in the study of dinosaur morphology. In: Carpenter K & Currie PJ (eds). *Dinosaur systematics: approaches and perspectives*. Cambridge University Press, Cambridge: 21-42.
- Chapman RE & Brett-Surman MK. 1990. Morphometric observations on hadrosaurid ornithopods. In: Carpenter K & Currie PJ (eds). *Dinosaur systematics: approaches and perspectives*. Cambridge University Press, Cambridge: 163-177.
- Chapman RE, Galton PM, Sepkoski Jr JJ & Wall WP. 1981. A morphometric study of the cranium of the pachycephalosaurid dinosaur *Stegoceras*. *Journal of Paleontology* 55: 608-618.
- Chapman RE, Weishampel DB, Hunt G & Rasskin-Gutman D. 1997. Sexual dimorphism in dinosaurs. In: Wohlberg DL, Stumps E & Rosenberg GD (eds). *Dinofest International*. Academy of Natural Sciences, Philadelphia: 83-93.
- Chiappe LM & Göhlich UB. 2010. Anatomy of *Juravenator starki* (Theropoda: Coelurosauria) from the Late Jurassic of Germany. *Neues Jahrbuch für Geologie und Paläontologie - Abhandlungen* 258: 257-296.
- Chiappe LM, Coria RA, Dingus L, Jackson F, Chinsamy A & Fox M. 1998. Sauropod dinosaur embryos from the Late Cretaceous of Patagonia. *Nature* 396: 258-261.
- Chiappe LM, Ji S, Ji Q & Norell MA. 1999. Anatomy and systematics of the Confuciusornithidae (Theropoda: Aves) from the Late Mesozoic of northeastern China. *Bulletin of the American Museum of Natural History* 242: 1-89.

- Chiappe LM, Kellner AWA, Rivarola D, Davila S & Fox M. 2000. Cranial morphology of *Pterodaustro guinazui* (Pterosauria: Pterodactyloidea) from the Lower Cretaceous of Argentina. *Contributions in Science* 483: 1-19.
- Chiappe LM, Salgado L & Coria RA. 2001. Embryonic skulls of titanosaur sauropod dinosaurs. *Science* 293: 2444-2446.
- Chiappe LM, Norell MA & Clark JM. 2002. The Cretaceous, short-armed Alvarezsauridae: *Mononykus* and its kin. In: Chiappe LM & Witmer LM (eds). *Mesozoic birds: above the heads of dinosaurs*. University of California Press, Berkeley: 87-120.
- Chiappe LM, Ji S & Ji Q. 2007. Juvenile birds from the Early Cretaceous of China: implications for enantiornithine ontogeny. *American Museum Novitates* 3594: 1-49.
- Chinsamy A, Codorniu L & Chiappe LM. 2009. Palaeobiological implications of the bone histology of *Pterodaustro guinazui*. *The Anatomical Record* 292: 1462-1477.
- Chinsamy A, Chiappe LM, Marugán-Lobón J, Gao C & Zhang F. 2013. Gender identification of the Mesozoic bird *Confuciusornis sanctus*. *Nature Communications* 4 (1381): 1-5. doi:10.1038/ncomms2377.
- Choiniere JN, Xu X, Clark JM, Forster CA, Guo Y & Han F. 2010. A basal alvarezsauroid theropod from the Early Jurassic of Xinjiang, China. *Science* 327: 571-574.
- Christiansen P & Fariña RA. 2004. Mass prediction in theropod dinosaurs. *Historical Biology* 16: 85-92.
- Chure DJ. 2000. *A new species of Allosaurus from the Morrison Formation of Dinosaur National Monument (UT-CO) and a revision of the theropod family Allosauridae*. PhD thesis, Columbia University, New York.

- Chure D, Britt BB, Whitlock JA & Wilson JA. 2010. First complete sauropod dinosaur skull from the Cretaceous of the Americas and the evolution of sauropod dentition. *Naturwissenschaften* 97: 379-391.
- Ciampaglio CN, Kemp M & McShea DW. 2001. Detecting changes in morphospace occupation patterns in the fossil record: characterization and analysis of measures of disparity. *Paleobiology* 27: 695-715.
- Clark JM, Norell MA & Makovicky PJ. 2002a. Cladistic approaches to the relationships of birds to other theropod dinosaurs. In: Chiappe LM & Witmer LM (eds). *Mesozoic birds: above the heads of dinosaurs*. University of California Press, Berkeley: 31-61.
- Clark JM, Norell MA & Rowe T. 2002b. Cranial anatomy of *Citipati osmolskae* (Theropoda, Oviraptorosauria), and a reinterpretation of the holotype of *Oviraptor philoceratops*. *American Museum Novitates* 3364: 1-24.
- Clark JM, Xu X, Forster CA & Wang Y. 2004. A Middle Jurassic “sphenosuchian” from China and the origin of the crocodylian skull. *Nature* 430: 1021-1024.
- Claessens LPAM, O'Connor PM & Unwin DM. 2009. Respiratory evolution facilitated the origin of pterosaur flight and aerial gigantism. *PLoS ONE* 4: e4497.
- Cleuren J & de Vree F. 2000. Feeding in crocodylians. In: Schwenk K (ed). *Feeding: form, function and evolution in tetrapod vertebrates*. Academic Press, New York: 337-358.
- Colbert EH. 1989. The Triassic dinosaur *Coelophysis*. *Museum of Northern Arizona Bulletin* 57: 1-160.
- Colbert EH. 1990. Variation in *Coelophysis bauri*. In: Carpenter K & Currie PJ (eds). *Dinosaur systematics: approaches and perspectives*. Cambridge University Press, Cambridge: 81-90.

- Colbert EH & Mook CC. 1951. The ancestral crocodylian *Protosuchus*. *Bulletin of the American Museum of Natural History* 97: 143-182.
- Collyer ML & Adams DC. 2007. Analysis of two-state multivariate phenotypic change in ecological studies. *Ecology* 88: 683-692.
- Cooper WE. & Vitt LJ. 1993. Female mate choice of large male broad-headed skinks. *Animal Behaviour* 45: 683-693.
- Coombs WP Jr. 1982. Juvenile specimens of the ornithischian dinosaur *Psittacosaurus*. *Palaeontology* 25: 89-107.
- Coria RA & Chiappe LM. 2007. Embryonic skin from Late Cretaceous sauropods (Dinosauria) of Auca Mahuevo, Patagonia, Argentina. *Journal of Paleontology* 81: 1528-1532.
- Cott HB. 1926. Observations on the life habits of some batrachians and reptiles from the lower Amazon, and note on some mammals from Marajó. *Proceedings of the Zoological Society of London* 29: 211-256.
- Cott HB. 1961. Scientific results of an inquiry into the ecology and economic status of the Nile crocodile (*Crocodilus niloticus*) in Uganda and northern Rhodesia. *Transactions of the Zoological Society of London* 29 : 211-356.
- Crompton AW & Attridge J. 1986. Masticatory apparatus of the larger herbivores during Late Triassic and Early Jurassic times. In: Padian K (ed). *The beginning of the age of dinosaurs*. Cambridge University Press, Cambridge: 223-236.
- Crowe R & Niswander L. 1998. Disruption of scale development by Delta-1 misexpression. *Developmental Biology* 195: 70-74.
- Csiki Z, Vremir M, Brusatte SL & Norell MA. 2010. An aberrant island-dwelling theropod dinosaur from the Late Cretaceous of Romania. *Proceedings of the National Academy of Sciences, U.S.A.* 107: 15357-15361.

- Currie PJ & Zhao X. 1993. A new carnosaur (Dinosauria, Theropoda) from the Jurassic of Xinjiang, People's Republic of China. *Canadian Journal of Earth Sciences* 30: 2037-2081.
- Currie PJ & Carpenter K. 2000. A new specimen of *Acrocanthosaurus atokensis* (Theropoda, Dinosauria) from the Lower Cretaceous Antlers Formation (Lower Cretaceous, Aptian) of Oklahoma, USA. *Geodiversitas* 22: 207-246.
- Currie PJ & Chen P. 2001. Anatomy of *Sinosauropteryx prima* from Liaoning, northeastern China. *Canadian Journal of Earth Sciences* 38: 1705-1727.
- Czechura GV & Wombey J. 1982. Three new striped skinks (Ctenotus, Lacertilia, Scincidae) from Queensland. *Queensland Museum Memoirs* 20: 639-645.
- Dacke CG, Arkle S, Cook DJ, Wormstone IM, Jones S, Zaidi M & Bascal ZA. 1993. Medullary bone and avian calcium regulation. *Journal of Experimental Biology* 184: 63-88.
- Dal Sasso C & Signore M. 1998. Exceptional soft-tissue preservation in a theropod dinosaur from Italy. *Nature* 392: 383-387.
- Dal Sasso C & Maganuco S. 2011. *Scipionyx samniticus* (Theropoda: Compsognathidae) from the Lower Cretaceous of Italy. *Memorie della Società Italiana di Scienze Naturali e del Museo Civico di Storia Naturale di Milano* 37: 1-281.
- D'Amore DC. 2009. A functional explanation for denticulation in theropod dinosaur teeth. *The Anatomical Record* 292: 1297-1314.
- Da Silveira R & Magnusson WE. 1999. Diets of Spectacled and black caiman in the Anavilhanas Archipelago, Central Amazonia, Brazil. *Journal of Herpetology* 33: 181-192.

- Dececchi TA & Larsson HCE. 2011. Assessing arboreal adaptations of bird antecedents: testing the ecological setting of the origin of the avian flight stroke. *PLoS ONE* 6: e22292.
- de Ricqlès AJ, Padian K & Horner JR. 2003. On the bone histology of some Triassic pseudosuchian archosaurs and related taxa. *Annales de Paléontologie* 89: 67-101.
- de Thoisy B, Hrbek T, Farias IP, Vasconcelos WR & Lavergne A. 2006. Genetic structure, population dynamics, and conservation of black caiman (*Melanosuchus niger*). *Biological Conservation* 133: 474-482.
- Dhouailly D. 2009. A new scenario for the evolutionary origin of hair, feather, and avian scales. *Journal of Anatomy* 214: 587-606.
- Dingus L & Rowe T. 1997. *The mistaken extinction: dinosaur evolution and the origin of birds*. Freeman, New York.
- Dodson P. 1975. Functional and ecological significance of relative growth in *Alligator*. *Zoology* 1975: 315-355.
- Dodson P. 1993. Comparative craniology of the Ceratopsia. *American Journal of Science* 293: 200-234.
- Drake AG. 2011. Dispelling dog dogma: an investigation of heterochrony in dogs using 3D geometric morphometric analysis of skull shape. *Evolution & Development* 13: 204-213.
- Drake AG & Klingenberg CP. 2008. The pace of morphological change: historical transformation of skull shape in St Bernard dogs. *Proceedings of the Royal Society B* 275: 71-76.
- Dyke GJ, Nudds RL & Rayner JM. 2006. Limb disparity and wing shape in pterosaurs. *Journal of Evolutionary Biology* 19: 1339-1342.

- Dyke GJ, McGowan AJ, Nudds RL & Smith D. 2009. The shape of pterosaur evolution: evidence from the fossil record. *Journal of Evolutionary Biology* 22: 890-898.
- Eddy DR & Clarke JA. 2011. New information on the cranial anatomy of *Acrocanthosaurus atokensis* and its implications for the phylogeny of Allosauroidea (Dinosauria: Theropoda). *PLoS ONE* 6: e17932.
- Elewa AMT. 2004. *Morphometrics: applications in biology and paleontology*. Springer-Verlag, Heidelberg.
- Elgin RA, Grau CA, Palmer C, Hone DWE, Greenwell D & Benton MJ. 2008. Aerodynamic characters of the cranial crest in *Pteranodon*. *Zitteliana B* 28: 167-174.
- Emerson SB & Bramble DM. 1993. Scaling, allometry, and skull design. In: Hanken J & Hall BK (eds). *The skull. Vol. 3. Patterns of structural and systematic diversity*. University of Chicago Press, Chicago: 384-421.
- Erickson GM & Brochu CA. 1999. How the “terror crocodile” grew so big. *Nature* 398: 205-206.
- Erickson GM, van Kirk SD, Su J, Levenston ME, Caler WE, Carter DR. 1996. Bite-force estimation for *Tyrannosaurus rex* from tooth-marked bones. *Nature* 382: 706-708.
- Erickson GM, Rogers KC & Yerby SA. 2001. Dinosaur growth patterns and rapid avian growth rates. *Nature* 412: 429-432.
- Erickson GM, Lappin AK & Vliet KA. 2003. The ontogeny of bite-force performance in American alligator (*Alligator mississippiensis*). *Journal of Zoology, London* 260: 317-327.
- Erickson GM, Makovicky PJ, Currie PJ, Norell MA, Yerby SA & Brochu CA. 2004a. Gigantism and comparative life-history parameters of tyrannosaurid dinosaurs. *Nature* 430: 772-775.

- Erickson GM, Lappin AK, Parker T & Vliet KA. 2004b. Comparison of bite-force performance between long-term captive and wild American alligators (*Alligator mississippiensis*). *Journal of Zoology* 262: 21-28.
- Erickson GM, Lappin AK & Larson P. 2005. Androgynous rex - The utility of chevrons for determining the sex of crocodylians and non-avian dinosaurs. *Zoology* 108: 277-286.
- Erickson GM, Rauhut OWM, Zhou Z, Turner AH, Inouye BD, Hu D & Norell MA. 2009. Was dinosaurian physiology inherited by birds? Reconciling slow growth in *Archaeopteryx*. *PLoS ONE* 4: e7390.
- Erickson GM, Gignac PM, Steppan SJ, Lappin AK, Villet KA, Brueggen JD, Inouye BD, Kledzik D & Webb GJW. 2012. Insights into the ecology and evolutionary success of crocodylians revealed through bite-force and tooth-pressure experimentation. *PLoS ONE* 7: e31781.
- Erwin DH. 2007. Disparity: morphological pattern and developmental context. *Palaeontology* 50: 57-73.
- Evans DC. 2010. Cranial anatomy and systematics of *Hypacrosaurus altispinus*, and a comparative analysis of skull growth in lambeosaurine hadrosaurids (Dinosauria: Ornithischia). *Zoological Journal of the Linnean Society* 159: 398-434.
- Evans DC & Reisz RR. 2007. Anatomy and relationships of *Lambeosaurus magnicristatus*, a crested hadrosaurid dinosaur (Ornithischia) from the Dinosaur Park Formation, Alberta. *Journal of Vertebrate Paleontology* 27: 373-393.
- Ezcurra MD. 2007. The cranial anatomy of the coelophysoid theropod *Zupaysaurus rougieri* from the Upper Triassic of Argentina. *Historical Biology* 19: 185-202.
- Ezcurra MD & Novas FE. 2007. Phylogenetic relationships of the Triassic theropod *Zupaysaurus rougieri* from NW Argentina. *Historical Biology* 19: 35-72.

- Fanti F, Currie PJ & Badamgarav D. 2012. New specimens of *Nemegtomaia* from the Baruungoyot and Nemegt Formations (Late Cretaceous) of Mongolia. *PLoS ONE* 7: e31330.
- Farias IP, Silveira R, de Thoisy B, Monjeló LA, Thorbjarnarson JB & Hrbek T. 2004. Genetic diversity and population structure of Amazonian crocodylians. *Animal Conservation* 7: 265-272.
- Farlow JO. 1976. Speculations about the diet and foraging behavior of large carnivorous dinosaurs. *American Midland Naturalist* 95: 186-191.
- Fastovsky DE & Weishampel DB. 2005. *The evolution and extinction of the dinosaurs*. University Press, Cambridge.
- Feduccia A, Lingham-Soliar T & Hinchliffe JR. 2005. Do feathered dinosaurs exist? Testing the hypothesis on neontological and paleontological evidence. *Journal of Morphology* 266: 125-166.
- Felsenstein J. 1985. Phylogenies and the comparative method. *The American Naturalist* 125: 1-15.
- Foote M. 1991. Morphological and taxonomic diversity in a clade's history: the blastoid record and stochastic simulations. *Contributions from the Museum of Paleontology, the University of Michigan* 28: 101-140.
- Foote M. 1993. Discordance and concordance between morphological and taxonomic diversity. *Paleobiology* 20: 185-204.
- Foote M. 1994. Morphological disparity in Ordovician-Devonian crinoids and the early saturation of morphological space. *Paleobiology* 20: 320-344.
- Forster CA. 1990. *The cranial morphology and systematics of Triceratops, with a preliminary analysis of ceratopsian phylogeny*. PhD thesis, University of Pennsylvania, Philadelphia.

- Foth C. 2012. On the identification of feather structures in stem-line representatives of birds: evidence from fossils and actuopalaeontology. *Paläontologische Zeitschrift* 86: 91-102.
- Foth C & Rauhut OWM. 2013. Macroevolutionary and morphofunctional patterns in theropod skulls: a morphometric approach. *Acta Palaeontologica Polonica* 58: 1-16.
- Foth C & Rauhut OWM. In press. The good, the bad, and the ugly: the influence of skull reconstructions and intraspecific variability in studies of cranial morphometrics in theropods and basal saurischians. *PloS ONE*.
- Foth C, Brusatte SL & Butler RJ. 2012. Do different disparity proxies converge on a common signal? Insights from the cranial morphometrics and evolutionary history of Pterosauria (Diapsida: Archosauria). *Journal of Evolutionary Biology* 25: 904-915.
- Foth C, Bona P & Desojo JB. In press. Intraspecific variation in the skull morphology of the black caiman *Melanosuchus niger* (Alligatoridae, Caimaninae). *Acta Zoologica*.
- Freckleton RP, Harvey PH & Pagel M. 2002. Phylogenetic analysis and comparative data: a test and review of the evidence. *The American Naturalist* 160: 712-726.
- Frey E, Tischlinger H, Buchy M-C & Martill DM. 2003. New specimens of Pterosauria (Reptilia) with soft parts with implications for pterosaurian anatomy and locomotion. In: Buffetaut E & Mazin J-M (eds). *Evolution and palaeobiology of pterosaurs*. The Geological Society, London: 233-266.
- Friedman M. 2010. Explosive morphological diversification of spiny-finned teleost fishes in the aftermath of the end-Cretaceous extinction. *Proceedings of the Royal Society of London B* 277: 1675-1683.
- Futuyma DJ. 2007. *Evolution*. Spektrum Akademischer Verlag, München.

- Gallina PA & Apesteguía S. 2011. Cranial anatomy and phylogenetic position of the titanosaurian sauropod *Bonitasaura salgadoi*. *Acta Palaeontologica Polonica* 56: 45-60.
- Galton PM. 1984. Cranial anatomy of the prosauropod dinosaur *Plateosaurus* from the Knollenmergel (Middle Keuper, Upper Triassic) of Germany. *Geologica et Palaeontologica* 18: 139-171.
- Galton PM. 1985. Cranial anatomy of the prosauropod dinosaur *Plateosaurus* from the Knollenmergel (Middle Keuper, Upper Triassic) of Germany. *Geologica et Palaeontologica* 19: 119-159.
- Galton PM. 2001. The prosauropod dinosaur *Plateosaurus* Meyer, 1837 (Saurischia: Sauropodomorpha; Upper Triassic). II. Notes on the referred species. *Revue de Paléobiologie* 20: 435-502.
- Galton PM & Jensen JA. 1979. A new large theropod dinosaur from the Upper Jurassic of Colorado. *Brigham Young University Geology Studies* 26: 1-12.
- Galton PM & Upchurch P. 2004. Prosauropoda. In: Weishampel DB, Dodson P, Osmólska H (eds). *The Dinosauria*. University of California Press, Berkeley: 232-258.
- García RA, Salgado L, Coria RA & Chiappe LM. 2010. Osteología embrionaria de saurópodos titanosaurios de Neuquén (Argentina): aspectos ontogenéticos y evolutivos. *Ameghiniana* 47: 409-430.
- Garland T, Harvey PH & Ives AR. 1992. Procedures for the analysis of comparative data using phylogenetically independent contrasts. *Systematic Biology* 41: 18-32.
- Gatesy SM. 1990. Caudofemoral musculature and the evolution of theropod locomotion. *Paleobiology* 16: 170-186.

- Gauthier JA. 1986. Saurischian monophyly and the origin of birds. *Memoirs of the California Academy of Science* 8: 1-55.
- Gauthier JA & Padian K. 1985. Phylogenetic, functional, and aerodynamic analyses of the origin of birds and their flight. In: Hecht MK, Ostrom JH, Viohl G & Wellnhofer P (eds). *The Beginnings of Birds*. Freunde des Jura-Museums Eichstätt, Eichstätt: 185-197.
- Gilmore GW. 1920. Osteology of the carnivorous dinosauria in the United States National Museum, with special reference to the genera *Antrodemus* (*Allosaurus*) and *Ceratosaurus*. *Bulletin - United States National Museum* 110: 1-159.
- Glut DF. 2003. *Dinosaurs. The encyclopedia. Supplement 3*. Mcfarland & Co, Jefferson.
- Godefroit P, Demuynck H, Dyke G, Hu D, Escuillié F & Claeys P. 2013a. Reduced plumage and flight ability of a new Jurassic paravian theropod from China. *Nature Communications* 4 (1394): 1-6.
- Godefroit P, Cau A, Hu D, Escuillié F, Wu W & Dyke G. In press. A Jurassic avialan dinosaur from China resolves the early phylogenetic history of birds. *Nature*.
- Göhlich UB & Chiappe LM. 2006. A new carnivorous dinosaur from the Late Jurassic Solnhofen archipelago. *Nature* 440: 329-332.
- Goloboff PA, Farris JS & Nixon KC. 2008. TNT, a free program for phylogenetic analysis. *Cladistics* 24: 774-786.
- Goodwin MB. 1990. Morphometric landmarks of pachycephalosaurid cranial material from the Judith River Formation of northcentral Montana. In: Carpenter K & Currie PJ (eds). *Dinosaur systematics: approaches and perspectives*. Cambridge University Press, Cambridge: 189-201.

- Goodwin MB, Clemens WA, Horner JR & Padian K. 2006. The smallest known *Triceratops* skull: new observations on ceratopsid cranial anatomy and ontogeny. *Journal of Vertebrate Paleontology* 26: 103-112.
- Gould SJ. 1991. The disparity of the Burgess Shale arthropod fauna and the limits of cladistic analysis: why we must strive to quantify morphospace. *Paleobiology* 17: 411-423.
- Gow CE, Kitching JW & Raath MA. 1990. Skulls of the prosauropod dinosaur *Massospondylus carinatus* Owen in the collections of the Bernard Price Institute for Palaeontological Research. *Palaeontologia Africana* 27: 45-58.
- Gower DJ. 2002. Braincase evolution in suchian archosaurs (Reptilia: Diapsida): evidence from the rauisuchian *Batrachotomus kupferzellensis*. *Zoological Journal of the Linnean Society* 136: 49-76.
- Gower DJ & Weber E. 1998. The braincase of *Euparkeria*, and the evolutionary relationships of birds and crocodylians. *Biological Reviews* 73: 367-411.
- Gower JC. 1975. Generalized Procrustes analysis. *Psychometrika* 40: 33-51.
- Hall PM & Portier KM. 1994. Cranial morphometry of New Guinea Crocodiles (*Crocodylus novaeguineae*): ontogenetic variation in relative growth of the skull and an assessment of its utility as a predictor of the sex and size of individuals. *Herpetological Monographs* 8: 203-225.
- Hammer O. 2009. *PAST: Paleontological Statistics. Reference manual*. 191 pp. <http://folk.uio.no/ohammer/past/>
- Hammer O & Harper D. 2006. *Paleontological data analysis*. Blackwell Publishing, Malden.
- Hammer O, Harper DAT & Ryan PD. 2001. PAST: Paleontological statistics software package for education and data analysis. *Palaeontologia Electronica* 4: 1-9.

- Harris MP, Fallon JF & Prum RO. 2002. Shh-Bmp2 signaling module and the evolutionary origin and diversification of feathers. *Journal of Experimental Zoology (MOL DEV EVOL)* 294: 160-176.
- Henderson DM. 2000. Skull and tooth morphology as indicators of niche partitioning in sympatric Morrison Formation theropods. *Gaia* 15: 219-226.
- Henderson DM. 2002. The eyes have it: The sizes, shapes, and orientations of theropod orbits as indicators of skull strength and bite force. *Journal of Vertebrate Paleontology* 22: 766-778.
- Henderson DM. 2010. Pterosaur body mass estimates from three-dimensional mathematical slicing. *Journal of Vertebrate Paleontology* 30: 768-785.
- Henderson DM & Weishampel DB. 2002. Convergent evolution of the maxilla-dental-complex among carnivorous archosaurs. *Senckenbergiana lethaea* 82: 77-92.
- Herron JC. 1991. Growth rates of black caiman *Melanosuchus niger* and spectacled caiman *Caiman crocodilus* and the recruitment of breeders in hunted caiman populations. *Biological Conservation* 55: 103-113.
- Hieronimus TL & Witmer LM. 2010. Homology and evolution of avian compound rhamphothecae. *The AUK* 127: 590-604.
- Hinić S. 2002. *Cranial osteology of Massospondylus carinatus Owen, 1854 and its implications for prosauropod phylogeny*. Master thesis, University of Toronto, Toronto.
- Holliday CM & Witmer LM. 2008. Cranial kinesis in dinosaurs: intracranial joints, protractor muscles, and their significance for cranial evolution and function in diapsids. *Journal of Vertebrate Paleontology* 28: 1073-1088.

- Holliday CM & Witmer LM. 2009. The epipterygoid of crocodyliforms and its significance for the evolution of the orbitotemporal region of eusuchians. *Journal of Vertebrate Paleontology* 29: 715-733.
- Holtz TR Jr. 2004. Tyrannosauroida. In: Weishampel DB, Dodson P & Osmólska H (eds). *The Dinosauria*. University of California Press. Berkeley: 111-136.
- Holtz TR Jr., Molnar RE & Currie PJ. 2004. Basal Tetanurae. In: Weishampel DB, Dodson P & Osmólska H (eds). *The Dinosauria*. University of California Press. Berkeley: 71-110.
- Hone DWE, Tischlinger H, Xu X & Zhang F. 2010. The extent of the preserved feathers on the four-winged dinosaur *Microraptor gui* under ultraviolet light. *PLoS ONE* 5: e9223.
- Hone D, Naish D & Cuthill I. 2012. Does mutual sexual selection explain the evolution of head crests in pterosaurs and dinosaurs? *Lethaia* 45: 139-156.
- Horna J, Horna V, Cintra R & Vásquez P. 2001. Feeding ecology of black caiman *Melanosuchus niger* in a western Amazonian forest: The effects of ontogeny and seasonality on diet composition. *Ecotropica* 7: 1-11.
- Horna V, Zimmermann R, Cintra R, Vásquez P & Horna J. 2003. Feeding ecology of the black caiman (*Melanosuchus niger*) in Manu National Park, Peru. *Lyonia* 4: 65-72.
- Horner JR & Goodwin MB. 2006. Major cranial changes during *Triceratops* ontogeny. *Proceedings of the Royal Society B* 273: 2757-2761.
- Hu D, Hou L, Zhang L & Xu X. 2009. A pre-*Archaeopteryx* troodontid theropod from China with long feathers on the metatarsus. *Nature* 461: 640-643.
- Hübner TR. 2012. Bone histology in *Dysalotosaurus lettowvorbecki* (Ornithischia: Iguanodontia) - variation, growth, and implications. *PLoS ONE* 7: e29958.

- Hübner TR & Rauhut OWM. 2010. A juvenile skull of *Dysalotosaurus lettowvorbecki* (Ornithischia: Iguanodontia), and implications for cranial ontogeny, phylogeny, and taxonomy in ornithopod dinosaurs. *Zoological Journal of the Linnean Society* 160: 366-396.
- Hunt G & Carrano MT. 2010. Models and methods for analyzing phenotypic evolution in lineages and clades. *The Paleontological Society Papers* 16: 245-269.
- Hurum JH & Sabath K. 2003. Giant theropod dinosaurs from Asia and North America: skulls of *Tarbosaurus bataar* and *Tyrannosaurus rex* compared. *Acta Palaeontologica Polonica* 48: 161-190.
- Hutchinson JR. 2001a. The evolution of pelvic osteology and soft tissues on the line to extant birds (Neornithes). *Zoological Journal of the Linnean Society* 131: 123-168.
- Hutchinson JR. 2001b. The evolution of femoral osteology and soft tissues on the line to extant birds (Neornithes). *Zoological Journal of the Linnean Society* 131: 169-197.
- Hutton JM. 1987. Growth and feeding ecology of the Nile crocodile *Crocodylus niloticus* at Ngezi, Zimbabwe. *Journal of Animal Ecology* 56: 25-38.
- Iordansky NN. 1973. The skull of the Crocodylia. In: Gans C & Parson TS (eds). *Biology of the Reptilia*. Academic Press, New York: 201-262.
- Irmis RB. 2007. Axial skeleton ontogeny in the Parasuchia (Archosauria: Pseudosuchia) and its implications for ontogenetic determination in archosaurs. *Journal of Vertebrate Paleontology* 27: 350-361.
- Irmis RB. 2011. Evaluating hypotheses for the early diversification of dinosaurs. *Earth and Environmental Science Transactions of the Royal Society of Edinburgh* 101: 397-426.

- Ji S, Ji Q, Lü J & Yuan C. 2007. A new giant compsognathid dinosaur with long filamentous integuments from Lower Cretaceous of northeastern China. *Acta Geologica Sinica* 81: 8-15.
- Johnson DR & O'Higgins P. 1996. Is there a link between changes in the vertebral "hox code" and the shape of vertebrae? A quantitative study of shape change in the cervical vertebral column of mice. *Journal of Theoretical Biology* 183: 89-93.
- Jones IL & Hunter FM. 1993. Mutual sexual selection in a monogamous seabird. *Nature* 362: 238-239.
- Jones IL & Hunter FM. 1999. Experimental evidence for mutual inter- and intrasexual selection favoured a crested auklet ornament. *Animal Behaviour* 57: 521-528.
- Jones KE & Goswami A. 2010. Quantitative analysis of the influence of phylogeny and ecology on phocid and otariid pinniped (Mammalia; Carnivora) cranial morphology. *Journal of Zoology* 280: 297-308.
- Jones M. 2008. Skull shape and feeding strategy in *Sphenodon* and other Rhynchocephalia (Diapsida: Lepidosauria). *Journal of Morphology* 269: 945-966.
- Kälin JA. 1933. Beiträge zur vergleichenden Osteologie des Crocodylidschädels. *Zoologisches Jahrbuch* 57: 535-714.
- Kellner AWA & Campos D de A. 2002. The function of the cranial crest and jaws of a unique pterosaur from the Early Cretaceous of Brazil. *Science* 279: 389-392.
- Kellner AWA, Wang X, Tischlinger H, Campos DA, Hone DWE & Meng X. 2010. The soft tissue of *Jeholopterus* (Pterosauria, Anurognathidae, Batrachognathinae) and the structure of the pterosaur wing membrane. *Proceedings of the Royal Society B* 277: 321-329.

- Kley NJ, Sertich JJW, Turner AH, Krause DW, O'Connor PM & Georgi JA. 2010. Craniofacial morphology of *Simosuchus clarki* (Crocodyliformes: Notosuchia) from the Late Cretaceous of Madagascar. *Journal of Vertebrate Paleontology* 30: 13-98.
- Klingenberg CP. 2009. Morphometric integration and modularity in configurations of landmarks: tools for evaluating a priori hypotheses. *Evolution & Development* 11: 405-421.
- Klingenberg CP. 2010. Evolution and development of shape: integrating quantitative approaches. *Nature Reviews Genetics* 11: 623-635.
- Klingenberg CP. 2011. MorphoJ: an integrated software package for geometric morphometrics. *Molecular Ecology Resources* 11: 353-357.
- Klingenberg CP & Gidaszewski NA. 2010. Testing and quantifying phylogenetic signals and homoplasy in morphometric data. *Systematic Biology* 59: 245-261.
- Knoll F & Ruiz-Omeñaca JI. 2009. Theropod teeth from the basalmost Cretaceous of Anoual (Morocco) and their palaeobiogeographical significance. *Geological Magazine* 146: 602-616.
- Kraaijeveld K, Gregurke J, Hall C, Komdeur J & Mulder R. 2004. Mutual ornamentation, sexual selection, and social dominance in the black swan. *Behavioral Ecology* 15: 380-389.
- Kulemeyer C, Asbahr K, Gunz P, Frahnert S, Bairlein F. 2009. Functional morphology and integration of corvid skulls - a 3D geometric morphometric approach. *Frontiers in Zoology* 6: 1-14.
- Kundrát M. 2009. Heterochronic shift between early organogenesis and migration of cephalic neural crest cells in two divergent evolutionary phenotypes of archosaurs: crocodile and ostrich. *Evolution & Development* 11: 535-546.

- Kundrát M, Cruickshank ARI, Manning TW & Nudds J. 2008. Embryos of therizinosauroid theropods from the Upper Cretaceous of China: diagnosis and analysis of ossification patterns. *Acta Zoologica (Stockholm)* 89: 231-251.
- Kurzanov SM. 1972. Sexual dimorphism in protoceratopsians. *Paleontologicheskii Zhurnal* 1: 104-112.
- Langer MC. 2004. Basal Saurischia. In: Weishampel DB, Dodson P & Osmólska H (eds). *The Dinosauria*. University of California Press, Berkeley: 25-46.
- Langer MC, Ezcurra MD, Bittencourt JS & Novas FE. 2009. The origin and early evolution of dinosaurs. *Biological Reviews* 84: 1-56.
- Langston W. 1965. Fossil crocodylians from Colombia and the Cenozoic history of the Crocodylia in South America. *University of California Publications in Geological Sciences* 52: 1-152.
- Larson PL. 1997. The king's new clothes: a fresh look at *Tyrannosaurus rex*. In: Wolberg DL, Stumps E & Rosenberg GD (eds). *Dinofest International*. Academy of Natural Sciences, Philadelphia: 65-71.
- Larson PL. 2008. Variation and sexual dimorphism in *Tyrannosaurus rex*. In: Larson P & Carpenter K (eds). *Tyrannosaurus rex, the tyrant king*. Indiana University Press, Bloomington: 103-128.
- Larsson HCE & Sues H-D. 2007. Cranial osteology and phylogenetic relationships of *Hamadasuchus rebouli* (Crocodyliformes: Mesoeucrocodylia) from the Cretaceous of Morocco. *Zoological Journal of the Linnean Society* 149: 533-567.
- Lauder GV. 1995. On the inference of function from structure. In: Thomason JJ (ed). *Functional Morphology in Vertebrate Paleontology*. Cambridge University Press, Cambridge: 1-18.

- Laurin M. 2004. The evolution of body size, Cope's rule and the origin of amniotes. *Systematic Biology* 53: 594-622.
- Lautenschlager S. 2013. Cranial myology and bite force performance of *Erlikosaurus andrewsi*: a novel approach for digital muscle reconstructions. *Journal of Anatomy* 222: 260-272.
- Leal LA, Azevedo SAK, Kellner AWA & Da Rosa AAS. 2004. A new early dinosaur (Sauropodomorpha) from the Caturrita Formation (Late Triassic), Paraná Basin, Brazil. *Zootaxa* 690: 1-24.
- Lee AH & Werning S. 2008. Sexual maturity in growing dinosaurs does not fit reptilian growth models. *Proceedings of the National Academy of Sciences, U.S.A.* 105: 582-587.
- Lefebvre B, Eble GJ, Navarro N. & David B. 2004. Diversification of atypical Paleozoic echinoderms: a quantitative survey of patterns of stylophoran disparity, diversity, and geography. *Paleobiology* 32: 483-510.
- Lehman TM. 1990. The ceratopsian subfamily Chasmosaurinae: sexual dimorphism and systematics. In: Carpenter K & Currie PJ (eds). *Dinosaur systematics: approaches and perspectives*. Cambridge University Press, Cambridge: 211-229.
- Lehman TM. 1998. A gigantic skull and skeleton of the horned dinosaur *Pentaceratops sternbergi* from New Mexico. *Journal of Paleontology* 72: 894-906.
- Li D, Sullivan C, Zhou Z & Zhang F. 2010. Basal birds from China: a brief review. *Chinese Birds* 1: 83-96.
- Lingham-Soliar T, Feduccia A & Wang X. 2007. A new Chinese specimen indicates that "protofeathers" in the Early Cretaceous theropod dinosaur *Sinosauropteryx* are degraded collagen fibres. *Proceedings of the Royal Society B* 274: 1823-1829.

- Link E & Fürsich FT. 2001. Hochauflösende Feinstratigraphie und Mikrofaziesanalyse der Oberjura Plattenkalke von Painten, Südliche Frankenalb. *Archaeopteryx* 19: 71-88.
- Lockwood CA, Kimbel WH & Lynch JM. 2005. Variation in early hominin temporal bone morphology and its implications for species diversity. *Transactions of the Royal Society of South Africa* 60: 1-5.
- Loewen MA. 2009. *Variation in the Late Jurassic theropod dinosaur Allosaurus: ontogenetic, functional, and taxonomic implications*. University of Utah, Salt Lake City.
- Long JA & McNamara KJ. 1997. Heterochrony: the key to dinosaur evolution. In: Wolberg DL, Stumps E & Rosenberg GD (eds). *Dinofest International*. Academy of Natural Sciences, Philadelphia: 113-123.
- Lü J & Ji Q. 2006. Preliminary results of a phylogenetic analysis of the pterosaurs from western Liaoning and surrounding areas. *Journal of the Paleontological Society of Korea* 22: 239-261.
- Lü J, Unwin DM, Xu L & Zhang X. 2008. A new azhdarchoid pterosaur from the Lower Cretaceous of China and its implications for pterosaur phylogeny and evolution. *Naturwissenschaften* 95: 891-897.
- Lü J, Unwin DM, Jin X, Liu Y & Ji Q. 2010a. Evidence for modular evolution in a long-tailed pterosaur with a pterodactyloid skull. *Proceedings of the Royal Society of London B* 277: 383-389.
- Lü J, Kobayashi Y, Li T & Zhong S. 2010b. A new basal sauropod dinosaur from the Lufeng Basin, Yunnan Province, southwestern China. *Acta Geologica Sinica* 84: 1336-1342.

- Lü J, Unwin DM, Deeming DC, Ji X, Liu J & Ji Q. 2011. An egg-adult association, gender, and reproduction in pterosaurs. *Science* 331: 321-324.
- Lü J, Currie PJ, Li X, Zhang X, Pu H, Jia S. In press. Chicken-sized oviraptorid dinosaurs from central China and their ontogenetic implications. *Naturwissenschaften*.
- Lucas AM & Stettenheim PR. 1972. *Avian anatomy. Integument, Part I & II*. U.S. Government Printing Office, Washington.
- Lupia R. 1999. Discordant morphological disparity and taxonomic diversity during the Cretaceous angiosperm radiation: North American pollen record. *Paleobiology* 25: 1-28.
- Makovicky PJ, Kobayashi Y & Currie PJ. 2004. Ornithomimosauria. In: Weishampel DB, Dodson P & Osmólska H (eds). *The Dinosauria*. University of California Press, Berkeley: 137-150.
- Maddison WP. 1991. Squared-change parsimony reconstructions of ancestral states for continuous-valued characters on a phylogenetic tree. *Systematic Zoology* 40: 304-314.
- Maddison WP & Maddison DR. 2009. *Mesquite: a modular system of evolutionary analysis. Version 2.72*. <http://mesquiteproject.org/>
- Madsen JH. 1976. *Allosaurus fragilis*: a revised osteology. *Utah Geological and Mineralogical Survey Bulletin* 109: 3-163.
- Madsen JH & Welles SP. 2000. *Ceratosaurus* (Dinosauria, Theropoda), a revised osteology. *Utah Geology Survey Miscellaneous Publication* 00-2: 1-80.
- Maganuco S, Cau A & Pasini G. 2005 First description of theropod remains from the Middle Jurassic (Bathonian) of Madagascar. *Atti della Società Italiana di Scienze Naturali e del Museo Civico di Storia Naturale in Milano* 146: 165-202.
- Maisey JG. 1991. *Santana Fossils*. TFH Publications, Neptune City, New Jersey.

- Maleev EA. 1974. Giant carnosaur of the family Tyrannosauridae. *Trudy Sovmestnaya Sovetsko-Mongolskaya Paleontologicheskaya Ekspeditsiya* 1: 132-191.
- Mallarino R, Grant PR, Grant BR, Herrel A, Kuo WP & Abzhanov A. 2011. Two developmental modules establish 3D beak-shape variation in Darwin's finches. *Proceedings of the National Academy of Sciences, U.S.A.* 108: 4057-4062.
- Mallon JC, Holmes R, Eberth DA, Ryan MJ & Anderson JS. 2011. Variation in the skull of *Anchiceratops* (Dinosauria, Ceratopsidae) from the Horseshoe Canyon Formation (Upper Cretaceous) of Alberta. *Journal of Vertebrate Paleontology* 31: 1047-1071.
- Marioni B, Da Silveira R, Magnusson WE & Thorbjarnarson JB. 2008. Feeding behavior of two sympatric caiman species, *Melanosuchus niger* and *Caiman crocodilus*, in the Brazilian Amazon. *Journal of Herpetology* 42: 768-772.
- Martill DM & Naish D. 2006. Cranial crest development in the azhdarchoid pterosaur *Tupuxuara*, with a review of the genus and tapejarid monophyly. *Palaeontology* 49: 925-941.
- Martinez RN & Alcober OA. 2009. A basal sauropodomorph (Dinosauria: Saurischia) from the Ischigualasto Formation (Triassic, Carnian) and the early evolution of Sauropodomorpha. *PLoS ONE* 4: e4397.
- Martinez RN, Sereno PC, Alcober OA, Colombi CE, Renne PR, Montañez IP & Currie BS. 2011. A basal dinosaur from the dawn of the dinosaur era in southwestern Pangaea. *Science* 331: 206-210.
- Marugán-Lobón J & Buscalioni AD. 2003. Disparity and geometry of the skull in Archosauria. *Biological Journal of Linnean Society* 80: 67-88.
- Marugán-Lobón J & Buscalioni AD. 2004. Geometric morphometrics in macroevolution: morphological diversity of skull in modern avian forms in contrast

- to some theropod dinosaurs. In: Elewa AMT (ed). *Morphometrics: applications in biology and paleontology*. Springer-Verlag, Berlin: 157-173.
- Marugán-Lobón J & Buscalioni AD. 2006. Avian skull morphological evolution: exploring exo- and endocranial covariation with two-block partial least squares. *Zoology* 109: 217-230.
- Maryańska T & Osmólska H. 1975. Protoceratopsidae (Dinosauria) of Asia. *Palaeontologia Polonica* 33: 133-182.
- Mateus O. 1998. *Lourinhanosaurus antunesi*, a new Upper Jurassic allosauroid (Dinosauria: Theropoda) from Lourinhã, Portugal. *Memórias da Academia de Ciências de Lisboa* 37: 111-124.
- Mateus O, Walen A & Antunes MT. 2006. The large theropod fauna of the Lourinhã Formation (Portugal) and its similarity to the Morrison Formation, with a description of a new species of *Allosaurus*. *New Mexico Museum of Natural History and Science, Bulletin* 36: 1-7.
- Mayr G & Clarke JA. 2003. The deep divergences of neornithine birds: a phylogenetic analysis of morphological characters. *Cladistics* 19: 527-553.
- Mayr G, Peters DS, Plodowski G & Vogel O. 2002. Bristle-like integumentary structures at the tail of the horned dinosaur *Psittacosaurus*. *Naturwissenschaften* 89: 361-365.
- Mazzetta GV, Fariña RA & Vizcaíno SF. 2000. On the palaeobiology of the South American horned theropod *Carnotaurus sastrei* Bonaparte. *Gaia* 15: 185-192.
- McClelland BK. 1990. *Anatomy and kinesis of the Allosaurus skull*. Texas Tech University, Lubbock.

- McGowan AJ & Dyke GJ. 2007. A morphospace-based test for competitive exclusion among flying vertebrates: did birds, bats and pterosaurs get in each other's space? *Journal of Evolutionary Biology* 20: 1230-1236.
- McHenry CR, Clausen PD, Daniel WJT, Meers MB & Pendharkar A. 2006. Biomechanics of the rostrum in crocodylians: a comparative analysis using finite-element modeling. *The Anatomical Record* 288: 827-849.
- McNamara KJ. 1982. Heterochrony and phylogenetic trends. *Paleobiology* 8: 130-142.
- Meloro C & Jones M. 2012. Tooth and cranial disparity in the fossil relatives of *Sphenodon* (Rhynchocephalia) dispute the persistent "living fossil" label. *Journal of Evolutionary Biology* 25: 2194-2209.
- Medem F. 1963. Osteología craneal, distribución geográfica y ecología de *Melanosuchus niger* (Spix), (Crocodylia, Alligatoridae). *Ibidem* 12: 5-19.
- Medem F. 1981. *Los Crocodylia de Sur América. Vol. I. Los Crocodylia de Colombia*. Colciencias, Bogotá.
- Meier R, Shiyang K, Vaidya G & Ng PKL. 2006. DNA barcoding and taxonomy in Diptera: a tale of high intraspecific variability and low identification success. *Systematic Biology* 55: 715-728.
- Meier R, Zhang G & Ali F. 2008. The use of mean instead of smallest interspecific distances exaggerates the size of the "barcoding gap" and leads to misidentification. *Systematic Biology* 57: 809-813.
- Meyer CP & Paulay G. 2005. DNA barcoding: error rates based on comprehensive sampling. *PloS Biology* 3: e422.
- Mickoleit G. 2004. *Phylogenetische Systematik der Wirbeltiere*. Verlag Dr. Friedrich Pfeil, München.

- Middleton KM & Gatesy SM. 2000. Theropod forelimb design and evolution. *Zoological Journal of the Linnean Society* 128: 149-187.
- Midford PE, Garland Jr T & Maddison WP. 2005. *PDAP Package of Mesquite*. Version 1.07. http://mesquiteproject.org/pdap_mesquite/
- Miller SC & Bowman BM. 1981. Medullary bone osteogenesis following estrogen administration to mature male Japanese quail. *Developmental Biology* 87: 52-63.
- Molnar RE. 1990. Variation in theory and in theropods. In: Carpenter K & Currie PJ (eds). *Dinosaur systematics: approaches and perspectives*. Cambridge University Press, Cambridge: 71-79.
- Molnar RE. 2005. Sexual selection and sexual dimorphism in theropods. In: Carpenter K (ed). *The carnivorous dinosaurs*. Indiana University Press, Bloomington: 284-312.
- Molnar RE, Kurzanov SM, Dong Z. 1990. Carnosauria. In: Weishampel DB, Dodson P, & Osmólska H (eds). *The Dinosauria*. University of California Press, Berkeley 169-209.
- Monteiro LR & Soares M. 1997. Allometric analysis of the ontogenetic variation and evolution of the skull in *Caiman* Spix, 1825 (Crocodylia: Alligatoridae). *Herpetologica*, 53: 62-69.
- Monteiro LR, Cavalcanti MJ & Sommer HSJ. 1997. Comparative ontogenetic shape changes in the skull of *Caiman* species (Crocodylia, Alligatoridae). *Journal of Morphology* 321: 53-62.
- Mook CC. 1921. Notes on the postcranial skeleton in the Crocodilia. *Bulletin of the American Museum of Natural History* 44: 67-100.
- Moser M. 2003. *Plateosaurus engelhardti* Meyer, 1937 (Dinosauria: Sauropodomorpha) aus dem Feuerletten (Mittelkeuper; Obertrias) von Bayern. *Zitteliana B* 24: 3-186.

- Nesbitt SJ. 2007. The anatomy of *Effigia okeeffeae* (Archosauria, Suchia), theropod-like convergence, and the distribution of related taxa. *Bulletin of the American Museum of Natural History* 302: 1-84.
- Nesbitt SJ. 2011. The early evolution of archosaurs: relationships and the origin of major clades. *Bulletin of the American Museum of Natural History* 352: 1-292.
- Nesbitt SJ & Butler RJ. 2013. Redescription of the archosaur *Parringtonia gracilis* from the Middle Triassic Manda beds of Tanzania, and the antiquity of Erpetosuchidae. *Geological Magazine* 150: 225-238.
- Norell MA. 1988. *Cladistics approaches to evolution and paleobiology as applied to the phylogeny of alligatorids*. Yale University, New Haven.
- Norell MA & Xu X. 2005. Feathered dinosaurs. *Annual Review of Earth and Planetary Sciences* 33: 277-299.
- Norell MA, Clark JM, Turner AH, Makovicky PJ, Barsbold R & Rowe T. 2006. A new dromaeosaurid theropod from Ukhaa Tolgod (Ömnögov, Mongolia). *American Museum Novitates* 3545: 1-51.
- Norman DB, Witmer LM & Weishampel DB. 2004. Basal Ornithischia. In: Weishampel DB, Dodson P & Osmólska H (eds). *The Dinosauria*. University of California Press, Berkeley: 325-334.
- Novas FE & Pol D. 2002. Alvarezsaurid relationships reconsidered. In: Chiappe LM & Witmer LM (eds). *Mesozoic birds: above the heads of dinosaurs*. University of California Press, Berkeley: 121-125.
- O'Connor JK & Chiappe LM. 2011. A revision of enantiornithine (Aves: Ornithothoraces) skull morphology. *Journal of Systematic Palaeontology* 9: 135-157.
- O'Higgins P. 2000. The study of morphological variation in the hominid fossil record: biology, landmarks and geometry. *Journal of Anatomy* 197: 103-120.

- O'Higgins P & Collard M. 2002. Sexual dimorphism and facial growth in papionin monkeys. *Journal of Zoology* 257: 255-272.
- Osborn HF. 1903. The skull of *Creosaurus*. *Bulletin of the American Museum of Natural History* 19: 697-701.
- Osborn HF. 1912. Crania of *Tyrannosaurus* and *Allosaurus*. *Memoirs of the American Museum of Natural History* 1: 1-30.
- Ósi A. 2010. Feeding-related characters in basal pterosaurs: implications for jaw mechanism, dental function and diet. *Lethaia* 44: 136-152.
- Ósi A, Weishampel DB & Jianu CM. 2005. First evidence of azhdarchid pterosaurs from the Late Cretaceous of Hungary. *Acta Palaeontologica Polonica* 50: 777-787.
- Osmólska H, Currie PJ & Barsbold R. 2004. Oviraptorosauria. In: Weishampel DB, Dodson P & Osmólska H (eds). *The Dinosauria*. University of California Press, Berkeley: 165-183.
- Ostrom JH. 1978. The osteology of *Compsognathus longipes* Wagner. *Zitteliana* 4: 73-118.
- Otte KC. 1974. Research programme *Melanosuchus niger* in the Manu National Park. *World Wildlife Yearbook* 1973-1974: 257-260.
- Ouyang H & Ye Y. 2002. *The first mamenchisaurian skeleton with complete skull*, *Mamenchisaurus youngi*. Sichuan Science and Technology Press. Chengdu.
- Pacheco LF. 1994. Estimating crocodylian abundance in forest lagoons. In: *Group, Proceedings of the 12th Working Meeting of the IUCN-SSC Crocodile Specialist. Crocodiles*. IUCN, Gland: 241-244.
- Padian K. 1983. A functional analysis of flying and walking in pterosaurs. *Paleobiology* 9: 218-239.

- Padian K. 1985. The origins and aerodynamics of flight in extinct vertebrates. *Palaeontology* 28: 413-433.
- Padian K 2008a. The Early Jurassic pterosaur *Dorygnathus banthensis* (Theorori, 1830). *Special Papers in Palaeontology* 80: 1-64.
- Padian K 2008b. The early Jurassic pterosaur *Campylognathoides* Strand, 1928. *Special Papers in Palaeontology* 80: 65-107.
- Padian K & Horner JR. 2011a. The definition of sexual selection and its implications for dinosaurian biology. *Journal of Zoology* 283: 23-27.
- Padian K & Horner JR. 2011b. The evolution of “bizarre structures” in dinosaurs: biomechanics, sexual selection, social selection or species recognition? *Journal of Zoology* 283: 3-17.
- Padian K & Horner JR. In press. Misconceptions of sexual selection and species recognition: a response to Knell et al. and to Mendelson and Shaw. *Trends in Ecology and Evolution*.
- Padian K, de Ricqlès A de & Horner JR. 2001. Dinosaurian growth rates and bird origins. *Nature* 412: 405-408.
- Palmer C & Dyke GJ. 2010. Biomechanics of the unique pterosaur pteroid. *Proceedings of the Royal Society B* 277: 1121-1127.
- Paradis E, Claude J & Strimmer K. 2004. APE: analyses of phylogenetics and evolution in R language. *Bioinformatics* 20: 289-290. <http://ape.mpl.ird.fr/>
- Paul GS. 2002. *Dinosaurs of the air: the evolution and loss of flight in dinosaurs and birds*. John Hopkins University Press, Baltimore.
- Paul GS. 2008. The extreme lifestyle and habits of the gigantic tyrannosaurid superpredators of the Late Cretaceous of North America and Asia. In: Larson P, &

- Carpenter K (eds). *Tyrannosaurus rex, the tyrant king*. Indiana University Press, Bloomington: 307-352.
- Paul GS. 2010. *The Princeton field guide to dinosaurs*. Princeton University Press, New Jersey.
- Peyer K. 2006. A reconsideration of *Compsognathus* from the Upper Tithonian of Canjuers, southeastern France. *Journal of Vertebrate Paleontology* 26: 879-896.
- Pierce SE & Benton MJ. 2006. *Pelagosaurus typus* Bronn, 1841 (Mesoeucrocodylia: Thalattosuchia) from the Upper Lias (Toarcian, Lower Jurassic) of Somerset, England. *Journal of Vertebrate Paleontology* 26: 621-635.
- Pierce SE, Angielczyk KD & Rayfield EJ. 2008. Patterns of morphospace occupation and mechanical performance in extant crocodylian skulls: a combined geometric morphometric and finite element modelling approach. *Journal of Morphology* 269: 840-864.
- Piña C, Larriera A, Siroski P & Verdade LM. 2007. Cranial sexual discrimination in hatchling broad-snouted caiman (*Caiman latirostris*). *Iheringia, Série Zoologia* 97: 17-20.
- Pinheiro FL, Fortier DC, Schultz CL, Artur J, Andrade FG de & Bantim RAM. 2011. New information on *Tupandactylus imperator*, with comments on the relationships of Tapejaridae (Pterosauria). *Acta Palaeontologica Polonica* 56: 567-580.
- Piras P, Teresi L, Buscalioni AD & Cubo J. 2009. The shadow of forgotten ancestors differently constrains the fate of Alligatoidea and Crocodyloidea. *Global Ecology and Biogeography* 18: 30-40.
- Piras P, Colangelo P, Adams DC, Buscalioni AD, Cubo J, Kotsakis T, Meloro C & Raia P. 2010. The *Gavialis-Tomistoma* debate: the contribution of skull ontogenetic

- allometry and growth trajectories to the study of crocodylian relationships. *Evolution & Development* 12: 568-579.
- Piras P, Salvi D, Ferrara G, Maiorino L, Delfino M, Pedde L & Kotsakis T. 2011. The role of post-natal ontogeny in the evolution of phenotypic diversity in *Podarcis* lizards. *Journal of Evolutionary Biology* 24: 2705-2720.
- Platt SG, Rainwater TR, Thorbjarnarson JB, Finger AG, Anderson TA & McMurry S. T. 2009. Size estimation, morphometrics, sex ratio, sexual size dimorphism, and biomass of Morelet's crocodile in northern Belize. *Caribbean Journal of Science* 45: 80-93.
- Plotkin MJ, Medem F, Mittermeier RA & Constable IA. 1983. Distribution and conservation of the black caiman (*Melanosuchus niger*). In: Rhodin A & Mitaya K (eds). *Advances in Herpetology and Evolutionary Biology*. Museum of Comparative Zoology, Cambridge: 695-705.
- Poe S. 1997. Data set incongruence and the phylogeny of crocodylians. *Systematic Biology* 45: 393-414.
- Pol D & Gasparini Z. 2009. Skull anatomy of *Dakosaurus andiniensis* (Thalattosuchia: Crocodylomorpha) and the phylogenetic position of Thalattosuchia. *Journal of Systematic Palaeontology* 7: 163-197.
- Pol D & Powell JE. 2007. Skull anatomy of *Mussaurus patagonicus* (Dinosauria: Sauropodomorpha) from the Late Triassic of Patagonia. *Historical Biology* 19: 125-144.
- Pol D & Rauhut OWM. 2012. A Middle Jurassic abelisaurid from Patagonia and the early diversification of theropod dinosaurs. *Proceedings of the Royal Society B* 279: 3170-3175.

- Pol D, Rauhut OWM, Lecuona A, Leardi JM, Xu X, Clark JM. In press. A new fossil from the Jurassic of Patagonia reveals the early basicranial evolution and the origins of Crocodyliformes. *Biological Reviews*.
- Porro LB, Holliday CM, Anapol F, Ontiveros LC, Ontiveros LT & Ross CF. 2011. Free body analysis, beam mechanics, and finite element modeling of the mandible of *Alligator mississippiensis*. *Journal of Morphology* 272: 910-937.
- Prentice KC, Ruta M & Benton MJ. 2011. Evolution of morphological disparity in pterosaurs. *Journal of Systematic Palaeontology* 9: 337-353.
- Prieto-Márquez A, Gignac PM & Joshi S. 2007. Neontological evaluation of pelvic skeletal attributes purported to reflect sex in extinct non-avian archosaurs. *Journal of Vertebrate Paleontology* 27: 603-609.
- Prieto-Márquez A. 2010. Global phylogeny of hadrosauridae (Dinosauria: Ornithopoda) using parsimony and Bayesian methods. *Zoological Journal of the Linnean Society* 159: 435-502.
- Prieto-Márquez A & Norell MA. 2011. Redescription of a nearly complete skull of *Plateosaurus* (Dinosauria: Sauropodomorpha) from the Late Triassic of Trossingen (Germany). *American Museum Novitates* 3727: 1-58.
- Prum RO. 1999. Development and evolutionary origin of feathers. *Journal of Experimental Zoology (MOL DEV EVOL)* 285: 291-306.
- Prum RO & Brush AH. 2002. The evolutionary origin and diversification of feathers. *The Quarterly Review of Biology* 77: 261-295.
- Purvis A. & Rambaut A. 1995. Comparative analysis by independent contrasts (CAIC) - an Apple Macintosh application for analysing comparative data. *Computer Applications in the Biosciences* 11: 247-251.

- Rauhut OWM. 2003a. The interrelationships and evolution of basal theropod dinosaurs. *Special Papers in Palaeontology* 69: 1-213.
- Rauhut OWM. 2003b. A tyrannosauroid dinosaur from the Upper Jurassic of Portugal. *Palaeontology* 46: 903-910.
- Rauhut OWM. 2004. Provenance and anatomy of *Genyodectes serus*, a large toothed ceratosaur (Dinosauria: Theropoda) from Patagonia. *Journal of Vertebrate Paleontology* 24: 894-902.
- Rauhut OWM. 2007. The myth of the conservative character: braincase characters in theropod phylogenies. *Hallesches Jahrbuch für Geowissenschaften, Beiheft* 23: 51-54.
- Rauhut OWM. In press. New observations on the skull of *Archaeopteryx*. *Paläontologische Zeitschrift*.
- Rauhut OWM & Fechner R. 2005. Early development of the facial region in a non-avian theropod dinosaur. *Proceedings of the Royal Society B* 272: 1179-1183.
- Rauhut OWM, Fechner R, Remes K & Reis K. 2011. How to get big in the Mesozoic: the evolution of the sauropodomorph body plan. In: Klein N, Remes K, Gee CT & Sander PM (eds). *Biology of the sauropod dinosaurs: understanding the life of giants*. Indiana University Press, Bloomington: 119-149.
- Rauhut OWM, Foth C, Tischlinger H & Norell MA. 2012. Exceptionally preserved juvenile megalosauroid theropod dinosaur with filamentous integument from the Late Jurassic of Germany. *Proceedings of the National Academy of Sciences, U.S.A.* 109: 11746-11751.
- Rayfield EJ. 2004. Cranial mechanics and feeding in *Tyrannosaurus rex*. *Proceedings of the Royal Society B* 271: 1451-1459.

- Rayfield EJ. 2005. Aspects of comparative cranial mechanics in the theropod dinosaurs *Coelophysis*, *Allosaurus* and *Tyrannosaurus*. *Zoological Journal of the Linnean Society* 144: 309-316.
- Rayfield EJ. 2007. Finite Element Analysis and understanding the biomechanics and evolution of living and fossil organisms. *Annual Review of Earth and Planetary Sciences* 35: 541-576.
- Rayfield EJ. 2011. Structural performance of tetanuran theropod skulls, with emphasis on the Megalosauridae, Spinosauridae and Charcharodontosauridae. *Special Papers in Palaeontology* 86: 241-253.
- Rayfield EJ, Norman DB, Horner CC, Horner JR, Smith PM, Thomason JJ & Upchurch P. 2001. Cranial design and function in a large theropod dinosaur. *Nature* 409: 1033-1037.
- R Development Core Team. 2011. *R: A Language and Environment for Statistical Computing*. R Foundation for Statistical Computing, Vienna. <http://www.R-project.org>
- Reisz RR, Evans DC, Sues H-D & Scott D. 2010. Embryonic skeletal anatomy of the sauropodomorph dinosaur *Massospondylus* from the Lower Jurassic of South Africa. *Journal of Vertebrate Paleontology* 30: 1653-1665.
- Richtsmeier JT, Corner BD, Grausz HM, Cheverud JM & Danahey SE. 1993. The role of postnatal growth pattern in the production of facial morphology. *Systematic Biology* 42: 307-330.
- Rieppel OC. 1993. Patterns of diversity in the reptilian skull. In: Hanken J & Hall BK (eds). *The skull. Vol. 2. Patterns of structural and systematic diversity*. University of Chicago Press, Chicago: 344-390.

- Robert P & Escoufier Y. 1976. A unifying tool for linear multivariate statistical methods: the RV-coefficient. *Applied Statistics* 25: 257-265.
- Rohlf FJ. 2000. Statistical power comparisons among alternative morphometric methods. *American Journal of Physical Anthropology* 111: 463-478.
- Rohlf FJ. 2003. *tpsRelw, relative warps analysis, version 1.36*. Department of Ecology and Evolution, State University of New York at Stony Brook.
<http://life.bio.sunysb.edu/morph/>
- Rohlf FJ. 2005. *tpsDig, digitize landmarks and outlines, version 2.05*. Department of Ecology and Evolution, State University of New York at Stony Brook.
<http://life.bio.sunysb.edu/morph/>
- Rohlf FJ & Corti M. 2000. Use of two-block partial least-squares to study covariation in shape. *Systematic Biology* 49: 740-753.
- Rohlf FJ & Marcus LF. 1993. A revolution in morphometrics. *Trends in Ecology and Evolution* 8: 129-132.
- Rohlf FJ & Slice DE. 1990. Extensions of the Procrustes method for the optimal superimposition of landmarks. *Systematic Zoology* 39: 40-59.
- Romer AS. 1956. *Osteology of the reptiles*. University of Chicago Press, Chicago.
- Rootes WL, Chabreck RH, Wright VL, Brown BW & Hess TJ. 1991. Growth rates of American alligators in estuarine and palustrine wetlands in Louisiana. *Estuaries* 14: 489-494.
- Russell DA. 1970. Tyrannosaurs from the Late Cretaceous of western Canada. *National Museum of Natural Sciences, Publications in Palaeontology* 1: 1-34.
- Ruta M. 2009. Patterns of morphological evolution in major groups of Palaeozoic Temnospondyli (Amphibia: Tetrapoda). *Special Papers in Palaeontology* 81: 91-120.

- Ruta M, Wagner PJ & Coates MI. 2006. Evolutionary patterns in early tetrapods. I. Rapid initial diversification followed by decrease in rates of character change. *Proceedings of the Royal Society B* 273: 2107-2111.
- Ryan MJ, Russell AP, Eberth DA & Currie PJ. 2001. The taphonomy of a *Centrosaurus* (Ornithischia: Certopsidae) bone bed from the Dinosaur Park Formation (upper Campanian), Alberta, Canada, with comments on cranial ontogeny. *Palaios* 16: 482-506.
- Ryan MJ, Holmes R & Russell AP. 2007. A revision of the late Campanian centrosaurine ceratopsid genus *Styracosaurus* from the western interior of North America. *Journal of Vertebrate Paleontology* 27: 944-962.
- Sadleir RW & Makovicky PJ. 2008. Cranial shape and correlated characters in crocodylian evolution. *Journal of Evolutionary Biology* 21: 1578-1596.
- Sadleir RW, Barrett PM & Powell HP. 2008. The anatomy and systematics of *Eustreptospondylus oxoniensis*, a theropod dinosaur from the Middle Jurassic of Oxfordshire, England. *Monograph of the Palaeontological Society* 627: 1-82.
- Sakamoto M. 2010. Jaw biomechanics and the evolution of biting performance in theropod dinosaurs. *Proceedings of the Royal Society B* 277: 3327-3333.
- Sánchez-Villagra MR & Aguilera OA. 2006. Neogene vertebrates from Urumaco, Falcón State, Venezuela: Diversity and significance. *Journal of Systematic Palaeontology* 4: 213-220.
- Sander PM, Klein N, Buffetaut E, Cuny G, Suteethorn V & Le Loeuff J. 2004. Adaptive radiation in sauropod dinosaurs: bone histology indicates rapid evolution of giant body size through acceleration. *Organisms, Diversity & Evolution* 4: 165-173.
- Sander PM, Mateus O, Laven T & Knötschke N. 2006. Bone histology indicates insular dwarfism in a new Late Jurassic sauropod dinosaur. *Nature* 441: 739-741.

- Sander PM, Klein N, Stein K & Wings O. 2011. Sauropod bone histology and its implications for sauropod biology. In: Klein N, Remes K, Gee CT & Sander PM (eds). *Biology of the sauropod dinosaurs: understanding the life of giants*. Indiana University Press, Bloomington: 276-302.
- Sanz JL, Chiappe LM, Pérez-Moreno BP, Moratalla JJ, Hernández-Carrasquilla F, Buscalioni, AD, Ortega F, Poyato-Ariza FJ, Rasskin-Gutman D & Martínez-Delcòs X. 1997. A nestling bird from the Lower Cretaceous of Spain: implications for avian skull and neck evolution. *Science* 276: 1543-1546.
- Sampson SD. 1997. Craniofacial ontogeny in centrosaurine dinosaurs (Ornithischia: Ceratopsidae): taxonomic and behavioral implications. *Zoological Journal of the Linnean Society* 121: 293-337.
- Sampson SD & Witmer LM. 2007. Craniofacial anatomy of *Majungasaurus crenatissimus* (Theropoda: Abelisauridae) from the Late Cretaceous of Madagascar. *Journal of Vertebrate Paleontology* 27: 32-102.
- Sawyer RH & Knapp LW. 2003. Avian skin development and the evolutionary origin of feathers. *Journal of Experimental Zoology (MOL DEV EVOL)* 298B: 57-72.
- Schumacher GH. 1973. The head muscles and hyolaryngeal skeleton of turtles and crocodylians. In: Gans C & Parsons TS (eds). *Biology of the Reptilia*. Academic Press, London: 101-199.
- Schweigert G. 2007. Ammonite biostratigraphy as a tool for dating Upper Jurassic lithographic limestones from South Germany - first results and open questions. *Neues Jahrbuch für Geologie und Paläontologie - Abhandlungen* 245: 117-125.
- Schweigert G, Tischlinger H & Dietl G. 2010. Eine fossile Feder aus dem Nusplinger Plattenkalk (Oberjura, Schwäbische Alb). *Archaeopteryx* 28: 31-40.

- Schweitzer MH & Marshall CL. 2001. A molecular model for the evolution of endothermy in the theropod-bird lineage. *Journal of Experimental Zoology (MOL DEV EVOL)* 291: 317-338.
- Schweitzer MH, Wittmeyer JL & Horner JR. 2005. Gender-specific reproductive tissue in ratites and *Tyrannosaurus rex*. *Science* 308: 1456-1460.
- Schweitzer MH, Elsey RM, Dacke CG, Horner JR & Lamm E-T. 2007. Do egg-laying crocodylian (*Alligator mississippiensis*) archosaurs form medullary bone? *Bone* 40: 1152-1158.
- Selander RK. 1966. Sexual dimorphism and differential niche utilization in birds. *The Condor* 68: 113-151.
- Sereno PC. 1999. The evolution of dinosaurs. *Science* 284: 2137-2147.
- Sereno PC & Brusatte SL. 2009. Comparative assessment of tyrannosaurid interrelationships. *Journal of Systematic Palaeontology* 7: 455-470.
- Sereno PC & Larsson HCE. 2009. Cretaceous crocodyliforms from the Sahara. *ZooKeys* 28: 1-143.
- Sereno PC, Forster CA, Rogers RR & Monetta AM. 1993. Primitive dinosaur skeleton from Argentina and the early evolution of Dinosauria. *Nature* 361: 64-66.
- Sereno PC, Larsson HCE, Sidor CA & Gado B. 2001. The giant crocodyliform *Sarcosuchus* from the Cretaceous of Africa. *Science* 294: 1516-1519.
- Shine R. 1989. Ecological causes for the evolution of sexual dimorphism: a review of the evidence. *The Quarterly Review of Biology* 64: 419-461.
- Singleton M. 2002. Patterns of cranial shape variation in the *Papionini* (Primates: Cercopithecinae). *Journal of Human Evolution* 42: 547-578.
- Smith DK. 1998. A morphometric analysis of *Allosaurus*. *Journal of Vertebrate Paleontology* 18: 126-142.

- Smith HF. 2011. The role of genetic drift in shaping modern human cranial evolution: a test using microevolutionary modeling. *International Journal of Evolutionary Biology* 2011: 1-11.
- Smith KK. 1993. The form of the feeding apparatus in terrestrial vertebrates: Studies of adaptation and constraint. In: Hanken J & Hall BK (eds). *The skull. Vol. 3. Patterns of structural and systematic diversity*. University of Chicago Press, Chicago: 150-196.
- Smith LH & Lieberman BS. 1999. Disparity and constraint in olenelloid trilobites and the Cambrian radiation. *Paleobiology* 25: 459-470.
- Smith ND, Makovicky PJ, Hammer WR & Currie PJ. 2007. Osteology of *Cryolophosaurus ellioti* (Dinosauria: Theropoda) from the Early Jurassic of Antarctica and implications for early theropod evolution. *Zoological Journal of the Linnean Society* 151: 377-421.
- Smith ND, Makovicky PJ, Agnolín FL, Ezcurra MD, Pais DF & Salisbury SW. 2008. A *Megaraptor*-like theropod (Dinosauria: Tetanurae) in Australia: support for faunal exchange across eastern and western Gondwana in the Mid-Cretaceous. *Proceedings of the Royal Society B* 275: 2085-2093.
- Soto M & Perea D. 2008. A ceratosaurid (Dinosauria, Theropoda) from the Late Jurassic-Early Cretaceous of Uruguay. *Journal of Vertebrate Paleontology* 28: 439-444.
- Starck D. 1979. *Vergleichende Anatomie der Wirbeltier auf evolutionsbiologischer Grundlage. Bd. 2: Das Skeletsystem. Allgemeines, Skeletsubstanzen, Skelet der Wirbeltiere einschließlich Lokomotionstypen*. Springer-Verlag, Berlin.

- Stecher R. 2008. A new Triassic pterosaur from Switzerland (Central Austroalpine, Grisons), *Raeticodactylus filisurensis* gen. et sp. nov. *Swiss Journal of Geosciences* 101: 185-201.
- Stein K, Csiki Z, Rogers KC, Weishampel DB, Redelstorff R, Carballido JL & Sander PM. 2010. Small body size and extreme cortical bone remodeling indicate phyletic dwarfism in *Magyarosaurus dacus* (Sauropoda: Titanosauria). *Proceedings of the National Academy of Sciences, U.S.A.* 107: 9258-9263.
- Stone JR. 2003. Mapping cladograms into morphospaces. *Acta Zoologica (Stockholm)* 84: 63-68.
- Stromer E. 1934. Die Zähne des *Compsognathus* und Bemerkungen über das Gebiß der Theropoda. *Centralblatt für Mineralogie, Geologie und Paläontologie, B* 1934: 74-85.
- Sudhaus W & Rehfeld K. 1992. *Einführung in die Phylogenetik und Systematik*. Gustav Fischer Verlag, Stuttgart.
- Sues H-D, Reisz RR, Hinić S & Raath MA. 2004. On the skull of *Massospondylus carinatus* Owen, 1854 (Dinosauria: Sauropodomorpha) from the Elliot and Clarens Formations (Lower Jurassic) of South Africa. *Annals of Carnegie Museum* 73: 239-257.
- Sues H-D, Nesbitt SJ, Berman D & Henrici AC. 2011. A late-surviving basal theropod dinosaur from the latest Triassic of North America. *Proceedings of the Royal Society B* 278: 3459-3464.
- Swafford DL. 2003. *PAUP**. *Phylogenetic analysis using parsimony (* and other methods)*. Version 4. Sinauer Associates, Sunderland, Massachusetts.
- <http://paup.csit.fsu.edu/>

- Tatarinov LP. 1960. [Discovery of pseudosuchians in the Upper Permian of the USSR]. *Paleontologicheskii Zhurnal* 1960: 74-80. [in Russian]
- Thompson HS. 1988. *Generation of swine. Tales of shame and degradation in the '80s*. Simon & Schuster, Inc., New York.
- Tischlinger H. 2002. Der Eichstätter *Archaeopteryx* im langwelligen UV-Licht. *Archaeopteryx* 20: 21-38.
- Tischlinger H. 2005a. Neue Informationen zum Berliner Exemplar von *Archaeopteryx lithographica* H.v.Meyer 1861. *Archaeopteryx* 23: 33-50.
- Tischlinger H. 2005b. Ultraviolet light investigations of fossils from the Upper Jurassic plattenkalks of Southern Frankonia. *Zitteliana B* 26: 26.
- Tischlinger H & Unwin DM. 2004. UV-Untersuchungen des Berliner Exemplars von *Archaeopteryx lithographica* H. v. Meyer 1861 und der isolierten *Archaeopteryx*-Feder. *Archaeopteryx* 22: 17-50.
- Tischlinger H & Frey E. 2010. Multilayered is not enough! New soft tissue structures in the *Rhamphorhynchus* flight membrane. *Acta Geoscientia Sinica* 31: 64.
- Tomkins JL, LeBas NR, Witton MP, Martill DM & Humphries S. 2010. Positive allometry and the prehistory of sexual selection. *American Naturalist* 176: 141-148.
- Trutnau L. 1994. *Krokodile*. Westarp Wissenschaften, Magdeburg.
- Tsuihiji T, Watabe M, Tsogtbaatar K, Tsubamoto T, Barsbold R, Suzuki S, Lee AH, Ridgely RC, Kawahara Y & Witmer LM. 2011. Cranial osteology of a juvenile specimens of *Tarbosaurus bataar* (Theropoda, Tyrannosauridae) from the Nemegt Formation (Upper Cretaceous) of Bugin Tsav, Mongolia. *Journal of Vertebrate Paleontology* 31: 497-517.
- Tumarkin-Deratzian AR. 2009. Evaluation of long bone surface textures as ontogenetic indicators in centrosaurine ceratopsids. *The Anatomical Record* 292: 1485-1500.

- Tumarkin-Deratzian AR, Vann DR & Dodson P. 2006. Bone surface texture as an ontogenetic indicator in long bones of the Canada goose *Branta canadensis* (Anseriformes: Anatidae). *Zoological Journal of the Linnean Society* 148: 133-168.
- Turner AH, Pol D, Clarke JA, Erickson GM & Norell MA. 2007. A basal dromaeosaurid and size evolution preceding avian flight. *Science* 317: 1378-1381.
- Turner AH, Makovicky PJ & Norell MA. 2012. A review of dromaeosaurid systematics and paravian phylogeny. *Bulletin of the American Museum of Natural History* 371: 1-206.
- Tykoski RS. 1998. *The osteology of Syntarsus kayentakatae and its implications for ceratosaurid phylogeny*. Master thesis, The University of Texas, Austin.
- Tykoski RS. 2005. *Anatomy, ontogeny, and phylogeny of Coelophysoid theropods*. PhD thesis, The University of Texas, Austin.
- Unwin DM. 2006. *The pterosaurs from deep time*. Pi Press, New York.
- van der Lubbe T, Richter U & Knötschke N. 2009. Velociraptorine dromaeosaurid teeth from the Kimmeridgian (Late Jurassic) of Germany. *Acta Palaeontologica Polonica* 54: 401-408.
- van Drongelen W & Dullemeijer P. 1982. The feeding apparatus of *Caiman crocodilus*; a functional–morphological study. *Anatomischer Anzeiger* 151: 337-366.
- Varricchio DJ. 1997. Growth and Embryology. In: Currie PJ & Padian K (eds). *Encyclopedia of Dinosaurs*. Academic Press, San Diego: 282-288.
- Vasconcelos WR, Hrbek T, Da Silveira R, de Thoisy B, Marioni B & Farias IP. 2006. Population genetic analysis of *Caiman crocodilus* (Linnaeus, 1758) from South America. *Genetics and Molecular Biology* 29: 220-230.

- Verdade LM. 2000. Regression equations between body and head measurements in the broad-snouted Caiman (*Caiman latirostris*). *Revista Brasileira de Biologia* 60: 469-482.
- Verdade LM. 2003. Cranial sexual dimorphism in captive adult broad-snouted caiman (*Caiman latirostris*). *Amphibia-Reptilia* 24: 92-99.
- Villamarín-Jurado F & Suárez E. 2007. Nesting of the black caiman (*Melanosuchus niger*) in northeastern Ecuador. *Journal of Herpetology* 41: 164-167.
- Villier L & Eble GJ. 2004. Assessing the robustness of disparity estimates: the impact of morphometric scheme, temporal scale, and taxonomic level in spatangoid echinoids. *Paleobiology* 30: 652-665.
- Wagner GP & Gauthier JA. 1999. 1,2,3 = 2,3,4: A solution to the problem of the homology of the digits in the avian hand. *Proceedings of the National Academy of Sciences, U.S.A.* 96: 5111-5116.
- Walker AD. 1990. A revision of *Sphenosuchus acutus* Haughton, a crocodylomorph reptile from the Elliot Formation (late Triassic or early Jurassic) of South Africa. *Philosophical Transactions of the Royal Society of London, Series B* 330: 1-120.
- Wang X, Zhou Z, Zhang F & Xu X. 2002. A nearly completely articulated rhamphorhynchoid pterosaur with exceptionally well-preserved wing membranes and “hair” from Inner Mongolia, northeast China. *Chinese Science Bulletin* 47: 226-230.
- Wang X, Kellner AWA, Zhou Z & Campos D de A. 2005. Pterosaur diversity and faunal turnover in Cretaceous terrestrial ecosystems in China. *Nature* 437: 875-879.
- Webb GJW & Messel H. 1978. Morphometric analysis of *Crocodylus porosus* from the north coast of Arnhem Land, northern Australia. *Australian Journal of Zoology* 26: 1-27.

- Webb GJW, Hollis GJ & Manolis SC. 1991. Feeding, growth, and food conversion rates of wild juvenile saltwater crocodiles (*Crocodylus porosus*). *Journal of Herpetology* 25: 462-473.
- Weishampel DB. 1981. Acoustic analyses of potential vocalization in lambeosaurine dinosaurs (Reptilia: Ornithischia). *Paleobiology* 7: 252-261.
- Weishampel DB. 1984. Evolution of jaw mechanisms in ornithopod dinosaurs. *Advances in Anatomy, Embryology and Cell Biology* 87: 1-110.
- Weishampel DB & Chapman RE. 1990. Morphometric study of *Plateosaurus* from Trossingen (Baden-Württemberg, Federal Republic of Germany). In: Carpenter K & Currie PJ (eds). *Dinosaur systematics: approaches and perspectives*. Cambridge University Press, Cambridge: 43-51.
- Weishampel DB, Dodson P & Osmólska H. 2004. *The Dinosauria*. University of California Press, Berkeley.
- Wellnhofer P. 1970. Die Pterodactyloidea (Pterosauria) der Oberjura-Plattenkalke Süddeutschlands. *Bayerische Akademie der Wissenschaften, Mathematisch-Naturwissenschaftliche Klasse, Abhandlungen* 141: 1-155.
- Wellnhofer P. 1975. Die Rhamphorhynchoidea (Pterosauria) der Oberjura-Plattenkalke Süddeutschlands. *Palaeontographica Abt. A* 148: 1-185.
- Wellnhofer P. 1978. *Pterosauria*. Gustav Fischer Verlag, Stuttgart.
- Wellnhofer P. 1987. New crested pterosaurs from the Lower Cretaceous of Brazil. *Mitteilungen der Bayerischen Staatssammlung für Paläontologie und historischen Geologie* 27: 175-186.
- Wellnhofer P. 1991. *The illustrated encyclopedia of pterosaurs*. Salamander Books Ltd., London.

- Wellnhofer P. 2008. *Archaeopteryx. Der Urvogel von Solnhofen*. Verlag Dr. Friedrich Pfeil, München.
- Wellnhofer P & Kellner AWA. 1991. The skull of *Tapejara wellnhoferi* Kellner (Reptilia, Pterosauria) from the Lower Cretaceous Santana Formation of the Araripe Basin, Northeastern Brazil. *Mitteilungen der Bayerischen Staatssammlung für Paläontologie und historischen Geologie* 31: 89-106.
- Westheide W & Rieger R. 2004. *Spezielle Zoologie. Teil 2: Wirbel- oder Schädeltiere*. Spektrum Akademischer Verlag, Heidelberg.
- Whitlock JA, Wilson JA & Lamanna MC. 2010. Description of a nearly complete juvenile skull of *Diplodocus* (Sauropoda: Diplodocoidea) from the Late Jurassic of North America. *Journal of Vertebrate Paleontology* 30: 442-457.
- Widelitz RB, Jiang T, Lu J & Chuong C. 2000. β -catenin in epithelial morphogenesis: Conversion of part of avian foot scales into feather buds with a mutated β -Catenin. *Developmental Biology* 219: 98-114.
- Wiesemüller B, Rothe H & Henke W. 2003. *Phylogenetische Systematik*. Springer-Verlag, Berlin.
- Wild R. 1984. Flugsaurier aus der Obertrias von Italien. *Naturwissenschaften* 71: 1-11.
- Wilkinson MT, Unwin DM & Ellington CP. 2006. High lift function of the pteroid bone and forewing of pterosaurs. *Proceedings of the Royal Society B* 273: 119-126.
- Wilkinson PM & Rhodes WE. 1997. Growth rates of American alligators in coastal South Carolina. *Journal of Wildlife Management* 61: 397-402.
- Wills MA. 1998. Crustacean disparity through the Phanerozoic: comparing morphological and stratigraphic data. *Biological Journal of Linnean Society* 65: 455-500.

- Wills MA, Briggs DEG & Fortey RA. 1994. Disparity as an evolutionary index: a comparison of Cambrian and Recent arthropods. *Paleobiology* 20: 93-130.
- Wilson JA. 2002. Sauropod dinosaur phylogeny: critique and cladistic analysis. *Zoological Journal of the Linnean Society* 136: 217-276.
- Wilson JA & Sereno PC. 1998. Early evolution and higher-level phylogeny of sauropod dinosaurs. *Society of Vertebrate Paleontology Memoir* 5: 1-68.
- Witmer LM. 1995. The Extant Phylogenetic Bracket and the importance of reconstructing soft tissues in fossils. In: Thomason JJ (ed). *Functional morphology in vertebrate paleontology*. Cambridge University Press, Cambridge: 19-33.
- Witmer LM. 1997. The evolution of the antorbital cavity of archosaurs: a study in soft-tissue reconstruction in the fossil record with an analysis of the function of pneumaticity. *Memoirs of the Society of Vertebrate Paleontology* 17: 1-73.
- Witmer LM. 2009. Fuzzy origins for feathers. *Nature* 458: 293-295.
- Witton MP. 2008. A new approach to determining pterosaur body mass and its implications for pterosaur flight. *Zitteliana B* 28: 143-158.
- Witton MP & Naish D. 2008. A reappraisal of azhdarchid pterosaur functional morphology and paleoecology. *PLoS ONE* 3: e2271.
- Witton MP & Habib MB. 2010. On the size and flight diversity of giant pterosaurs, the use of birds as pterosaur analogues and comments on the pterosaur flightlessness. *PLoS ONE* 5: e13982.
- Witzel U & Preuschoft H. 2005. Finite-element model construction for the virtual synthesis of the skulls in vertebrates: case study of *Diplodocus*. *The Anatomical Record* 283A: 391-401.
- Witzel U, Mannhardt J, Goessling R, Micheeli P & Preuschoft, H. 2011. Finite element analyses and virtual syntheses of biological structures and their application to

- sauropod skulls. In: Klein N, Remes K, Gee GT & Sander PM (eds). *Biology of the sauropod dinosaurs: understanding the life of giants*. Indiana University Press, Bloomington: 171-181.
- Wu P, Jiang T, Suksaweang S, Widelitz RB & Chuong C. 2004. Molecular shaping of the beak. *Science* 305: 1465-1466.
- Wu P, Jiang T, Shen J, Widelitz RB & Chuong C. 2006. Morphoregulation of avian beaks: comparative mapping of growth zone activities and morphological evolution. *Developmental Dynamics* 235: 1400-1412.
- Wu XB, Xue H, Wu LS, Zhu JL & Wang RP. 2006. Regression analysis between body and head measurements of Chinese alligators (*Alligator sinensis*) in captive population. *Animal Biodiversity and Conservation* 29: 65-71.
- Wu X & Chatterjee S. 1993. *Dibothrosuchus elaphros*, a crocodylomorph from the Lower Jurassic of China and the phylogeny of the Sphenosuchina. *Journal of Vertebrate Paleontology* 13: 58-89.
- Xing L, Peng G & Shu C. 2008. Stegosaurian skin impressions from the Upper Jurassic Shangshaximiao Formation, Zigong, Sichuan, China: A new observation. *Geological Bulletin of China* 27: 1049-1053.
- Xu X & Wu X. 2001. Cranial morphology of *Sinornithosaurus millenii* Xu et al. 1999 (Dinosauria: Theropoda: Dromaeosauridae) from the Yixian Formation of Liaoning, China. *Canadian Journal of Earth Sciences* 38: 1739-1752.
- Xu X & Guo Y. 2009. The origin and early evolution of feathers: insights from recent paleontological and neontological data. *Vertebrata Palasiatica* 47: 311-329.
- Xu X, Norell MA, Kuang X, Wang X, Zhao Q & Jia C. 2004. Basal tyrannosauroids from China and evidence for protofeathers in tyrannosauroids. *Nature* 431: 680-684.

- Xu X, Clark JM, Forster CA, Norell MA, Erickson GM, Eberth DA, Jia C & Zhao Q. 2006. A basal tyrannosauroid dinosaur from the Late Jurassic of China. *Nature* 439: 715-718.
- Xu X, Clark JM, Mo J, Choiniere J, Forster CA, Erickson GM, Hone DWE, Sullivan C, Eberth DA, Nesbitt S, Zhao Q, Hernandez R, Jia C, Han F & Guo Y. 2009a. A Jurassic ceratosaur from China helps clarify avian digital homologies. *Nature* 459: 940-944.
- Xu X, Zhao Q, Norell MA, Sullivan C, Hone D, Erickson GM, Wang X, Han F & Guo Y. 2009b. A new feathered maniraptoran dinosaur fossil that fills a morphological gap in avian origin. *Chinese Science Bulletin* 54: 430-435.
- Xu X, Zheng X & You H. 2010. Exceptional dinosaur fossils show ontogenetic development of early feathers. *Nature* 464: 1338-1341.
- Xu X, You H, Du K & Han F. 2011. An *Archaeopteryx*-like theropod from China and the origin of Avialae. *Nature* 475: 465-470.
- Xu X, Wang K, Zhang K, Ma Q, Xing L, Sullivan C, Hu D, Cheng S & Wang S. 2012. A gigantic feathered dinosaur from the Lower Cretaceous of China. *Nature* 484: 92-95.
- Yates A. 2003. The species taxonomy of the sauropodomorph dinosaurs from the Löwenstein Formation (Norian, Late Triassic) of Germany. *Palaeontology* 46: 317-337.
- Yates A. 2007. The first complete skull of the Triassic dinosaur *Melanorosaurus* Haughton (Sauropodomorpha: Anchisauria). *Special Papers in Palaeontology* 77: 9-55.

- Yates A. 2012. Basal Sauropodomorpha: the “prosauropods.” In: Brett-Surman MK, Holtz TR Jr & Farlow JO (eds). *The complete dinosaur*. Indiana University Press, Bloomington: 425-444.
- You H, Lamanna MC, Harris JD, Chiappe LM, O'Connor JK, Ji S, Lü J, Yuan C, Li D, Zhang X, Lacovara KJ, Dodson P & Ji, Q. 2006. A nearly modern amphibious bird from the Early Cretaceous of northwestern China. *Science* 312: 1640-1643.
- Young MT & Larvan MD. 2010. Macroevolutionary trends in the skull of sauropodomorph dinosaurs - the largest terrestrial animals to have ever lived. In: Elewa AMT (ed). *Morphometrics for non-morphometricans* Springer-Verlag, Berlin: 259-269.
- Young MT, Brusatte SL, Ruta M & Andrade MB. 2010. The evolution of Metriorhynchoidea (Mesoeucrocodylia, Thalattosuchia): an integrated approach using geometric morphometrics, analysis of disparity, and biomechanics. *Zoological Journal of the Linnean Society* 158: 801-859.
- Zanno LE. 2010. A taxonomic and phylogenetic re-evaluation of Therizinosauria (Dinosauria: Maniraptora). *Journal of Systematic Palaeontology* 8: 503-543.
- Zanno LE & Makovicky PJ. 2011. Herbivorous ecomorphology and specialization patterns in theropod dinosaur evolution. *Proceedings of the National Academy of Sciences, U.S.A.* 108: 232-237.
- Zeiss A. 1977. Jurassic stratigraphy of Franconia. *Stuttgarter Beiträge zur Naturkunde - Serie B* 31: 1-32.
- Zelditch ML, Swiderski DL, Sheets HD & Fink WL. 2004. *Geometric morphometrics for biologists: a primer*. Elsevier Academic Press, San Diego.
- Zhao X & Currie PJ. 1993. A large crested theropod from the Jurassic of Xinjiang, People's Republic of China. *Canadian Journal of Earth Sciences* 30: 2027-2036.

- Zhang F, Zhou Z, Xu X, Wang X & Sullivan C. 2008. A bizarre Jurassic maniraptoran from China with elongate ribbon-like feathers. *Nature* 455: 1105-1108.
- Zheng X, You H, Xu X & Dong Z. 2009. An Early Cretaceous heterodontosaurid dinosaur with filamentous integumentary structures. *Nature* 458: 333-336.
- Zhong Z. 1996. *Cranial anatomy of Shunosaurus and Camarasaurus (Dinosauria: Sauropoda) and the phylogeny of Sauropoda*. PhD thesis, Texas Tech University, Lubbock.
- Zhou Z. 2004. The origin and early evolution of birds: discoveries, disputes, and perspectives from fossil evidence. *Naturwissenschaften* 91: 455-471.
- Zhou Z & Zhang F. 2003. Anatomy of the primitive bird *Sapeornis chaoyangensis* from the Early Cretaceous of Liaoning, China. *Canadian Journal of Earth Sciences* 40: 731-747.
- Zhou Z & Zhang F. 2004. A precocial avian embryo from the Lower Cretaceous of China. *Science* 306: 653.
- Zhou Z, Wang X, Zhang F & Xu X. 2000. Important features of *Caudipteryx* - Evidence from two nearly complete new specimens. *Vertebrata Palasiatica* 38: 241-254.
- Zhou Z, Clarke J, Zhang Z & Wings O. 2004. Gastroliths in *Yanornis*: an indication of the earliest radical diet-switching and gizzard plasticity in the lineage leading to living birds? *Naturwissenschaften* 91: 571-574.
- Ziegler T & Olbort S. 2007. Genital structures and sex identification in crocodiles. *Crocodile Specialist Group Newsletter* 26: 16-17.
- Zusi RL. 1993. Patterns of diversity in the avian skull. In: Hanken J & Hall BK (eds). *The skull. Vol. 2. Patterns of structural and systematic diversity*. University of Chicago Press, Chicago: 391-437.

Curriculum vitae

PERSONAL DATA

- Name: Christian Foth
- Date of birth: 12th November 1984
- Place of birth: Rostock
- Nationality: German
- christian.foth@gmx.net

EDUCATION

PhD thesis: Ontogenetic, macroevolutionary and morphofunctional patterns in archosaur skulls: a morphometric approach (Supervisor: PD Dr. Oliver Rauhut, Bayerische Staatssammlung für Paläontologie und Geologie).

since 01/2011 PhD program Evolution, Ecology and Systematics at the Ludwig-Maximilians-University of Munich

since 04/2010 PhD study of Palaeontology at the Ludwig-Maximilians-University of Munich

Diploma thesis: Die Morphologie des Erstlingsgefieders ausgewählter Vogeltaxa unter Berücksichtigung der Phylogenie (The morphology of neoptile feathers from subset bird taxa under regard of their phylogeny), 183 p. (Supervisor/reviewer: Prof. Stefan Richter, Allgemeine und Spezielle Zoologie, University of Rostock; Dr. Gerald Mayr, Forschungsinstitut Senckenberg, Frankfurt).

10/2004-12/2009 study of Biology at the University of Rostock, with final degree
06/2004 A level at the Käthe-Kollwitz-Gymnasium, Rostock

CAREER HISTORY

- 01/2011- researcher in the DFG project: Macroevolutionary patterns in the evolution of the skull in theropod dinosaurs: a morphometric approach (PD Dr. Oliver Rauhut, Bayerische Staatssammlung für Paläontologie und Geologie)
- 08/2011-10/2011 researcher in the DFG project: The early evolution of the Neopterygii (Dr. Adriana López-Arbarello, Bayerische Staatssammlung für Paläontologie und Geologie)
- 03/2011-07/2011 researcher in the DFG project: Middle to Late Jurassic archosaurs from Chubut Province, Argentinean Patagonia and Jurassic archosaurs radiation in the southern hemisphere (PD Dr. Oliver Rauhut, Bayerische Staatssammlung für Paläontologie und Geologie)
- 09/2010-02/2011 researcher in the DFG project: Saurischian dinosaurs from the Elliot Formation, South Africa (PD Dr. Oliver Rauhut, Bayerische Staatssammlung für Paläontologie und Geologie)
- 11/2009-07/2010 student helper at the Max Planck Institute for Demographic Research, Rostock. Working group: Evolutionary Biodemography (Dr. Alexander Scheuerlein)
- 2007 volunteer helper for the special exhibition “Evolution der Vögel” (Evolution of birds) by the Zoological Collection of the University of Rostock
- 2005-2008 assistance at zoological practises at the University of Rostock

GRANTS

- 06/2007-12/2009 scholarship of the Studienstiftung des deutschen Volkes (“German National Merit Foundation”)
- 04/2008 Travel grant of the Studienstiftung des deutschen Volkes (“German National Merit Foundation”) for the field work in China

FIELD WORK

02/2011	Cerro Condor, Chubut Province, Argentina (Dr. Oliver Rauhut, ten days)
11-12/2010	Cerro Condor, Chubut Province, Argentina (Dr. Oliver Rauhut, three weeks)
04/2008	Turpan Basin, Xinjiang, China (Dr. Oliver Wings, four weeks)
09/2005	Münchehagen, Germany (Dr. Annette Richter, one week)

RESEARCH INTERESTS

- Archosaur evolution
- Evolution and morphology of vertebrate integuments
- Ontogeny and life history of reptiles

SOFTWARE EXPERIENCES

- Cladistics: TNT, Mesquite
- Geometric morphometrics: Tps, MorphoJ, Morphologika, Landmark
- Statistics: PAST, R (basic knowledge)
- Image processing and 3D reconstruction: Photoshop, GIMP, CorelDraw, Inkscape, Imaris, VGStudio Max

SCIENTIFIC PUBLICATIONS

- Foth C**, Rauhut OWM. In press. The good, the bad, and the ugly: the influence of skull reconstructions and intraspecific variability in studies of cranial morphometrics in theropods and basal saurischians. *PLoS ONE*.
- Foth C**, Bona P, Desojo JB. In press. Intraspecific variation in the skull morphology of the black caiman *Melanosuchus niger* (Alligatoridae, Caimaninae). *Acta Zoologica*.
- Foth C**, Rauhut OWM. 2013. Macroevolutionary and functional-morphological patterns in theropod skulls: a morphometric approach. *Acta Palaeontologica Polonica* 58: 1-16.
- Butler RJB, Yates AM, Rauhut OWM, **Foth C**. 2013. A pathological tail in a basal sauropodomorph dinosaur from South Africa: Evidence of traumatic amputation? *Journal of Vertebrate Paleontology* 33: 224-228.
- Rauhut OWM, **Foth C**, Tischlinger H, Norell MA. 2012. Exceptionally preserved juvenile megalosauroid theropod dinosaur with filamentous integument from the Late Jurassic of Germany. *Proceedings of the National Academy of Sciences, U.S.A.* 109: 11746-11751.
- Buchwitz M, **Foth C**, Kogan I, Voigt S. 2012. On the use of osteoderm features for a cladistic approach on the internal relationships of the Chroniosuchia (Tetrapoda: Reptiliomorpha). *Palaeontology* 55: 623-640.
- Foth C**, Brusatte SL, Butler, RJ. 2012. Do different disparity proxies converge on a common signal? Insights from the cranial morphometrics and evolutionary history of Pterosauria (Diapsida: Archosauria). *Journal of Evolutionary Biology* 25: 904-915.
- Foth C**. 2012. On the identification of feather structures in stem-line representatives of birds: evidence from fossils and actuopalaeontology. *Paläontologische Zeitschrift* 86: 91-102.
- Foth C**, Kalbe J, Kautz R. 2011. First evidence of Elasmosauridae (Reptilia: Sauropterygia) in an erratic boulder of Campanian age originating from southern Sweden or the adjacent Baltic Sea area. *Zitteliana A* 51: 285-290
- Foth C**. 2011. The morphology of neoptile feathers: ancestral state reconstruction and its phylogenetic implications. *Journal of Morphology* 272: 387-403.
- Foth C**. 2008. Konvergente Entstehung des Fluges bei Amniota und ihre Bedeutung zum Verständnis der Vogelevolution. *Sitzungsberichte der Gesellschaft Naturforschender Freunde zu Berlin* 47: 33-66.

REVIEWS FOR SCIENTIFIC JOURNALS

- Paläontologische Zeitschrift (2)
- PloS ONE (1)

PUBLIC LECTURES

- Foth C.** 2009. Dinosaurier. *Kinder-Campus, Universität Rostock*, 13.05.2009.
- Foth C.** 2009. Konvergente Evolution des Flugs in der Stammlinie der Vögel. *Darwin Colloquium "Evolution of organisms and environment"*, TU Bergakademie Freiberg, 12.-13.06.2009.
- Foth C.** 2008. Dinosaurierjagd in China. *Vorweisung der Zoologischen Sammlung der Universität Rostock*, 03.12.2008.
- Foth C.** 2008. Zur Evolution des Fluges bei terrestrischen Wirbeltieren. *Vorweisung der Zoologischen Sammlung der Universität Rostock*, 02.07.2008.
- Foth C.** 2006. Über die Biologie der Tyrannosauroida. *Vorweisung der Zoologischen Sammlung der Universität Rostock*, 08.11.2006.

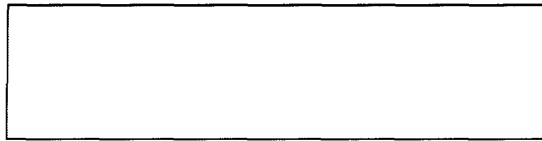
PUBLISHED ABSTRACTS

- Foth C**, Bona P, Desojo JB. 2013. Intraspecific variation in the skull morphology of the black caiman *Melanosuchus niger* (Alligatoridae, Caimaninae). *10th International Congress of Vertebrate Morphology*, 08-12 July 2013, Barcelona, *Anatomical Record* 296, *Special Feature*: 250.
- Rauhut OWM, **Foth C.** 2013. A new look for an old bird: new observations on the morphology of *Archaeopteryx*. *10th International Congress of Vertebrate Morphology*, 08-12 July 2013, Barcelona, *Anatomical Record* 296, *Special Feature*: 235.
- Foth C**, Brusatte S, Butler, R. 2012. Cranial morphometrics, disparity and evolutionary history of Pterosauria (Diapsida: Archosauria). *72nd Annual Meeting of the Society of Vertebrate Paleontology*, 17-20 October 2012, Raleigh, *Journal of Vertebrate Paleontology*, *Program and Abstracts*, 2012: 96.
- Hübner T, **Foth C**, Heinrich W-D. 2012. Reappraisal of the Upper Jurassic *Dysalotosaurus* locality 'Ig/WJ' at Tendaguru, based on historic, taphonomic, and demographic data. *Centenary Meeting of the Paläontologische Gesellschaft*, 24-29 September 2012, Berlin, *Terra Nostra* 2012 (3): 83-84.

- Foth C**, Yates AM, Rauhut OWM, Butler RJ. 2012. A pathological tail in a basal sauropodomorph dinosaur from South Africa. *Centenary Meeting of the Paläontologische Gesellschaft*, 24-29 September 2012, Berlin, *Terra Nostra* 2012 (3): 56-57.
- Foth C**. 2012. The influence of taphonomy on fossil body plumages and the identification of feather structures in stem-line representatives of birds. *10th Annual Meeting of the European Association of Vertebrate Palaeontologists*, 19-24 June 2012, Teruel, *Fundamental* 20: 77-79.
- Rauhut OWM, **Foth C**. 2011. New information on Late Jurassic theropod dinosaurs from Southern Germany. *IV Congress of Latin-American Vertebrate Paleontology*, 21-24 September 2011, San Juan, *Ameghiniana* 48, Suplemento: R120-R121.
- Foth C**, Scheuerlein A. 2010. When do dinosaurs become mature? - A case study on *Psittacosaurus* from the Lower Cretaceous in China. *80. Jahrestagung der Paläontologischen Gesellschaft*, 05-08 October 2010, München, *Zitteliana B* 29: 37.
- Foth C**, Kalbe J, Kautz R. 2010. First evidence of an Elasmosauridae (Reptilia: Sauropterygia) in a Geschiebe from the Campanian (Upper Cretaceous) of South Scandinavia. *80. Jahrestagung der Paläontologischen Gesellschaft*, 05-08 October 2010, München, *Zitteliana B* 29: 36.
- Foth C**. 2009. The morphology of neoptile feathers in extant birds - implications for feather evolution in theropod dinosaurs. *79. Jahrestagung der Paläontologischen Gesellschaft*, 05-07 October 2009, Bonn, *Terra Nostra* 2009 (3): 34.

PROFESSIONAL ASSOCIATIONS

- Society of Vertebrate Paleontology
- European Association of Vertebrate Palaeontology
- Verein der Freunde und Förderer der Zoologischen Sammlung Rostock
- Deutsche Zoologische Gesellschaft (German Zoological Society)
- Paläontologische Gesellschaft (German Palaeontological Society)



Eidesstattliche Versicherung

Ich versichere hiermit an Eides statt, dass die Dissertation von mir selbstständig, ohne Beihilfe angefertigt worden ist.

München, den 22.07.2013

(Unterschrift)

Erklärung

Hiermit erkläre ich, dass die Dissertation, ganz oder in Teilen, noch keiner anderen Promotionskommission vorgelegt worden ist.

München, den 22.07.2013

(Unterschrift)

Erklärung

Hiermit erkläre ich, dass ich mich anderweitig einer Doktorprüfung ohne Erfolg **nicht** unterzogen habe.

München, den 22.07.2013

(Unterschrift)

Appendix

of

Ontogenetic, macroevolutionary and morphofunctional patterns in
archosaur skulls: a morphometric approach

by Christian Foth

Supplementary information of Chapter 1 to Chapter 6

SUPPLEMENTARY INFORMATION OF CHAPTER 1

Introduction and summary of the thesis

1. Taxon sampling
2. Description of Landmarks
3. Methods
4. Phylogeny

1. TAXON SAMPLING

For both geometric morphometric analyses performed in Chapter 1 the skulls of 21 pseudosuchians (19 Crocodylomorpha and two outgroup taxa) and 54 saurischian taxa were sampled. The datasets are mainly based on published reconstructions, except the skulls of the ontogenetic series of *Melanosuchus niger*. The skulls for the later based on photo material (see Chapter 3).

Table S1.1. List of crocodylomorph taxa with data of occurrences (in million years, Ma). **SMF**

Senckenberg Naturmuseum Frankfurt (Germany); **NHMW** Naturhistorisches Museum Wien (Austria); **ZSM** Zoologische Staatssammlung München (Germany). *Ontogenetic series of *Melanosuchus niger*: SMF 30113; SMF 40172; ZSM 13/1911; ZSM 130/1911; ZSM 64/1911; NHMW 2025 (Table S3.1, see supplementary information of Chapter 3).

Taxon	Systematic affinities	Age (Ma)	Sources
<i>Erpetosuchus granti</i>	Pseudosuchia (outgroup)	220.3	Benton & Walker 2002
<i>Gracilisuchus stipanicorum</i>	Pseudosuchia (outgroup)	241.1	Nesbitt 2011
<i>Dibothrosuchus elaphros</i>	basal Crocodylomorpha	193.1	Wu & Chatterjee 1993
<i>Dromicosuchus grallator</i>	basal Crocodylomorpha	220.3	Nesbitt 2011
<i>Sphenosuchus acutus</i>	basal Crocodylomorpha	195.6	Nesbitt 2011
<i>Protosuchus richardsoni</i>	basal Crocodyliformes	199.1	Nesbitt 2011
<i>Anatosuchus minor</i>	Notosuchia	112.5	Sereno & Larsson 2009
<i>Araripesuchus wegneri</i>	Notosuchia	112.5	Sereno & Larsson 2009
<i>Baurusuchus salgadoensis</i>	Notosuchia	88.5	Carvalho et al. 2005
<i>Simosuchus clarki</i>	Notosuchia	68.1	Kley et al. 2010
<i>Dakosaurus andiniensis</i>	Thalattosuchia	145.5	Pol & Gasparini 2009
<i>Pelagosaurus typus</i>	Thalattosuchia	182.5	Pierce & Benton 2006
<i>Hamadasuchus rebouli</i>	Neosuchia	102.7	Larsson & Sues 2007
<i>Kaprosuchus saharicus</i>	Neosuchia	96.6	Sereno & Larsson 2009
<i>Sarcosuchus imperator</i>	Neosuchia	119.5	Sereno et al. 2001
<i>Alligator sinensis</i>	Crocodylia	Recent	Iordansky 1973
<i>Crocodylus thorbjarnarsoni</i>	Crocodylia	2.7	Brochu & Storrs 2012
<i>Gavialis gangeticus</i>	Crocodylia	Recent	Iordansky 1973
* <i>Melanosuchus niger</i>	Crocodylia	Recent	see Chapter 3
<i>Osteolaemus tetraspis</i>	Crocodylia	Recent	Iordansky 1973
<i>Tomistoma schlegelii</i>	Crocodylia	Recent	Iordansky 1973

Table S1.2. List of saurischian taxa with data of occurrences (in million years, Ma). *ontogenetic series (see also taxonomical comments below); **juvenile specimens.

Taxon	Systematic affinities	Age (Ma)	Sources
<i>Herrerasaurus ischigualastensis</i>	basal Saurischia	220.3	Nesbitt 2011
<i>Chuxiongosaurus lufengensis</i>	basal Sauropodomorpha	195.6	Lü et al. 2010b
<i>Eoraptor lunensis</i>	basal Sauropodomorpha	228.3	Martinez et al. 2011
<i>Jingshanosaurus xinwaensis</i>	basal Sauropodomorpha	199.1	Yates 2012
* <i>Massospondylus carinatus</i>	basal Sauropodomorpha	195.6	Gow et al. 1990; Reisz et al. 2010
<i>Melanorosaurus readi</i>	basal Sauropodomorpha	211.6	Yates 2007
<i>Pampadromaeus barberenai</i>	basal Sauropodomorpha	220.3	Cabreira et al. 2011
<i>Plateosaurus engelhardti</i>	basal Sauropodomorpha	208.6	Yates 2003
<i>Unaysaurus tolentinoi</i>	basal Sauropodomorpha	213.6	Leal et al. 2004
<i>Mamenchisaurus youngi</i>	basal Sauropoda	153.4	Ouyang & Ye 2002
<i>Shunosaurus lii</i>	basal Sauropoda	158.6	Zhong 1996
<i>Diplodocus longus</i>	Neosauropoda	150.6	Wilson & Sereno 1998; Whitlock et al. 2010
<i>Abydosaurus mcintoshi</i>	Macronaria	101.3	Chure et al. 2010
* <i>Antarctosaurus wichmannianus</i>	Macronaria	77.1	Gallina & Apesteguía 2011
*Titanosaurid embryo	Macronaria	c. 81.5	Garcia et al. 2010
<i>Camarasaurus lentus</i>	Macronaria	150.6	Wilson & Sereno 1998
<i>Giraffatitan brancai</i>	Macronaria	153.4	Wilson & Sereno 1998
<i>Daemonosaurus chauliodus</i>	basal Theropoda	203.6	Sues et al. 2011
<i>Tawa hallae</i>	basal Theropoda	213.6	Nesbitt 2011
<i>Coelophysis bauri</i>	Coelophysoidea	213.6	Nesbitt 2011
<i>Dilophosaurus wetherilli</i>	Coelophysoidea	189.8	Rauhut 2003a
<i>Syntarsus kayentakatae</i>	Coelophysoidea	189.8	Tykosky 2005
<i>Zupaysaurus rougieri</i>	Coelophysoidea	213.6	modified after Ezcurra 2007
<i>Carnotaurus sastrai</i>	Ceratosauria	77.1	Rauhut 2003a
<i>Ceratosaurus nasicornis</i>	Ceratosauria	153.3	Sampson & Witmer 2007
<i>Limusaurus inextricabilis</i>	Ceratosauria	158.5	Xu et al. 2009a
<i>Majungasaurus crenatissimus</i>	Ceratosauria	68.1	Sampson & Witmer 2007
<i>Monolophosaurus jiangi</i>	basal Tetanurae	163.0	Brusatte et al. 2010b
* <i>Dubreuillosaurus valesdunensis</i>	Megalosauridae	166.2	Allain 2002
* <i>Sciurumimus albersdoerferi</i>	Megalosauridae	153.3	This study
Spinosauridae	Megalosauria	108.1	Rauhut 2003a
<i>Acrocanthosaurus atokensis</i>	Allosauroidae	117.2	Eddy & Clarke 2011
* <i>Allosaurus</i> spp.	Allosauroidae	153.4	Loewen 2009
<i>Sinraptor dongi</i>	Allosauroidae	158.6	Currie & Zhao 1993

Supplementary information of Chapter 1

<i>Alioramus altai</i>	Tyrannosauroida	68.1	Brusatte et al. 2009
<i>Bistahieversor sealeyi</i>	Tyrannosauroida	77.5	Carr & Williamson 2010
<i>Daspletosaurus torosus</i>	Tyrannosauroida	74.5	Holtz 2004
<i>Dilong paradoxus</i>	Tyrannosauroida	126.2	Xu et al. 2004
<i>Gorgosaurus libratus</i>	Tyrannosauroida	77.1	Carr 1999
<i>Guanlong wucaii</i>	Tyrannosauroida	158.5	Xu et al. 2006
* <i>Tarbosaurus baatar</i>	Tyrannosauroida	74.5	Hurum & Sabbath 2003; Tsuihiji et al. 2011
* <i>Tyrannosaurus rex</i>	Tyrannosauroida	74.5	Carr & Williamson 2004
<i>Gallimimus bullatus</i>	Ornithomimosauria	74.5	Makovicky et al. 2004
<i>Garudimimus brevipes</i>	Ornithomimosauria	91.6	Makovicky et al. 2004
<i>Ornithomimus velox</i>	Ornithomimosauria	74.5	Rauhut 2003a
<i>Compsognathus longipes</i>	Compsognathidae	148.2	Peyer 2006
<i>Erlikosaurus andrewsi</i>	Therizinosauroida	91.6	Rauhut 2003a
* <i>Citipati osmolskae</i>	Oviraptorosauria	74.5	Osmólska et al. 2004
* <i>Conchoraptor gracilis</i>	Oviraptorosauria	77.1	Osmólska et al. 2004
* <i>Nemegtomaia barsboldi</i>	Oviraptorosauria	68.1	Fanti et al. 2012
* <i>Yulong mini</i>	Oviraptorosauria	82.6	Lü et al. in press
<i>Anchiornis huxleyi</i>	Paraves	159.3	Hu et al. 2009
<i>Archaeopteryx lithographica</i>	Paraves	148.2	Rauhut in press
<i>Bambiraptor feinbergi</i>	Paraves	78.2	Burnham 2004
<i>Sinornithosaurus millenii</i>	Paraves	126.2	Xu & Wu 2001
<i>Tsaagan mangas</i>	Paraves	74.5	Turner et al. 2012
<i>Velociraptor mongoliensis</i>	Paraves	74.5	Turner et al. 2012
** <i>Juravenator starki</i>		153.3	modified after Chiappe & Göhlich 2010
** <i>Scipionyx samniticus</i>		110.5	Dal Sasso & Maganuco 2011

TAXONOMICAL COMMENTS TO THE ONTOGENETIC SERIES USED FOR SAURISCHIA

Not all ontogenetic series used in the analyses for heterochronic patterns in saurischians represent true monospecific series. Due to the incomplete fossil record some series were created artificially by adding skulls of adult species, which are closely related to known juvenile species/specimens. To describe the ontogenetic series in titanosaurids we used

skull reconstruction of titanosaurid embryos, which were found in the locality Auca Mahuevo, Argentina (Upper Neuquén Group, Campanian) (Chiappe et al. 2001). For adult specimen, a skull reconstruction of the titanosaurid *Antarctosaurus* was used, which lived about the same time (Gallina & Apesteguía 2011). However, one has to consider that only the posterior part of the skull of *Antarctosaurus* is present (Gallina & Apesteguía 2011). For Megalosauridae, the juvenile specimen is represented by *Sciurumimus* from the upper Jurassic of southern Germany (see Chapter 6).

Unfortunately, skull material of adult individuals of basal megalosaurids known so far (e.g. *Afrovenator*, *Dubreuillosaurus*, *Eustreptospondylus*, *Torvosaurus*) is usually incomplete. The most complete skull material is known from *Dubreuillosaurus* from Middle Jurassic of France (Allain 2002) and *Eustreptospondylus* from the Middle Jurassic of England (Sadleir et al. 2008). However, in comparison the skull material from *Dubreuillosaurus* is slightly more complete than that of *Eustreptospondylus*. For Oviraptoridae the juvenile species *Yulong mini* from the Upper Cretaceous of China was chosen as juvenile representative of an ontogenetic series. For the adult Oviraptoridae, a consensus shape was calculated *a posteriori* from *Citipati osmolskae*, *Conchoraptor gracilis*, *Nemegtomaia barsboldi* based on the Procrustes coordinates and principal components.

Both *Juravenator* and *Scipionyx* were originally described as juvenile compsognathids (Göhlich & Chiappe 2006; Dal Sasso & Maganuco 2011). The discovery of the juvenile megalosaurid *Sciurumimus* (see Chapter 6) however showed that juvenile individuals of basal tetanurans resemble basal coelurosaurs in their morphology (see Chapter 6). Thus, it is likely that the taxonomic ascertainment of *Juravenator* and *Scipionyx* as compsognathids based simply on juvenile characters. This

has to be tested in future investigations in more detail. Therefore, no skull material from adult species was added to these two juveniles.

2. DESCRIPTION OF LANDMARKS

The skull shape of Crocodylomorpha was captured by 15 homologous landmarks (LM) and 14 homologous semi-landmarks (semi-LM) and that of the Saurischia by 17 homologous landmarks and 32 homologous semi-landmarks. Landmarks and semi-landmarks were plotted on the skull reconstructions / photos with help of the program tpsDig2 (Rohlf 2005). The chosen landmarks are of type 1 (points where two bones meet) and type 2 (points of maximal curvature or extremities) following the terminology of Bookstein (1991).

CROCODYLOMORPHA

- 1 anteroventral corner of the premaxilla
- 2 contact of premaxilla and maxilla along the tooth row
- 3 contact of maxilla and jugal along the ventral margin of the skull
- 4 most posterior point of the quadratojugal
- 5 contact between jugal and postorbital on the posterior margin of the orbit
- 6 contact between jugal and postorbital on the anterior margin of the lateral temporal fenestra
- 7 contact between jugal and quadratojugal on the posteroventral margin of the lateral temporal fenestra
- 8 contact between postorbital and postorbital on the dorsal margin of the lateral temporal fenestra

- 9 contact between postorbital and frontal on the posterodorsal margin of the orbit
- 10 contact between prefrontal and frontal on the anterodorsal margin of the orbit
- 11 contact between squamosal and quadrate on the posterior end of the skull
- 12 contact between lacrimal and jugal on the anteroventral margin of the orbit
- 13-21 nine semi-LMs on the dorsal margin of the skull between LM 1 and LM 11
- 22* contact between maxilla and lacrimal on the dorsal margin of the antorbital fenestra
- 23* most ventral point of the lacrimal on the posterior margin of the antorbital fenestra
- 24* most anterior point of the antorbital fenestra
- 25-27 three semi-LMs on the ventral margin of the maxilla between LM 2 and LM 3
- 28-29 two semi-LMs on the ventral margin of the skull between LM 3 and LM 4

*Landmarks describing the shape of the external antorbital fenestra. In *Crocodylia* and *Sarcosuchus* this skull opening is absent. Thus, for these taxa three landmarks were plotted at the meeting point of lacrimal, jugal and maxilla.

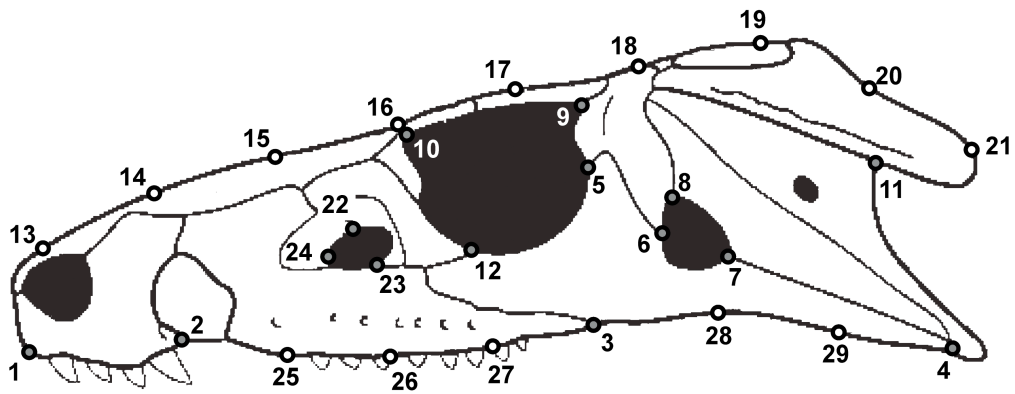


Fig. S1.1. Landmarks and semi-landmarks plotted on the skull reconstruction of *Protosuchus richardsoni* (modified after Nesbitt 2011) used for the crocodylomorph data set. Grey circles represent landmarks and white circles represent semi-landmarks.

SAURISCHIA

- 1 anteroventral corner of the premaxilla
- 2 contact of premaxilla and maxilla along the tooth row
- 3 contact of maxilla and jugal along the ventral margin of the skull
- 4 posteroventral corner of the quadratojugal (postorbital region)
- 5 most ventral point of the lacrimal on the posterior margin of the antorbital fenestra
- 6 contact between maxilla and lacrimal on the dorsal margin of the antorbital fenestra
- 7 contact between lacrimal and jugal on the anteroventral margin of the orbit
- 8 contact between jugal and postorbital on the posterior margin of the orbit
- 9 contact between jugal and postorbital on the anterior margin of the lateral temporal fenestra
- 10 contact between jugal and quadratojugal on the posteroventral margin of the lateral temporal fenestra
- 11 contact between postorbital and frontal on the posterodorsal margin of the orbit
- 12 contact between postorbital and squamosal on the dorsal margin of the lateral temporal fenestra
- 13 anteroventral tip of the squamosal on the posterior margin of the lateral temporal fenestra
- 14 contact of premaxilla and nasal on the dorsal margin of the external naris
- 15 most anteroventral point of the subnarial process of the nasal on the ventral margin of the external naris
- 16-18 three semi-LMs on the ventral margin of the maxilla between LM 2 and LM 3

- 19-20 two semi-LMs on the ventral margin of the skull between LM 3 and LM 4
- 21 one semi-LM on the posterodorsal margin of the antorbital fenestra between LM 5 and LM 6
- 22 dorsal contact between postorbital and squamosal
- 23 anteroventral tip of the squamosal on the posterior margin ventral process
- 24-26 three semi-LMs on the anteroventral margin of the antorbital fenestra between LM 6 and LM 5
- 27-30 four semi-LMs on the anterodorsal margin of the orbit between LM 7 and LM 11
- 31-45 fifteen semi-LMs on the dorsal margin of the skull between LM 1 and LM 23
- 46-47 two semi-LMs on the posterior margin of the orbit between LM 11 and LM 8
- 48 one semi-LM on the anteroventral margin of the lateral temporal fenestra between LM 9 and LM 10
- 49 one semi-LM on the posterodorsal margin of the lateral temporal fenestra between LM 12 and LM 13

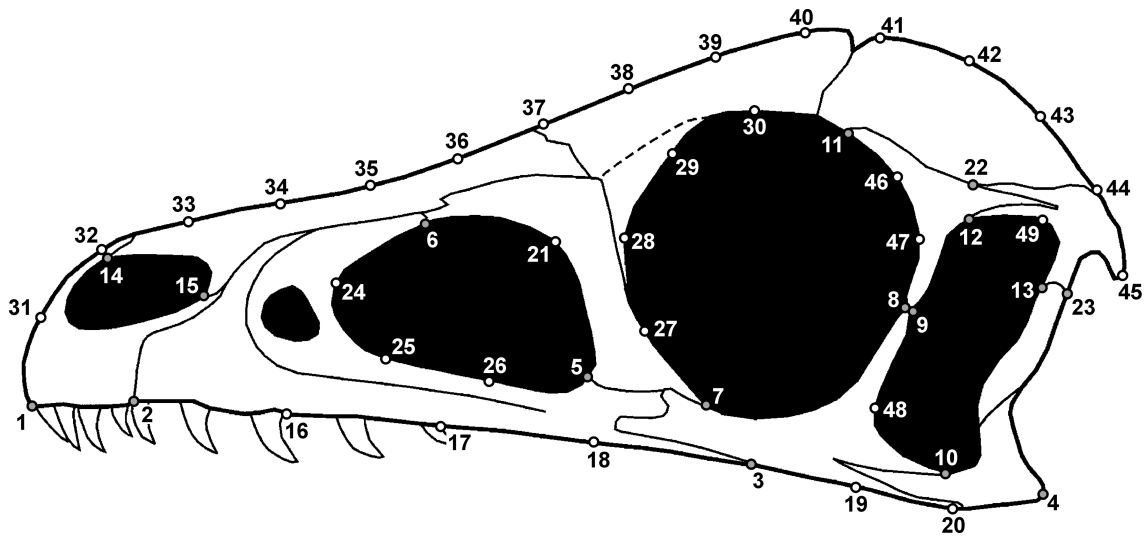


Fig. S1.2. Landmarks and semi-landmarks plotted on the skull reconstruction of *Sciurumimus albersdoerferi* used for the saurischian data set. Grey circles represent landmarks and white circles represent semi-landmarks.

3. METHODS

The methods used of the current analyses are only briefly described. A more detailed description of some of the methods is given in the actual chapters. After plotting the landmark and semi-landmark coordinates both datasets were superimposed separately using Generalized Procrustes Analysis (GPA) in tpsrelw (Rohlf 2003), which minimizes non-shape variation between species, including that caused by size, location, orientation and rotation (Gower 1975; Rohlf & Slice 1990). To minimize the effects of variation due to the arbitrary spacing of the semi-landmarks over the sampled curves, semi-landmarks were slid along their tangent to align with the perpendicular of corresponding landmarks, minimizing the Procrustes distance. Thus, semi-landmarks capture primarily information about the bowing of the sampled curve (Bookstein 1997; Zelditch et al. 2004). Afterwards, the Procrustes coordinates were loaded into MorphoJ.

The Procrustes coordinates of both datasets were subjected to Principal Component Analysis (PCA) in MorphoJ (Klingenberg 2011). This method assimilates data from all Procrustes coordinates and reduces it to a set of Principal components that summarize the skull shape of each sample and describes maximal shape variation within the morphospace (Hammer & Harper 2006). Additionally, the skull shape captured by Procrustes coordinates was tested against centroid size (log-transformed) in MorphoJ.

Similarities between Procrustes shapes between different taxa and ontogenetic stages were estimated by calculating a hierarchic clusters with Ward's method with help of the program PAST 2.17b (Hammer et al. 2001). Here, the clusters are joined by minimizing the increase of within-group variance (Hammer 2009). Additionally, for Saurischia shape similarities were quantified by calculating a matrix with Euclidean distance in PAST. Furthermore, pairwise angles between different ontogenetic trajectories were estimated based on the PC values of the first two axes. For that each ontogenetic trajectory was described as phenotypic change vector $\Delta \vec{y}_i = \vec{y}_{ij} - \vec{y}_{ik}$ with two shape traits (PC 1 and PC 2), in which i stands for a specific ontogeny between two fixed stages, juvenile j and adult k (Collyer & Adam 2007). The difference in direction (=

angle) between the ontogenetic phenotypic change vectors $\Delta \vec{y}_a, \Delta \vec{y}_b$ was calculated

with help of the dot product
$$\cos^{-1}(\Delta \vec{y}_a, \Delta \vec{y}_b) = \frac{\Delta \vec{y}_a \cdot \Delta \vec{y}_b}{|\Delta \vec{y}_a| |\Delta \vec{y}_b|}$$
. Furthermore, the angle

was computed based on Procrustes shape change against centroid size (log-transformed).

To estimate cranial shape changes during evolution all juvenile taxa were excluded from the data set. For that an informal supertree (Butler & Goswami 2008) was created for both Crocodylomorpha and Saurischia (see below). For both phylogenies branch lengths were assigned based on the mid-point age of the existence of taxa (this information was taken from the Paleobiology Database), and zero branch lengths were adjusted by sharing out the time equally between branches (see Ruta et al. 2006; Brusatte et al. 2008; Brusatte 2011). An arbitrary length of 10 Ma was added to the root. The assignment of branch lengths was estimated with help of the software package R (R Development Core Team, 2011) using the APE package (version 2.7-2; Paradis et al. 2004) and a function written by Graeme Lloyd (see <http://www.graemetlloyd.com/methdpf.html>). Afterwards the trees were loaded into MorphoJ and Procrustes coordinates were mapped as continuous characters on the topology (Klingenberg & Gidaszewski 2010). The reconstruction of hypothetical ancestral shapes based on square change parsimony by minimizing the total sum of square changes across the phylogeny (Maddison 1991). Afterwards ontogenetic and evolutionary shape changes were compared. To compare the evolutionary shape changes in Crocodylomorpha with their body size evolution, centroid size of the Procrustes coordinates were mapped with square change parsimony on the respective phylogeny with help of the software package Mesquite 2.72 (Maddison & Maddison 2009).

4. PHYLOGENY

PHYLOGENETIC INTERRELATIONSHIP OF CROCODYLOMORPHA

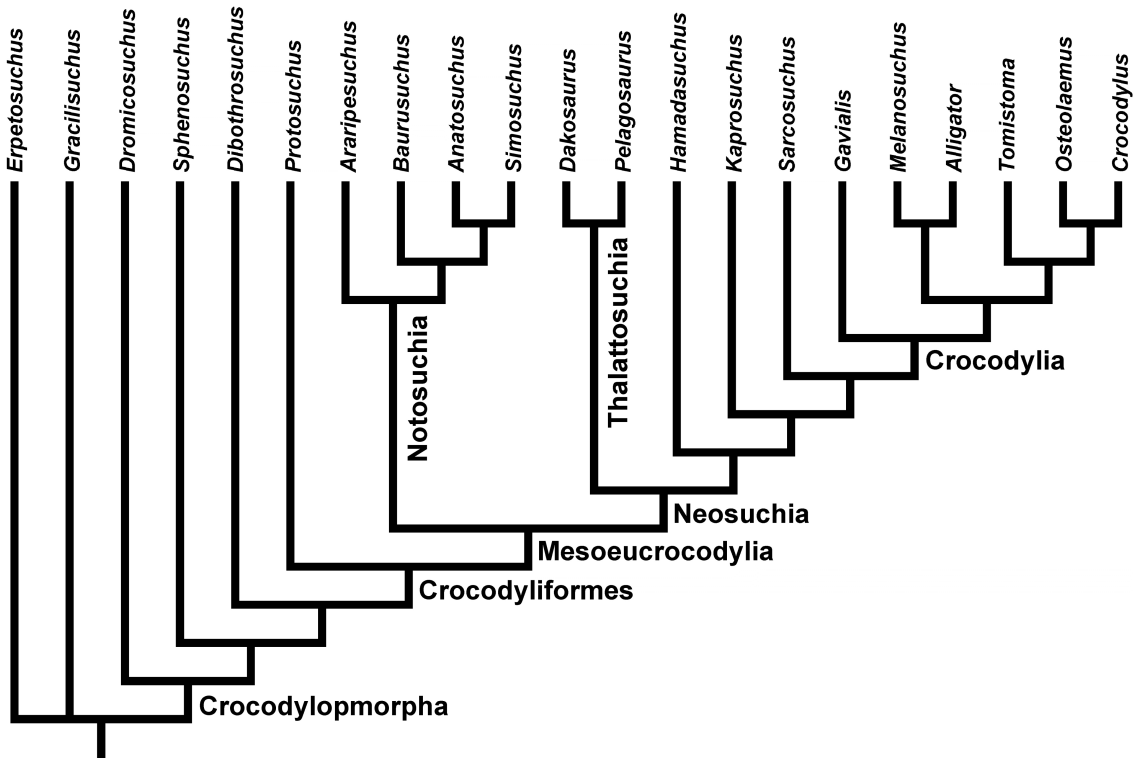


Fig. S1.4. Phylogenetic interrelationship of Crocodylomorpha. The interrelationship of basal Crocodylomorpha based on Nesbitt (2011), in which the phylogenetic position of *Erpetosuchus* follows Nesbitt & Butler (2013). The phylogenetic interrelationship of Crocodyliformes follows Pol & Gasparini (2009) and that of Crocodylia after Brochu et al. (2012). The phylogenetic positions of *Anatosuchus* and *Kaprosuchus* follow Sereno & Larsson (2009).

PHYLOGENETIC INTERRELATIONSHIP OF SAURISCHIA

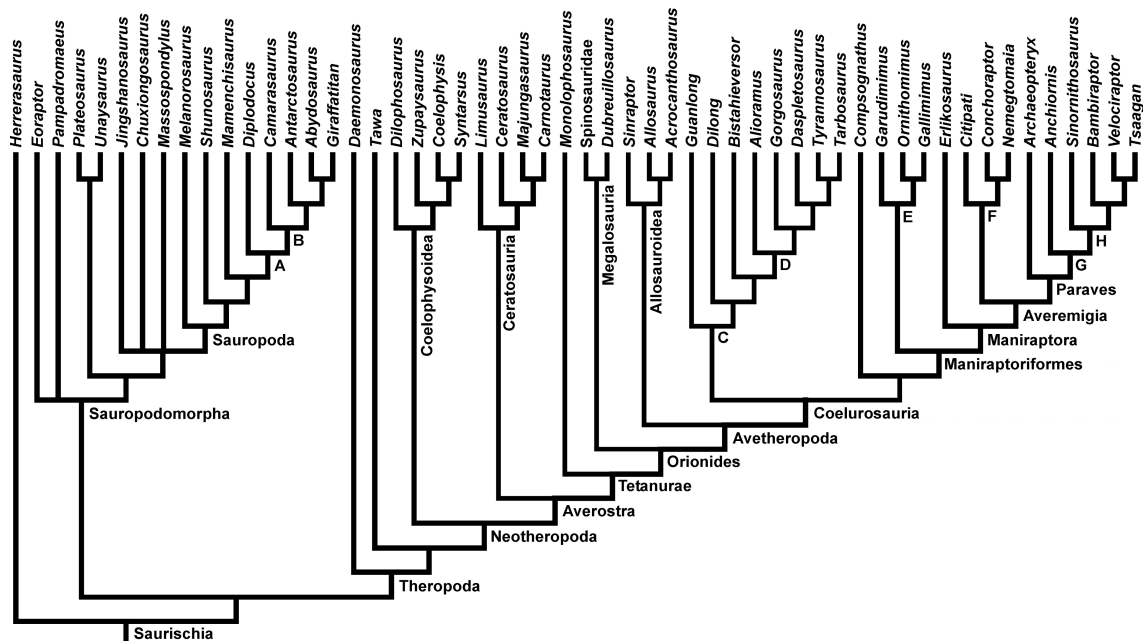


Fig. S1.5. Phylogenetic interrelationship of Crocodylomorpha. **A** Neosauropoda, **B** Macronaria, **C** Tyrannosauroidae, **D** Tyrannosauridae, **E** Ornithomimosauria, **F** Oviraptoridae, **G** Deinonychosauria, **H** Dromaeosauridae. The phylogenetic interrelationship of basal Sauropodomorpha and Herrerasaurus based on Cabreira et al. (2011), in which the phylogenetic position of *Eoraptor* follows Martinez et al. (2011) and that of *Chuxiongosaurus* follows Lü et al. (2010b). The phylogenetic interrelationship of Sauropoda based on Carballido et al. (2011), in which the phylogenetic position of *Abydosaurus* follows Chure et al. (2010). The phylogenetic position of *Tawa* and *Daemonosaurus* within Theropoda follows Sues et al. (2011). The phylogenetic interrelationship of Coelophysoidea based on Ezcurra & Novas (2007) and that of Ceratosauria after Pol & Rauhut (2012). The phylogenetic interrelationship of basal Tetanurae follows Carrano et al. (2012) and that of Coelurosauria follows Turner et al. (2012). The phylogenetic interrelationship of Tyrannosauroidae based on after Brusatte et al. (2010a), in which the phylogenetic position of *Alioramus* based on Thompson (1988).

SUPPLEMENTARY INFORMATION OF CHAPTER 2

The good, the bad, and the ugly: the influence of skull reconstructions and intraspecific variability in studies of cranial morphometrics in theropods and basal saurischians

1. Institutional abbreviations
2. Taxon sampling
3. Description of landmarks
4. Skull shape variation

1. INSTITUTIONAL ABBREVIATIONS

AMNH, American Museum of Natural History, New York; BHI, Black Hills Institute, Hill City; BP, Bernard Price Institute for Palaeontological Research, University of the Witwatersrand, Johannesburg; FMNH, The Field Museum, Chicago; GPIT, Geologisch-Paläontologisches Institut, Tübingen (IFGT Institut für Geowissenschaften, Eberhard-Karls-Universität, Tübingen); IVPP, Institute of Vertebrate Palaeontology and Palaeoanthropology, Beijing; LACM, Los Angeles County Museum, Los Angeles; MB, Museum für Naturkunde, Berlin; MOR, Museum of the Rockies, Bozeman; NM, National Museum, Bloemfontein; NMC, National Museum of Canada, Ottawa; NMMNH, New Mexico Museum of Natural History and Science, Albuquerque; NCSM, North Carolina Museum of Natural Sciences, Raleigh; PIN, Paleontological Institute, Russian Academy of Sciences, Moscow; PVSJ, Museo de Ciencias Naturales, Universidad Nacional de San Juan, San Juan; QMNS, Qatar Museum of Nature and Science; SMA, Sauriermuseum, Aathal; SMNS, Staatliches Museum für Naturkunde Stuttgart, Stuttgart; TMP, Royal Tyrrell Museum of Palaeontology, Drumheller; TTU, Texas Tech University, Lubbock; ULBRA, Museu de Ciências Naturais, Universidade Luterana do Brasil, Canoas; UUVP, Utah Museum of Natural History, Salt Lake City; ZPAL, Institute of Palaeobiology, Polish Academy of Sciences, Warsaw.

2. TAXON SAMPLING

Table S2.1. List of specimens used in the study

Taxon	Collection number	Reference
Allosauroidae + basal Tetanurae		
<i>Acrocanthosaurus atokensis</i>	NCSM 14345	Currie & Carpenter 2000; Eddy & Clarke 2011
<i>Allosaurus</i> spp.	TTU P9269	McClelland 1990
	AMNH 600	Osborn 1903; Molnar et al. 1990
	DINO 11541	Chure 2000
	MOR 693	Rauhut 2003a; Foth & Rauhut, this study
	UUVP 6000	Madsen 1976; Molnar et al. 1990; Holtz et al. 2004; Paul 2002; 2008; Fastovsky & Weishampel 2005; Westheide & Rieger 2009; Foth & Rauhut, this study
	SMA 0005	Foth & Rauhut, this study
	QMNS-FO-456	Foth & Rauhut, this study
<i>Monolophosaurus jiangi</i>	IVPP 84019	Zhao & Currie 1993; Rauhut 2003a; Brusatte et al. 2010b
<i>Sinoraptor dongi</i>	IVPP 10600	Currie & Zhao 1993
Sauropodomorpha + basal Saurischia		
<i>Eoraptor lunensis</i>	PVSJ 512	Sereno et al. 1993; Rauhut 2003a; Langer 2004; Paul 2002; Martinez et al. 2011, Nesbitt 2011
<i>Massospondylus carinatus</i>	BP/I/4934	Gow et al. 1990
	BP/I/5241	Gow et al. 1990
<i>Melanorosaurus</i>	NM QR3314	Yates 2007
<i>Pampadromaeus barberenai</i>	ULBRA-PVT016	Cabreira et al. 2011
<i>Plateosaurus engelhardti</i>	AMNH 6810	Galton 2001
	Composite	Wilson & Sereno 1998;
	GPIT 1	Galton 2001
	MB R. 1937	Galton 2001; Rauhut 2003a
	SMNS 12949	Galton 2001
	SMNS 13200	Galton 2001, Yates 2003; Nesbitt 2011

Taxon	Collection number	Reference
Tyrannosauroidae		
<i>Bistahieversor sealeyi</i>	NMMNH P-27469	Carr & Williamson 2010
<i>Daspletosaurus torosus</i>	NMC 8506	Russell 1970; Molnar 1990; Holtz 2004, Paul 2008
	FMNH PR308	Russell 1970; Molnar et al. 1990; Rauhut 2003a
<i>Gorgosaurus libratus</i>	composite	Carr 1999; Paul 2008
	TMP 91.36.500	Carr et al. 2011
<i>Tarbosaurus bataar</i>	PIN 551-1	Maleev 1974; Paul 2008
	ZPAL MgD-I/4	Hurum & Sabath 2003
<i>Tyrannosaurus rex</i>	AMNH 5027	Osborn 1912; Carpenter 1992; Molnar et al. 1990; Carr & Williamson 2004; Holtz 2004; Paul 2008; 2010
	BHI 3033	Larson 1997
	LACM 23844	Carr & Williamson 2004

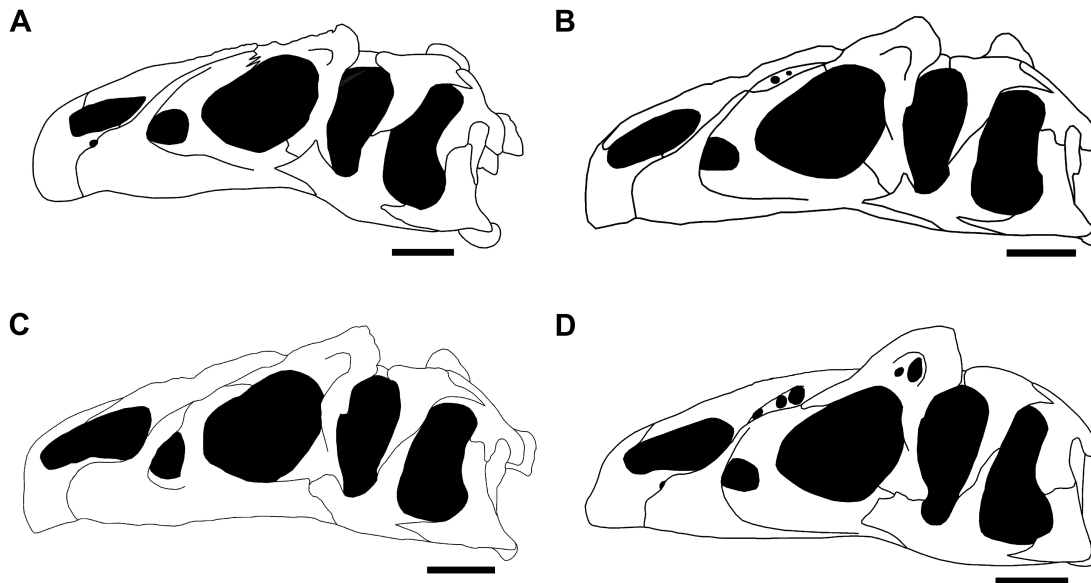


Fig. S2.1. Additional skull reconstructions of some *Allosaurus* specimens used for this study. A:

UUVP 6000. B: MOR 693. C: SMA 0005. D: QMNS-FO-456. Scale bar = 10 cm.

3. DESCRIPTION OF LANDMARKS

Table S2.2. Description of landmarks used for the different dataset.

No	Landmark
1	anteroventral corner of the premaxilla
2	contact of premaxilla and maxilla along the tooth row
3	contact of maxilla and jugal along the ventral margin of the skull
4	contact between jugal and quadratojugal along the ventral margin of the skull
5	posteroventral corner of the quadratojugal
6	contact of premaxilla and nasal along the dorsal margin of the skull
7	contact of premaxilla and nasal along the dorsal margin of the external naris
8	tip of the maxillary process of the premaxilla
9	tip of the maxillary process of the nasal
10	most-anterior point of the antorbital fenestra
11	ventralmost point of the lacrimal along the margin of the antorbital fenestra
12	anteriormost contact of the lacrimal along the dorsal margin of the antorbital fenestra
13	contact between lacrimal and jugal on the orbital margin
14	contact between postorbital and jugal on the orbital margin
15	contact between postorbital and jugal on the margin of the lateral temporal fenestra
16	contact between jugal and quadratojugal on the margin of the lateral temporal fenestra
17	anteroventral tip of the ventral process of the squamosal on the margin of the lateral temporal fenestra
18	ventral contact of postorbital and squamosal on the margin of the lateral temporal fenestra
19	dorsal contact between postorbital and squamosal
20	anteriormost point of the jugal
21	posteriormost point of the postorbital
22	contact between frontal and postorbital on the dorsal margin of the orbit

4. SKULL SHAPE VARIATION

Table S2.3. Variation of different skull reconstructions within basal Saurischia.

	Percentage error			Euclidean distance		
	Median	25 prntil	75 prntil	Median	25 prntil	75 prntil
Plateosaurus SMNS 13200	2.965	2.114	4.152	0.045	0.034	0.070
Plateosaurus SMNS 13200*	3.143	2.163	4.332	0.049	0.040	0.055
Plateosaurus MB.R 1937	2.605	1.220	4.863	0.043	NA	NA
Plateosaurus MB.R 1937*	3.062	1.495	5.337	0.051	0.039	0.056
Plateosaurus	5.978	4.179	8.981	0.063	0.055	0.092
Plateosaurus*	5.466	3.906	7.733	0.071	0.060	0.081
Massospondylus	3.148	1.919	4.369	0.049	NA	NA
Massospondylus*	3.042	2.052	4.920	0.058	0.046	0.074
Eoraptor	2.910	2.363	3.600	0.052	0.037	0.058
Eoraptor*	2.806	2.363	4.382	0.048	0.044	0.056
basal Saurischia	9.471	7.730	11.894	0.090	0.079	0.124
basal Saurischia*	9.181	7.347	11.401	0.103	0.098	0.112
Saurischia	10.437	8.793	12.167	0.098	0.084	0.146
Saurischia*	9.288	7.567	11.136	0.101	0.097	0.110

NA = not available due to small sample size, (*) Randomized dataset.

Table S2.4. Variation of different skull reconstructions within basal Tetanurae

	Percentage error			Euclidean distance		
	Median	25 prentil	75 prentil	Median	25 prentil	75 prentil
Allosaurus MOR 693	1.466	0.483	3.289	0.041	NA	NA
Allosaurus MOR 693*	2.122	1.091	4.076	0.048	0.036	0.078
Allosaurus AMNH 600	0.437	0.161	1.074	0.013	NA	NA
Allosaurus AMNH 600*	0.481	0.306	1.218	0.016	0.013	0.019
Allosaurus UVP 6000	3.271	2.444	4.615	0.034	0.031	0.053
Allosaurus UVP 6000*	3.321	2.479	4.507	0.048	0.041	0.051
Allosaurus	6.209	5.131	8.014	0.071	0.069	0.088
Allosaurus*	5.636	4.842	7.467	0.067	0.064	0.078
Acroncathosaurus	2.309	0.894	4.818	0.034	NA	NA
Acroncathosaurus*	2.595	1.526	4.609	0.039	0.032	0.049
Monolophosaurus	3.057	2.298	5.710	0.036	0.035	0.069
Monolophosaurus*	3.649	2.246	5.916	0.048	0.045	0.066
basal Tetanurae	5.316	4.507	7.301	0.064	0.056	0.086
basal Tetanurae*	6.289	5.040	7.778	0.074	0.069	0.082
Saurischia	10.437	8.793	12.167	0.098	0.084	0.146
Saurischia*	9.288	7.567	11.136	0.101	0.097	0.110

NA = not available due to small sample size, (*) Randomized dataset.

Table S2.5. Variation of different skull reconstructions within Tyrannosauroidae

	Percentage error			Euclidean distance		
	Median	25 prentil	75 prentil	Median	25 prentil	75 prentil
Tyrannosaurus AMNH 5027	2.284	1.969	3.396	0.039	0.023	0.046
Tyrannosaurus AMNH 5027*	2.410	1.902	3.088	0.035	0.029	0.041
Tyrannosaurus	4.794	2.396	6.468	0.051	0.047	0.065
Tyrannosaurus*	5.483	2.566	6.449	0.062	0.050	0.066
Tarbosaurus	5.310	3.924	6.454	0.059	0.058	0.065
Tarbosaurus*	4.904	3.659	7.474	0.063	0.055	0.071
Gorgosaurus	5.140	3.721	7.119	0.062	0.057	0.067
Gorgosaurus*	5.813	4.131	7.111	0.073	0.066	0.081
Daspletosaurus NMC 8506	0.680	0.399	1.047	0.014	0.011	0.014
Daspletosaurus NMC 8506*	0.649	0.501	1.006	0.012	0.011	0.014
Daspletosaurus FMNH PR308	0.842	0.328	1.312	0.023	0.018	0.039
Daspletosaurus FMNH PR308*	0.745	0.378	1.456	0.018	0.016	0.041
Daspletosaurus	2.614	1.197	4.133	0.039	NA	NA
Daspletosaurus*	3.100	1.876	4.721	0.044	0.043	0.052
Tyrannosauridae	4.656	3.269	6.191	0.056	0.043	0.076
Tyrannosauridae*	4.805	3.049	6.232	0.060	0.053	0.064
Saurischia	10.437	8.793	12.167	0.098	0.084	0.146
Saurischia*	9.288	7.567	11.136	0.101	0.097	0.110

NA = not available due to small sample size, (*) Randomized dataset.

Table S2.6. Errors of single landmarks with same specimens, same species and different species based on original data

Lm	Same specimen			Same species			Different species		
	Median	25 prcentil	75 prcentil	Median	25 prcentil	75 prcentil	Median	25 prcentil	75 prcentil
1	1.993	0.715	4.232	4.553	1.442	6.018	10.964	1.570	12.597
2	1.900	0.314	2.199	3.551	2.655	6.203	5.362	2.988	10.998
3	2.798	0.742	4.842	5.481	3.403	9.436	8.029	4.702	8.487
4	3.069	1.908	8.477	8.766	6.434	14.366	10.278	8.147	14.768
5	1.828	1.016	3.280	6.136	4.617	6.808	6.365	5.989	9.655
6	4.774	2.191	5.677	1.797	1.375	9.554	13.762	4.820	14.532
7	1.732	1.395	3.767	3.927	2.363	5.902	5.052	2.305	10.105
8	1.283	0.417	2.632	3.930	2.384	7.241	3.963	2.005	10.713
9	1.664	0.425	2.904	8.770	3.186	10.795	8.571	5.361	13.805
10	1.595	0.829	2.695	3.418	1.138	3.942	3.594	3.365	11.800
11	1.263	0.914	2.751	5.142	4.396	5.411	4.793	2.408	9.496
12	3.147	0.583	7.000	6.477	4.092	7.909	5.851	4.240	9.447
13	2.610	1.169	3.349	4.062	1.475	4.543	5.976	5.271	6.349
14	2.423	0.785	3.998	6.302	3.675	8.460	6.007	5.361	6.415
15	1.448	0.737	2.347	2.933	1.618	3.412	4.543	4.050	8.494
16	2.389	1.419	3.325	4.780	3.458	6.217	4.547	3.362	5.421
17	2.064	0.501	4.113	6.262	3.881	6.912	7.705	4.491	7.971
18	3.342	0.385	5.682	4.808	2.008	6.202	6.912	2.052	7.008
19	2.388	2.147	4.096	5.419	4.422	10.006	9.027	4.399	12.499
20	1.490	0.500	3.127	3.947	1.553	6.280	6.116	4.040	6.227
21	2.476	0.893	3.041	4.176	2.411	5.221	7.167	4.202	8.405
22	1.436	0.593	3.560	4.830	2.282	8.926	5.522	5.419	12.177

Table S2.7. Errors of single landmarks with same specimens, same species and different species based on randomized data

LM	Same specimen			Same species			Different species		
	Median	25 prntil	75 prntil	Median	25 prntil	75 prntil	Median	25 prntil	75 prntil
1	1.666	0.824	4.409	4.365	2.496	5.749	10.085	1.878	12.322
2	1.685	0.387	2.779	3.465	2.536	4.641	5.691	1.828	13.685
3	3.466	0.622	4.764	7.360	3.681	9.149	9.077	4.955	9.267
4	3.585	1.864	7.711	9.497	7.826	10.585	11.065	6.266	17.061
5	2.657	0.922	3.950	5.421	4.888	5.594	7.388	5.988	9.407
6	4.208	2.280	7.424	2.576	1.802	8.819	11.198	2.800	12.019
7	1.957	1.498	3.577	4.228	2.546	4.557	6.699	2.101	10.596
8	1.545	0.717	2.340	3.959	2.869	6.588	5.845	2.398	13.942
9	1.735	1.108	3.168	7.070	3.309	9.997	7.024	3.794	9.284
10	1.644	1.365	2.793	3.601	1.901	5.867	4.081	3.434	7.593
11	1.447	0.956	3.624	5.631	4.649	5.954	5.068	3.132	8.056
12	3.718	0.750	6.943	7.686	6.490	8.352	7.091	5.180	12.322
13	2.212	1.280	4.137	3.123	2.830	5.328	6.819	6.704	7.243
14	2.421	1.384	3.261	5.614	4.113	7.530	6.220	4.141	8.572
15	1.972	1.089	2.886	2.966	2.774	3.990	5.452	5.214	8.439
16	2.303	1.768	3.569	4.054	3.810	6.236	5.587	4.329	5.654
17	1.936	0.895	4.506	5.747	4.361	7.446	5.235	4.234	9.283
18	2.511	1.446	4.374	4.741	3.047	5.830	5.767	2.559	7.523
19	2.711	1.662	4.776	6.402	4.786	7.614	9.518	5.879	9.652
20	1.617	0.817	3.945	3.821	1.971	4.423	6.446	4.091	8.773
21	2.785	0.787	3.440	4.921	3.439	5.300	7.513	4.429	8.633
22	2.337	0.703	3.460	6.012	2.188	8.738	6.104	3.587	11.195

SUPPLEMENTARY INFORMATION OF CHAPTER 3

Intraspecific variation in the skull morphology of the black caiman *Melanosuchus niger*
(Alligatoridae, Caimaninae)

1. List of specimens
2. Description of Landmarks
3. Error test after Singleton (2002)

1. LIST OF SPECIMENS

Table S3.1. List of specimens of *Melanosuchus niger* used in the geometric morphometric analysis with information on sex, skull length SL, bite force, and data sets in which in was included (dorsal, ventral and lateral views). The bite force BF estimation based on the equation of Erickson et al. (2003): **LogBF = 2.75 x LogSL – 0.65**; **j** juvenile, **j*** juvenile specimens, which were x-rayed; **f** female, **m** male, **m*** identification of males by one of the authors (CF) based on the large size compared to the largest female. **SMF** Senckenberg Naturmuseum Frankfurt (Germany); **ZFMK** Zoologisches Forschungsmuseum Alexander Koenig, Bonn (Germany); **NHMW** Naturhistorisches Museum Wien (Austria); **ZMH** Zoologisches Museum Hamburg (Germany); **ZSM** Zoologische Staatssammlung München (Germany).

Specimen	sex	SL (cm)	logSL (cm)	logBF (N)
ZFMK 52355	j*	4.70	0.67	1.20
ZFMK 52353	j*	5.85	0.77	1.46
ZSM 858/1920	j*	6.10	0.79	1.51
ZSM 139/1982	j*	6.20	0.79	1.53
ZSM 2414/2006	j*	7.90	0.90	1.82
ZMH R08660	j*	8.00	0.90	1.83
SMF 30113	j	8.80	0.94	1.95
SMF 30102	j	10.20	1.01	2.12
ZSM 3/1971	j*	11.10	1.05	2.22
SMF 40142	j	13.10	1.12	2.42
SMF 40172	j	13.90	1.14	2.49
ZSM 13/1911	j	16.30	1.21	2.68
ZSM 130/1911	f	26.80	1.43	3.28
ZSM 27/1911	f	29.00	1.46	3.37
ZSM 87/1911	f	29.00	1.46	3.37
ZSM 76/1911	f	29.80	1.47	3.40
ZSM 85/1911	f	31.10	1.49	3.46
ZSM 84/1911	f	31.50	1.50	3.47
ZSM 77/1911	f	32.00	1.51	3.49
ZSM 86/1911	f	33.30	1.52	3.54
ZSM 83/1911	f	34.00	1.53	3.56
ZSM 91/1911	f	34.00	1.53	3.56
ZSM 68/1911	f	35.50	1.55	3.61
ZSM 14/1911	f	36.40	1.56	3.64
ZSM 89/1911	f	36.80	1.57	3.66
ZSM 70/1911	f	38.50	1.59	3.71

Supplementary information of Chapter 3

SMF 40171	m	25.70	1.41	3.23
ZSM 80/1911	m	30.00	1.48	3.41
ZSM 79/1911	m	30.30	1.48	3.42
ZSM 90/1911	m	33.50	1.53	3.54
ZSM 73/1911	m	34.50	1.54	3.58
ZSM 74/1911	m	35.50	1.55	3.61
ZSM 75/1911	m	35.90	1.56	3.63
ZSM 3/1911	m	36.60	1.56	3.65
ZSM 67/1911	m	37.50	1.57	3.68
ZSM 46/1911	m	38.50	1.59	3.71
ZSM 69/1911	m	39.50	1.60	3.74
ZSM 64/1911	m	39.80	1.60	3.75
ZSM 11/1911	m	40.30	1.61	3.76
ZSM 62/1911	m	42.30	1.63	3.82
ZSM 57/1911	m	43.50	1.64	3.86
ZSM 3039/0	m*	43.50	1.64	3.86
ZSM 1/1906	m*	45.00	1.65	3.90
NHMW 2024	m*	45.30	1.66	3.90
ZSM 35/1911	m	45.50	1.66	3.91
ZSM 52/1911	m	45.70	1.66	3.91
ZSM 2416/2006	m*	47.50	1.68	3.96
ZSM 63/1911	m*	49.50	1.69	4.01
ZSM 12/1911	m	50.00	1.70	4.02
SMF 28182	m*	50.00	1.70	4.02
ZSM 223/1295	m*	52.00	1.72	4.07
NHMW 2025	m*	52.50	1.72	4.08

2. DESCRIPTION OF LANDMARKS

Anatomical description of the landmarks (the landmarks are visualized in Fig. 3.1

Chapter 3; LM = landmark; semi-LM = semi-landmark)

DORSAL VIEW

- 1 most anterior contact between both premaxillae
- 2 midpoint of the posterior margin of the skull table
- 3 contact between the supraoccipital and parietal along the posterior margin of the skull table
- 4 most posterolateral point of the squamosal (contact with the exoccipital)
- 5 most posterolateral point of the quadrate
- 6 contact of jugal process of the postorbital with skull table
- 7 most posterolateral point of the orbit
- 8 most anterior point of the orbit
- 9 contact between the premaxilla and maxilla along the lateral margin of the skull
- 10 one semi-LM on the anterolateral margin of the skull between LM 1 and LM 9
- 11-12 two semi-LMs on the medial margin of the orbit between LM 8 and LM 6, from anterior to posterior
- 13-15 three semi-LMs on the lateral margin of the skull between LM 9 and LM 5, from anterior to posterior

LATERAL VIEW

- 1 most anteroventral point of the premaxillae
- 2 contact between the maxilla and jugal along the ventral margin of the skull
- 3 most posterior point of the quadratojugal at the jaw joint
- 4 most posterior point of the skull roof surface
- 5 postorbital foramen
- 6 most ventral contact between the jugal and postorbital
- 7 most anterior point of the orbit
- 8 contact of the premaxilla and maxilla along the margin of the tooth row
- 9 one semi-LM on the ventral margin of the premaxilla between LM 1 and LM 8
- 10-12 three semi-LMs on the ventral margin of the maxilla between LM 8 and LM 2, from anterior to posterior
- 13-14 two semi-LMs on the ventral margin of the jugal between LM 2 and LM 3, from anterior to posterior
- 15-21 seven semi-LMs on the dorsal margin of the skull between LM 1 and LM 4, from anterior to posterior

3. ERROR TEST AFTER SINGLETON (2002)

For the error test, estimating the methodological error of plotting landmarks on the skulls, Procrustes distances of the Procrustes coordinates to the respective consensus coordinates of each landmark were calculated. Then, the relation of these distances to the mean distance of the consensus landmarks to the centroid of the consensus shape was calculated as a percentage of the former from the latter. Based on the test all landmarks possess only a small percentage error for plotting landmarks ($\approx 0.08-1.27\%$).

Table S3.2. Percentage error for each landmark for both photographed (ZSM 2416/2006) and the X-rayed specimens (ZSM 3/1971) (in dorsal and lateral view) with n = 10.

LM	Dorsal view		Lateral view	
	Photograph	X-ray	Photograph	X-ray
1	0.326	0.311	0.650	0.659
2	0.451	0.508	0.204	0.958
3	0.318	0.887	0.611	0.528
4	0.477	0.628	0.308	0.538
5	0.566	0.612	0.527	0.638
6	0.508	0.824	0.268	0.410
7	0.956	1.271	0.325	0.695
8	0.262	0.407	0.474	0.644
9	0.255	0.248	0.309	0.498
10	0.112	0.163	0.373	0.259
11	0.200	0.341	0.179	0.368
12	0.173	0.345	0.144	0.360
13	0.082	0.321	0.173	0.269
14	0.119	0.294	0.310	0.390
15	0.153	0.535	0.273	0.393
16	-	-	0.300	0.355
17	-	-	0.309	0.256
18	-	-	0.417	0.292
19	-	-	0.328	0.419
20	-	-	0.238	0.286
21	-	-	0.240	0.315

SUPPLEMENTARY INFORMATION OF CHAPTER 4

Do different disparity proxies converge on a common signal? Insights from the cranial morphometrics and evolutionary history of Pterosauria (Diapsida: Archosauria)

1. List of species
2. Description of Landmarks
3. Phylogeny
4. Time
5. Morphospace
6. Skull shape evolution based on the supertree topology
7. Morphological disparity based on supertree topology

***All figures of the supplementary information of Chapter 4 are modified after Foth et al. (2012)**

1. LIST OF SPECIES

Table S4.1. Sources for skull images used in the morphometric analysis. *indicates skulls which are used as silhouettes in Fig. 4.2.

Taxon	Reference
<i>Eudimorphodon ranzii</i>	Wild 1984, Naturwissenschaften
<i>Raeticodactylus filisurensis</i> *	Stecher 2008, Swiss Journal of Geosciences
<i>Dimorphodon macronyx</i>	Wellnhofer 1978, Pterosauria (Gustav Fischer Verlag)
<i>Campylognathoides</i>	Padian 2008b, Special Papers in Palaeontology
<i>Rhamphorhynchus muensteri</i>	Wellnhofer 1975, Palaeontographica, Abt. A
<i>Dorygnathus banthensis</i>	Padian 2008a, Special Papers in Palaeontology
<i>Scaphognathus crassirostris</i>	Wellnhofer 1975, Palaeontographica, Abt. A
<i>Darwinopterus modularis</i>	Lü et al. 2010a, Proceedings of the Royal Society, Series B
<i>Anurognathus ammoni</i> *	Bennett 2007, Paläontologische Zeitschrift
<i>Gnathosaurus subulatus</i>	Wellnhofer 1970, Bayerische Akademie der Wissenschaften, Math. Nat. Klasse, Abh.
<i>Ctenochasma elegans</i> *	Wellnhofer 1978, Pterosauria (Gustav Fischer Verlag)
<i>Pterodaustro guinazui</i>	Chiappe et al. 2000, Contributions in Science
<i>Feilongus youngi</i>	Wang et al., 2005, Nature
<i>Gallodactylus canjuersensis</i>	Wellnhofer 1978, Pterosauria (Gustav Fischer Verlag)
<i>Pterodactylus antiquus</i>	Wellnhofer 1970, Bayerische Akademie der Wissenschaften, Math. Nat. Klasse, Abh.
<i>Germanodactylus cristatus</i>	Wellnhofer 1970, Bayerische Akademie der Wissenschaften, Math. Nat. Klasse, Abh.
<i>Germanodactylus rhamphastinus</i>	Wellnhofer 1970, Bayerische Akademie der Wissenschaften, Math. Nat. Klasse, Abh.
<i>Nyctosaurus gracilis</i>	Bennett 2003, Paläontologische Zeitschrift
<i>Anhanguera santanae</i>	Maisey 1991, Santana fossils (TFH publications)
<i>Anhanguera blittersdorffi</i>	Wellnhofer 1987, Mitteilungen der Bayerischen Staatssammlung und historischen Geologie
<i>Tropeognathus mesembrinus</i>	Maisey 1991, Santana fossils (TFH publications)
<i>Pteranodon longiceps</i>	Wellnhofer 1978, Pterosauria (Gustav Fischer Verlag)
<i>Pteranodon sternbergi</i> *	Wellnhofer, 1991, The Illustrated Encyclopedia of Pterosaurs (Salamnder Books, Ltd.)
<i>Tapejara wellnhoferi</i>	Wellnhofer & Kellner 1991, Mitteilungen der Bayerischen Staatssammlung und historischen Geologie
<i>Ingridia imperator</i> *	Pinheiro et al. 2011, Acta Palaeontologica Polonica
<i>Tupuxuara leonardii</i>	Martill & Naish 2006, Palaeontology
<i>Thalassodromeus sethi</i> *	Kellner & Campos 2002, Science

<i>"Phobetor" parvus</i>	Wellnhofer 1991, The Illustrated Encyclopedia of Pterosaurs (Salamnder Books, Ltd.)
<i>Dsungaripterus weii</i>	Wellnhofer 1978, Pterosauria (Gustav Fischer Verlag)
<i>Shenzhoupterus chaoyangensis</i>	Lü et al. 2008, Naturwissenschaften
<i>Zhejiangopterus linhaiensis</i>	Averianov 2004, Paleontological Journal

2. DESCRIPTION OF LANDMARKS

1. Anteroventral corner of premaxilla (= anteroventral corner of the skull; type 2)
2. Anteroventral corner of external naris or nasoantorbital fenestra (NAOF) (type 2)
3. Ventral-most point of the orbit (type 2)
4. Dorsal border of the skull constructed by a line at 90° to the midpoint between LM 1 and 2 (type 3)
5. Ventral border of the skull constructed by a line at 90° to the midpoint between LM 1 and 2 (type 3)
6. Dorsal border of the skull constructed by a line at 135° to line between LM 2 and 3 at LM 2 (type 3)
7. Ventral border of the skull constructed by a line at 135° to line between LM 2 and 3 at LM 2 (type 3)
8. Dorsal border of the skull constructed by a line at 90° to the midpoint between LM 2 and 3 (type 3)
9. Dorsal border of the naris-antorbital fenestra (AOF) unit constructed by a line at 90° to the midpoint between LM 2 and 3 (type 3)
10. Ventral border of the naris-AOF unit constructed by a line at 90° to the midpoint between LM 2 and 3 (type 3)

11. Ventral border of the skull constructed by a line at 90° to the midpoint between LM 2 and 3 (type 3)
12. Posterior border of the orbit constructed by a line at 90° to the line between LM 3 and 13 (type 3)
13. Posterodorsal border of the orbit constructed by a line at 45° to line between LM 2 and 3 at LM 3 (type 3)
14. Dorsal border of the orbit constructed by a line at 90° to the line between LM 13 and 15 (type 3)
15. Anterordorsal border of the orbit constructed by a line at 90° to the line between LM 3 and 13 (type 3)
16. Dorsal border of the skull constructed by a line at 90° to the line between LM 3 and 13 (type 3)
17. Dorsal border of the skull constructed by a line at 90° to the line between LM 13 and 18 (type 3)
18. Posterodorsal border of the skull constructed by a line at 45° to line between LM 2 and 3 at LM 3 (type 3)
19. Posterior border of the skull constructed by a line at 90° to the line between LM 13 and 18 (type 3)
20. Anteroventral corner of the AOF or NAOF (type 2)
21. Posteroventral corner of the quadrate (posteroventral corner of the skull, type 2)

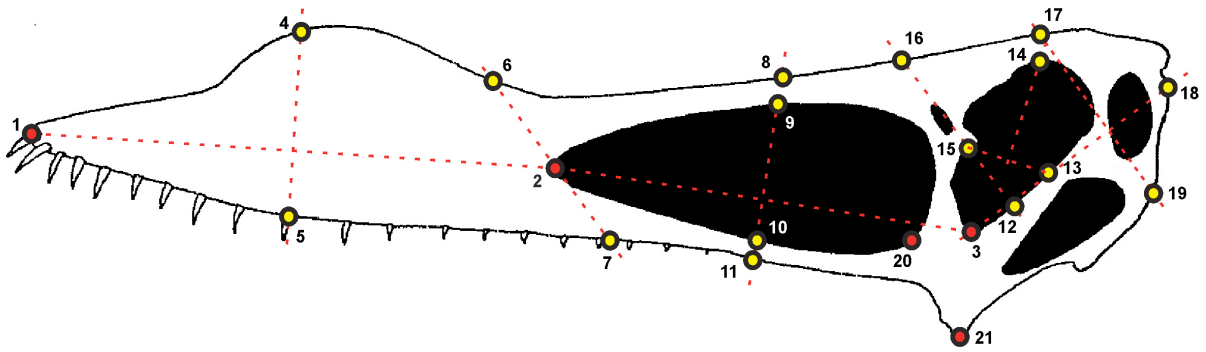


Fig. S4.1. Homologous landmarks plotted onto an exemplar pterosaur skull in left lateral view. Red points indicate type 2 landmarks and yellow points indicate type 3 landmarks (*Anhanguera santanae* skull, modified after Maisey 1991).

3. PHYLOGENY

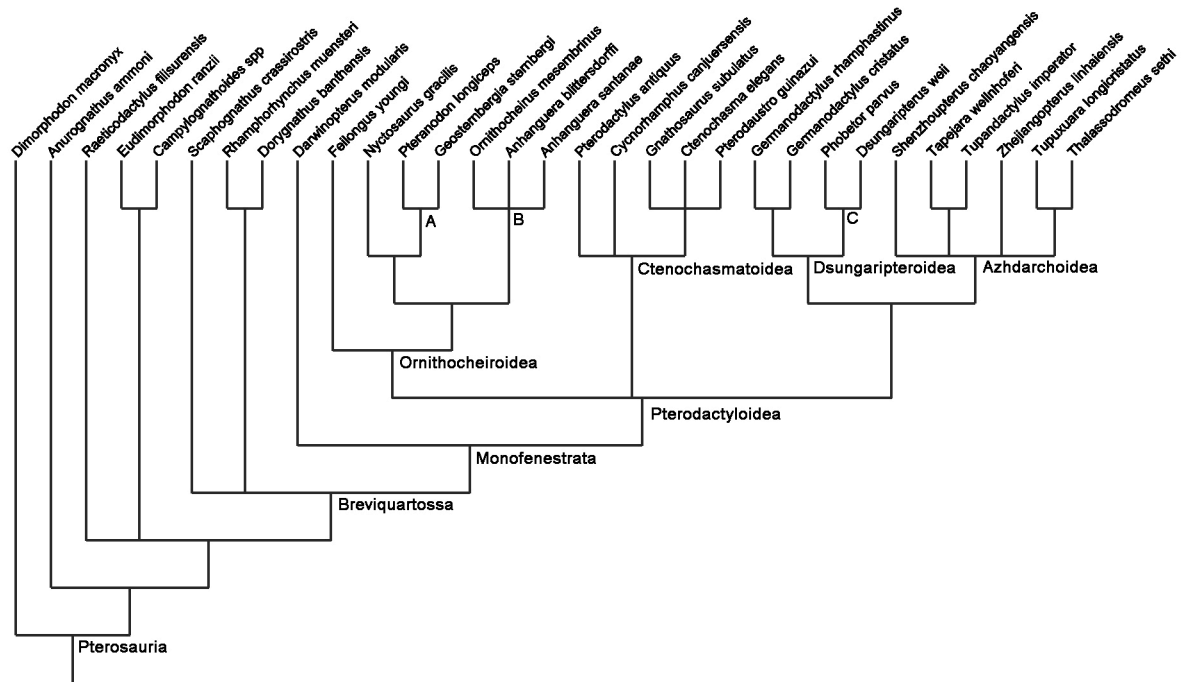


Fig. S4.2. Phylogeny of pterosaurs after Lü et al. (2010a). Clades used in this study (numbers refer to those positioned next to nodes): A) Pteranodontidae; B) Ornithocheiridae; C) Dsungaripteroidea.

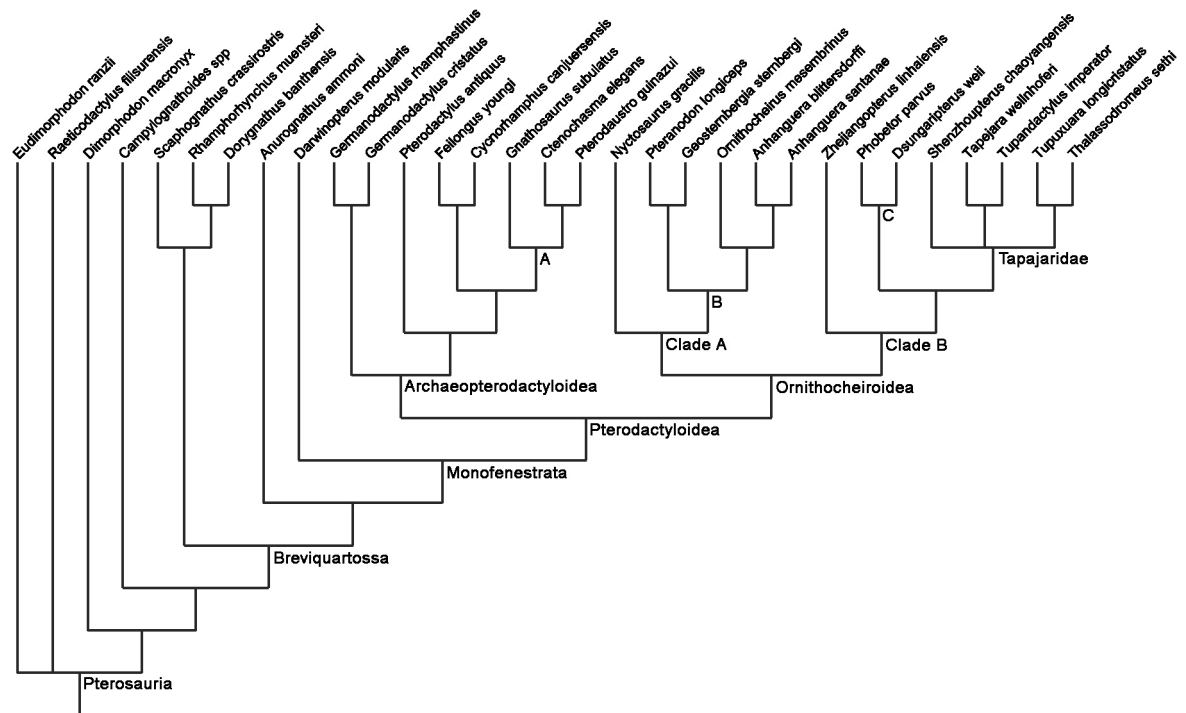


Fig. S4.3. Informal supertree of pterosaurs based on the phylogenies of Andres & Ji (2008) and Andres et al. (2010). Clades used in this study (numbers refer to those positioned next to nodes): A) Ctenochasmatidae; B) Pteranodontoidea; C) Dsungaripteridae.

4. TIME

Table S4.2. First occurrence dates (million of years ago, Ma) for pterosaurs used to calculate branch lengths for the phylogenetic significance test (correlation between cranial form and phylogeny).

Taxon	Age
<i>Dimorphodon macronyx</i>	196.5
<i>Anurognathus ammoni</i>	148.15
<i>Eudimorphodon ranzii</i>	205.75
<i>Campylognathoides</i> spp.	181.85
<i>Raeticodactylus filisurensis</i>	203.65
<i>Scaphognathus crassirostris</i>	148.15
<i>Rhamphorhynchus muensteri</i>	149.25
<i>Dorygnathus banthensis</i>	181.85
<i>Darwinopterus modularis</i>	161.5
<i>Pteranodon longiceps</i>	82.3
<i>Geosternbergia sternbergi</i>	85.9
<i>Nyctosaurus gracilis</i>	82.4
<i>Ornithocheirus mesembrinus</i>	110.4
<i>Ananguera blittersdorffi</i>	110.4
<i>Ananguera santanae</i>	110.4
<i>Feilongus youngi</i>	125.9
<i>Pterodactylus antiquus</i>	148.15
<i>Cycnorhamphus canjuersensis</i>	148.15
<i>Gnathosaurus subulatus</i>	148.15
<i>Ctenochasma elegans</i>	148.15
<i>Pterodaustro guinazui</i>	105.8
<i>Germanodactylus rhamphastinus</i>	148.15
<i>Germanodactylus cristatus</i>	148.15
<i>Phobetor parvus</i>	140.95
<i>Dsungaripterus weii</i>	140.95
<i>Tapejara wellnhoferi</i>	110.4
<i>Tupandactylus imperator</i>	116.5
<i>Shenzhoupterus chaoyangensis</i>	117.05
<i>Tupuxuara longicristatus</i>	116.5
<i>Thalassodromeus sethi</i>	116.5
<i>Zhejiangopterus linhaiensis</i>	82.05

5. MORPHOSPACE

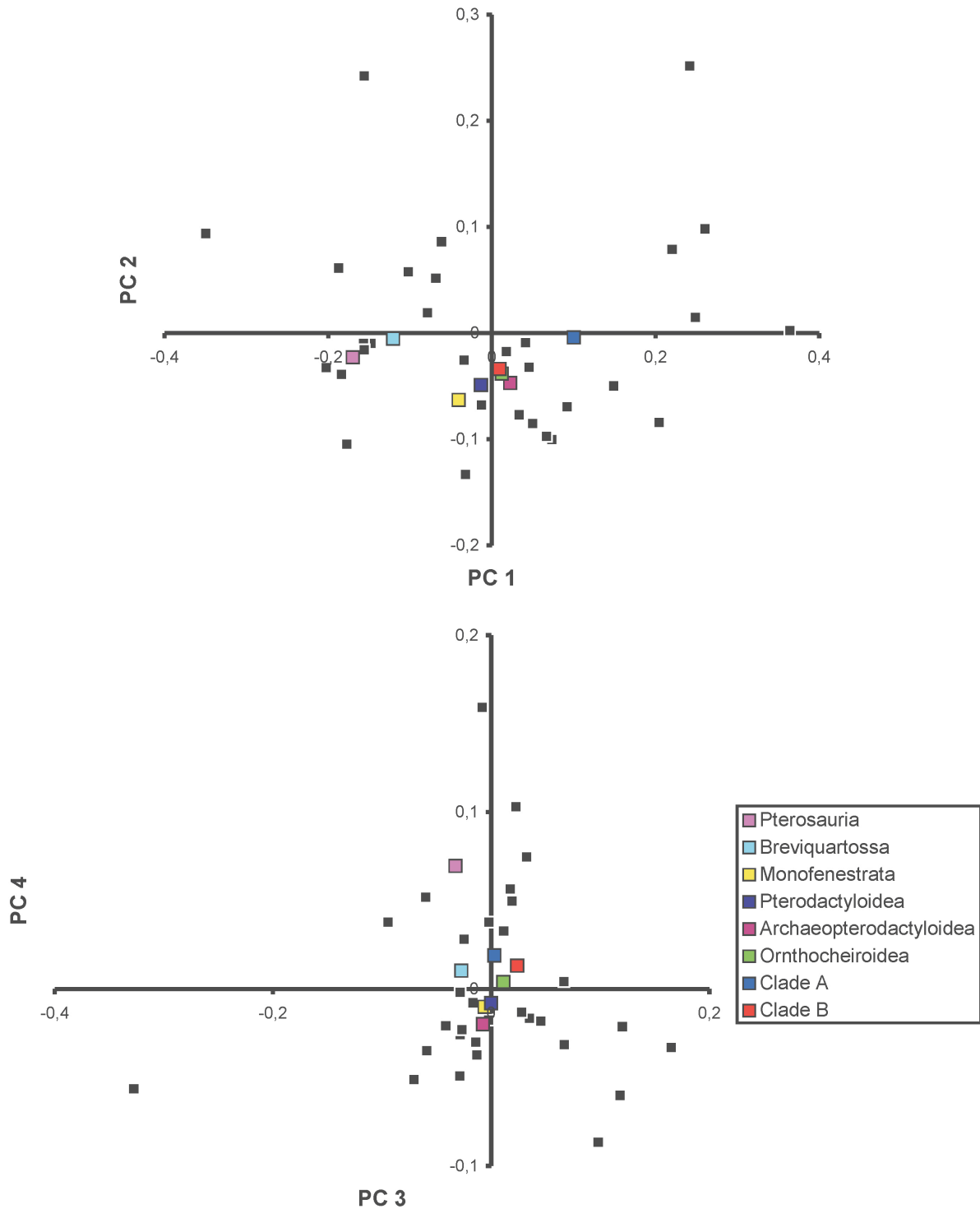


Fig. S4.4. Diagram of the first four PC axes with position of the hypothetical ancestors of several pterosaur clades based on the supertree topology. Clade A (Pteranodontoidea + *Nyctosaurus*), Clade B (Tapejaridae + Dsungaripteridae + *Zhejiangopterus*)

6. SKULL SHAPE EVOLUTION BASED ON THE SUPERTREE TOPOLOGY

The results from the ancestral state analysis based on the supertree are similar to those based on the Lü et al. (2010a) topology (Fig. S4.5). The skull of the hypothetical ancestor of all pterosaurs had a short, stout snout (negative position of PC 1, positive position of PC 4), a triangular naris-antorbital fenestra region (positive position of PC 4), a relatively large orbit (negative position of PC 3) and a relatively large postorbital region, whereas the hypothetical ancestor of the clade Breviquartossa had a more pointed tip of the snout. Compared to the basal pterosaur clades, the hypothetical ancestors of Monofenestrata, Pterodactyloidea, Archaeopterodactyloidea and Ornithocheiroidea possessed a more elongated skull with a long snout (more positive position of PC 1), a more trapezoidal naris-antorbital fenestra region (more negative position of PC 4) and a relatively smaller orbit and postorbital region (more positive position of PC 1). The skull of the hypothetical ancestor of clade A (Pteranodontoidea + *Nyctosaurus*) had a more elongated snout with a shallower antorbital region than the ancestor of Ornithocheiroidea (more positive position of PC 1, more negative position of PC 3), whereas the skull of the hypothetical ancestor of clade B (Tapejaridae + Dsungaripteridae + *Zhejiangopterus*) had a shortened snout (more negative position of PC 1) and deeper antorbital region (more positive position of PC 3).

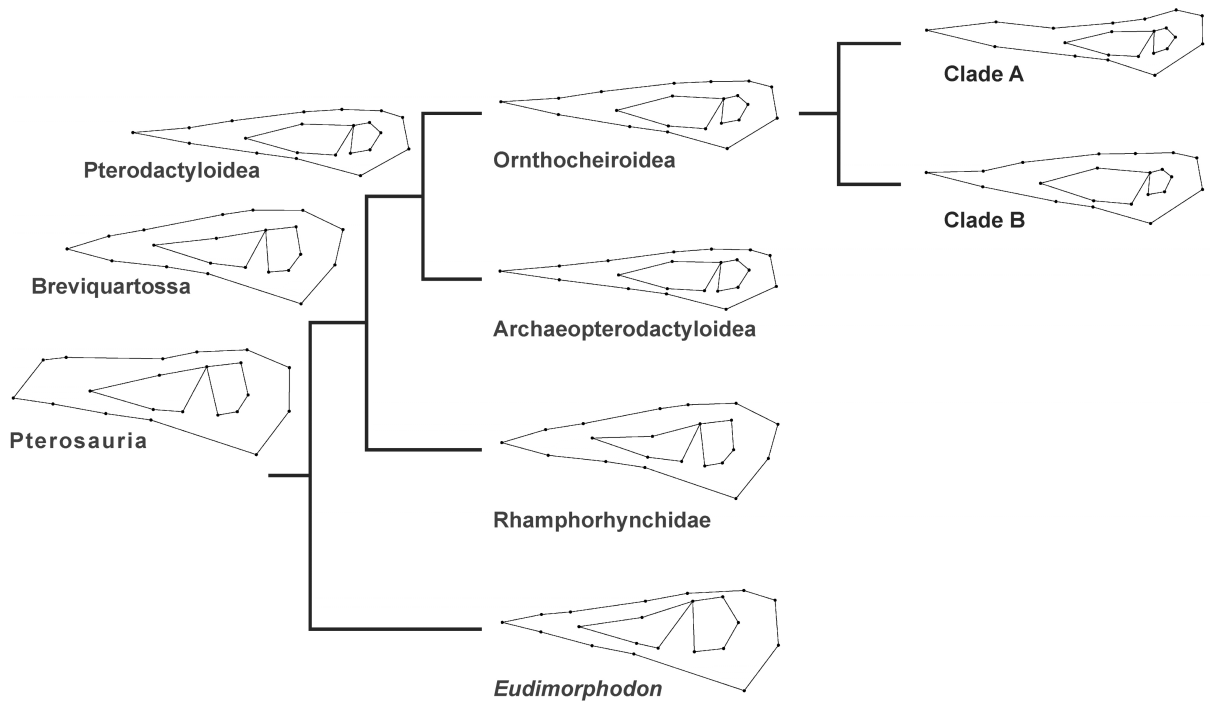


Fig. S4.5. Diagram of the ancestral shape reconstruction of pterosaur skulls based on the supertree topology. Clade A (Pteranodontoidea + *Nyctosaurus*), Clade B (Tapejaridae + Dsungaripteridae + *Zhejiangopterus*).

7. MORPHOLOGICAL DISPARITY

Table S4.3. Temporal bins analyzed in the disparity analysis.

Temporal bins	Species
Late Triassic-Early Jurassic	<i>Dimorphodon macronyx</i>
	<i>Eudimorphodon ranzii</i>
	<i>Raeticodactylus filisurensis</i>
	<i>Campylognathoides spp.</i>
	<i>Dorygnathus banthensis</i>
Middle Jurassic-Late Jurassic	<i>Rhamphorhynchus muensteri</i>
	<i>Scaphognathus crassirostris</i>
	<i>Anurognathus ammoni</i>
	<i>Darwinopterus modularis</i>
	<i>Gnathosaurus subulatus</i>
	<i>Ctenochasma elegans</i>
	<i>Cynorhamphus canjuersensis</i>
	<i>Pterodactylus antiquus</i>
	<i>Germanodactylus rhamphastinus</i>
	<i>Germanodactylus cristatus</i>
Early Cretaceous	<i>Pterodaustro guinazui</i>
	<i>Feilongus youngi</i>
	<i>Ananguera santanae</i>
	<i>Ananguera blittersdorffi</i>
	<i>Ornithocheirus mesembrinus</i>
	<i>Tapejara wellnhoferi</i>
	<i>Tupandactylus imperator</i>
	<i>Tupuxuara longicristatus</i>
	<i>Thalassodromeus sethi</i>
	<i>Phobetor parvus</i>
	<i>Dsungaripterus weii</i>
<i>Shenzhoupterus chaoyangensis</i>	
Late Cretaceous	<i>Nyctosaurus gracilis</i>
	<i>Zhejiangopterus linhaiensis</i>
	<i>Geosternbergia sternbergi</i>
	<i>Pteranodon longiceps</i>

Table S4.4. Phylogenetic groups within Pterosauria after Lü et al. (2010a) analyzed in the disparity analysis.

Phylogenetic groups	Species	
non-monofenestratan pterosaurs	<i>Dimorphodon macronyx</i>	
	<i>Eudimorphodon ranzii</i>	
	<i>Raeticodactylus filisurensis</i>	
	<i>Campylognathoides</i> spp.	
	<i>Dorygnathus banthensis</i>	
	<i>Rhamphorhynchus muensteri</i>	
	<i>Scaphognathus crassirostris</i>	
	<i>Anurognathus ammoni</i>	
	Monofenestrata	<i>Darwinopterus modularis</i>
		<i>Gnathosaurus subulatus</i>
<i>Ctenochasma elegans</i>		
<i>Cycnorhamphus canjuersensis</i>		
<i>Pterodactylus antiquus</i>		
<i>Germanodactylus rhamphastinus</i>		
<i>Germanodactylus cristatus</i>		
<i>Pterodaustro guinazui</i>		
<i>Feilongus youngi</i>		
<i>Anhanguera santanae</i>		
<i>Anhanguera blittersdorffi</i>		
<i>Ornithocheirus mesembrinus</i>		
<i>Tapejara wellnhoferi</i>		
<i>Tupandactylus imperator</i>		
<i>Tupuxuara longicristatus</i>		
<i>Thalassodromeus sethi</i>		
<i>Phobetor parvus</i>		
<i>Dsungaripterus weii</i>		
<i>Shenzhoupterus chaoyangensis</i>		
<i>Nyctosaurus gracilis</i>		
<i>Zhejiangopterus linhaiensis</i>		
<i>Geosternbergia sternbergi</i>		
<i>Pteranodon longiceps</i>		
Dsungaripteroidea	<i>Phobetor parvus</i>	
	<i>Dsungaripterus weii</i>	
	<i>Germanodactylus rhamphastinus</i>	
	<i>Germanodactylus cristatus</i>	

Azhdarchoidea	<i>Tapejara wellnhoferi</i>
	<i>Tupandactylus imperator</i>
	<i>Tupuxuara longicristatus</i>
	<i>Thalassodromeus sethi</i>
	<i>Shenzhoupterus chaoyangensis</i>
	<i>Zhejiangopterus linhaiensis</i>
Ctenochasmatoidea	<i>Gnathosaurus subulatus</i>
	<i>Ctenochasma elegans</i>
	<i>Cycnorhamphus canjuersensis</i>
	<i>Pterodactylus antiquus</i>
	<i>Pterodaustro guinazui</i>
Ornithocheiroidea	<i>Nyctosaurus gracilis</i>
	<i>Geosternbergia sternbergi</i>
	<i>Pteranodon longiceps</i>
	<i>Anhanguera santanae</i>
	<i>Anhanguera blittersdorffi</i>
	<i>Ornithocheirus mesembrinus</i>
	<i>Feilongus youngi</i>

Table S4.5. Phylogenetic groups within Pterodactyloidea after Andres & Ji (2008) analyzed in the disparity analysis.

Phylogenetic groups	Species	
Archaeopterodactyloidea	<i>Gnathosaurus subulatus</i>	
	<i>Ctenochasma elegans</i>	
	<i>Cycnorhamphus canjuersensis</i>	
	<i>Pterodactylus antiquus</i>	
	<i>Pterodaustro guinazui</i>	
	<i>Feilongus youngi</i>	
	<i>Germanodactylus rhamphastinus</i>	
	<i>Germanodactylus cristatus</i>	
	Ornithocheiroidea	<i>Tapejara wellnhoferi</i>
		<i>Tupandactylus imperator</i>
<i>Tupuxuara longicristatus</i>		
<i>Thalassodromeus sethi</i>		
<i>Shenzhoupterus chaoyangensis</i>		
<i>Zhejiangopterus linhaiensis</i>		
<i>Phobetor parvus</i>		
<i>Dsungaripterus weii</i>		
<i>Nyctosaurus gracilis</i>		
<i>Geosternbergia sternbergi</i>		
<i>Pteranodon longiceps</i>		
<i>Anhanguera santanae</i>		
<i>Anhanguera blittersdorffi</i>		
<i>Ornithocheirus mesembrinus</i>		
Pteranodontoidea + <i>Nyctosaurus</i>	<i>Nyctosaurus gracilis</i>	
	<i>Geosternbergia sternbergi</i>	
	<i>Pteranodon longiceps</i>	
	<i>Anhanguera santanae</i>	
	<i>Anhanguera blittersdorffi</i>	
	<i>Ornithocheirus mesembrinus</i>	
<i>Zhejiangopterus</i> + Tapejaridae + Dsungaripteridae + Azhdarchidae	<i>Tapejara wellnhoferi</i>	
	<i>Tupandactylus imperator</i>	
	<i>Tupuxuara longicristatus</i>	
	<i>Thalassodromeus sethi</i>	
	<i>Shenzhoupterus chaoyangensis</i>	
	<i>Zhejiangopterus linhaiensis</i>	
	<i>Phobetor parvus</i>	
	<i>Dsungaripterus weii</i>	

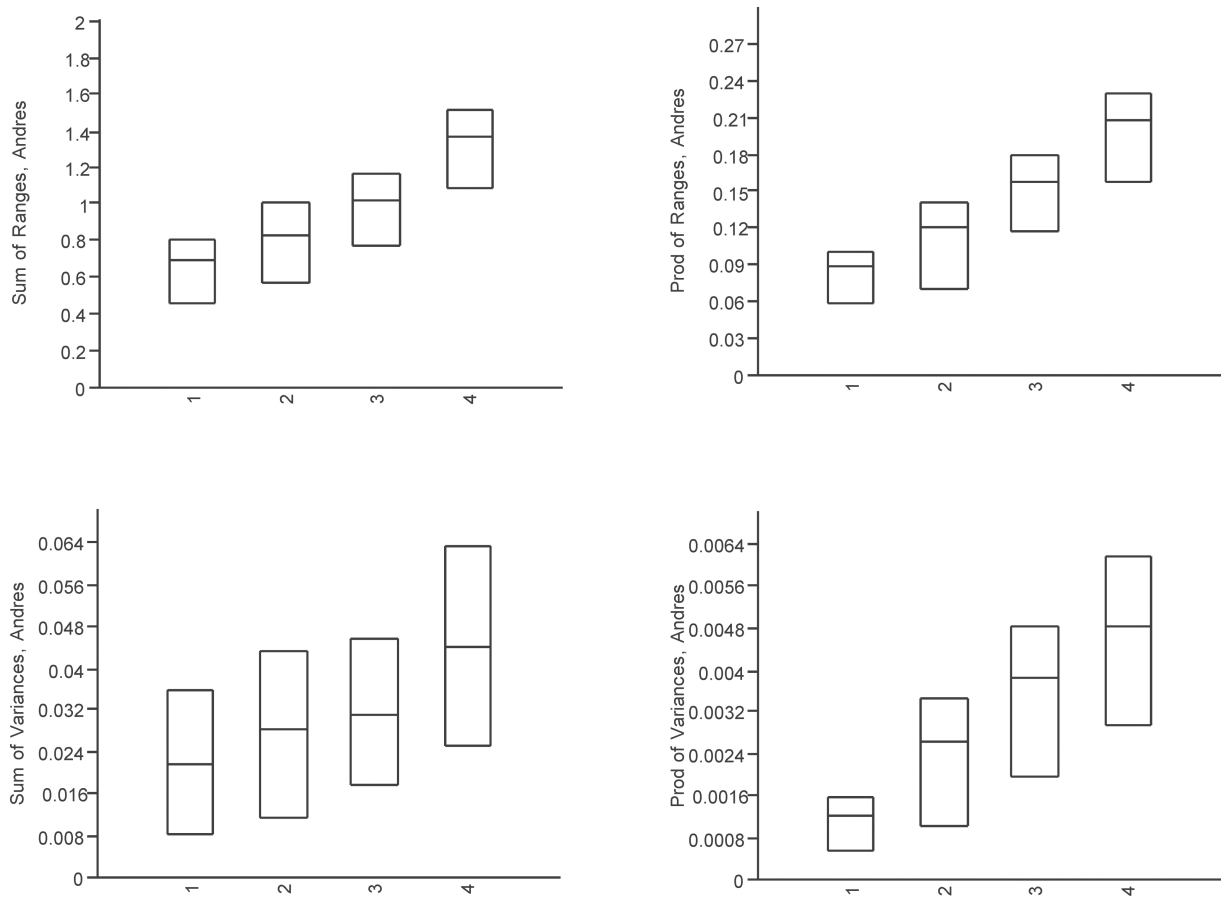


Fig. S4.6. Four disparity metrics compared in four taxonomic groups (numbers refer to the numbers on the x axis in each plot). 1) Archaeopterodactyloidea. 2) Clade A (Pteranodontoidea + *Nyctosaurus*). 3) Clade B (Tapejaridae + Dsungaripteridae + *Zhejiangopterus*). 4) Ornithocheiroidea. The boxes represent the extent of 95 % error bars and the horizontal line inside the box is the disparity measure for the group in question. The overlap (non-significant) or non-overlap (significant) of the error bars denotes statistical significance.

SUPPLEMENTARY INFORMATION OF CHAPTER 5

Macroevolutionary and morphofunctional patterns in theropod skulls: a morphometric approach

1. Taxon sampling
2. Description of landmarks
3. Biomechanic and ecological parameters
4. Phylogeny and cluster topologies
5. Phylogenetic signals of functional proxies (SSI and AMS) and diagnostic test for PIC analysis

***All figures of the supplementary information of Chapter 5 are modified after Foth & Rauhut (2013)**

1. TAXON SAMPLING

Table S5.1. List of taxa used in the present analyses with data of occurrences (in million of years, Ma) and sources of images.

Taxon	Systematic affinities	Age (Ma)	Sources
<i>Euparkeria</i>	Basal archosauriform	Anisian (241.5)	Rauhut 2003a
<i>Lesothosaurus</i>	Ornithischia	Hettangian/Sinemurian (202)	Norman et al. 2004
<i>Massospondylus</i>	Sauropodomorpha	Sinemurian (198.5)	Gow et al. 1990
<i>Plateosaurus</i>	Sauropodomorpha	Norian (215.5)	Galton 1985
<i>Herrerasaurus</i>	Herrerasauridae	Carnian (224)	Langer 2004
<i>Eoraptor</i>	Basal theropod	Carnian (224)	Langer 2004
<i>Daemonosaurus</i>	Basal theropod	Rhaetian (208)	Sues et al. 2011
<i>Syntarsus kayentakatae</i>	Coelophysidae	Sinemurian/Pliensbachian (195)	Tykosky 1998
<i>Coelophysis</i>	Coelophysidae	Carnian/Norian (221)	Colbert 1989
<i>Zupaysaurus</i>	Basal neotheropod	Norian (215.5)	Ezcurra 2007
<i>Limusaurus</i>	Ceratosauria	Oxfordian (156.5)	Xu et al. 2009a
<i>Ceratosaurus</i>	Ceratosauria	Kimmeridgian/Tithonian (151)	Sampson & Witmer 2007
<i>Carnotaurus</i>	Abelisauridae	Campanian/Maastrichtian (71.3)	Rauhut 2003a
<i>Majungasaurus</i>	Abelisauridae	Campanian (77.4)	Sampson & Witmer 2007
<i>Monolophosaurus</i>	Megalosauroida	Callovian (161.5)	Brusatte et al. 2010b
Spinosaurid	Megalosauroida	Albian (105.5)*	Rauhut 2003a
<i>Sinraptor</i>	Allosauroida	Oxfordian (156.5)	Currie & Zhao 1993
<i>Acrocanthosaurus</i>	Allosauroida	Aptian/Albian (112)	Eddy & Clarke 2011
<i>Allosaurus</i>	Allosauroida	Kimmeridgian/Tithonian (151)	Rauhut 2003a
<i>Guanlong</i>	Tyrannosauroida	Oxfordian (156.5)	Xu et al. 2006
<i>Dilong</i>	Tyrannosauroida	Barremian (124)	Xu et al. 2004
<i>Bistahieversor</i>	Tyrannosauroida	Campanian (77.4)	Carr & Williamson 2010
<i>Alioramus</i>	Tyrannosauridae	Maastrichtian (68.15)	Brusatte et al. 2009
<i>Daspletosaurus</i>	Tyrannosauridae	Campanian (77.4)	Holtz 2004
<i>Gorgosaurus</i>	Tyrannosauridae	Campanian (77.4)	Rauhut 2003a
<i>Tarbosaurus</i>	Tyrannosauridae	Campanian/Maastrichtian (71.3)	Hurum & Sabbath 2003
<i>Tyrannosaurus</i>	Tyrannosauridae	Campanian/Maastrichtian (71.3)	Holtz 2004
<i>Compsognathus</i>	Compsognathidae	Kimmeridgian (152.5)	Peyer 2006

<i>Garudimimus</i>	Ornithomimosauria	Cenomanian-Santonian (89)	Makovicky et al. 2004
<i>Gallimimus</i>	Ornithomimosauria	Maastrichtian (68.15)	Makovicky et al. 2004
<i>Ornithomimus</i>	Ornithomimosauria	Campanian/Maastrichtian (71.3)	Rauhut 2003a
<i>Erlikosaurus</i>	Therizinosauridae	Cenomanian-Santonian (89)	Rauhut 2003a
<i>Conchoraptor</i>	Oviraptoridae	Campanian (77.4)	Osmólska et al. 2004
<i>Citipati</i>	Oviraptoridae	Campanian (77.4)	Osmólska et al. 2004
<i>Oviraptor</i>	Oviraptoridae	Campanian (77.4)	Osmólska et al. 2004
<i>Archaeopteryx</i>	Avialae	Kimmeridgian (152.5)	Rauhut 2003a
<i>Confuciusornis</i>	Avialae	Barremian (124)	Chiappe et al. 1999
<i>Pengornis</i>	Avialae	Barremian (124)	O'Connor & Chiappe 2011
<i>Shenquiornis</i>	Avialae	Barremian (124)	O'Connor & Chiappe 2011
<i>Anchiornis</i>	Troodontidae	Oxfordian (156.5)	Hu et al. 2009
<i>Sinornithosaurus</i>	Dromaeosauridae	Barremian (124)	Xu & Wu 2001
<i>Bambiraptor</i>	Dromaeosauridae	Campanian (77.4)	Burnham 2004
<i>Velociraptor</i>	Dromaeosauridae	Campanian (77.4)	Barsbold & Osmólska 1999
<i>Shuvuuia</i>	Alvarezsauridae	Campanian (77.4)	Chiappe et al. 2002

*The reconstruction of a generalized spinosaurid is based on several taxa (the orbital and postorbital region mainly based on *Irritator*, and the snout based on *Suchomimus*, with some elements reconstructed after *Baryonyx*; see Rauhut 2003a), which range in age from the Barremian to the Cenomanian, so we used an intermediate stage between these extremes for the age estimate of this reconstruction.

2. DESCRIPTION OF LANDMARKS

Homologous landmarks plotted on all theropod skulls in lateral view. The landmarks present in both data sets are bold. Landmark 21 is only present in the smaller data set (latin). Marked (*) landmarks are identical with Brusatte et al. (2012a).

1. anteroventral corner of the premaxilla (this point is reconstructed in *Alioramus* and *Zupaysaurus* due to a missing premaxilla) (preorbital region)*
2. contact of premaxilla and nasal above the external naris (preorbital region)*
3. contact of premaxilla and maxilla along the tooth row (preorbital region)*
4. tip of the maxillary process of the premaxilla (preorbital region)
5. anterodorsal contact between lacrimal and nasal (preorbital region)
6. contact between maxilla and jugal along the margin of antorbital fenestra (in those taxa where the jugal do not reach the antorbital fenestra – the most anterior point of the jugal is chosen, as in most theropods the contact between maxilla and jugal along the antorbital fenestra is also the most anterior point of the jugal) (preorbital region)
7. contact of maxilla and jugal along the ventral margin of the skull (preorbital region)*
8. contact between lacrimal and jugal on the orbital margin (preorbital region)
9. contact between postorbital and jugal on the orbital margin (postorbital region)*
10. contact between postorbital and jugal on the margin of the lateral temporal fenestra (postorbital region)*
11. contact between jugal and quadratojugal on the margin of the lateral temporal fenestra (postorbital region)*
12. anteroventral tip of the squamosal on the margin of the lateral temporal fenestra (postorbital region)*

- 13. ventral contact of postorbital and squamosal on the margin of the lateral temporal fenestra (postorbital region)**
- 14. anterior tip of the postorbital on the orbital margin (postorbital region)**
- 15. most-anterior point of the antorbital fenestra (preorbital region)***
16. dorsal contact between postorbital and squamosal (postorbital region)
17. posteroventral corner of the quadratojugal (postorbital region)*
18. posteroventral tip of the squamosal posterior process (postorbital region)*
19. most-ventral point of the orbit (postorbital region)
- 20. posterior tip of the lacrimal on the orbital margin (postorbital region)**
- 21. *contact of the frontal with the parietal on the skull roof***

3. BIOMECHANICAL AND ECOLOGICAL PARAMETERS

The respective skull lengths and depths were estimated with help of the program tpsDig2 (Rohlf 2005) using the measure mode. The skull length was measured from the anterior tip of the premaxilla to the posterior end of the quadratojugal. The skull depth was measured at the height of the orbit. The average maximum stress was estimated using the data from Rayfield (2011). To estimate the skull strength indicator (SSI) the original data from Henderson (2002) were used to calculate a regression between skull depth and SSI (see Fig. S5.1). The estimated average maximum stress based on a regression of the original data from Rayfield (2011) (see Fig. S5.2).

Table S5.2. List of taxa used for the functional and ecological analyses with relevant parameters. C carnivorous; H herbivorous; O omnivorous (herbivorous and omnivorous taxa are summarized in non-carnivorous taxa); G generalist; W weak-biting; S strong-biting.

Taxon	Average				Diet	Feeding ecology
	Skull lengths (cm)	maximum stress (N/m ²)	Skull depth (cm)	Skull strength indicator		
<i>Euparkeria</i>	8.1	141.2	2.8	0.6	C	G
<i>Lesothosaurus</i>	6.4	107.4	2.4	0.5	O	G
<i>Massospondylus</i>	15.0	288.3	6.3	3.8	O	G
<i>Plateosaurus</i>	32.2	698.3	8.4	7.2	O	G
<i>Herrerasaurus</i>	29.7	636.1	8.8	7.9	C	G
<i>Eoraptor</i>	13.5	254.5	5.2	2.5	O	G
<i>Daemonosaurus</i>	13.4	251.2	6.9	4.7	C	G
<i>Syntarsus</i>	20.7	418.2	5.4	2.7	C	W
<i>Coelophysis</i>	21.0	425.0	7.4	5.5	C	W
<i>Zupaysaurus</i>	44.7	1023.6	13.3	19.4	C	W
<i>Limusaurus</i>	10.0	179.4	6.1	3.6	H	W
<i>Ceratosaurus</i>	68.8	1688.8	23.2	65.6	C	S
<i>Carnotaurus</i>	57.7	1377.3	38.1	193.4	C	S
<i>Majungasaurus</i>	55.7	1320.9	28.0	98.8	C	S
<i>Monolophosaurus</i>	66.6	1625.9	20.6	50.8	C	G
<i>Spinosaurid</i>	78.2	1958.1	22.0	58.4	C	W
<i>Sinraptor</i>	83.2	2104.5	30.0	114.9	C	S
<i>Acrocanthosaurus</i>	129.0	3506.4	50.9	363.8	C	S
<i>Allosaurus</i>	66.0	1608.3	23.3	66.4	C	S
<i>Guanlong</i>	33.2	724.6	9.0	8.3	C	G
<i>Dilong</i>	18.7	371.6	6.1	3.5	C	G
<i>Bistahieversor</i>	99.2	2584.6	30.6	119.9	C	S
<i>Alioramus</i>	62.0	1497.2	15.0	25.4	C	G
<i>Daspletosaurus</i>	103.4	2710.7	35.2	162.9	C	S
<i>Gorgosaurus</i>	102.3	2676.3	31.6	128.5	C	S
<i>Tarbosaurus</i>	127.1	3445.8	34.7	158.1	C	S
<i>Tyrannosaurus</i>	123.9	3347.0	51.1	366.0	C	S
<i>Compsognathus</i>	9.3	165.1	2.9	0.7	C	W
<i>Garudimimus</i>	24.8	514.7	9.9	10.2	H	W
<i>Gallimimus</i>	28.2	599.7	10.0	10.5	H	W
<i>Ornithomimus</i>	21.2	428.8	7.9	6.2	H	W
<i>Erlikosaurus</i>	21.3	432.8	6.6	4.2	H	G

<i>Conchoraptor</i>	8.7	152.4	4.1	1.5	O	S
<i>Citipati</i>	13.4	252.3	6.3	3.8	O	S
<i>Oviraptor</i>	17.1	335.4	7.9	6.2	O	S
<i>Archaeopteryx</i>	3.0	44.8	1.2	0.1	O	W
<i>Confuciusornis</i>	6.7	133.2	2.8	0.6	O	G
<i>Anchiornis</i>	5.4	87.3	3.0	0.8	O	W
<i>Sinornithosaurus</i>	13.7	258.5	4.5	1.9	C	G
<i>Bambiraptor</i>	11.2	205.3	3.7	1.2	C	G
<i>Velociraptor</i>	25.4	530.4	7.3	5.3	C	G
<i>Pengornis</i>	-	-	-	-	O	W
<i>Shenquiornis</i>	-	-	-	-	O	W
<i>Shuvuuia</i>	-	-	-	-	O	W

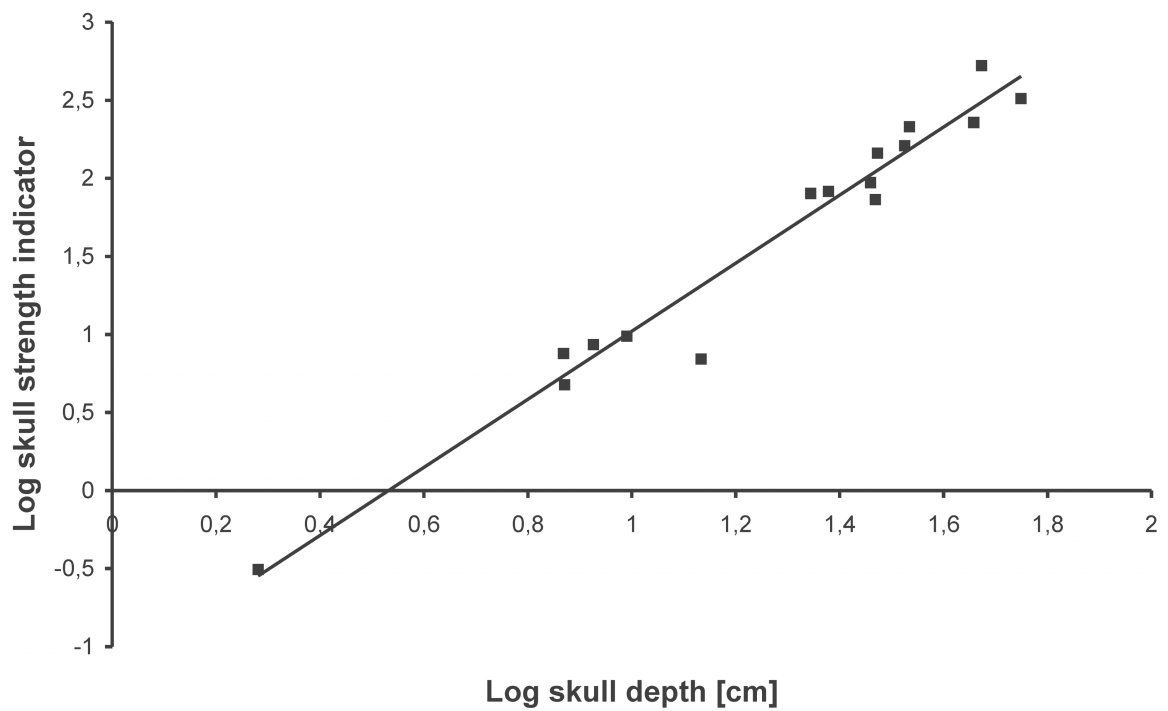


Fig. S5.1. Correlation between skull depth and skull strength indicator ($\text{LogSSI} = 2.18 \text{LogSD} - 1.1602$, $R^2 = 0.963$, p value < 0.001) (based on the data set from Henderson 2002).

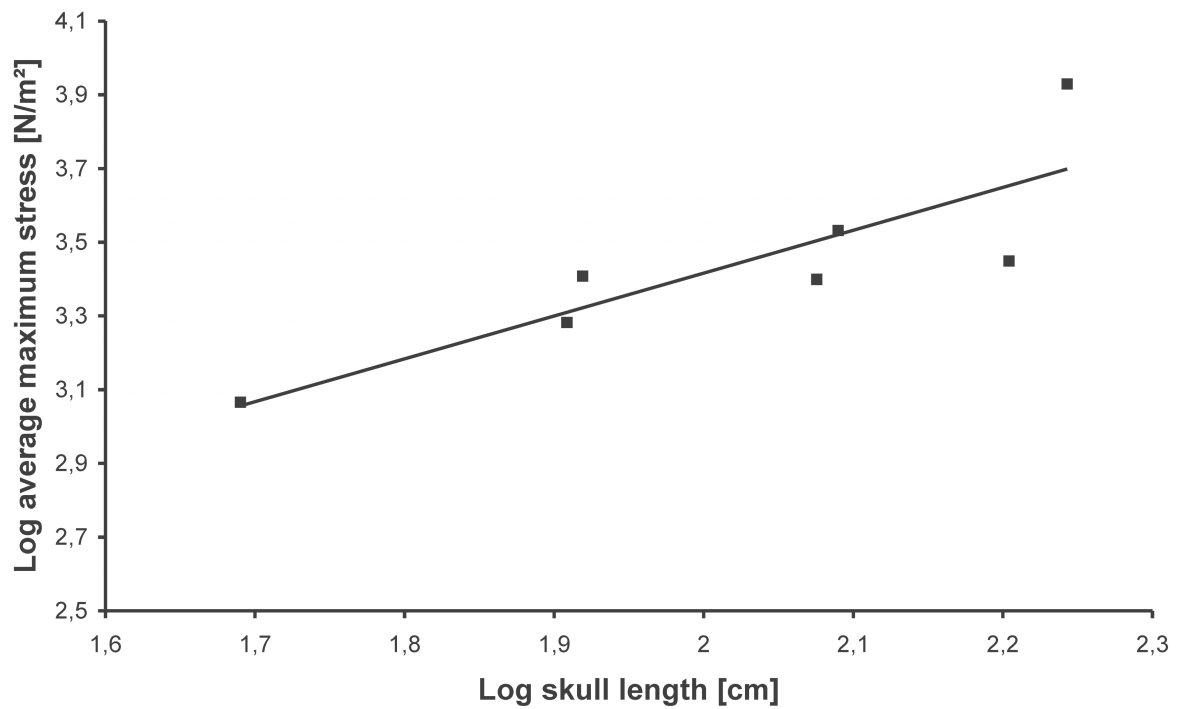


Fig. S5.2. Correlation between skull length and average maximum stress ($\text{LogAMS} = 1.16 \text{LogSL} - 1.0913$, $R^2 = 0.725$, p value < 0.001) (based on the data set from Rayfield 2011, without a crestless *Monolophosaurus*).

Table S5.3. Correlation of specimen centroid size (log transformed) with Procrustes Coordinates and the first three PC axes.

	R²	p value
Procrustes Coordinates (large data set)	0.159	<0.001
Procrustes Coordinates (small data set – Paraves)	0.140	<0.001
PC 1 (large data set)	0.166	0.007
PC 1 (small data set – Paraves)	0.083	0.335
PC 2 (large data set)	0.452	<0.001
PC 2 (small data set – Paraves)	0.169	0.147
PC 3 (large data set)	0.163	0.009
PC 3 (small data set – Paraves)	0.139	0.188

4. PHYLOGENY AND CLUSTER TOPOLOGIES

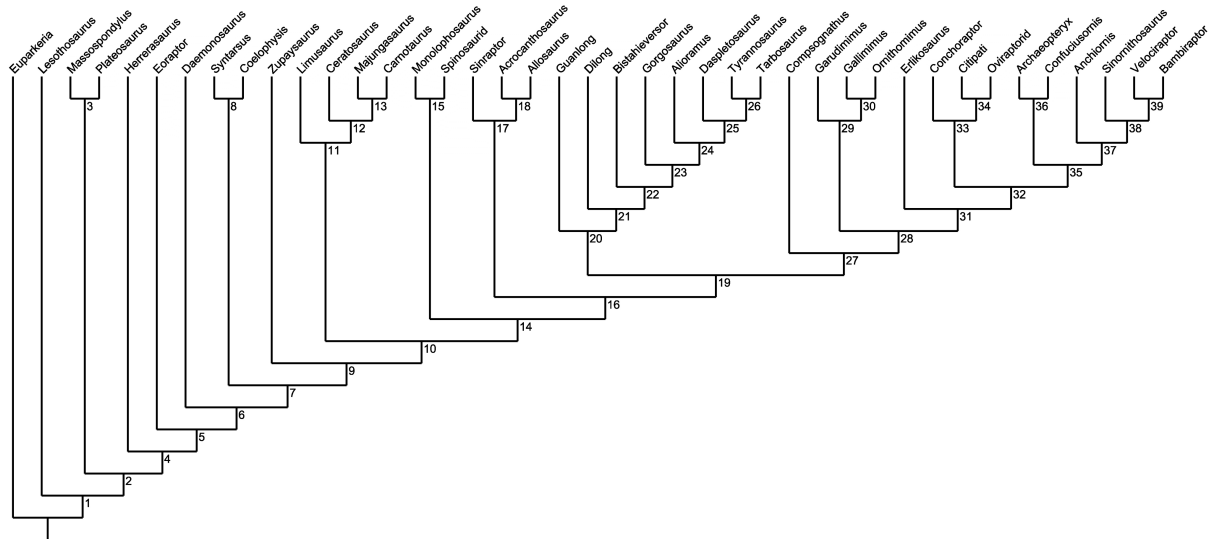


Fig. S5.3. Topology of the informal supertree used in all phylogenetic comparative analyses based on the large data set. 1 Dinosauria; 2 Saurischia; 3 Sauropodomorpha; 4 Theropoda; 7 Neotheropoda; 8 Coelophysidae; 10 Averostra; 11 Ceratosauria; 13 Abelisauridae; 14 Tetanurae; 15 Megalosauroida; 16 Neotetanurae; 17 Allosauroidae; 19 Coelurosauria; 20 Tyrannosauroida; 23 Tyrannosauridae; 27 Maniraptoriformes; 28 Maniraptora; 31 Clade A; 32; Averoimia; 33 Oviraptoridae; 35 Paraves; 36 Avialae; 37 Deinonychosauria; 38 Dromaeosauridae.

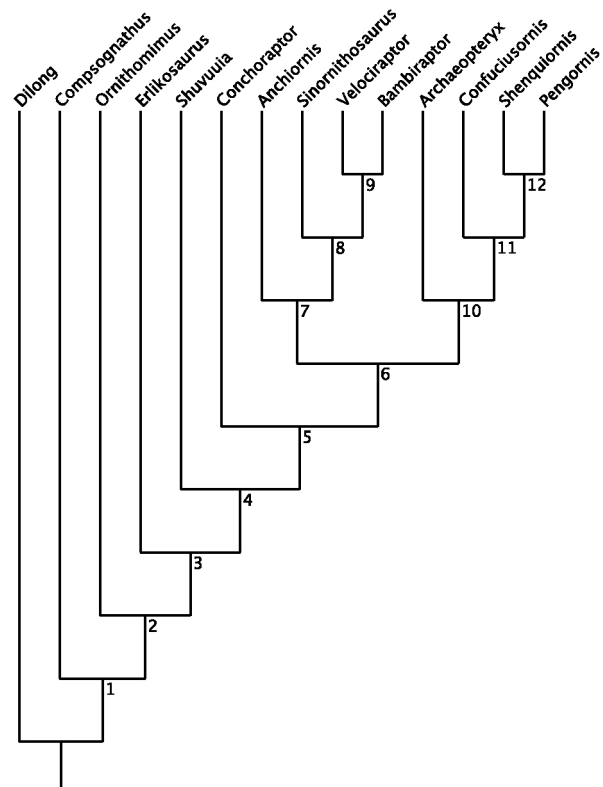


Fig. S5.4. Topology of the informal supertree used for the small data set. 2 Maniraptoriformes; 3 Maniraptora; 5 Aviremigia; 6 Paraves, 7 Deinonychosauria; 8 Dromaeosauridae; 10 Avialae; 11 Pygostylia; 12 Enantiornithes

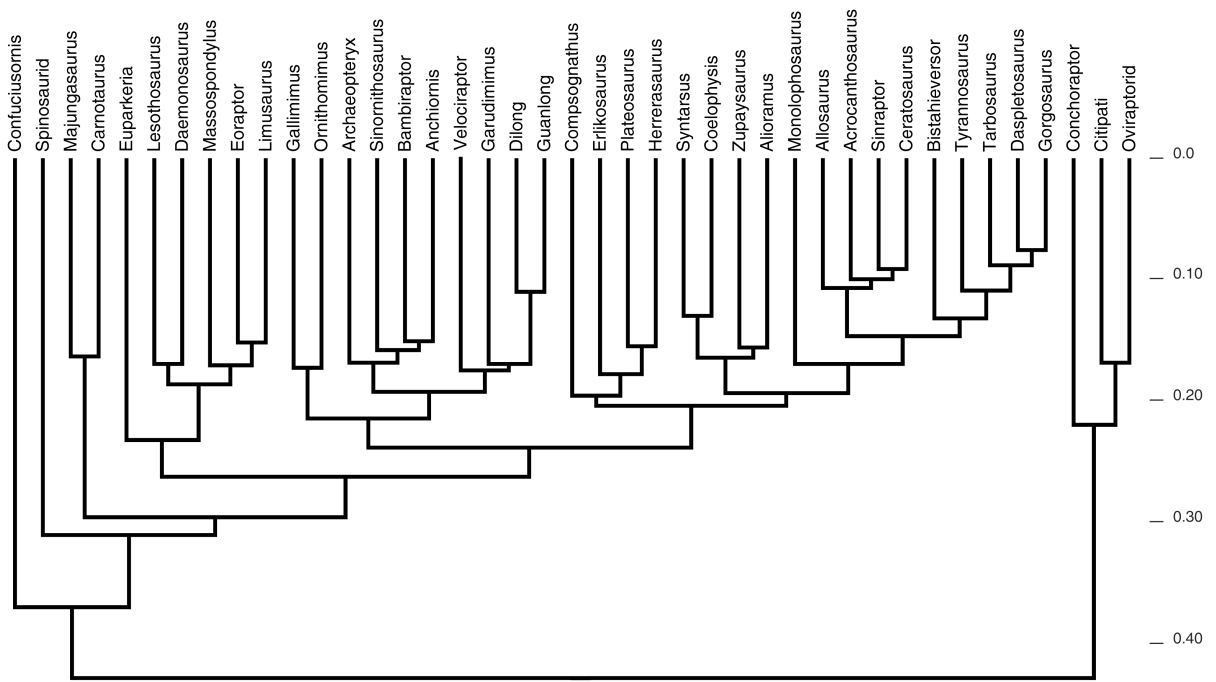


Fig. S5.5. UPGMA Cluster based on morphometric data. Numbers on the right side represent the distance.

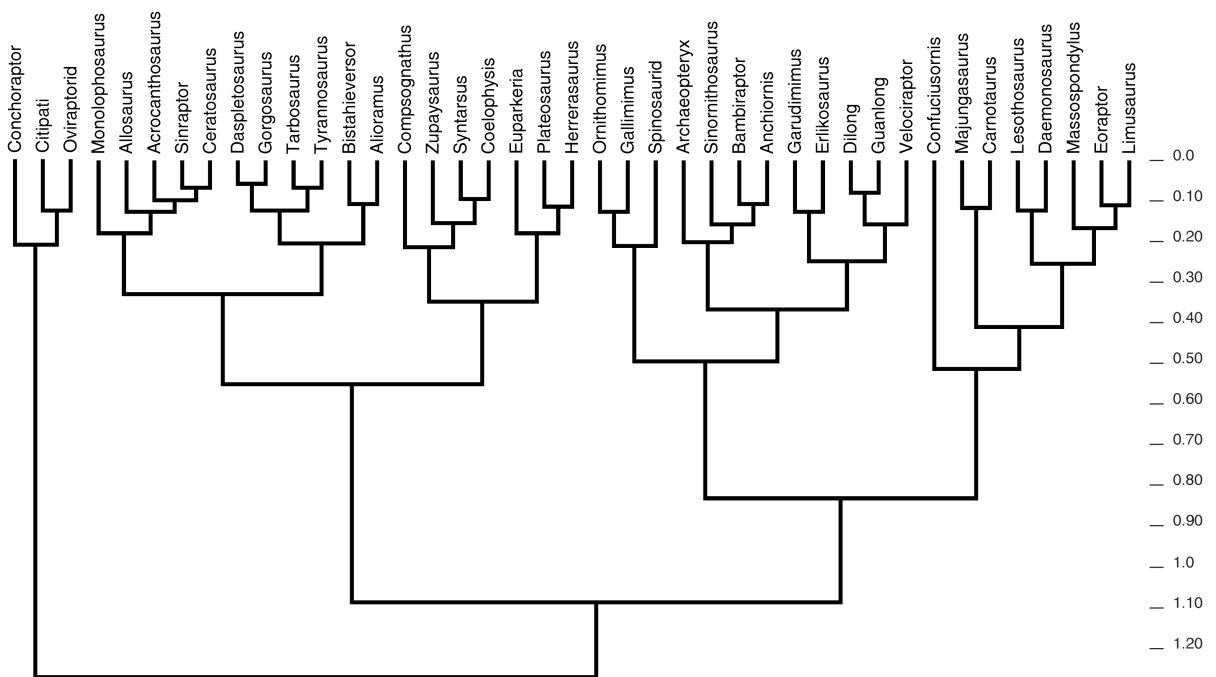


Fig. S5.6. Ward Cluster based on morphometric data. Numbers on the right side represent the distance.

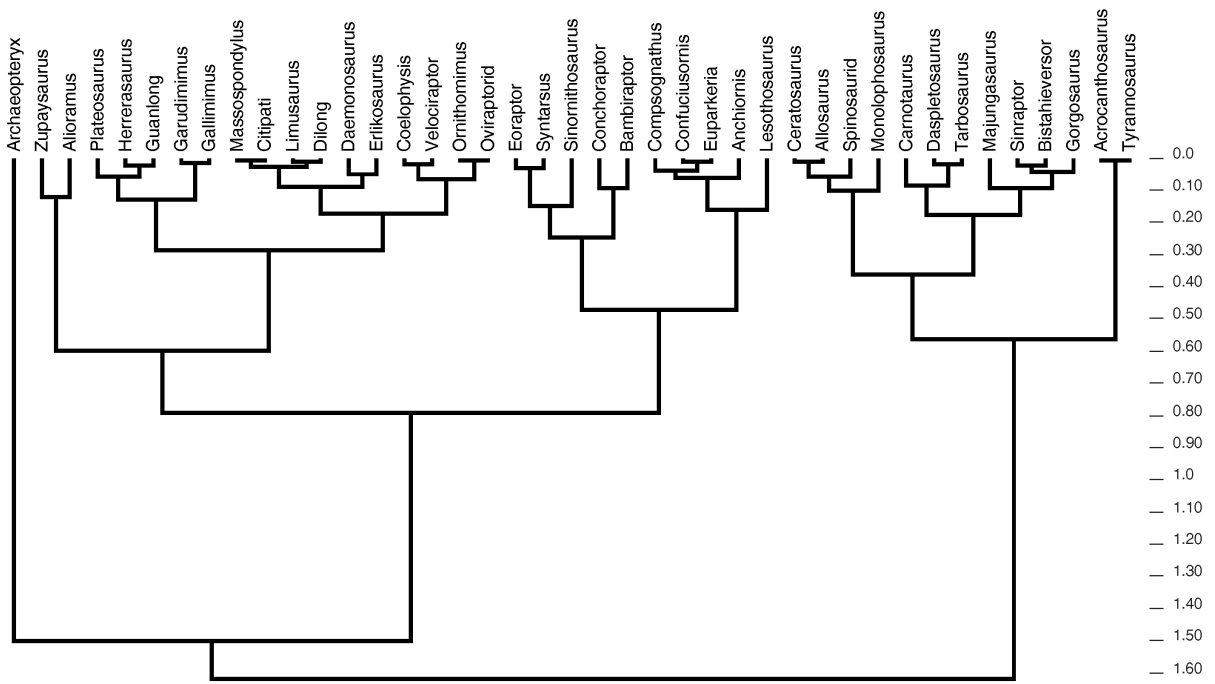


Fig. S5.7. UPGMA cluster based on skull strength indicator (log transformed). Numbers on the right side represent the distance.

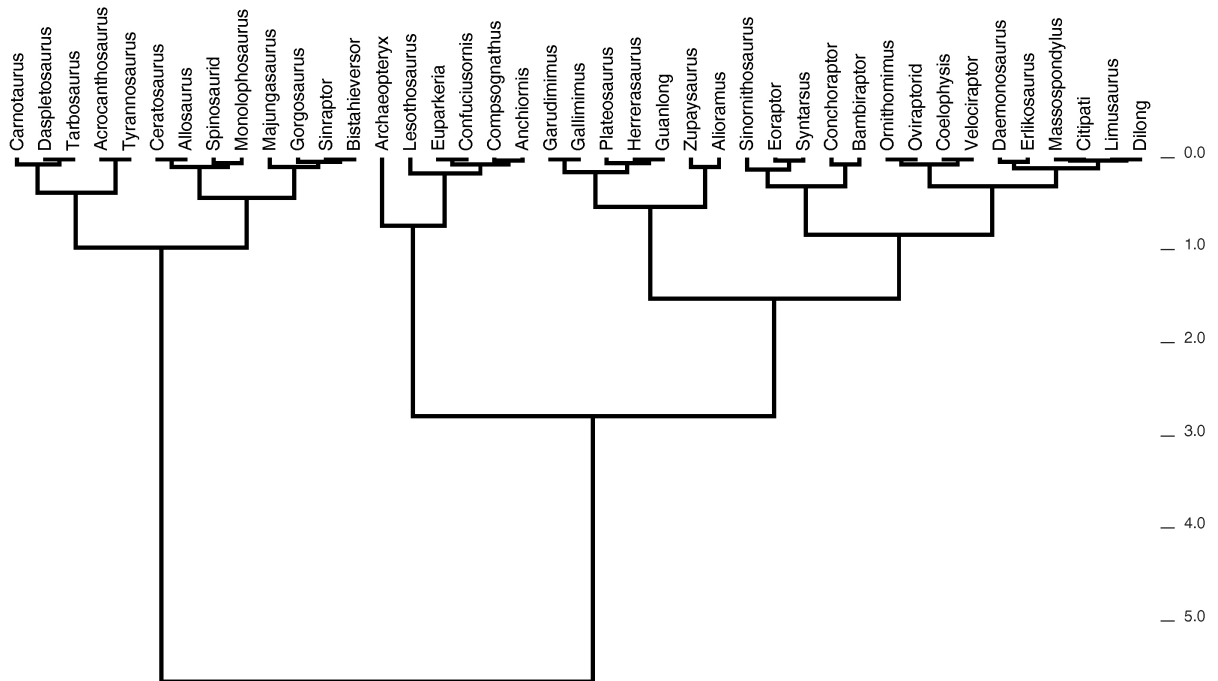


Fig. S5.8. Ward cluster based on skull strength indicator (log transformed). Numbers on the right side represent the distance.

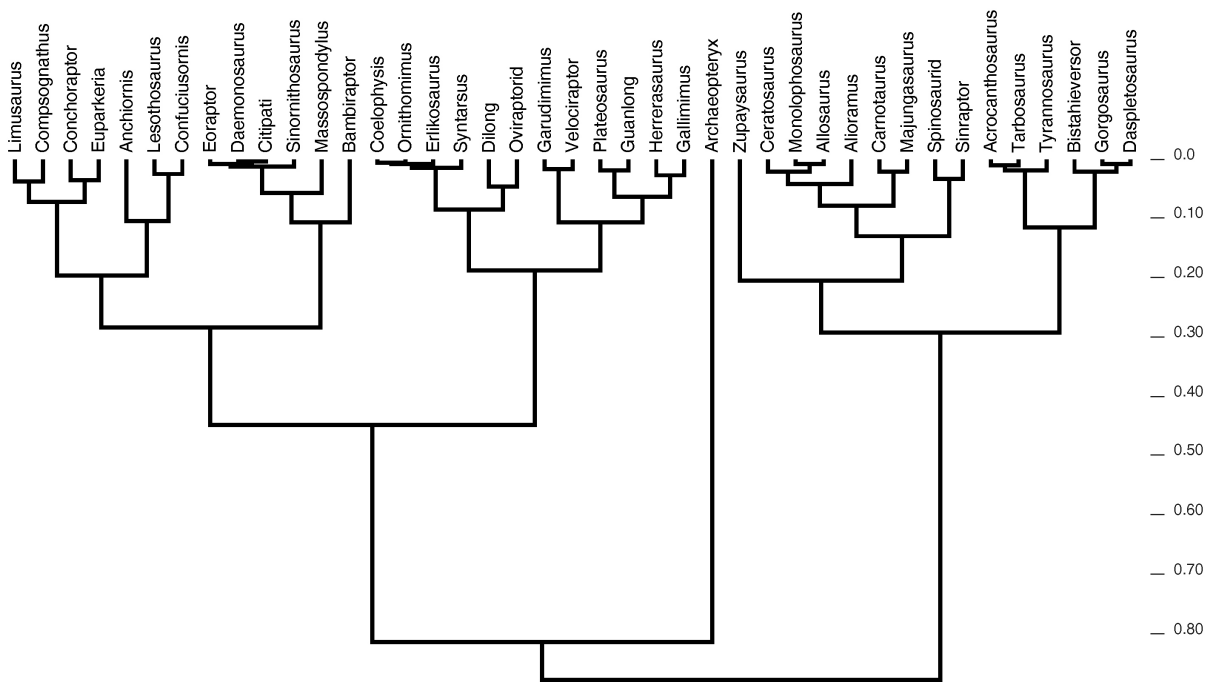


Fig. S5.9. UPGMA cluster based on average maximum stress (log transformed). Numbers on the right side represent the distance.

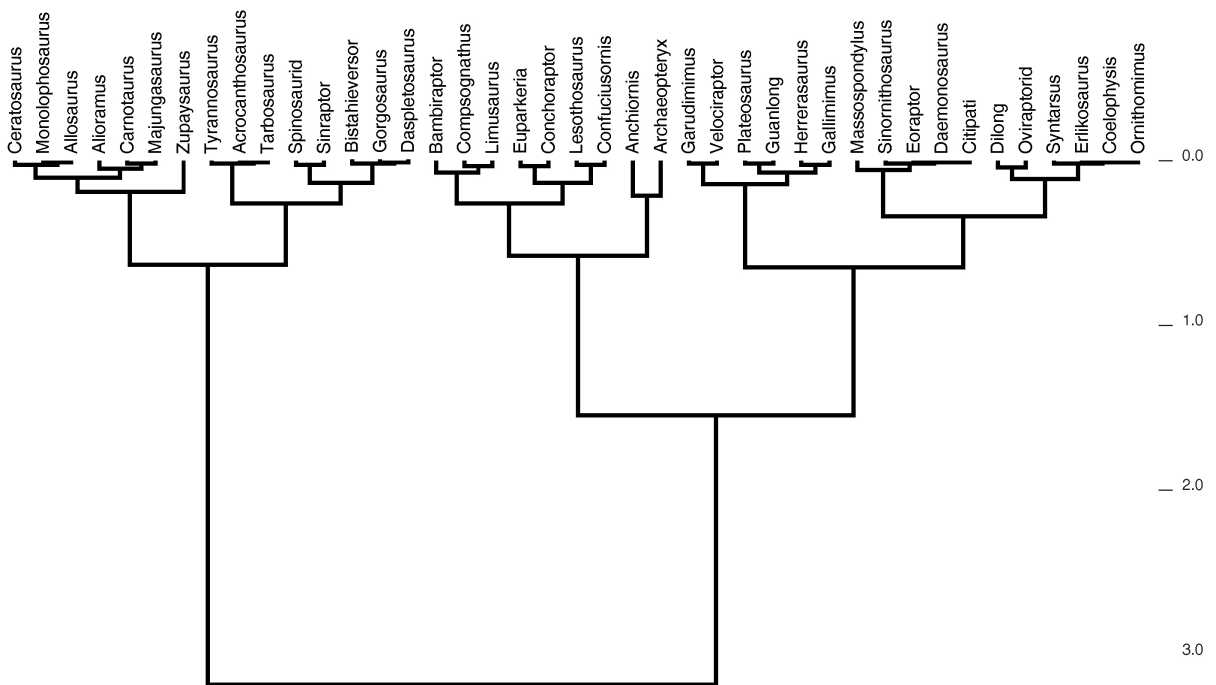


Fig. S5.10. Ward cluster based on average maximum stress (log transformed). Numbers on the right side represent the distance.

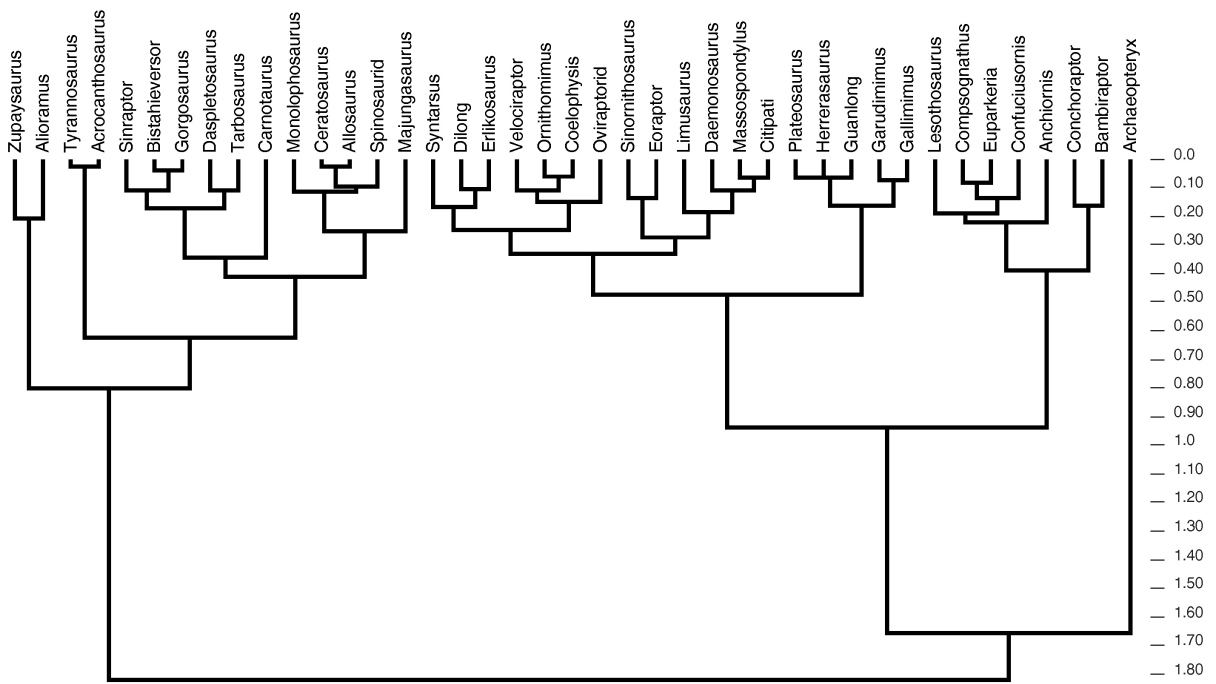


Fig. S5.11. UPGMA cluster based on skull strength indicator and average maximum stress (both log transformed). Numbers on the right side represent the distance.

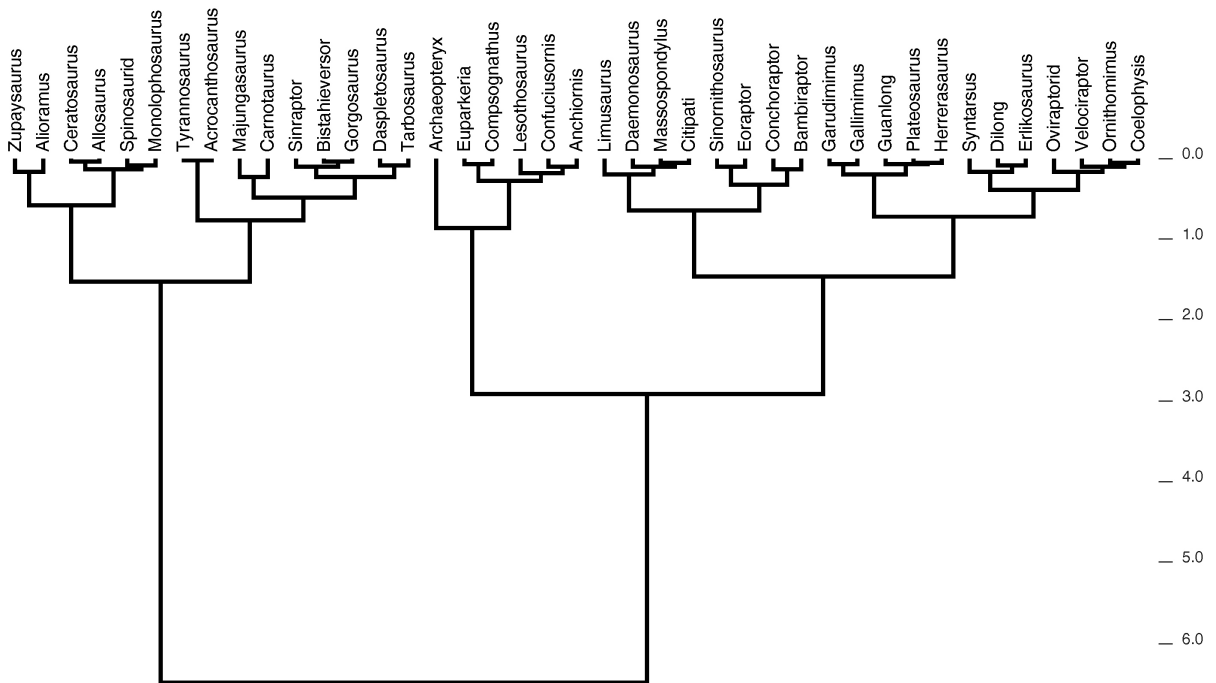


Fig. S5.12. Ward cluster based on skull strength indicator and average maximum stress (both log transformed). Numbers on the right side represent the distance.

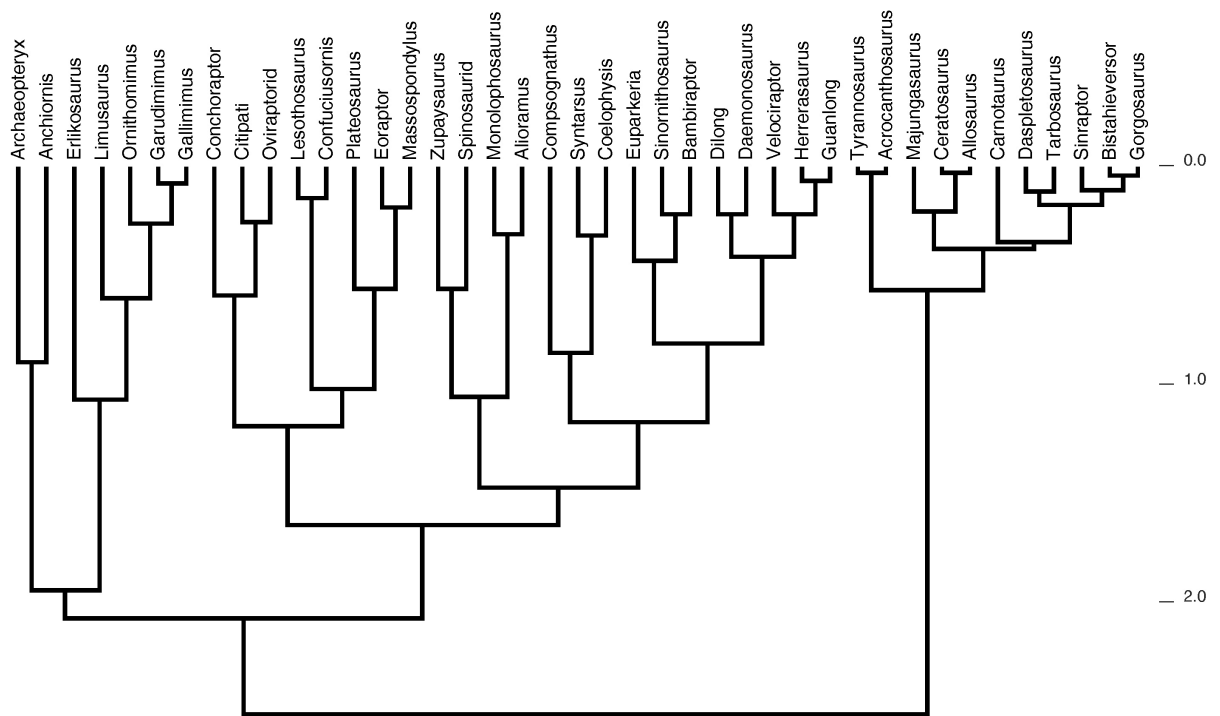


Fig. S5.13. UPGMA cluster based on feeding ecology, skull strength indicator and average maximum stress (both log transformed). Numbers on the right side represent the distance.

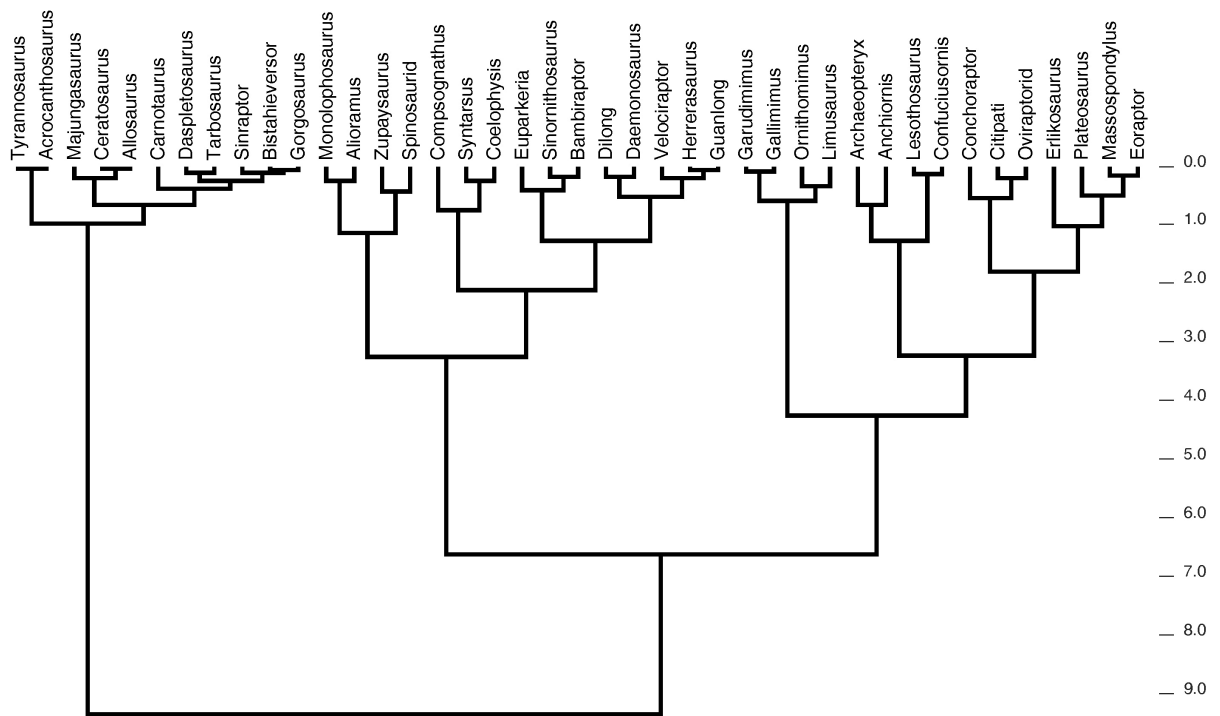


Fig. S5.14. Ward cluster based on feeding ecology, skull strength indicator and average maximum stress (both log transformed). Numbers on the right side represent the distance.

**5. PHYLOGENETIC SIGNALS OF FUNCTIONAL PROXIES (SSI AND AMS) AND
DIAGNOSTIC TEST FOR PIC ANALYSIS**

Both morphometric data and functional factors (SSI and AMS) show a phylogenetic signal (Fig. S5.15, Table 5.4). After transforming the scores into PIC values, we first analysed if they fulfil the four criteria listed in the materials and methods section (Table S5.4). Here, PC 1 and 2 as well as SSI and AMS show no significant correlations. For PC 3 a correlation is present for the fourth criterion (estimated node values vs. the corrected node high). However, as the fourth test indicates primarily evolutionary trends and it is not strictly diagnostic (Midford et al. 2005), all scores can be modelled as random walk with a uniform rate of change, and thus, fulfil the assumptions for PIC analyses. In contrast, the SSI based on Henderson's (2002) original data poses a significant correlation with the first criterion (standard deviation). However, this could be the result of the small sample size.

Table S5.4. Diagnostic test of the contrasts of PC, logSSI and logAMS scores. Degree of correlation and significance are given by R^2 and p value. * represents the small data set which includes only the original data from Henderson et al. (2002).

	Standard deviation	PIC node value	PIC node high	PIC node value vs. PIC node high
PC 1	0.009/0.554	0.035/0.245	0.002/0.794	0.02/0.388
PC 2	0.009/0.564	0.0003/0.921	0.0022/0.773	0.022/0.357
PC 3	0.032/0.266	0.056/0.14	0.022/0.366	0.563/<0.001
logSSI	0.0004/0.897	0.08/0.077	0.007/0.621	0.026/0.322
logAMS	0.052/0.156	0.175/0.007	0.002/0.788	0.003/0.626
PC 1*	0.048/0.496	<0.001/0.927	0.339/0.047	0.010/0.761
PC 2*	0.377/0.034	0.291/0.070	<0.001/0.995	0.051/0.479
PC 3*	0.100/0.316	<0.001/0.970	<0.001/0.983	0.543/0.006
logSSI*	0.438/0.019	0.251/0.097	0.032/0.580	0.177/0.174

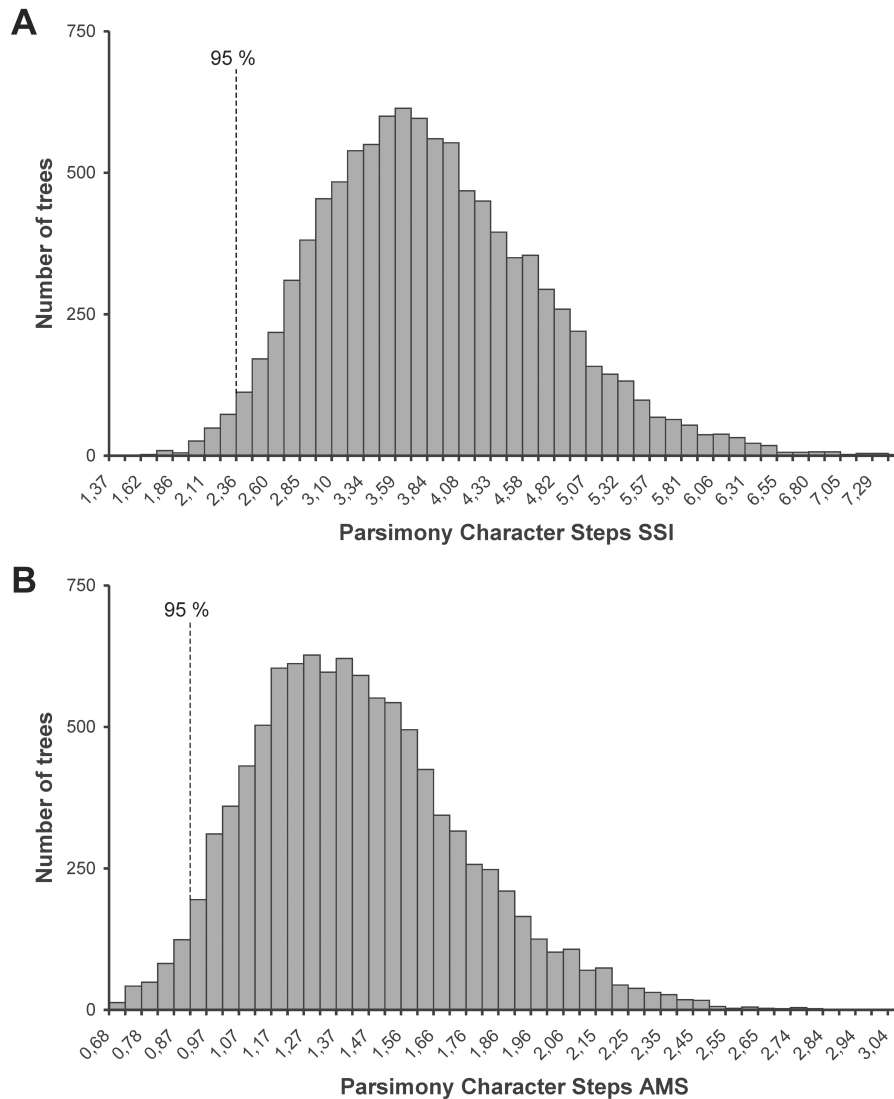


Fig. S5.15. Results from the permutation test for morphofunctional proxies skull strength indicator (SSI) and average maximum stress (AMS). **A.** Permutation of the skull strength character (logarithmic transformed) showing that the squared length of the supertree (= 0.987) is smaller than in 95 % of the 10 000 simulated tree topologies indicating that the skull strength indicator is phylogenetic constrained. The asterisk marks the 95% border. **B.** Permutation of the average maximum stress character (logarithmic transformed) showing that the squared length of the supertree (= 0.685) is smaller than in 95 % of the 10 000 simulated tree topologies indicating that the bite force is phylogenetic constrained.

SUPPLEMENTARY INFORMATION OF CHAPTER 6

Macroevolutionary and morphofunctional patterns in theropod skulls: a morphometric approach

1. Methods: UV photography
2. Additional information on *Sciurumimus*
3. Ontogenetic stage of the specimen
4. Phylogenetic analysis
5. Comparison with *Juravenator starki*
6. Comparisons with other Jurassic theropods
7. Additional discussion of soft tissues
8. Repository of the specimen

***All figures of the supplementary information of Chapter 6 are modified after Rauhut et al. (2012)**

1. METHODS: UV PHOTOGRAPHY

Most fossil skeletal remains and sometimes mineralized soft parts from the Upper Jurassic plattenkalks of southern Germany and from the Middle to Late Mesozoic localities of Northeastern China are fluorescent under ultraviolet radiation. In most cases, this fluorescence allows a more precise investigation of morphological details of skeletal remains as well as soft parts. Delicate skeletal elements and remains of soft parts are poorly or not discernable in visible light but shine conspicuously under filtered UV. The technique can be used to differentiate bone sutures from cracks, more clearly establish outlines of compressed skeletal elements, and to separate bones or soft parts from the underlying matrix or each other.

During the past 10 years, one of us (Helmut Tischlinger) has considerably improved ultraviolet investigation techniques and ultraviolet-light photography of fossils from Solnhofen and Solnhofen-type-Lagerstaetten as well as from the Middle Jurassic to Early Cretaceous lacustrine deposits of the Jinlingsi and Jehol Group, Northeastern China, using powerful UV lamps and new photographic documentation techniques (Tischlinger 2002, 2005a, b; Tischlinger & Unwin 2004; Arratia & Tischlinger 2010; Tischlinger & Frey 2010; Hone et al. 2010; Kellner et al. 2010; Schweigert et al. 2010). For our investigations we predominantly use UVA lamps with a wavelength of 365-366 nanometers.

Sometimes essential details of bones and soft parts are poorly or not visible even under UV light with the naked eye or even under a microscope, and can exclusively be demonstrated by ultraviolet-light photography. The application of different filters allows a selective visualisation of peculiar fine structures. In most cases a selection of

different colour correction filters is necessary. Each limestone slab and bone or tissue will react differently to different light wavelengths and is captured differently with varying exposures and filters. The right combination is needed to highlight the area of interest. The optimum filtering and exposure time has to be tested in a series of experiments (Tischlinger 2002). The number and combination of filters varies greatly and exposure times vary between 1 second and some minutes, depending on the nature of the fossil material and the magnification, intensity, and incident angle of the ultraviolet lamps. Filtering works optimally with analogue photography using slide films, although digital cameras can be used, too.

2. ADDITIONAL INFORMATION ON *SCIURUMIMUS*

HISTORY OF FIND AND PREPARATION

The specimen was found during systematic excavations in the Rygol Quarry at Painten, Bavaria, Germany. First bony elements of the central area of the body appeared after cleaning on the floor of the excavation area, so the slab with the skeleton was excavated and brought into the lab for preparation. In the lab, the upper surface (the one exposed in the quarry) was stabilized with a ceramic glue (Uniflott) and fixed to another slab. Then, the specimen was mechanically prepared from the underside. Damaged areas were reconstructed with Keraquick, which is clearly visible under UV light. Loose bones and sections were glued onto the specimen, but no arrangement or orientation of bones was changed. The specimen was studied by one of us (Helmut Tischlinger) prior to preparation, so that there can be no doubt about its authenticity.

Table S6.1. Selected measurements of *Sciurumimus albersdoerferi*

Body part	Length
Total length of skeleton	719 mm
Skull length	79 mm
Posterior skull height:	c. 32 mm
Length of orbit	19.7 mm
Height of orbit	21.5 mm
Length of mandible	73.2 mm
Length of cervical series	69 mm
Length of dorsal series	102 mm
Length of sacrum	37.25 mm
Length of preserved caudal series	432 mm
Length of humerus	26.8 mm
Length of radius	17 mm
Length of metacarpal II	11 mm
Length of femur	50.6 mm
Length of tibiotarsus	54.2 mm
Length of metatarsal III	32.1 mm

3. ONTOGENETIC STAGE OF THE SPECIMEN

Although no histological sampling is possible in this unique specimen, several lines of evidence indicate that the holotype is an early juvenile, probably early posthatchling individual. First, there is no fusion of any skeletal elements in the skeleton. In the vertebral column, the neurocentral sutures of the cervical, dorsal and at least anterior caudal vertebrae are open, and the neural arches even have slightly disarticulated from the centra in at least some elements. The sacral centra are preserved in articulation, but the posterior two sacrals are displaced ventrally from the anterior end of the sacrum, demonstrating that there is neither fusion of the sacral vertebrae with each other, nor of the sacral ribs with the ilium. Although the pattern of neurocentral suture closure varies within dinosaurs (Irmis 2007), the lack of fusion in all vertebrae, with the possible

exception of the distalmost caudals (which are already closed in hatchling crocodiles; Brochu 1996), clearly indicates that the specimen of *Sciurumimus* is an immature individual. This is furthermore supported by disarticulation in other elements that usually show very tight sutures or even fusion in theropods, such as the basioccipital and exoccipital, or the distal ischium. Likewise, several skeletal elements, such as the carpal and distal tarsal bones show poor ossification and several joint surfaces, including the proximal articular end of the humerus, exhibit strongly porous surfaces, indicating poorly ossified articular ends.

Another indicator of the early juvenile stage of *Sciurumimus* is found in the surface structure of basically all bony elements. Both dermal and enchondral elements show a coarsely striated surface (Fig. S6.1, S6.2). Such a surface structure corresponds to bone texture type I of Tumarkin-Deratzian et al. (2006). According to these authors, in birds, this texture occurs only in individuals of 50 % or less skeletal maturity, and hatching-year birds only exhibit this type of texture, as it is the case in *Sciurumimus*. Bone surface textures were found to be useful as ontogenetic indicator in a number of fossil amniotes (summary in Tumarkin-Deratzian 2009) and thus this represents an independent indication of an early ontogenetic stage for the specimen.



Fig. S6.1. Lateral side of the left dentary of *Sciurumimus*, showing striated bone surface texture.

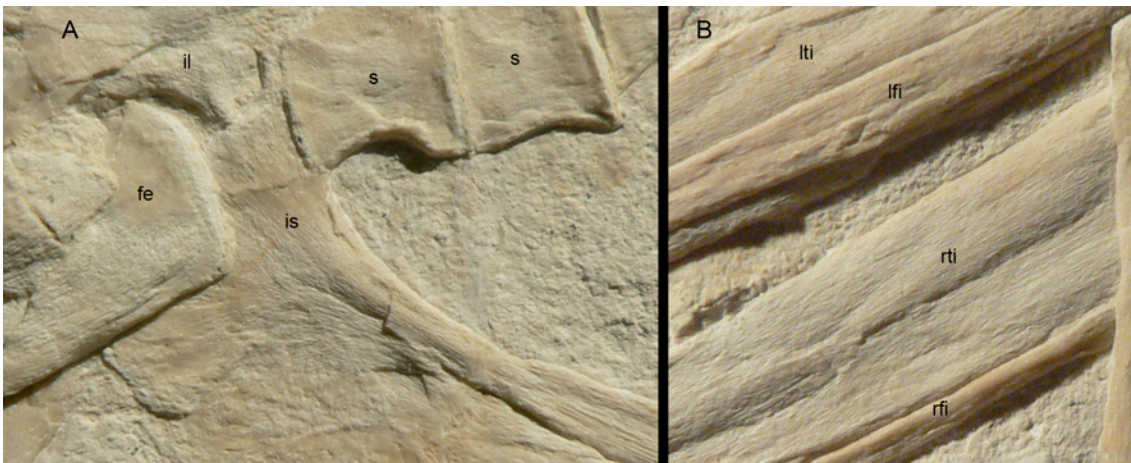


Fig. S6.2. Striated bone surface texture in sacral vertebrae and pelvic and limb elements of *Sciurumimus*.

A, Ischial peduncle of the left ilium, posterior sacral vertebrae, proximal end of femur and ischium. B, tibiae and fibulae. Abbreviations: fe, femur; il, ilium; is, ischium; lfi, left fibula; lti, left tibia; rfi, right fibula; rti, right tibia; s, sacral vertebra.

Finally, the maxillary dentition of *Sciurumimus* shows a conspicuous pattern of fully erupted teeth intercalated with empty tooth positions. A very similar pattern in

Scipionyx was interpreted as an indication that no complete wave of tooth replacement has occurred by Dal Sasso & Signore (1998), again indicating an early post-hatchling stage for the animal. If the presence of a frontoparietal gap can be substantiated by future studies, this would represent a further argument for regarding the specimen as an early post-hatchling individual (Dal Sasso & Maganuco 2011).

Given this early ontogenetic stage of the type specimen of *Sciurumimus*, the small size of the latter does not necessarily indicate that this taxon was a small theropod as an adult. Indeed, a hatchling *Allosaurus* maxilla described by Rauhut & Fechner (2005) is considerably smaller (23 mm) than the same element in *Sciurumimus* (42 mm), although *Allosaurus* grows to sizes in excess of seven metres. Thus, unless *Sciurumimus* had a strongly reduced growth rate, as it is the case in island dwarf sauropods (Sander et al. 2006 Stein et al. 2010), this taxon probably grew to adult sizes in excess of five meters, as it is the case in other megalosaurids.

4. PHYLOGENETIC ANALYSIS

To establish the phylogenetic position of the new taxon, we coded it into three recent phylogenetic analyses. Two of these, those of Smith et al. (2008) and of Choiniere et al. (2010) were chosen because they are among the largest theropod analysis published so far, including a high number of characters and a taxon sampling that represents all major groups of non-avian theropods. Both of these analyses depicted *Sciurumimus* consistently as a basal tetanuran, though with rather poor resolution at the base of this clade and somewhat differing results (see below). Therefore, we ran a third analysis, using the most comprehensive matrix on basal tetanurans published so far, that of

Benson et al. (2010). The results of the latter analysis were used for the phylogenetic placement of the new taxon presented in the main manuscript.

Given the juvenile status of the specimen, one important question is, of course, the possible affect of ontogenetically variable characters on its phylogenetic position. Clearly age-dependant characters, such as fusion of skeletal elements, were coded as “?” for *Sciurumimus* in all analysis. Furthermore, in addition to the analyses reported on below, we ran additional analyses of the three data matrices with all characters we considered to be potentially variable with ontogeny (characters concerning cranial ornamentation [crests, rugosities], orbit shape and size, morphometric ratios between different elements or between different structures within one element, development of muscle attachments) coded as “?” for *Sciurumimus*. Although this considerably increased the amount of missing data in *Sciurumimus*, the phylogenetic results remained the same as those reported below.

ANALYSIS BASED ON SMITH ET AL. (2008)

Smith et al. (2008) presented a phylogenetic analysis of six outgroup and 51 neotheropod ingroup taxa, plus one single specimen from the Early Cretaceous of Australia, coded across 353 morphological characters. This matrix is a slightly expanded version of the matrix of Smith et al. (2007) and includes a wide array of non-avian theropods, from coelophysoids to paravians, though with emphasis on non-coelurosaurian forms (39 of the ingroup OTUs). We coded *Sciurumimus* in the same matrix, without changes to other codings, and ran the analysis in PAUP* 4.0 (Swofford 2003), using a heuristic search with TBR branch swapping and random addition sequence with 100 replicates. The analysis resulted in the recovery of 3 720 equally

parsimonious trees with a length of 887 steps. The strict consensus of these trees (Fig. S6.3) generally agrees with that found by Smith et al. (2008), though with slightly less resolution within Megalosauroidea (=Spinosauroidea). *Sciurumimus* was found to be the sister taxon to *Monolophosaurus* and Neotetanurae in this analysis. However, only one additional step is needed to place this taxon within Megalosauroidea, whereas a placement within Neotetanurae implies at least six additional steps. Tree support is low, with bootstrap values below 50 for the vast majority of nodes within Theropoda, with the exception of some coelurosaur clades.

Codings for Sciurumimus in the matrix of Smith et al. (2008)

00200[0/1]0101??100?10?000?21000011???00?00?10?1[1/2]0?01????0001000?00????
 00?000?????0121??0??0?100????00000?????????????????0100100?11?1000[0/1]0?11
 ?0110?1110[0/1]?0?0?0120?00?00101????000?10020????000?0010001000000?????
 01[0/1]000000[0/1]0000000?00?011111010110?010010000000??001100?1?[0/1]1?0?0
 ???00?10?00000011?0?1??201?????10?????????00?????????????1100?0?01??1201?00
 00100

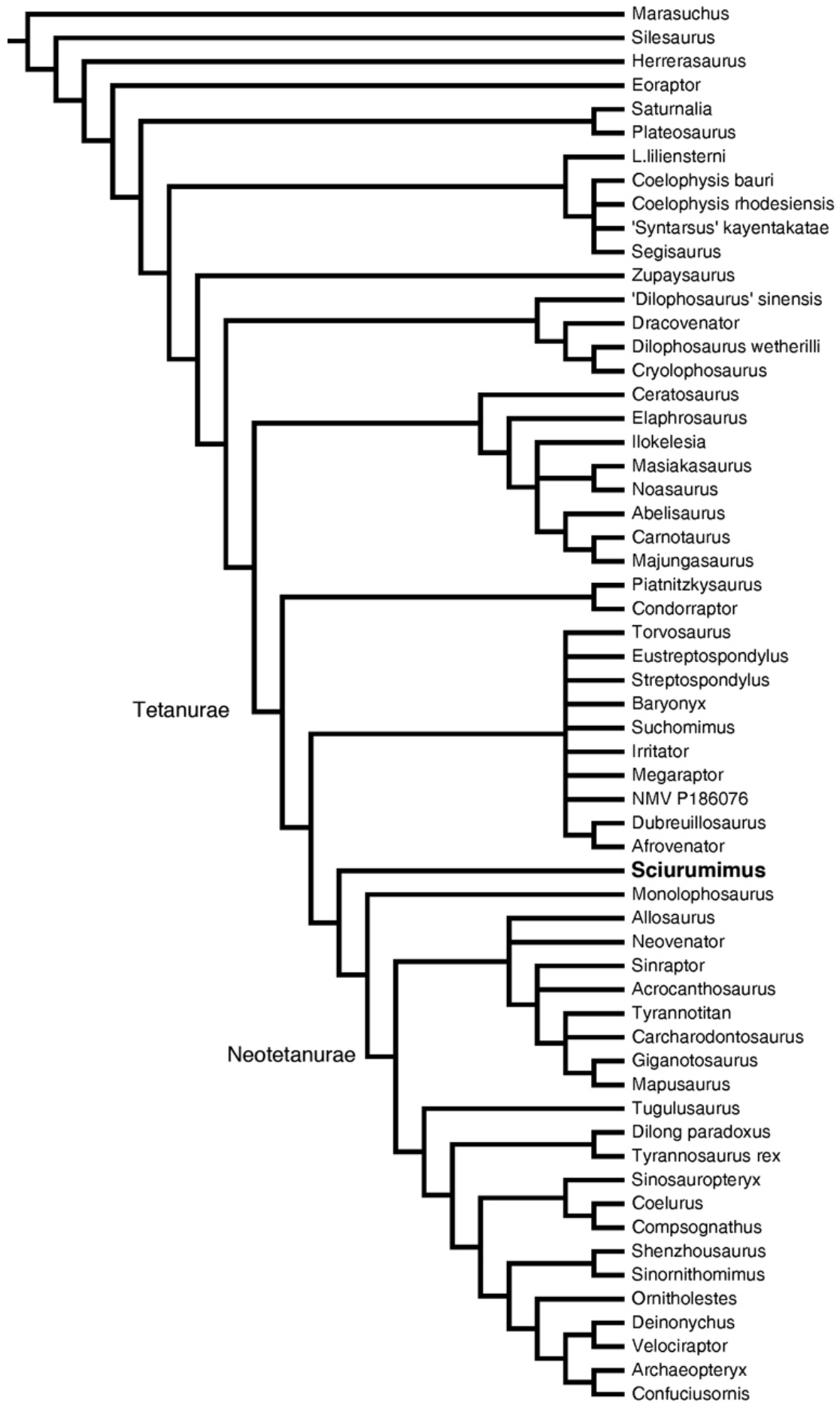


Fig. S6.3. Strict consensus cladogram of the analysis based on Smith et al. (2008).

ANALYSIS BASED ON CHOINIÈRE ET AL. (2010)

In the supplementary information of their paper, Choiniere et al. (2010) presented one of the largest phylogenetic analyses of non-avian theropods published so far, including two outgroup and 92 neotheropodan ingroup taxa, scored across 421 characters. As in the case of the Smith et al. (2008) analysis, this analysis includes a wide array of taxa, but with emphasis on coelurosaurs (71 of the ingroup taxa). *Sciurumimus* was coded for the 421 characters of Choiniere et al. (2010), and the analysis was run in TNT 1.1 (Goloboff et al. 2008), using a heuristic search strategy with random addition sequence, performing 1 000 replicates of Wagner trees, followed by TBR branch swapping. TNT was chosen as analytic program in the case of this matrix, since analysis in PAUP resulted to be prohibitively long. The analysis resulted in 1 210 equally parsimonious trees with a length of 1 866 steps. The strict consensus tree agrees with that found by Choiniere et al. (2010), and *Sciurumimus* was found to be a basal, non-neotetanuran tetanuran, forming a polytomy with *Afrovenator* and a spinosaurid-*Torvosaurus* clade (Fig. S6.4).

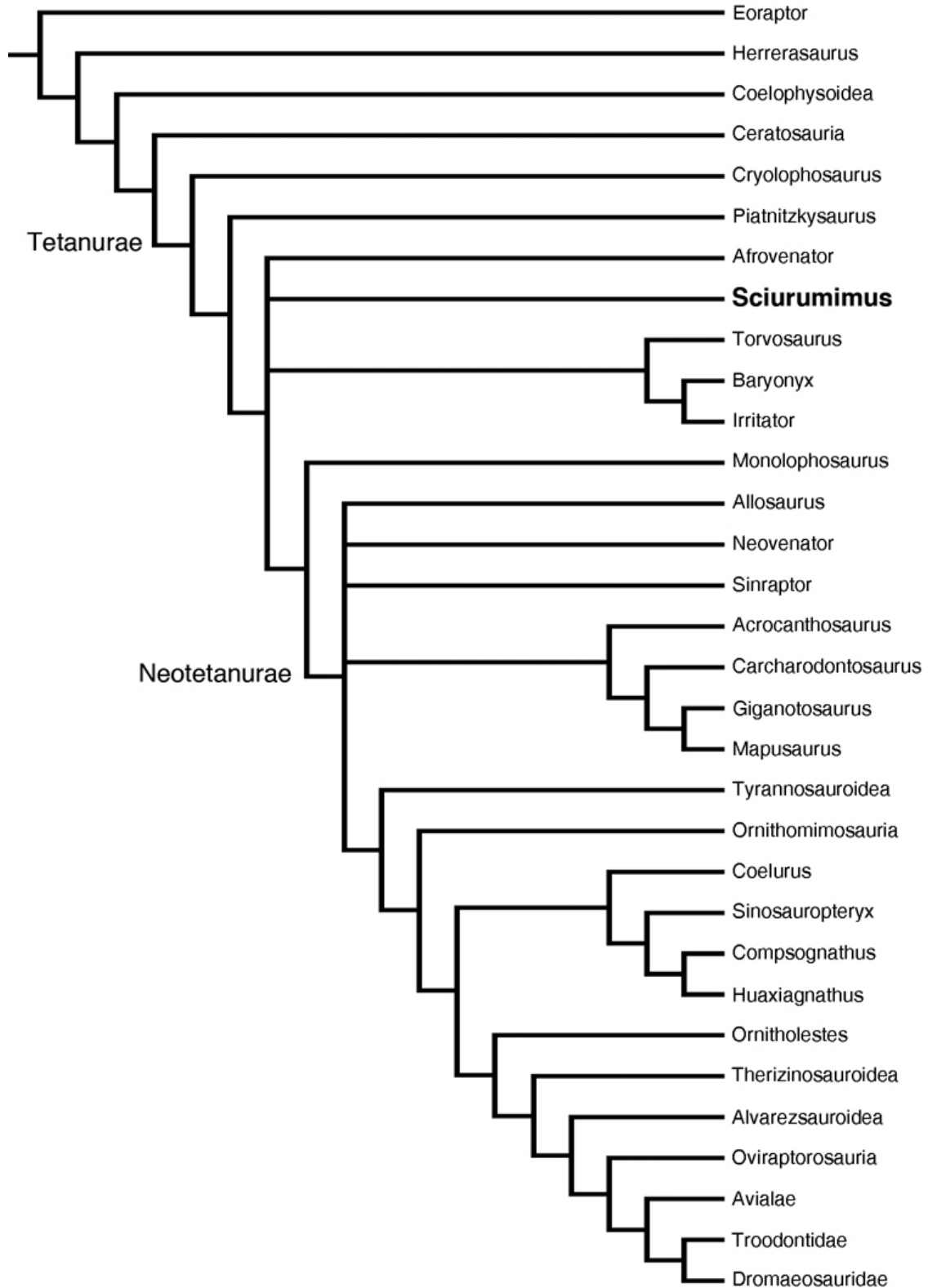


Fig. S6.4. Strict consensus tree of the analysis based on Choiniere et al. (2010). Several clades were collapsed for clarity. Ingroup relationships in these clades is as in Choiniere et al. (2010).

Codings for Sciurumimus in the matrix of Choiniere et al. (2010)

10?0[01]00?00?11010?????20001?00?0?0000?000?11100000??1??0010?????000?00
 ?????0100??0?10??????000????????????000?1?0000?????????0?1000100?01110?
 0?011??00??01001?00002000?0?00?0202??[01]0?00111??0?00??00?00011001?23???
 ?0000000000??0000100001000??1??0000?11000?00001000?0000?000001?1??0111
 00010?012112111?1000000100?02?0??0?0?1??1?0?00??01??0?00001000010?1?000
 ?01??0?000100????1???1????00????????????0010??00?0?2000?

ANALYSIS BASED ON BENSON ET AL. (2010)

After establishing that *Sciurumimus* is a basal, non-coelurosaurian theropod in the analyses of Smith et al. (2010) and Choiniere et al. (2010), we decided to test its detailed phylogenetic position in the most extensive phylogenetic analysis of basal tetanurans published so far, that of Benson et al. (2010). This matrix included four outgroup and 41 tetanuran ingroup taxa, with emphasis on basal, non-coelurosaurian taxa [38 of the ingroup taxa, as opposed to 20 in Smith et al. (2008) and 13 in Choiniere et al. (2010)], scored across 233 characters. We included *Sciurumimus* in this matrix and reran the analysis in PAUP* 4.0, using the same settings described above for the Smith et al. (2008) analysis. The analysis resulted in 7 383 equally parsimonious trees with a length of 656 steps. The strict consensus of these trees recovered *Sciurumimus* in a large polytomy within Megalosauroidae more derived than *Monolophosaurus*. After the exclusion of *Piveteausaurus*, a reduced consensus tree depicts *Sciurumimus* as the most basal representative of the Megalosauridae (Fig. 6.4, S6.5). As in the previous analyses, tree support is rather low, with most clades showing bootstrap values below 50 %.

An interesting result of the analysis is that the inclusion of *Sciurumimus*, without any other changes to the original matrix of Benson et al. (2010), led to the recovery of the monophyletic Carnosauria, including the Megalosauroidea and Allosauroidea. This relationship was also found by Rauhut (2003a), but is in contrast to most recent analyses, which recovered megalosauroids (or spinosauroids) as outgroup to a monophyletic Neotetanurae that includes allosauroids and coelurosaur e.g. Smith et al. (2008), Choiniere et al. (2010) and Benson et al. (2010). Synapomorphies of carnosaurs include the presence of a subnarial foramen, the presence of at least weakly developed enamel wrinkles in the lateral teeth, opisthocoelous cervical vertebrae, a kinked anterior edge of the anterior caudal neural spines, the presence of an indentation between the acromion process of the scapula and the coracoid, a biceps tubercle that is developed as an obliquely oriented ridge, the presence of a broad ridge above the acetabulum on the ilium, and the presence of a well-developed extensor groove on the anterior side of the distal femur. However, making Neotetanurae monophyletic, to the exclusion of megalosauroids, requires only two additional steps. Thus, the interrelationships of basal tetanurans remain problematic and need additional investigation.

Codings for Sciurumimus in the matrix of Benson et al. (2010)

[0/1]??01?0?1001101?0??????0?0000?010210??010000??000?0?00??11????00101??
 1????1??0?110000010020?00101?00?111?0[1/2]?10[0/1]?11??0000000??001001?0020
 0000?1????0000[0/1]001011?0001????[0/1]0??00??0?101001?1??11??????01?????
 ??02???0010?010??00?00?0??

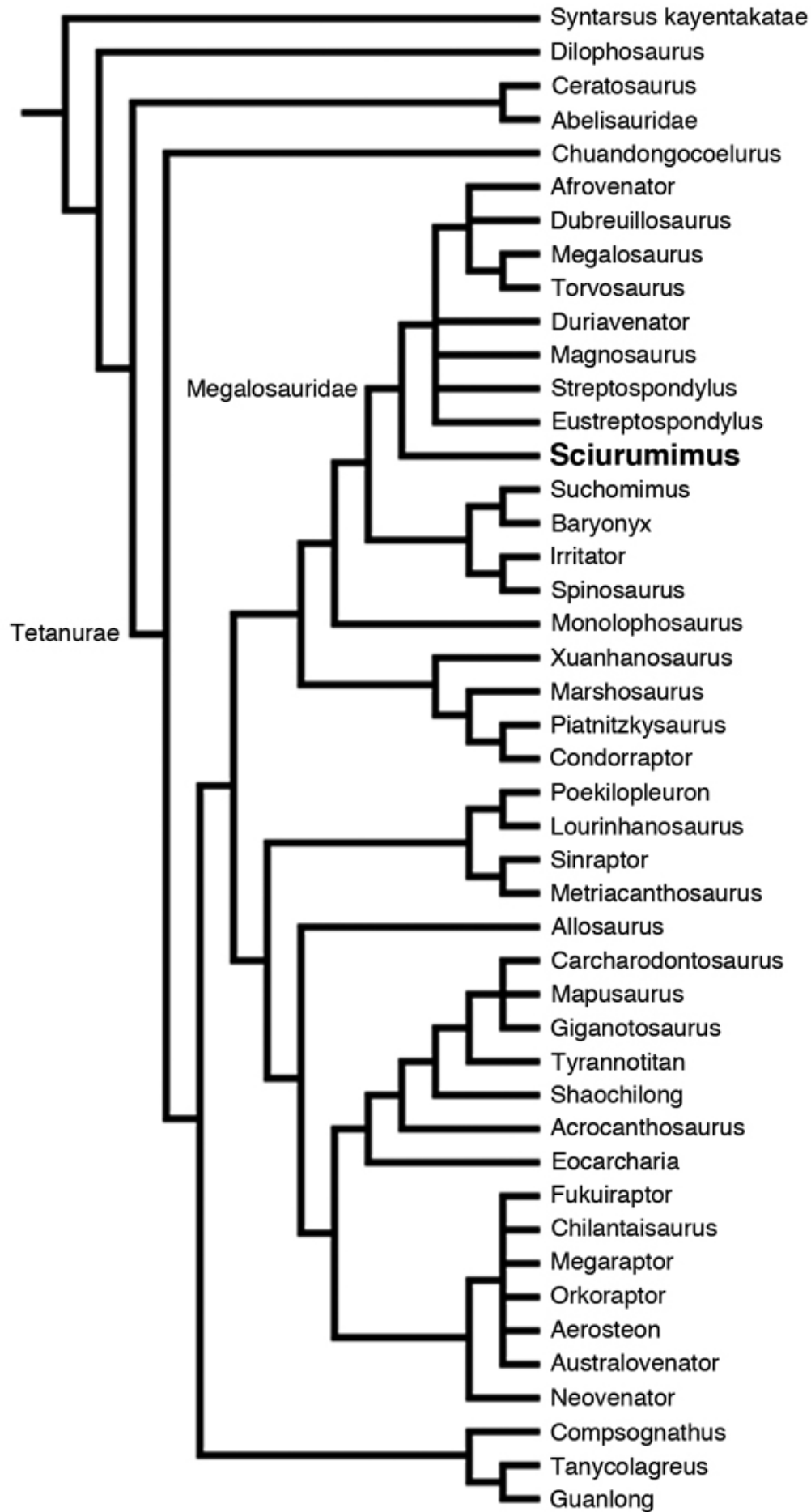


Fig. S6.5. Reduced consensus tree of the analysis based on the matrix of Benson et al. (2010).

DISCUSSION

The congruent results of the three phylogenetic analyses provide strong support for a basal tetanuran relationship of *Sciurumimus*, although some uncertainty about the exact phylogenetic position remains. As demonstrated by the analysis based on the matrix of Benson et al. (2010), the character combination shown by the new taxon is most compatible with megalosauroid relationships. Although this is supported by analyses with all characters that we considered to be potentially ontogenetically variable coded as “?” for *Sciurumimus*, the very early ontogenetic stage of the specimen leaves room for speculation about the possible effects of ontogenetic changes on the phylogenetic results, since little is still known about ontogenetic changes in non-avian theropod dinosaurs. On the other hand, however, the results show that even such very young individuals preserve enough phylogenetically relevant information to at least establish their approximate phylogenetic position.

5. COMPARISON WITH *JURAVENATOR STARKI*

At first glance, the skeleton of *Sciurumimus* seems to be strikingly similar to that of *Juravenator starki*, from the Kimmeridgian of Schamhaupten (Göhlich & Chiappe 2006; Chiappe & Göhlich 2010). Not only are the two animals contemporaneous up to the same horizon within the same ammonite subzone (Schweigert 2007) and come from the same geographical area (though from different subbasins within the Upper Jurassic limestone deposits of southern Germany), but they are also of closely matching size.

Indeed, even in detailed comparison, the proportions of *Juravenator* and *Sciurumimus* are strikingly similar (Table S6.2).

Table S6.2. Comparison of selected measurements of *Juravenator* and *Sciurumimus*. Measurements of *Juravenator* from (Chiappe & Göhlich 2010).

	<i>Juravenator</i>	<i>Sciurumimus</i>
Skull length	82 mm	79 mm
Scapula length	42 mm	42 mm
Humerus length	27 mm	26.8 mm
Radius length	c. 19 mm	17 mm
Mc II length	9 mm	8.8 mm
Femur length	52 mm	50.6 mm
Tibiotarsus length	58.1 mm	54.2 mm
Mt III length	34 mm	32.1 mm

However, despite these similarities in general morphometrics, the two taxa show numerous differences in anatomical details [based on Chiappe & Göhlich (2010) and own observations on the type of *Juravenator*], even though comparison is sometimes hampered by the different preservation [*Sciurumimus* is exposed in lateral view, but *Juravenator* in dorsolateral view for most elements; see Chiappe & Göhlich (2010)]. Thus, in the skull of *Juravenator*, the anterior margin of the antorbital fossa is rectangular, rather than gently rounded, the maxillary fenestra is relatively smaller, the antorbital fossa is smaller, the ventral process of the postorbital is more massive and notably curved, the ventral (quadratojugal) process of the squamosal tapers to a point, and the posterior premaxillary teeth bear serrations, whereas they are more slender and devoid of serrations in *Sciurumimus*. In the vertebral column, *Juravenator* differs from *Sciurumimus* in the following characters: cervical epiphyses small, barely if at all overhanging the postzygapophyses; prezygoepiphyseal laminae in the cervical

vertebrae absent; presence of a posterior pleurocoel in a mid-cervical centrum; anteriormost dorsal vertebrae distinctly elongate; strongly posteriorly inclined, triangular neural spines in the anterior caudal vertebrae; relatively more elongate posterior caudal vertebrae; posterior caudal prezygapophyses more elongate and anteriorly directed, rather than anterodorsally; distal chevrons skid-like. In the pectoral girdle and forelimb, the following differences can be established: the scapula is less slender and has a distinctly curved blade; the supraglenoid fossa is triangular, with an acutely angled posterior rim; the internal tuberosity of the humerus is confluent with the proximal humeral articular surface, forming a rectangular edge on the medial side of the proximal humerus; the ulna lacks a proximal expansion and olecranon process; shaft of ulna more massive than shaft of radius. In the pelvis and hindlimb, *Juravenator* differs from *Sciurumimus* in the lack of an anterior dorsal lip of the ilium (the presence of which represents an autapomorphy of *Sciurumimus*), the relatively smaller pubic peduncle of the ilium, a more reduced supraacetabular crest, which is confluent posteriorly with the lateral brevis shelf, a pronounced antitrochanteric lip on the ischial peduncle of the ilium, a rectangular, rather than undulate posterior end of the postacetabular blade of the ilium, an obturator process on the ischium [erroneously identified as pubis by Chiappe & Göhlich (2010)] that is offset from the pubic peduncle, the lack of a distal expansion of the ischial shaft, the short and triangular metatarsal I, a metatarsal IV that is distinctly longer than metatarsal II, and the shorter and more robust metatarsal V. Thus, these numerous differences strongly indicate that the two animals cannot be referred to the same taxon, despite the similar size and proportions.

Looking at the phylogenetic position of *Juravenator* led to some interesting results. To test the position of this taxon, we also coded it in the matrices of Smith et al.

2008 and Choiniere et al. (2010), and analysed the matrices under the same parameters outlined above. When analysed together with *Sciurumimus*, *Juravenator* was found to be the sister taxon to this genus in both analyses, with otherwise no changes in the phylogenetic position of *Sciurumimus* (i.e. both taxa were found to be basal, non-neotetanuran tetanurans). However, when *Sciurumimus* was removed from the analyses, *Juravenator* was found to be a basal coelurosaur in both cases (Fig. S6.6, S6.7).

As it is the case with *Sciurumimus*, the type of *Juravenator* is most probably an early posthatchling individual, since it lacks any fusion of skeletal elements, even lacks ossified carpal and distal tarsal elements altogether, and shows coarsely striated surface texture in all skeletal elements (see Chiappe & Göhlich 2010). Several of the characters shared by *Sciurumimus* and *Juravenator*, and interpreted as synapomorphies of these taxa in the analyses, are probably ontogenetically variable, such as the round orbit, anterodorsally sloping ventral strut of the lacrimal (related to the size and shape of the orbit), absence of a posteroventral process in the coracoid, absence of a ventral hook on the preacetabular blade of the ilium, and poorly developed attachment of the m. iliofibularis on the fibula (all three muscle attachment areas). Thus, analysis of these two early juveniles together with otherwise subadult and adult theropods might give erroneous results, and we consider the phylogenetic position of *Juravenator* as uncertain. *Juravenator* shows a highly unusual character combination (Chiappe & Göhlich 2010) and further analysis of its affinities is necessary to firmly establish its phylogenetic position. However, such a detailed reappraisal of *Juravenator* is beyond the scope of the current paper.

These phylogenetic results furthermore suggest that the frequent referral of early juvenile theropods, such as *Juravenator* (Göhlich & Chiappe 2006) and *Scipionyx* (Dal Sasso & Maganuco 2011) to the Compsognathidae might simply be due to similarities between these taxa and the also juvenile type specimen of *Compsognathus bavarica*, and thus the phylogenetic status and content of the Compsognathidae need to be reevaluated.

Codings for Juravenator in the matrix of Smith et al. (2008)

00200[0/1]0[0/1]01???00100??00?21010[0/1]111??20??0?10?1[1/2]0?101[0/1]0?0001
 00?000?0?00[0/1]??0000?0?00?????????????????????????????????????0??0?0?????
 ?????????????01101???0??100100000??0[0/1]01?????0?100?0????00011?00???10010
 00?????0101100000000?001?00???111101111??0100100?0000??001002?0000?101??
 ??????0?0100000????2011?????1????????00?????????2??11?0??????1200?0?????
 ?

Codings for Juravenator in the matrix of Choiniere et al. (2010)

10?0[01]00?00?11010?1????20101?00?0?0?00000??[12]110000??110?0010?1????000
 ?00?000??00????????????????0?0????????????????????????????????????0?0000?0???0??
 ???0???0???0???0?000020???0????01?10???00101???10??????????[01]011?1?????
 ??000000?????0?0?100?1000??1???0?0?10?01??00?10000???1?0000????????011100?
 11?0?2?12111?10000001002000011?0?0?100111?00????????????????10?00?1?000?0?01
 ??0?0001?00???1????????00????????????1??0?10?????1?2000?

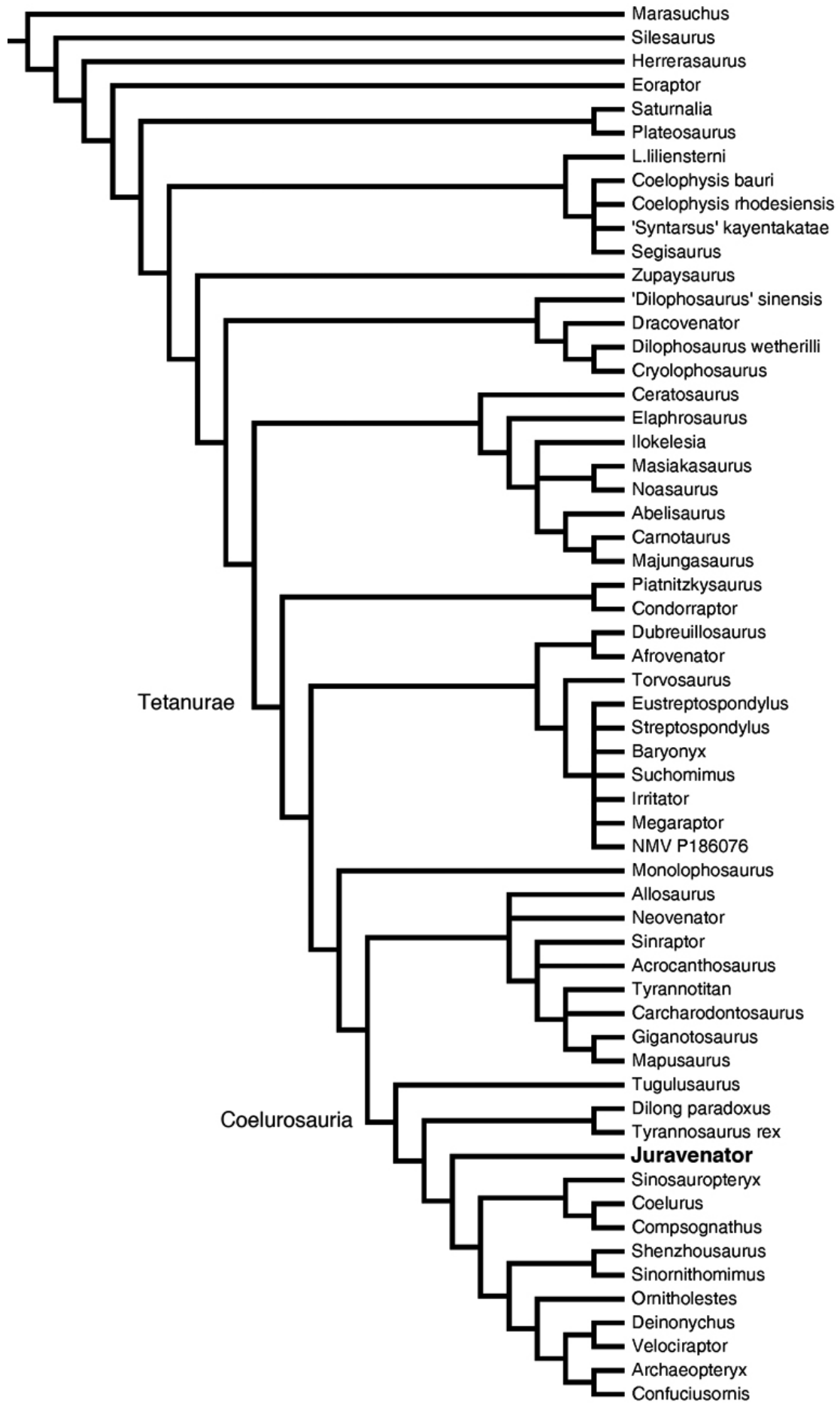


Fig. S6.6. Phylogenetic analysis of *Juravenator*, excluding *Sciurumimus*, based on the matrix of Smith et al. (2008).

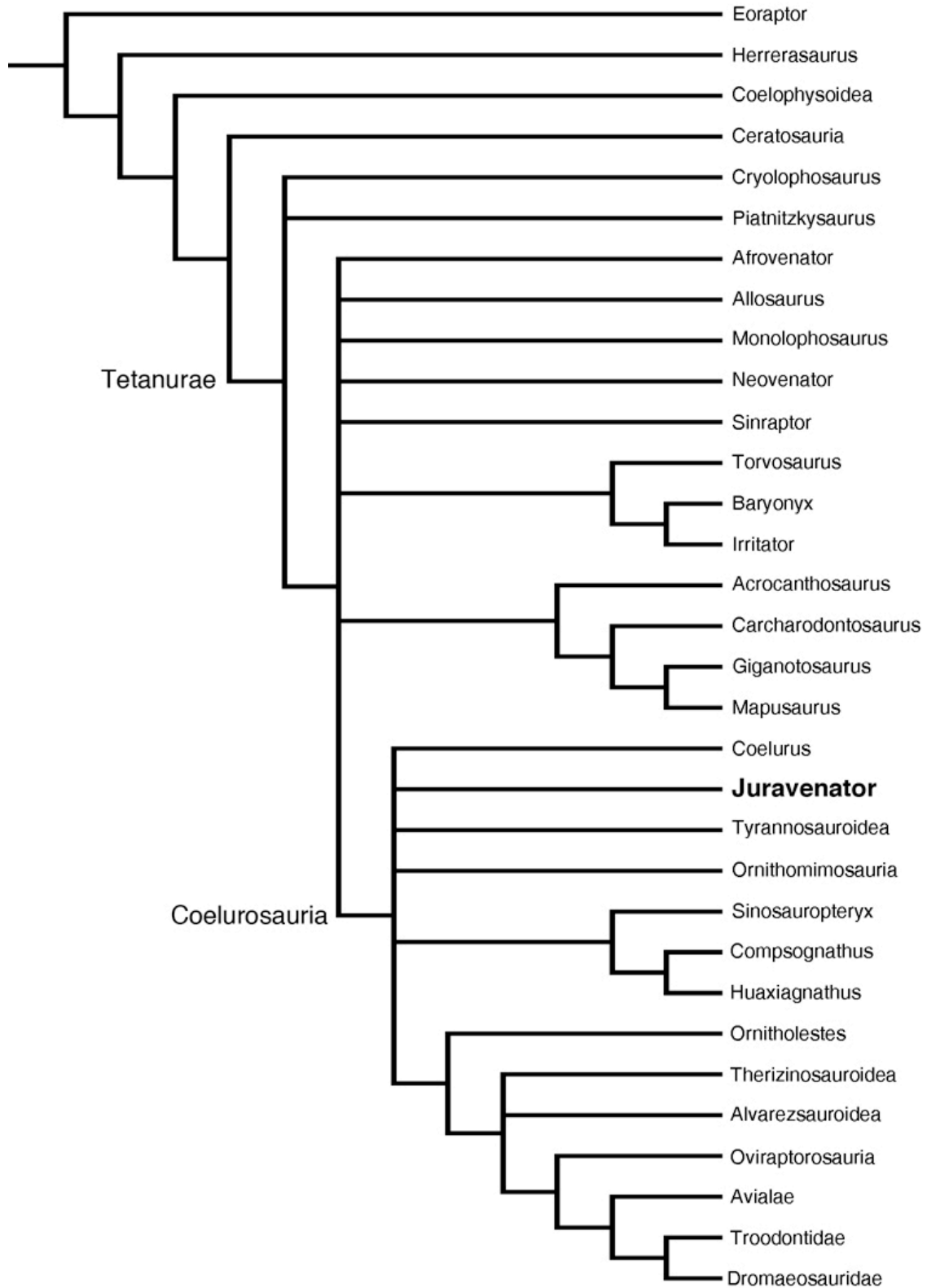


Fig. S6.7. Phylogenetic analysis of *Juravenator*, excluding *Sciurumimus*, based on the matrix of Choiniere et al. (2010). Several clades have been collapsed for clarity.

6. COMPARISONS WITH OTHER JURASSIC THEROPODS

Given the early juvenile stage of the type specimen of *Sciurumimus albersdoerferi*, one might ask whether this animal represents a juvenile of another, known taxon of theropods from the Late Jurassic. Apart from *Juravenator*, theropods known from the Late Jurassic of Europe include the ceratosaur *Ceratosaurus* (Mateus et al. 2006; Soto & Perea 2008), the megalosaurid *Torvosaurus* (Mateus et al. 2006), the allosauroids *Allosaurus europaeus*, *Lourinhanosaurus* and *Metriacanthosaurus* (Mateus et al. 2006; Benson et al. 2010), and the coelurosaurs *Compsognathus* (Ostrom 1978; Peyer 2006), *Aviatyrannis* (Rauhut 2003b), *Stokesosaurus langhami* (Benson 2008b) and *Archaeopteryx* (Wellnhofer 2008)

First of all, *Sciurumimus* differs from all of these taxa, in which comparable material is preserved, in its apomorphic characters. Numerous differences with *Ceratosaurus* further include most tetanuran synapomorphies, such as the presence of a maxillary fenestra, the presence of only one pleurocoel in the cervical vertebrae, a hand with only three metacarpals, and the presence of a wing-like lesser trochanter that reaches at least half the height of the femoral head (Gilmore 1920; Madsen & Welles 2000).

Given that the phylogenetic analysis indicates that *Sciurumimus* represents a basal megalosaurid, comparisons with the megalosaurid *Torvosaurus* might be most important. However, numerous differences between the two taxa include the number of premaxillary teeth (three in *Torvosaurus*, four in *Sciurumimus*), the offset of the maxillary fenestra from the anterior rim of the antorbital fossa in *Sciurumimus*, the lack of a well-developed prezygoepipophyseal lamina in the cervical vertebrae of

Torvosaurus, the straight and much more robust humerus, relatively shorter radius and ulna, and relatively shorter and much more robust metacarpals in *Torvosaurus*, and the widely laterally exposed medial brevis shelf, flexed ischial shaft and lack of a distal incision between the obturator process and ischial shaft in this taxon (Galton & Jensen 1979; Britt 1991).

Establishing differences with the European allosauroids is somewhat more difficult, since all of them are based on very fragmentary material and/or have not been described in detail yet. Differences between *Sciurumimus* and *Allosaurus europaeus* include the pneumatized nasal and raised lateral margins of the nasals in the latter (Mateus et al. 2006), and further differences with other species of *Allosaurus* include the anteroposteriorly short axial neural spine, lack of well-developed prezygoepipophyseal laminae in the cervical vertebrae, presence of an anterior kink in the anterior caudal neural spines, presence of an anterior spur in mid-caudal vertebrae, presence of strongly elongate distal caudal prezygapophyses, distally expanded mid-caudal chevrons, strongly sigmoidal humerus, well-developed anterior hook in the preacetabular blade of the ilium, and an obturator process that is offset from the pubic peduncle of the ischium in the latter taxon (Madsen 1976). Differences with *Metriacanthosaurus* are the less steeply sloping posterior dorsal margin of the ilium and the much lower dorsal neural spines in *Sciurumimus*. The latter taxon also differs from *Lourinhanosaurus* in the lack of an anterior spur in the mid-caudal vertebrae, the lack of an anterior hook in the preacetabular blade and a lateral exposure of the medial brevis shelf of the ilium, and an obturator process that is not offset from the pubic peduncle of the ischium (Mateus 1998).

Sciurumimus lacks coelurosaurian synapomorphies, which already makes a referral to one of the known coelurosaurian taxa from the Late Jurassic of Europe improbable. Apart from the fact that *Archaeopteryx* is known from juvenile to subadult specimens that are even smaller than the early juvenile specimen of *Sciurumimus*, a comparison between these two taxa finds more differences than similarities, for example in the shape and placing of the teeth, the shape of the jaws, the form of the vertebrae, the much more slender and bird-like forelimbs of *Archaeopteryx*, etc. (see Wellnhofer 2008).

Compsognathus is known from two specimens (Ostrom 1978; Peyer 2006), one of which is closely comparable in size to *Sciurumimus*. However, numerous differences are found between these animals, from overall body proportions to anatomical details such as the shape and extent of the antorbital fossa and maxillary fenestra, the much more slender dentary in *Compsognathus*, the shape of the cervical vertebrae, the presence of a triangular obturator process in the ischium in *Compsognathus*, etc.

Comparison with *Aviatyrannis* and *Stokesosaurus langhami* is more problematic, since both are based on very limited material. Nevertheless, the ilium of *Aviatyrannis* differs considerably in overall shape and in the presence of a sharply defined vertical ridge above the acetabulum from *Sciurumimus* (Rauhut 2003a), and *Stokesosaurus langhami* differs in the same features and the lack of a well-developed prezygoepipophyseal lamina in the cervical vertebrae.

In summary, it seems very unlikely that *Sciurumimus* represents a juvenile of a known taxon of theropod dinosaurs. Furthermore, the quite unusual anatomy in many parts of the skeleton clearly indicates that the specimen represents a new taxon.

7. ADDITIONAL DISCUSSION OF SOFT TISSUES

The new specimen possesses patches of skin and filamentous integument structures, which are visible under UV light (Figs. 6.3, S6.8-S6.10). Skin remains are preserved in the forelimb region and on the dorsal and ventral side of the tail (Fig. S6.9). Differences in the reflection of UV light indicate that further skin remains are probably preserved on the surface of some bones (e.g. femur). In contrast to *Juravenator* (Chiappe & Göhlich 2010), and other examples of theropods where skin remains are preserved (Xu & Guo 2009), the patches show no evidence of a scaly surface.

Filaments are preserved on the dorsal and ventral side of the trunk and on the dorsal and ventral side of the tail. However, the best preservation is present on the dorsal side of the anterior-mid section of the tail. Here, the filaments are extremely elongated and present in high density, forming a bushy tail (Figs. S6.8, S6.9), as it is the case in some other theropods (Ji et al. 2007). Due to the actual state of preparation, it is not possible to judge if the filaments reach equal lengths on the dorsal side of the presacral region. The filaments are very fine and show no branching pattern, indicating that these structures are similar to protofeathers found in some coelurosaurian theropods, e.g. *Dilong* (Tyrannosauroidae), probably *Sinosauropteryx* (Compsognathidae), *Beipiaosaurus* (Therizinosauroidae), *Shuuvia* (Alvarezsauridae) (Norell & Xu 2005; Xu & Guo 2009), and *Juravenator* (basal Coelurosauria) (Chiappe & Göhlich 2010). Similar looking structures were described for some small

ornithischian dinosaurs [*Psittacosaurus* (Mayr et al. 2002) and *Tianyulong* (Zheng et al. 2009)]. Assuming homology between the protofeathers found in coelurosaurs and these ornithischians, the new specimen helps to bridge the considerable gap between both filamentous integument structures. Thus, protofeathers probably represent the plesiomorphic state for dinosaurs (Witmer 2009; Brusatte et al. 2010c). However, in many dinosaur groups, e.g. Ceratopsia, Stegosauria, Hadrosauridae, Sauropodomorpha, Ceratosauria, basal Tetanurae, and basal coelurosaurs scaly skin impressions are known (Bonaparte et al. 1990; Anderson et al. 1999; Glut 2003; Göhlich & Chiappe 2006, Coria & Chiappe 2007; Xing et al. 2008; Xu & Guo 2009; Bell 2012). These scales are usually non-overlapping and polygonal in shape (Xu & Guo 2009).

However, we regard the presence of both scales and protofeathers in early dinosaurs as not problematic. Most fossil skin impressions are usually incomplete and preserved only as small, regionally distributed patches, indicating only that this respective body region was covered with scaly skin. However, the examples of *Psittacosaurus* and *Juravenator* where both scales and protofeathers are present, show that different kind of integument structures can be present in the same animal. Furthermore, recent studies in evolutionary developmental biology indicate that scale and feather development are regulated by the same set of signal molecules. Thus, only small changes within the pathways can lead to different integument structures (Crowe & Niswander 1998; Widelitz et al. 2000; Harris et al. 2002; Dhouailly 2009), and it seems likely that feathers could get secondarily lost in several lines independently. Finally, whereas scaly skin impressions might be preserved in various sediments, including even coarse sandstones, the preservation of fine filaments, such as those found in *Sciurumimus*, requires very special conditions, so taphonomic processes also play a

major role in our understanding of the distribution of integumentary structures in theropod dinosaurs. The latter conclusion is supported by the recent find of the large tyrannosauroid theropod *Yutyrannus*, which was preserved in a suitable environment and has filamentous feathers preserved (Xu et al. 2012).



Fig. S6.8. Impressions of filaments dorsal to anterior caudal vertebrae under normal light. Abbreviation: C, caudal vertebra. Scale bar is 10 mm.

Interestingly, the body of pterosaurs was also covered with monofilaments (Bakhurina & Unwin 1995; Wang et al. 2002), recently named pycnofibers (Kellner et al. 2010). If filamentous protofeathers are primitive for dinosaurs, it seems very likely

that these structures are homologous to the protofeathers of dinosaurs (Zhou 2004), and, thus, the origin of feathers leads back to ornithodiran origins.

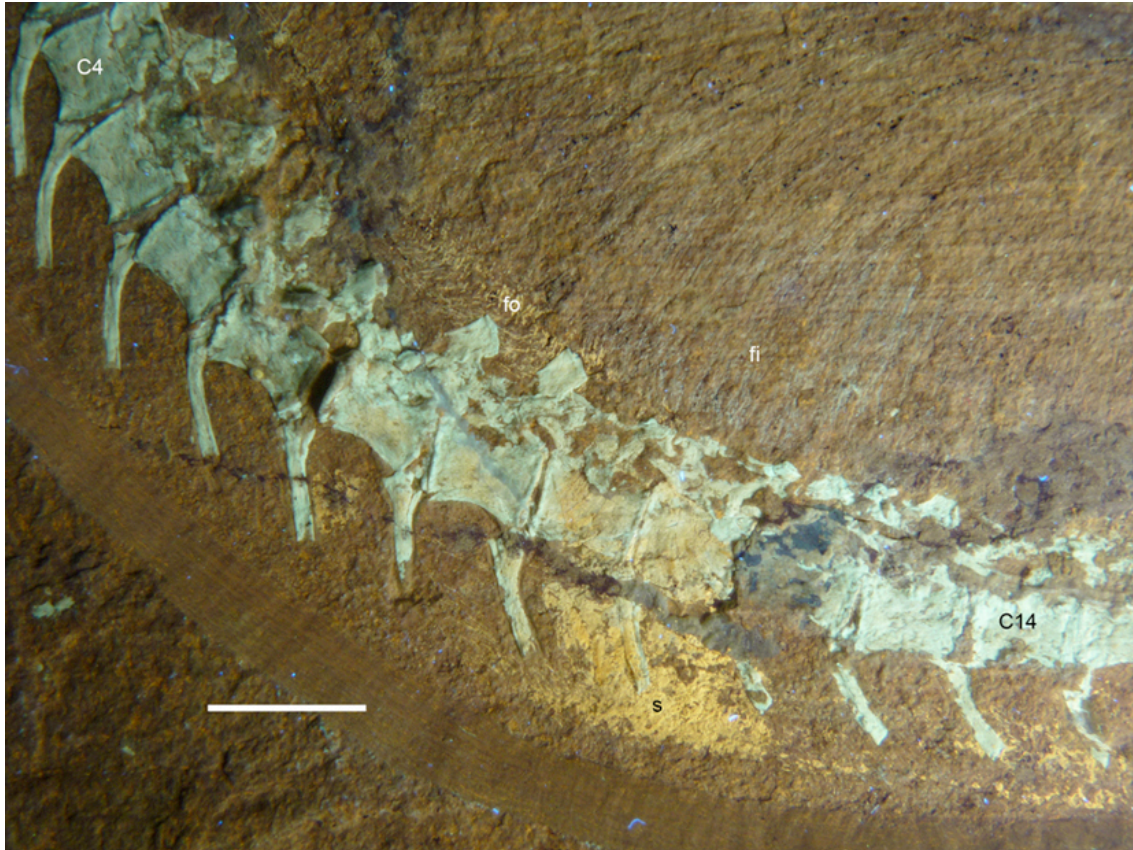


Fig. S6.9. Soft tissue preservation in the anterior caudal region of *Sciurumimus* under ultraviolet light. Abbreviations: C, caudal vertebra; fi, filaments; fo, possible follicles at the base of filaments; s, skin. Scale bar is 10 mm.

The preserved integument structures of *Sciurumimus* provide new information on the morphology of protofeathers and the origin of feathers. In one area, on the dorsal side of the tail, protofeathers and skin are preserved in direct association. Both structures can be differentiated by their different luminescence under UV light. The protofeathers seem to be anchored in the skin, indicating that these integument

structures might have grown from follicles. Indeed, there are conspicuous, dorsoventrally elongate skin structures preserved where the filaments reach the skin, which might represent direct evidence for these follicles. This is interesting, because it has been suggested that follicle formation was a late event in feather evolution, which took place with the evolution of vaned feathers (Sawyer & Knapp 2003; Alibardi & Sawyer 2006; Alibardi & Toni 2008). This scenario was based on the feather embryogenesis of some recent bird species, where barb ridge formation occurs before follicle formation. The hypothesis that unbranched protofeathers apparently grow from a follicle supports the idea that feather evolution is highly correlated with follicle formation (Prum 1999; Prum & Brush 2002). Further support for this comes from *Psittacosaurus*, where the bristles extend under the skin layer (Mayr et al. 2002), also lending additional support for the homology of ornithischian filaments with theropod protofeathers and bird feathers.

8. REPOSITORY OF THE SPECIMEN

The holotype specimen of *Sciurumimus* belongs to the private Painten collection of the Albersdörfer family, where it bears the collection number 1687. However, the scientific availability of the specimen is guaranteed by its inclusion in the register of cultural objects of national importance of Germany (Verzeichnis national wertvollen Kulturgutes). Under the Act to prevent the exodus of German Cultural Property (KultSchG; Bundesgesetzblatt I: 1754; 1999), the inclusion of the specimen in this list prevents it from being sold outside Germany and guarantees that its current repository is always known and changes of repository have to be announced. Furthermore, the type specimen of *Sciurumimus albersdoerferi* is deposited as a permanent loan at the

municipal Bürgermeister Müller Museum in Solnhofen, Bavaria, where it is also available for additional scientific study and bears the specimen number BMMS BK 11.

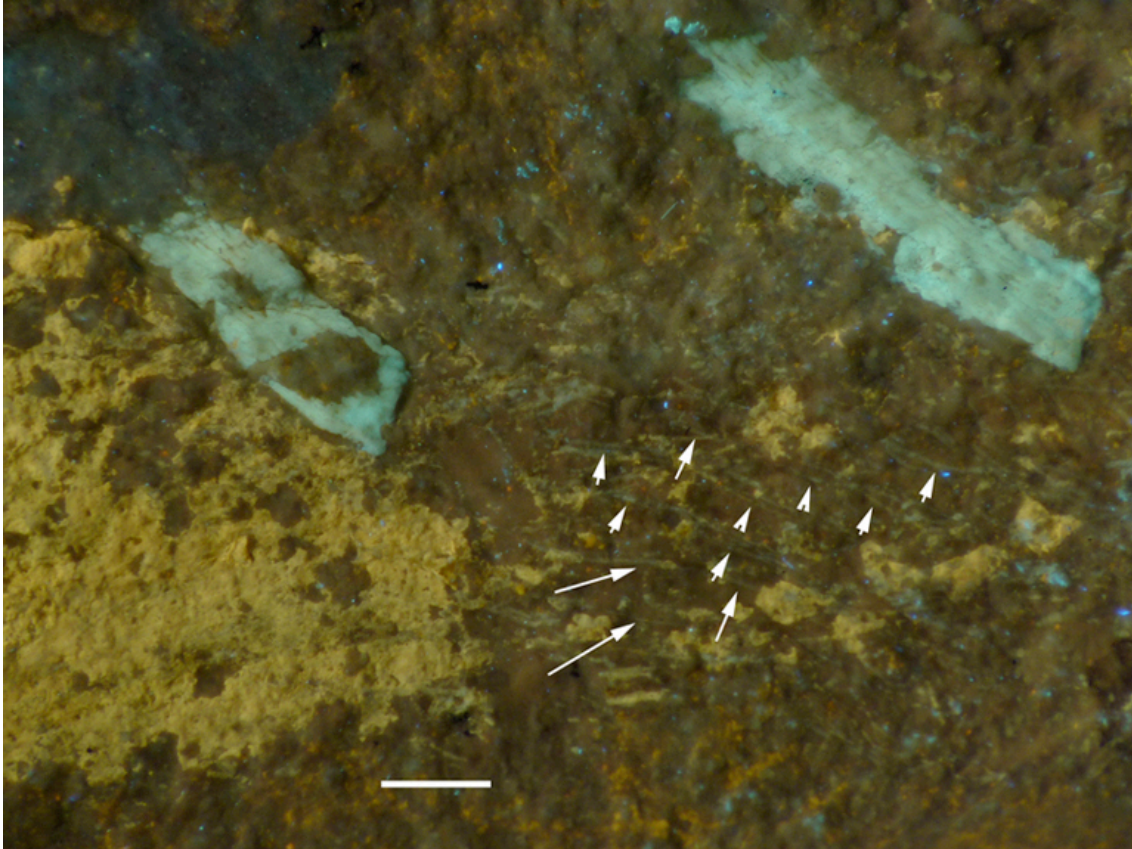


Fig. S6.10. Short filaments on the ventral tail flank below the 12th and 13th caudal vertebra. Arrows point to single filaments.
